Univerzita Karlova v Praze
Přírodovědecká fakulta

Studijní program:
Environmentální vědy

Nicholas Talbot MSc

A detailed study on aerosol particle size distribution in indoor and outdoor environments with attention to ammonium nitrate transformations.

Detailní studie rozdělení velikosti částic aerosolu ve vnitřním a venkovním prostředí s důrazem na přeměny dusičnanu amonného.

Disertační práce

Supervisor: Ing. Vladimír Ždímal, Dr.

Supervisor Specialist: Ing. Jakub Ondráček, Ph.D.

Praha, 2016

Declaration:

I declare that I prepared this final work independently and that all the information sources and literature used within this thesis has been correctly referenced. I also declare that this work or a substantial portion thereof has not been submitted to obtain another academic degree or equivalent.

Signature

Prohlášení:

Prohlašuji, že jsem závěrečnou práci zpracoval samostatně a že jsem uvedl všechny použité informační zdroje a literaturu. Tato práce ani její podstatná část nebyla předložena k získání jiného nebo stejného akademického titulu.

Podpis

.....

Acknowledgements

I would like to take this opportunity to thank the people who have contributed in some way to this thesis and the research documented herein. Firstly, thank you to my lead supervisor Vladimir Zdimal for his wonderful patience and excellent guidance. The experiment of teaching an environmental scientist foundational physical chemistry was certainly a challenging one. Sorry for asking the kinds of questions that made you close your eyes and shake your head solemnly. I have enjoyed my time with the group and regard it as successful and fruitful experience. Thanks for allowing me the opportunity.

Thanks, or rather na zdravi to my supervisor specialist and friend Jakub Ondracek for all the practical help in work and liquid refreshments, from now on I will always check to see if the signal cable is plugged in, hopefully we can toast to a successful defence soon. Finally a big thanks to my co-supervisor Jaroslav Schwarz for all the precise and detailed advice, not least for providing excellent internet support on impactor measurement techniques.

To all my colleagues and co-authors here in ICPF Prague, a big thank you for tolerating my complete inability to pick up the Czech language, you are all friends and if ever you are looking for a getaway to New Zealand it would be my pleasure to show you around. Thanks to Irena and Pepa in the labs for preparing so much of the experimental work and helping weigh all those filters. A special mention also to Lucie Kubelova, thanks for all the math help and your work on Articles 2 and 3. Kayleigh Kavanagh, editor in chief and proof reader extraordinaire. You turned up at the lab at just the wrong time, or the right time as far as I'm concerned. Your work on this thesis and the Articles has been priceless.

I would like to thank Guy Coulson for recommending this PhD position and for enabling my previous MSc to proceed whilst working with NIWA. Michael Cusack, friend and collegue, thanks for also not learning to speak Czech as moral support to me. Along with the rest of the Prague expat crew, we had some good times over the last couple of years.

Thanks also to my parents, sis and the gang, I'm sorry for disappearing to the other hemisphere for a few years. Hopefully this will all be worthwhile and I'll be back in New Zealand soon to enjoy a few brunches on the beach and grills on the deck in the evenings. How I will miss the 7am Sunday morning Skype catch-up calls.

Finally I would like to thank the Marie Curie European Union Seventh Framework Programme (FP7/2007-2013) under grant agreement n° 315760 HEXACOMM project for supporting the research in this document.

When I was 12 I was given an Oxford English dictionary, on the inside cover was written;
Words are the swords by which every war is won. I reiterate that here.

Contents

Figures

Tables

Terminology

Throughout this document the terms particulate and aerosol will be used interchangeably. However, they can be defined separately. Particles are solid or liquid droplet suspended in air, where-as aerosols refer to both the particulate and the gas (air) in which it is suspended.

This thesis will often refer to the dissociation of ammonium nitrate. We use the term dissociation to define the reversible thermodynamic reaction of the ammonium nitrate (solid/aqueous) – nitric acid / ammonia (gas) partitioning in the atmosphere. It is understood that when ammonium nitrate becomes dissolved in an aqueous droplet, the release of ammonia and nitric acid from this droplet can be described as evaporation. However, for continuity, the term dissociation will be used throughout this thesis.

Abstrakt

Dusičnan amonný je důležitou chemickou sloučeninou z hlediska aerosolového výzkumu především pro své široké zastoupení nad velkými hustě zalidněnými oblasti. Nicméně díky své těkavosti za normálních podmínek a při nízkých teplotních gradientech je poměrně obtížné přesně měřit jeho koncentraci. Je všeobecně známo, že těkavost dusičnanu amonného je závislá na teplotě, relativní vlhkosti, konkrétním složení dané aerosolové částice a dostupnosti příslušných plynných prekurzorů. Skupenství dané částice ovlivňuje hodnotu rovnovážné konstanty reakce dusičnan amonný - kyselina dusičná/amoniak a následně i rychlost disociace. Z hlediska aerosolového výzkumu zabývajícího se vnitřním prostředím jsou tyto termodynamické procesy umocněny přechodem částic pocházejících z vnějšího prostředí do nových podmínek v prostředí vnitřním. Náhlé změny teploty a relativní vlhkosti, spolu s povrchovými reakcemi v uzavřeném vnitřním mikroprostředí urychlují disociaci dusičnanu amonného. Tato zvýšená rychlost disociace může způsobovat chyby v měřených datech, zvyšovat tvorbu nových částic ve vnitřním prostředí a urychlovat korozi kulturních památek jejich okyselením. Míra těchto dopadů je nejistá především díky nedostatku znalostí o přeměně částic při jejich přechodu z venkovního do vnitřního prostředí. Proto bylo v rámci této disertační práce provedeno pět experimentálních kampaní, z nichž každá byla pozorně navržena tak, aby zodpověděla určitou otázku týkající se přeměny částic. Speciální pozornost byla věnována chování dusičnanu amonného a to především, nikoliv však výhradně, ve vztahu k vnitřnímu prostředí.

Nejprve bylo nutné získat širší porozumění základního chování dusičnanu amonného v „čistém“ prostředí. Za tímto účelem byly provedeny kontrolované laboratorní experimenty, které jsou popsány v Článku 1 (Article 1). Tyto experimenty umožnily sledovat rychlost disociace čistého dusičnanu amonného na kyselinu dusičnou a amoniak v uzavřeném systému v závislosti na velikosti částic. V rámci experimentů byly generovány monodisperzní částice čistého dusičnanu amonného o třech velikostech (50, 100 a 200 nm). Výsledky ukázaly, že při transportu částic 2 m dlouhým reaktorem s kontrolovanou teplotou docházelo k nejrychlejšímu zmenšování 200 nm částic v porovnání s ostatními dvěma velikostmi (50 a 100 nm). Proces zmenšování probíhal rychleji při delších zdržných dobách a vyšších teplotách v reaktoru. Nicméně při výpočtu rychlostí disociace na základě naměřené integrální hmoty byly dosaženy přesně opačné výsledky. Menší částice dle výpočtu ztrácely hmoty rychleji než částice větší. Tento rozdíl mezi matematickým modelem a reálnými experimenty ukazuje, že i přes snahu zajistit, aby byl vygenerovaný dusičnan amonný ve formě suchých krystalických částic, nejspíše stále zůstával v částicích jistý obsah vody. Molekuly vody se pak postupně vypařovaly během transportu reaktorem a tím docházelo ke zmenšování částic.

Pro ověření výsledků laboratorních experimentů (Article 1) v reálných podmínkách byla provedena intenzivní měřící kampaň v průběhu léta 2014 a její výsledky jsou uvedeny v Článku 2 (Article 2). Cílem této kampaně bylo sledování změn ve složení částic mezi vnějším a vnitřním prostředím s vysokým časovým rozlišením při typických okolních podmínkách. Pro téměř souběžné vzorkování z vnějšího a vnitřního prostředí s vysokým časovým rozlišením bylo nutné využít systém přepínacího ventilu. Těžištěm výzkumu v této kampani bylo především vnitřní prostředí. Nicméně získaná data s vysokým časovým rozlišením umožnila provedení detailní analýzy denních fluktuací NH_4NO_3 – HNO_3/NH_3 koncentrací ve vnějším prostředí. Z naměřených dat bylo zjištěno, že sledované koncentrace byly přímo ovlivněné teplotou, solárním zářením a změnami výšky mezní vrstvy.

V průběhu tohoto experimentu byl pozorován také vznik nových částic ve vnějším prostředí, což následně způsobilo nárůst počtu částic menších než 100 nm pronikajících do vnitřního prostředí. Tato epizoda byla využita pro zjištění infiltračních rychlostí v reálném čase, vypočtených v závislosti na velikosti částic, čase a dynamické změně koncentrací. Poměr koncentrací ve vnitřním a vnějším prostředí (I/O) vypočtených pro tento případ byl následně porovnán s celkovým průměrným poměrem I/O vypočteným z početních koncentrací naměřených pomocí spektrometru SMPS (pro částice <0.71µm). Dále bylo pozorováno snížení hmotnostní koncentrace dusičnanů při přechodu z vnějšího do vnitřního prostředí, přesně jak bylo očekáváno. Data naměřená pomocí aerosolového hmotnostního spektrometru (AMS) ukázala, že chemické složení naměřené ve vnitřním prostředí bylo úměrné chemickému složení ve vnějším prostředí. Tato podobnost může být vysvětlena malým rozdílem teplot mezi vnějším a vnitřním prostředím v průběhu dne. Vyšší venkovní teploty snižují koncentraci dusičnanu amonného již před transportem do vnitřního prostředí, a tudíž následně nedochází k tak výraznému poklesu jeho koncentrace. Tyto závěry byly potvrzeny i daty z off-line Bernerových nízkotlakých impaktorů (BLPI) umístěných současně ve vnějším a vnitřním prostředí.

Díky výrazné teplotní závislosti stability dusičnanu amonného, byla v zimě 2014-2015 provedena srovnávací experimentální kampaň, jejíž výsledky jsou uvedeny v Článku 3 (Article 3). Metodika měření byla zachována shodná s předcházející letní kampaní. Výsledky naměřené ve venkovním prostředí ukázaly značný nárůst koncentrací dusičnanů v porovnání s výsledky z letní kampaně. Odpařitelná (non-refractory - NR) složka organických sloučenin a dusičnany vykazovaly podobné trendy průměrných koncentrací ve vnějším prostředí. Sezónní změny v chemickém složení byly vypočteny z hmotnostních koncentrací naměřených pomocí AMS a byl zjištěn 33-37% pokles I/O pro všechny měřené složky při porovnání zimního a letního období. Shodný pokles poměrů I/O pro všechny složky ukazuje na spíše fyzikální než chemický mechanismus úbytku částic. Výsledky z BLPI impaktorů potvrdily tato zjištění, když ukázaly více hmoty síranů a dusičnanů ve vnitřním prostředí na patrech pro tři nejmenší frakce aerosolu (<200 nm).

Důvodem pro tento posun ve velikostní distribuci směrem k menším částicím je zmenšování částic při jejich přechodu z vnějšího do vnitřního prostředí v zimním období a to za následujících předpokladů: není aktivní žádný vnitřní zdroj částic a možný odraz částic na patrech pro větší částice je minimalizován díky mazání impakčních fólií. Toto zmenšování částic nebylo zjištěno v průběhu letní kampaně a ani výsledky z AMS nebyly v tomto ohledu průkazné. Nicméně I/O poměr, získaný z SMPS měření, pro částice akumulačního módu v zimním období (0,56) dosáhl odlišné hodnoty od stejného poměru naměřeného v letním období (0,80). Bylo zjištěno, že díky relativně vysokým venkovním teplotám a nižší relativní vlhkosti v letním období byl venkovní aerosol suchý nebo téměř suchý před vstupem do vzorkovacích potrubí nebo vstupem do přístrojů umístěných ve vnitřním prostředí. Ve výsledku tak byly venkovní částice v letním období již ve venkovním prostředí v podobném stavu, jaký dosáhly částice v zimním období teprve při přechodu do vnitřního prostředí.

Na závěr Článku 3 (Article 3) byly vypočteny Spearmanovy korelační koeficienty a s nimi spojený P-test na datech vnitřních a vnějších hmotnostních koncentrací ze zimního období a meteorologických datech. Celá sada dat byla zpracována jako 24-hodinové průměry. Na základě statistické analýzy bylo zjištěno, že rychlost proudění vzduchu vykazovala korelaci s koncentracemi všech analyzovaných chemických sloučenin. Pomocí této analýzy byl také odhalen částečný vliv směru a rychlosti větru na poměr I/O.

Na základě nejistot v měření mezi různými přístroji odhalených v Článku 3 (Article 3), byl Článek 4 (Article 4) zaměřen na porovnání různých kaskádních impaktorů. V průběhu zimy 2014 v Praze a léta 2015 v Barceloně byly provedeny dvě porovnávací kampaně. Tyto kampaně byly zaměřeny na porovnání několika různých typů kaskádních impaktorů ve dvou různých prostředích s dobře definovaným typem aerosolu - kontinentální (v Praze) a přímořský (v Barceloně). V rámci kampaně byly použity 4 různé typy kaskádních impaktorů: (i) Sioutasův osobní kaskádní impaktor - Personal Cascade Impactor Sampler (PCIS; 250 nm - 10 µm), (ii) Bernerův nízkotlaký impaktor - Berner Low-Pressure Impactor (BLPI; 25nm -13.5µm), (iii) Bernerův nízkotlaký impaktor v úpravě pro měření nanočástic - nano-Berner Low-Pressure Impactor (nano-BLPI; 11nm-1.95µm) a (iv) impaktor pro měření nanočástic s rovnoměrnou depozicí vzorkovaného aerosolu - nano Micro-Orifice Uniform Deposit Impactor (nano-MOUDI; 10nm-10µm). V rámci porovnávací kampaně byl BLPI stanoven interním standardem, a to především díky jeho detailní znalosti a charakterizaci v rámci předchozích kalibračních měření. Z hlediska porovnání velikostního rozdělení hmotnostní koncentrace vykazoval nejlepší shodu s referenčním BLPI nano-BLPI impaktor a to nezávisle na ročním období (celkové hmotě aerosolu) a prostředí (chemickém složení aerosolu). Nano-MOUDI impaktor ukázal dobrou shodu s referenčním BLPI pro částice >320 nm. Naopak pro částice <320 nm byly hodnoty hmotnostních koncentrací ve venkovním prostředí naměřené nano-MOUDI impaktorem vyšší než hodnoty BLPI. Vysvětlení pro rozdíly v daném velikostním rozmezí jsou ne zcela dobře definovatelné, i když jedním z hlavních důvodů bude pravděpodobně disociace dusičnanu amonného.

Toto vysvětlení je velmi pravděpodobné zejména pro výsledky získané z měřicí kampaně v Praze, kde mohlo dojít ke zmenšování větších částic díky umístění nano-MOUDI impaktoru ve vnitřním, i když nevytápěném, prostředí. Mechanická rotující patra tohoto impaktoru a kovová schránka mohou způsobovat zahřívání celého impaktoru a tak podporovat případnou disociaci a vypařování. Dalším faktorem, který mohl způsobovat zmenšování částic v nano-MOUDI impaktoru jsou ztráty díky rozptylování vzorku na celou plochu impakčního substrátu, což následně zvyšuje možné interakce. Také ztráty z Teflonových filtrů (použitých v nano-MOUDI) mohou být významnější než z polykarbonátových filtrů, které byly použité v ostatních impaktorech. Předchozí výzkumné práce odhalily významný nárůst rychlosti disociace v případech, kdy teplota vzorkovaného vzduchu byla nejméně o 5°C vyšší než teplota filtru (Hering & Cass, 1999). I přesto, že není možné učinit zcela nezpochybnitelné závěry ohledně odlišného chování jednotlivých impaktorů, je zcela jasné, že dusičnany hrají klíčovou úlohu v případných odlišnostech v měření těchto impaktorů. Tato fakta zdůrazňují důležitost této disertační práce z hlediska většího porozumění vlivu chování dusičnanu amonného na jednotlivé přístroje, sběr dat a dynamické chování aerosolových částic při jejich přechodu z vnějšího do vnitřního prostředí.

Závěrem nelze nezmínit měřicí kampaň uskutečněnou ve stanici pražského metra za reálných podmínek. Měření probíhalo po 24 hodin během provozu metra. Měření zahrnovalo umístění rozsáhlé sady měřících online a offline přístrojů ve velmi hustě zalidněném vnitřním prostředí. Mechanicky uvolněné částice z kolejnic, brzd a dalších součástí vozů metra tvořily největší příspěvek k celkové hmotě aerosolu. Nicméně, sekundární organické aerosoly tvořily nezanedbatelnou složku naměřeného aerosolu, přičemž tento aerosol pocházel z vnějšího prostředí. Tato zjištění dokládají důležitost a význam vlivu dynamického chování aerosolových částic na lidské zdraví při každodenní expozici v dopravním prostředku.

Abstract

Due to its prevalence over large, densely populated areas, ammonium nitrate is an important chemical species in aerosol research. However, due to its volatility at ambient temperatures and over low temperature gradients, ammonium nitrate can be a difficult species to accurately measure. The volatility of ammonium nitrate is known to be dependent on temperature, relative humidity, the internal mixing state of the particle, and availability of the precursor gas constituents. The particle's physical state affects the equilibrium constant value of the ammonium nitrate - nitric acid / ammonia exchange and helps determine the dissociation rate. For indoor aerosol research, the outdoor originating aerosol particles' exposure to the new physical conditions indoors, such as changes in temperature, humidity, and particle-surface reactions within the microenvironment all accelerate ammonium nitrate dissociation. This increased rate of partitioning can generate artifacts on datasets, increase indoor particle formation, and accelerate the corrosion of cultural antiquities through acidification. The magnitude of these impacts is uncertain due to the current lack of knowledge on particle transformation processes when outdoor originating particles migrate indoors. To address this gap in knowledge, this thesis describes 5 experiments, each carefully designed to help answer specific questions regarding particle transformations, with attention to ammonium nitrate behaviour, explicitly, but not exclusively, in regards to indoor environments.

To commence, it was necessary to establish a broad understanding of the fundamental behaviour of ammonium nitrate in a 'pure' environment. To this end, laboratory controlled experiments were carried out, and are described in Article 1. These experiments allowed for the observation of the shrinking / dissociation rates of a non-internally mixed ammonium nitrate (NH_4NO_3) - nitric acid (NHO_3) / ammonia (NH_3) exchange in a closed system. From a chosen size specific monodisperse NH_4NO_3 aerosol, results showed the 200nm particles shrank quicker than the 50/100nm particles when transported through the 2m long, laminar flow, temperature controlled reactor. Longer residence times and higher temperatures within the reactor accelerated this shrinking process. However, when dissociation rates were calculated using integrated mass measurements, the results were reversed. The smaller particles were found to lose mass faster than the larger particles. This indicated that, despite efforts to make sure the ammonium nitrate aerosol were dry, crystalline particles, it was considered likely that the particle wasn't completely dried, with further dehydration occurring as it travelled through the reactor.

To test the results of Article 1 in real-world conditions, an intensive field experiment was carried out during the summer of 2014, with the results reported in Article 2. The experimental objectives were to identify changes in particle composition between indoor and outdoor environments, under typical ambient conditions, and with a high temporal resolution. To help achieve this, a switching system was utilized to alternate between the indoor and outdoor environments, allowing almost real-time analysis of particle dynamics with online, high time-resolution instrumentation. The focus was intended to be on the indoor environment during this experiment. However, the high resolution data afforded by the instrumentation also allowed for detailed observations of a diurnal fluctuation in NH_4NO_3 – HNO_3/NH_3 concentrations outdoors. This was found to be directly influenced by temperature, solar radiation and changes in boundary layer height.

During the same campaign, a new particle formation event outdoors enabled the rapid increase of outdoor to indoor migrating particles to be observed for particles less than 100 nm. This was then used to identify real-time I/O ratios, which were calculated by considering size, time and particle concentration dynamics. The I/O ratio obtained for this event was then set against an overall averaged I/O ratio calculated via particle number concentrations from scanning mobility particle sizer (SMPS) data, with a mobility diameter of <0.71µm. A reduction in NO_3^- mass concentrations from the outdoors to indoor environment was expected and observed. Moreover, compositional analysis carried out with aerosol mass spectrometer (AMS) measurements observed indoor chemical composition to be proportionally equivalent to that outdoors. This was explained by the similarity in temperatures indoors during daytime, reducing concentrations of ammonium nitrate before they entered indoors. These findings were supported by filter measurements taken from off-line Berner Low-Pressure Impactors which were also deployed indoors and outdoors.

Due to the volatile behaviour of NH_4NO_3, a seasonal comparative experiment was undertaken during winter 2014-15, with the methodology consistent with the previous campaign. The results, described in Article 3, showed non-refractory (NR) - organics and NO_3^- had similar mean outdoor concentrations, with a marked increase in winter NO_3^- concentrations compared to summer. Seasonal changes in chemical composition were calculated from AMS mass concentrations, and a 33-37% decrease in I/O ratio was observed from summer to winter. The similarity in proportional loss of mass of all species presented evidence of physical rather than chemical processes. BLPI results confirmed these findings by revealing more mass indoors than outdoors on the ultrafine stages for both SO_4^2 and NH_4^+. With no emission sources indoors, and particle bounce discounted due to greasing of the capture substrates, it was concluded that the particles were shrinking when penetrating indoors, and were therefore being counted in the ultrafine mode during the winter. This shrinking was not observed during the summer, nor was it as prominent on AMS measurements. However, the winter accumulation mode, obtained by SMPS measurements, showed an I/O ratio (. 56) that was anomalous to those of summer (. 80). It was determined that, due to higher ambient temperatures and lower relative humidity during summer, the aerosol outdoors were dry or mainly dry before entering the sampling room or the sampling inlet. In effect, during summer, the outdoor aerosols were in conditions comparable to the indoor aerosol during the winter.

Statistical tests, including Spearman Rank correlation and P-tests were carried out using winter, indoor and outdoor chemical mass concentrations, which were then set against meteorological conditions averaged over 24 hours. Wind speed was found to be well correlated with concentrations of all species. Further analysis revealed a small influence of wind direction and speed on I/O relationships. It was concluded that the increased loss of mass indoors during winter was attributed to concentrations of chemical species outdoors, the increased temperature gradient between indoors and outdoors and higher mean wind speed during the winter season.

With uncertainties between different instruments highlighted in Article 3, instrument behaviour was the focus of research detailed in Article 4. Two field campaigns were carried out during winter 2014 in Prague and summer 2015 in Barcelona to compare the response of several types of cascade impactors in two different and well-characterised aerosol airmass types, namely continental (Prague) and marine (Barcelona). The types of impactors used were: (i) Personal cascade impactor Sioutas (PCIS; 250 nm - 10 µm), (ii) Berner low-pressure impactor (BLPI; 25nm -13.5µm), (iii) nano-

Berner low-pressure impactor (nano-BLPI; 11nm-1.95µm) and (iv) nano micro-orifice uniform deposit impactor (nano-MOUDI; 10nm-10µm).

Taking the well characterised BLPI as an internal reference, the best agreement regarding mass size distributions was obtained with the nano-BLPI, independently of season (aerosol load) and location (aerosol chemical composition). The nano-MOUDI showed good agreement for particle sizes >320 nm, whereas, for particle diameters <320 nm this instrument recorded larger mass concentrations outdoors than the BLPI. The reason for the observed differences in these size ranges are inconclusive, yet dissociation processes of ammonium nitrate are suspected as being influential. This is especially true from the Prague results, during which, the shrinking of larger particles could have occurred due to the nano-MOUDI being located indoors, although in an unheated shed. The mechanics (rotating stages) and the metal housing of the stages may also have caused warming, and, therefore, encouraged dissociation and evaporation processes to occur. Another factor that may have reduced particle sizes within the nano-MOUDI were losses due to the spreading of the sample over the filter substrate, which increased interaction. Losses off the Teflon filter substrate may have been more significant than from the polycarbonate substrate used for the other impactors. Prior research found a significant increase in dissociation rates, especially when the sampled air temperature was >5 degrees Celsius more than the filter (Hering & Cass, 1999). Even though no absolute conclusions can be drawn for the reasons behind the different behaviours of different impactors, it is clear that nitrate plays a key part in the performance of these instruments. This highlights, once more, the importance of this work in establishing a greater understanding of ammonium nitrate on instrumentation, data collection and indoor and outdoor particle dynamics.

Finally, an experiment set in a real-world situation was undertaken in Prague metro over a period of 24 hours, with data collection carried out whilst the transportation hub was open. This placed the use of a suite of online and offline instrumentation together, in a heavily populated indoor setting. Mechanically formed particles from tracks, brakes and cables accounted for the majority of aerosol mass. However, there was also a significant presence of secondary inorganics that had migrated into the metro from street level. These findings demonstrate the importance and relevance of aerosol dynamics to human exposure in every day settings.

1. Atmospheric Aerosols

1.1. Atmospheric aerosols: an overview

Aerosols, tiny particles suspended in air, are everywhere, from the Polar Regions to the Tropics, aerosol partciles are found, and have always been since the moment of Earth's creation. In fact we owe our existence to aerosol particles. Without aerosols, there would be no clouds, no fresh water, the earth would be a lot hotter and life would be impossible. Aerosol particles are consistently emitted from natural sources, including dust storms, volcanic eruptions, biomass fires, vegetation and sea spray, from which sea salt is released into the atmosphere. More recently, human activity has contributed to the total aerosol loading through the modification of natural surface cover, release of industrial pollutants and the burning of fossil fuels resulting in direct and indirect harmful effects to ourselves and the biosphere. It is at this point when particles become a pollutant.

In more recent times, awareness of air pollution has increased due to media coverage. No longer is the awareness of 'air pollution' purely the domain of the scientist or academics. Whether it is the Los Angeles' photochemical smog's of the 1980's, the Asian brown cloud, or metropolitan India's worsening air quality, numbers are presented, chocked brown skies photographed, and physiological and social consequences reported upon. Yet as population's wealth increases, so does the need and desire for transportation, power, engineered materials, good and services. It seems that a lowering of air quality is a cost we pay for socio-economic progress.

'Stay indoors' is the normal response to days when meteorological conditions fail to disperse the worst of our emissions, yet as populations spend ever increasing amounts of time indoors so the proportional exposure to indoor aerosols increases. There appears to be little perception of poor air quality indoors, i.e. there are usually no brown clouds or toxic smells. This results in less awareness of the risks, amplifying the health threat. Indoor micro-environments are usually sealed to enhance warmth and comfort, yet this may trap outdoor pollutants indoors, physically transform particles, or generate new particles. It is this inward migration of outdoor particulate and the transformations to the particles during and after transportation from outdoors to indoors that defines the primary motivation for this thesis.

It is understood that some chemical species are volatile under what are considered normal atmospheric conditions which can result in changes to the physico-chemical properties of the particle. These changes can occur outdoors according to the time of the day, usually, but not exclusively, due to meteorology and season. The outdoor aerosol then directly affects indoor aerosol dynamics. However, within the new environment, aerosol particles meet the new conditions that can then further enhance physico-chemical transformations. These changes create uncertainties within datasets, reduce comfort, can be physiologically harmful to humans and can increase the rate of degradation of antiquities. It is within the context of these uncertainties and concerns that the results within this document, will add to a greater understanding of the dynamic nature of indoor aerosols.

1.2. Definitions and classifications of aerosol particles

An aerosol can be defined as a liquid or solid particle suspended in a gas (Seinfeld & Pandis, 2012). Particle diameters typically range from 10^{-9}–10^{-4} m, with the lower limit related to molecules and molecular clusters and the upper limit, is defined by fast sedimentation. The most evident example of aerosols in the atmosphere are clouds, which mostly consist of condensed water with droplet diameter of approximately 2 mm, however they are formed around a particle nucleus an estimated 10^{th} of the size. In atmospheric science and throughout this thesis, the term aerosol particles refer to suspended particles that contain a large proportion of condensed matter other than water.

1.3. Aerosol origin

Atmospheric aerosol particles can be attributed to either natural or anthropogenic sources. The majority of aerosol particles are released from natural sources, with an combined estimated mass flux of ~12,100 Tg y^{-1}, compared to anthropogenic emissions, which has an estimated emission flux of ~300 Tg y^{-1} (Chin, 2009). These figures are not reliable when considering locally polluted environments such as cities when anthropogenic sources will be more prevalent. All major sources are displayed in Figure 1-1 along with typical sizes. Aerosol particles of natural origin are dominated by windborne crustal material, mostly from arid lands, and marine aerosols, released by the frictional action of wind, creating waves which release aerosol or gas precursors through bubbles bursting on the sea surface (Andreae & Rosenfeld 2008). Other contributing natural sources include volcanic emissions (dust and sulfates from volcanic SO_2), naturally occurring biomass burning (such as wild forest fires), biogenic emissions such as spores, pollens and sulfates from biogenic gases and other organic matter (Kulkarni and Baron 2011). Anthropogenic sources of aerosols are dominated by combustion emissions from vehicles in urban areas, other contributing factors include cement manufacturing, metallurgy, energy, agricultural and fertiliser manufacturing activities. A further important addition to anthropogenic origin particulate is via chemical reactions from gases released by human activities, these are mostly from SO_2, NO_x and volatile organic compounds (VOCs) which are emitted from industrial and combustion processes.

1.4. Aerosol shape and size

The research described within this thesis will often refer to particle size distributions, a typical starting point for analysis of air quality. Atmospheric particles are often described as having a diameter, and this diameter used as a tool to garner knowledge about aerosol composition. This implies, often incorrectly, that aerosol particles are spherical. Atmospheric particles are composed of a wide variety of shapes of which geometrical diameters are rarely meaningful. Some means of expressing the size of such particles is necessary, as important properties

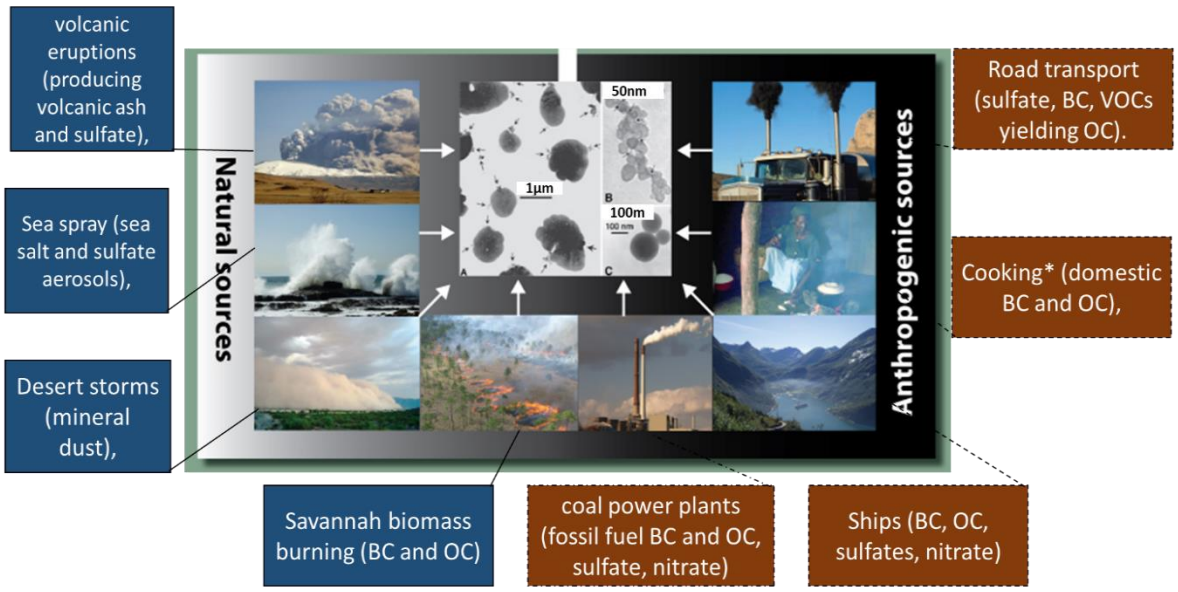

Figure 1-1 Natural and anthropogenic sources of aerosol particles with typical size shown as inset (Pósfai et al., 1999).

To compensate for these irregularly shaped aerosol an equivalent diameter is introduced. This depends on a physical, rather than a geometrical, property. An equivalent diameter is defined as the diameter of the sphere that would have the same value of a particular physical property as that of the irregular particle (Hinds, 2012). Figure 1.2 presents a demonstration of 4 different types of carbonaceous material under an electron microscope. The differences between just this one species as well as the differences in the surface area of each particle is clear to see.

It is important to note that various types of aerosol instrumentation report different measures of particle diameter depending on the employed methodology and application. For example, a scanning mobility particle sizer (SMPS) will use the electrical mobility of a particle, whilst an impactor or the aerosol mass spectrometer (AMS) will measure a particle's aerodynamic properties. A universal measure of aerosol particle size does not exist and, as a result, the sizing definition will be specified for particle diameters reported in this thesis.

1.5. Catergorisation of aerosol sizes

Atmospheric aerosols are most typically categorised according to their size. As previously mentioned particle sizes range through several orders of magnitude and can often be linked to its formation mechanism and composition (Vu et al., 2015). The specific ranges of particle sizes are called modes, which include the nucleation mode (<20 nm), the Aitken mode (20-100 nm), the accumulation mode (100 nm – 1 µm) and the coarse mode (1-10 µm) (Zhu et al., 2005). Particles can also be sub-classified as nanoparticles (<50 nm), ultrafine (<100 nm) and fine modes (<1 µm) (Figure 1-3).

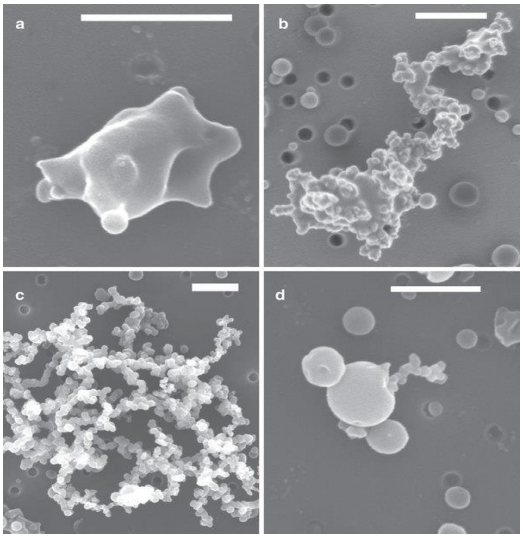

Figure 1-2 Electron microscope images of four different categories of carbonaceous particle, with prevalence in research presented by China et al. (2013): (**a**) embedded, (50%) (**b**) partly coated, (34%) (**c**) bare (12%) and (**d**) with inclusions (4%) 500nm size is defined.

The *nucleation mode* incorporates all particles below 20 nm in diameter. Particles in this mode are associated with the formation of new particles through precursor gaseous emissions and are therefore called secondary particles. These gaseous precursors include H_2SO_4, NH_3 and VOCs (Kulmala & Kerminen, 2008). Nucleation mode particles can also be emitted directly by combustion from exhaust emissions as primary particles. Several nucleation mechanisms have been proposed (Salma et al, 2011), however, particles in the atmosphere can scavenge the gaseous precursors necessary for nucleation through condensation processes and, thus, clean air conditions are often more favourable for new particle formation processes. Because of this, meteorology can play a vital role in new particle formation. Rain events (wet deposition) serve to remove aerosol from the lower atmosphere whilst solar radiation increases photochemistry. Photochemistry plays a pivotal role in new particle formation through the generation of free radicals in the atmosphere. These react with gaseous precursors to produce the vapours necessary for nucleation (O'Dowd & de Leeuw, 2007). Following the formation of stabilised clusters through nucleation of the gaseous precursors mentioned (<1 nm), organic vapours are believed to activate these clusters and cause the fresh particles to grow in size (Kulmala et al., 2013).

Nucleation has been observed in almost all types of environments, including Polar (Wiedensohler et al., 1996), high altitude (Venzac et al., 2009), boreal forests (Kulmala et al. 1998), remote areas (Birmili et al., 2001) and urban environments Pey et al. (2009); Dall'Osto et al. (2013), and many others. In urban environments, traffic emissions contribute significantly to nucleation processes through emissions of precursor gases necessary for nucleation, while also emitting primary particles with a typical size distribution in the nucleation mode (Harris & Maricq, 2001). The residence time of these particles are typically short as they grow rapidly through condensation and coagulation processes (Zhang et al. 2004). In rural and remote regions, nucleation episodes are typically favoured under clean air conditions, as nucleation and the condensation of gaseous precursors on pre-existing particles are

competing processes (Birmili et al, 2001; Rodríguez et al. 2005). However, nucleation still occurs under polluted atmospheric conditions provided the growth rate of the nucleating particles is sufficiently quick to avoid being scavenged by pre-existing particles (Hamed et al., 2006). Nucleation mode particles are typically removed from the atmosphere through condensation and coagulation processes, causing the particles to grow into Aitken and accumulation modes. Coagulation is produced by Brownian motion and diffusion and is the most common removal process for nanoparticles (Mészáros, 1999). The rate of coagulation is relative to the concentration of particles in the atmosphere, as a higher number of particles increases the probability of interaction.

The Aitken mode refers to all particles of a diameter between 20 and 100nm. Particles in this mode result from primary emissions and coagulation between pre-existing particles that are usually from the nucleation mode (Dall'Osto et al., 2013). In the urban environment, this mode is especially prevalent owing to primary emissions from traffic, such as black carbon from the incomplete combustion of fuels associated with diesel engines (Morawska et al. 1999).

The accumulation mode includes all fine particles between 100 nm and 1 μm. This mode is associated with particles resulting from processes of coagulation. These particles may act as condensation nuclei whereby low vapour gaseous species such as H_2SO_4, NH_3, HNO_3 and non-methane VOCs can condense on the existing particle surface (Rose et al., 2006). The adsorption or condensation of gas phase components and the coagulation of smaller particles to form accumulation mode particles acts to reduce particle number concentrations, but conversely, increases particle mass concentrations. The accumulation mode is so named because particle removal mechanisms are least efficient in this regime, and thus, have a longer residence time in the atmosphere than the lower size modes (Seinfeld & Pandis, 2012). They can be transported over longer distances, are usually

considered regional, and are often significant when considering pollution transportation from urban to rural locations.

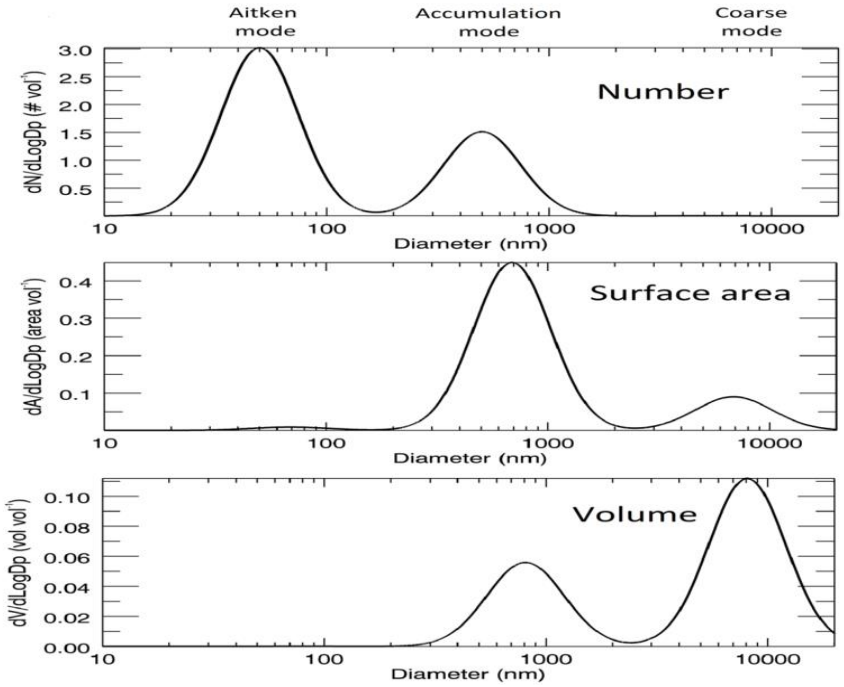

Figure 1-3 Size distributions of particle numbers (a), surface areas (b), and volumes / mass (c) (taken from Turner and Colbeck (1994).

Coarse particles are those of diameter greater than 1 µm. Air quality studies normally refer to mass concentrations of particulate matter with aerodynamic diameters less than 1 µm, 2.5 µm and 10 µm as PM_1, $PM_{2.5}$ and PM_{10}, respectively. Coarse particles are mostly primary and are generated from mechanical processes such as re-suspended mineral dust, marine aerosol, products from tyre and brake abrasion, and biogenic emissions. However, coarse secondary particles can occur when gases chemically react with particles of marine or crustal origin (Querol et al., 2009). Whereas coarse particles are typically primary and result from mechanical processes, the fine fraction (< 1µm) is dominated by secondary species (NO_3^-, SO_4^{2-} and NH_4^+ ions) and emissions from combustion processes (carbonaceous material) (Seinfeld & Pandis, 2012) and/or the condensation of semi-volatile compounds on the surface of these particles (Seinfeld & Pandis, 2012). Aerosol particle origins will be discussed in detail during chapter 3 in this thesis

1.6. Residence time of aerosols

Residence time can be defined as a metric of the time a particle remains in an airborne state and is closely aligned with its evolution over this time period. Attempts to calculate aerosol residence times must consider the compositional properties and the physical forces acting upon the particle; with photolysis by solar radiation a prime example. Environmental factors, such as meteorology can significantly affect the residence time of aerosol, with variables such as relative humidity, temperature and pressure. The dynamic nature of these physical forces mean they can change during the

atmospheric transport of the aerosol, resulting in a constant flux in a particles expected residence time. Ahmed et al. (2004), reported a strong correlation between increased relative humidity and increased particle condensation and associated growth by coagulation. By this mechanism, the deposition velocity is increased and residence time is decreased.

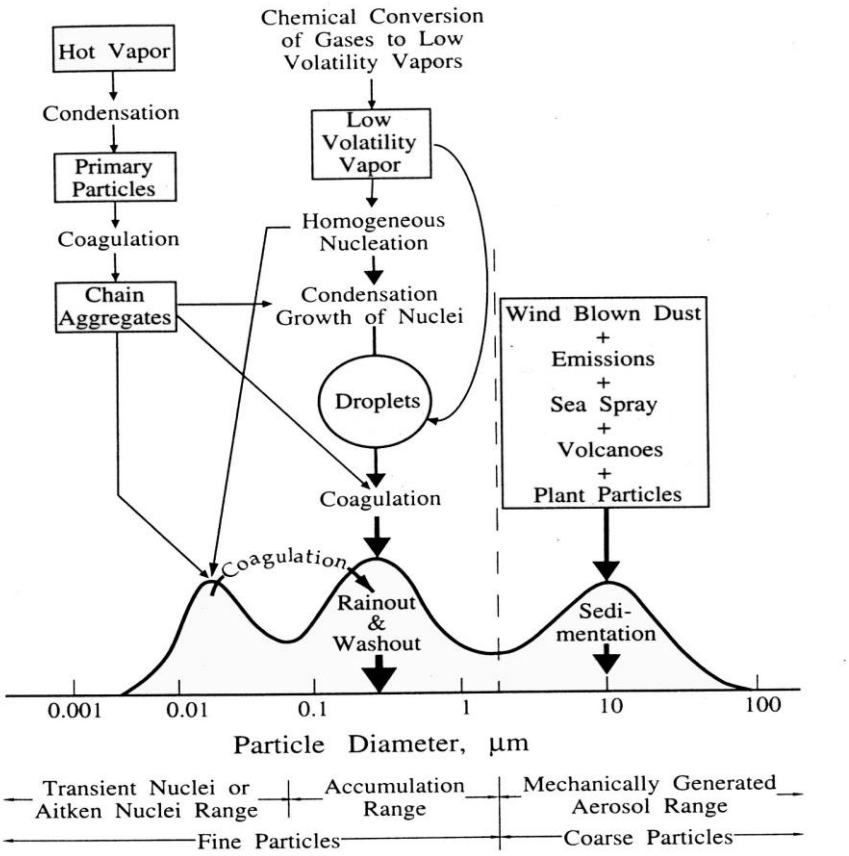

Figure 1-4 A simplified schematic of particle size with emission sources (Whitby et al, 1976).

Seasonal changes bring different meteorological conditions which can effect aerosol residence time. For example, lower temperatures and higher humidity in cooler season increasing particle deposition rates. Atmospheric composition and pressure also effect the residence time of aerosol (Georgii & Pankrath, 1982). A study carried out over the Pacific Ocean reported that the upper atmosphere aerosols of 65 nm in size have residence times of approximately 1 month and can be transported on a hemispheric scale, whilst in the boundary layer their lifetime is reduced by one order of magnitude (Williams et al. 2002). Clearly, residence time is a key factor to consider when attempting to understand the composition of our aerosol.

1.7. Meteorology and air pollution

Broadly, meteorology is the redistribution of heat from the tropics to the poles via a fluid dynamic system within the lower portion of the atmosphere. This is approximately 6 km at the poles and 16 km at the equator and is known as the troposphere. It is within this thin basis in which almost all life is housed. On local and regional scales, the weather is a major factor in influencing both the production

and fate of aerosol pollutants. Meteorological parameters, such as air temperature, humidity, rainfall, solar radiation, wind speed and wind direction, play an important role in the formation, transformation, transport, mixing, dispersion and dilution of aerosols and other air pollutants (Kulkarni and Baron 2011). These effects are expressed as spatial variations in concentrations, chemical composition, and particle size distribution (Seinfeld & Pandis, 2012). Meteorological conditions effect the accuracy of the predictions derived from mathematical models such as dispersion models (Kousa et al.,2002). It is therefore very important that meteorological data is recorded and reported alongside monitored or researched air quality data.

Diurnal variations observed in previous research (Kubelová et al., 2015; Long et al., 2014; Poulain et al., 2011) are usually attributed to changes in meteorology from night to day. For example, correlations have been identified between brown haze formation events and wintertime local and regional meteorology (Salmond et al., 2015). Additionally, wind speed has been anti-correlated with air pollution build-up (Longley et al., 2003), this is attributed to better mixing, and dilution (Hussein et al., 2005). There are often observed changes between summer and winter concentrations, with increases typically observed during summer. This has been related to semi volatile species evaporating/dissociating to vapour form at certain temperatures and relative humidity (Hering & Cass, 1999; Putaud et al., 2010).Mixing depth is increased under unstable meteorological conditions, which are usually associated with wind conditions.

Conversely, the mixing height is reduced under stable, high pressure conditions. Atmospheric stability is highest when temperature close to the ground cools quicker than the air above the ground. These conditions can last for long periods, and with such little mixing and dilution, levels of pollution can build quickly, causing considerable problems. This has been most notable over many major cities in more recent years (Zhao et al., 2013). However, due to certain sources and the movement of pollutants, air quality issues can effect far less dense populated areas. (Trompetter et al., 2010).

1.8. References

Ahmed, A., Mohamed, A, Ali, A Barakat, A., Abd El-Hady, M., & El-Hussein, A. (2004). Seasonal variations of aerosol residence time in the lower atmospheric boundary layer. *Journal of Environmental Radioactivity*, *77*(3), 275–283. http://doi.org/10.1016/j.jenvrad.2004.03.011

Andreae, M. O., & Rosenfeld, D. (2008). Aerosol–cloud–precipitation interactions. Part 1. The nature and sources of cloud-active aerosols. *Earth-Science Reviews*, *89*(1-2), 13–41. http://doi.org/10.1016/j.earscirev.2008.03.001

Birmili, W., Wiedensohler, A., Heintzenberg, J., & Lehmann, K. (2001). Atmospheric particle number size distribution in central Europe: Statistical relations to air masses and meteorology. *Journal of Geophysical Research: Atmospheres*, *106*(D23), 32005–32018. http://doi.org/10.1029/2000JD000220

Chin, M. (2009). *Atmospheric Aerosol Properties and Climate Impacts*. DIANE Publishing. Retrieved from https://books.google.com/books?id=IgJZXXgtHmQC&pgis=1

China, S., Mazzoleni, C., Gorkowski, K., Aiken, A. C., & Dubey, M. K. (2013). Morphology and mixing state of individual freshly emitted wildfire carbonaceous particles. *Nature Communications*, *4*, 2122. http://doi.org/10.1038/ncomms3122

Dall'Osto, M., Querol, X., Alastuey, A., O'Dowd, C., Harrison, R. M., Wenger, J., & Gómez-Moreno, F. J. (2013). On the spatial distribution and evolution of ultrafine particles in Barcelona. *Atmospheric Chemistry and*

Physics, *13*(2), 741–759. http://doi.org/10.5194/acp-13-741-2013

Georgii, H.-W., & Pankrath, J. (Eds.). (1982). *Deposition of Atmospheric Pollutants*. Dordrecht: Springer Netherlands. http://doi.org/10.1007/978-94-009-7864-5

Hamed, a., Joutsensaari, J., Mikkonen, S., Sogacheva, L., Dal Maso, M., Kulmala, M., … Laaksonen, a. (2006). Nucleation and growth of new particles in Po Valley, Italy. *Atmospheric Chemistry and Physics Discussions*, *6*(5), 9603–9653. http://doi.org/10.5194/acpd-6-9603-2006

Harris, S. J., & Maricq, M. M. (2001). Signature size distributions for diesel and gasoline engine exhaust particulate matter. *Journal of Aerosol Science*, *32*(6), 749–764. http://doi.org/10.1016/S0021-8502(00)00111-7

Hering, S., & Cass, G. (1999). The Magnitude of Bias in the Measurement of PM25 Arising from Volatilization of Particulate Nitrate from Teflon Filters. *Journal of the Air & Waste Management Association*, *49*(6), 725–733. http://doi.org/10.1080/10473289.1999.10463843

Hinds, W. C. (2012). *Aerosol Technology: Properties, Behavior, and Measurement of Airborne Particles*. John Wiley & Sons. Retrieved from https://books.google.com/books?hl=en&lr=&id=qIkyjPXfWK4C&pgis=1

Hussein, T., Hämeri, K., Heikkinen, M. S. A., & Kulmala, M. (2005). Indoor and outdoor particle size characterization at a family house in Espoo–Finland. *Atmospheric Environment*, *39*(20), 3697–3709. http://doi.org/10.1016/j.atmosenv.2005.03.011

Turner J and Colbeck I. (1994). Physical and Chemical Properties of Atmospheric Aerosols, *85*, 75–83.

Kousa, A., Kukkonen, J., & Karppinen, A. (2002). A model for evaluating the population exposure to ambient air pollution in an urban area. *Atmospheric …*. Retrieved from http://www.sciencedirect.com/science/article/pii/S1352231002002285

Kubelová, L., Vodička, P., Schwarz, J., Cusack, M., Makeš, O., Ondráček, J., & Ždímal, V. (2015). A study of summer and winter highly time-resolved submicron aerosol composition measured at a suburban site in Prague. *Atmospheric Environment*, *118*, 45–57. http://doi.org/10.1016/j.atmosenv.2015.07.030

Kulmala, M., & Kerminen, V.-M. (2008). On the formation and growth of atmospheric nanoparticles. *Atmospheric Research*, *90*(2-4), 132–150. http://doi.org/10.1016/j.atmosres.2008.01.005

Kulmala, M., Kontkanen, J., Junninen, H., Lehtipalo, K., Manninen, H. E., Nieminen, T., … Worsnop, D. R. (2013). Direct observations of atmospheric aerosol nucleation. *Science (New York, N.Y.)*, *339*(6122), 943–6. http://doi.org/10.1126/science.1227385

Kulmala, M., Toivonen, A., Makela, J. M., & Laaksonen, A. (1998). Analysis of the growth of nucleation mode particles observed in Boreal forest. *Tellus B*, *50*(5), 449–462. http://doi.org/10.1034/j.1600-0889.1998.t01-4-00004.x

Long, S., Zeng, J., Li, Y., Bao, L., Cao, L., Liu, K., … Zhao, Y. (2014). Characteristics of secondary inorganic aerosol and sulfate species in size-fractionated aerosol particles in Shanghai. *Journal of Environmental Sciences (China)*, *26*(5), 1040–51. http://doi.org/10.1016/S1001-0742(13)60521-5

Longley, I. D., Gallagher, M. W., Dorsey, J. R., Flynn, M., Allan, J. D., Alfarra, M. R., & Inglis, D. (2003). A case study of aerosol (4.6nm<Dp<10µm) number and mass size distribution measurements in a busy street canyon in Manchester, UK. *Atmospheric Environment*, *37*(12), 1563–1571. http://doi.org/10.1016/S1352-2310(03)00010-4

Mészáros:, E. (n.d.). Fundamentals of Atmospheric Aerosol Chemistry. *Journal of Atmospheric Chemistry*, *39*(1), 99–103. http://doi.org/10.1023/A:1010753724116

Morawska, L., Thomas, S., Jamriska, M., & Johnson, G. (1999). The modality of particle size distributions of environmental aerosols. *Atmospheric Environment*, *33*(27), 4401–4411. http://doi.org/10.1016/S1352-2310(99)00217-4

O'Dowd, C. D., & de Leeuw, G. (2007). Marine aerosol production: a review of the current knowledge. *Philosophical Transactions. Series A, Mathematical, Physical, and Engineering Sciences*, *365*(1856), 1753–

1774. http://doi.org/10.1098/rsta.2007.2043

Pey, J., Querol, X., Alastuey, A., Rodr??guez, S., Putaud, J. P., & Van Dingenen, R. (2009). Source apportionment of urban fine and ultra-fine particle number concentration in a Western Mediterranean city. *Atmospheric Environment*, *43*(29), 4407–4415. http://doi.org/10.1016/j.atmosenv.2009.05.024

Pósfai, M., Anderson, J. R., Buseck, P. R., & Sievering, H. (1999). Soot and sulfate aerosol particles in the remote marine troposphere. *Journal of Geophysical Research: Atmospheres*, *104*(D17), 21685–21693. http://doi.org/10.1029/1999JD900208

Poulain, L., Spindler, G., Birmili, W., Plass-Dülmer, C., Wiedensohler, A., & Herrmann, H. (2011). Seasonal and diurnal variations of particulate nitrate and organic matter at the IfT research station Melpitz. *Atmospheric Chemistry and Physics*, *11*(24), 12579–12599. http://doi.org/10.5194/acp-11-12579-2011

Kulkarni, P A. Baron, K. W. (2011). *Aerosol Measurement: Principles, Techniques, and Applications*. John Wiley & Sons. Retrieved from https://books.google.com/books?id=ETvXooNW4-EC&pgis=1

Putaud, J.-P., Van Dingenen, R., Alastuey, A., Bauer, H., Birmili, W., Cyrys, J., … Raes, F. (2010). A European aerosol phenomenology – 3: Physical and chemical characteristics of particulate matter from 60 rural, urban, and kerbside sites across Europe. *Atmospheric Environment*, *44*(10), 1308–1320. http://doi.org/10.1016/j.atmosenv.2009.12.011

Querol, X., Alastuey, a., Pey, J., Cusack, M., Pérez, N., Mihalopoulos, N., … Koçak, M. (2009). Variability in regional background aerosols within the Mediterranean. *Atmospheric Chemistry and Physics Discussions*, *9*(2), 10153–10192. http://doi.org/10.5194/acpd-9-10153-2009

Rodríguez, S., Van Dingenen, R., Putaud, J. P., Martins-Dos Santos, S., & Roselli, D. (2005). Nucleation and growth of new particles in the rural atmosphere of Northern Italy - Relationship to air quality monitoring. *Atmospheric Environment*, *39*(36), 6734–6746. http://doi.org/10.1016/j.atmosenv.2005.07.036

Rose, D., Wehner, B., Ketzel, M., Engler, C., Voigtländer, J., Tuch, T., & Wiedensohler, A. (2006). Atmospheric number size distributions of soot particles and estimation of emission factors. *Atmospheric Chemistry and Physics*, *5*, 10125–10154. http://doi.org/10.5194/acpd-5-10125-2005

Salma, I., Borsòs, T., Weidinger, T., Aalto, P., Hussein, T., Dal Maso, M., & Kulmala, M. (2011). Production, growth and properties of ultrafine atmospheric aerosol particles in an urban environment. *Atmospheric Chemistry and Physics*, *11*(3), 1339–1353. http://doi.org/10.5194/acp-11-1339-2011

Salmond, J. A., Dirks, K. N., Fiddes, S., Pezza, A., Talbot, N., Scarfe, J., … Petersen, J. (2015). A climatological analysis of the incidence of brown haze in Auckland, New Zealand. *International Journal of Climatology*, n/a–n/a. http://doi.org/10.1002/joc.4509

Seinfeld, J., & Pandis, S. (2012). *Atmospheric chemistry and physics: from air pollution to climate change*. Retrieved from http://www.google.com/books?hl=en&lr=&id=YH2K9eWsZOcC&oi=fnd&pg=PA1991&dq=seinfeld+and+pandis&ots=hK3xLmaXHx&sig=YBgCj_Ct7vI-a5Aso7JIigN3958

Trompetter, W. J., Davy, P. K., & Markwitz, A. (2010). Influence of environmental conditions on carbonaceous particle concentrations within New Zealand. *Journal of Aerosol Science*, *41*(1), 134–142. http://doi.org/10.1016/j.jaerosci.2009.11.003

Venzac, H., Sellegri, K., Villani, P., Picard, D., & Laj, P. (2009). Seasonal variation of aerosol size distributions in the free troposphere and residual layer at the puy de Dôme station, France. *Atmospheric Chemistry and Physics*, *9*(4), 1465–1478. http://doi.org/10.5194/acp-9-1465-2009

Vu, T. V., Delgado-Saborit, J. M., & Harrison, R. M. (2015). Review: Particle Number size distributions from seven major sources and implications for source apportionment studies. *Atmospheric Environment*, *122*, 114–132. http://doi.org/10.1016/j.atmosenv.2015.09.027

Whitby, K. T., Kittelson, D. B., Cantrell, B. K., Barsic, N. J., & Bolan, D. F. (1976). Aerosol size distributions and concentrations measured during the General Motors proving grounds sulfate study. In *American Chem. Soc*. Retrieved from http://experts.umn.edu/en/publications/aerosol-size-distributions-and-concentrations-measured-during-the-general-motors-proving-grounds-sulfate-study(e79f0dca-92f6-

4f30-99d7-cf6fe9975d34).html

Wiedensohler, A., Covert, D. S., Swietlicki, E., Aalto, P., Heintzenberg, J., & Leck, C. (1996). Occurrence of an ultrafine particle mode less than 20 nm in diameter in the marine boundary layer during Arctic summer and autumn. *Tellus, Series B: Chemical and Physical Meteorology*. http://doi.org/10.1034/j.1600-0889.1996.t01-1-00006.x

Williams, J., de Reus, M., Krejci, R., Fischer, H., & Ström, J. (2002). Application of the variability-size relationship to atmospheric aerosol studies: estimating aerosol lifetimes and ages. *Atmospheric Chemistry and Physics Discussions*, *2*(1), 43–74. http://doi.org/10.5194/acpd-2-43-2002

Zhang, K. M., Wexler, A. S., Zhu, Y. F., Hinds, W. C., & Sioutas, C. (2004). Evolution of particle number distribution near roadways. Part II: the "Road-to-Ambient" process. *Atmospheric Environment*, *38*(38), 6655–6665. http://doi.org/10.1016/j.atmosenv.2004.06.044

Zhao, X. J., Zhao, P. S., Xu, J., Meng, W., Pu, W. W., Dong, F., … Shi, Q. F. (2013). Analysis of a winter regional haze event and its formation mechanism in the North China Plain. *Atmospheric Chemistry and Physics*, *13*(11), 5685–5696. http://doi.org/10.5194/acp-13-5685-2013

Zhu, Y., Hinds, W. C., Krudysz, M., Kuhn, T., Froines, J., & Sioutas, C. (2005). Penetration of freeway ultrafine particles into indoor environments. *Journal of Aerosol Science*, *36*(3), 303–322. http://doi.org/10.1016/j.jaerosci.2004.09.007

2. Implications of Atmospheric Aerosols

2.1. Atmospheric aerosols and health

Epidemiological studies have linked exposure to fine and ultrafine particulate air pollution to acute and chronic health effects, such as the exacerbations of respiratory and cardiovascular disease (Dockery et al., 1993; Pope et al., 2014; Schwartz et al., 1996). Worldwide, it has been estimated that air pollution kills 7 million people annually, accounting for 1 in 8 of all deaths, and represents up to 8% of lung cancer deaths, 5% of cardiopulmonary deaths and 3% of respiratory infection deaths (Worlds Health Organization, 2014). Figure 2-1 shows averaged premature death rates (given in months) from World Health Organisation (WHO) global health risks (Worlds Health Organization, 2014).

As one would expect, inhalation is the most common form of exposure to airborne pollutants. The effects of inhalation are found to be dependent on the concentration, size, shape and composition of the particles, and length of exposure (Oberdörster, 2001). Short-term exposure to fine particles has been associated with adverse respiratory and cardiovascular health effects (Figure 2-1), including premature mortality (Pope et al., 2014). Considering the complex composition of particles, it is inherently difficult to identify with any great surety which components are culpable for the adverse health effects (Dockery et al., 1993). The non-uniform nature of air quality risks is highlighted in Figure 2-1. The loss in statistical life expectancy that can be attributed to anthropogenic contributions to particulate matter $PM_{2.5}$ is shown. It should be noted that pollutants cross international borders, and countries with heavy industry may find that their emissions greatly effect a neighbouring country or county's population (EEA, 2014).

A standard metric for assessing air quality is to refer to mass measurements of particulate matter. However, as stated in the previous section, mass is dominated by larger particles which do not penetrate as deeply into the lung system (Figure 2-2). Ultrafine particles contribute little to PM mass but can contribute up to 90% to the particle number concentration when major sources, such as busy roads, are close by (Zhu et al., 2005). Due to their small size and larger surface areas, these tiny particles are understood to pose the greatest danger. Figure 2-2 shows that a particle's ability to penetrate deeper into the respiratory system, enter the circulatory system stream and deposit in the brain, is size dependent (Oberdörster, 2001).

As already discussed, ultrafine particles are often associated with freshly released traffic emissions. These emissions sources release poorly combusted carbonaceous materials, which are often conglomerates, and, therefore, have a very large surface area to size ratio. These emissions can also contain organics and metals. Together, these aerosols are believed to increase the risk of diseases; with a recent report linked 7500 premature deaths to car exhaust emissions in the UK alone (Yim & Barrett, 2012).

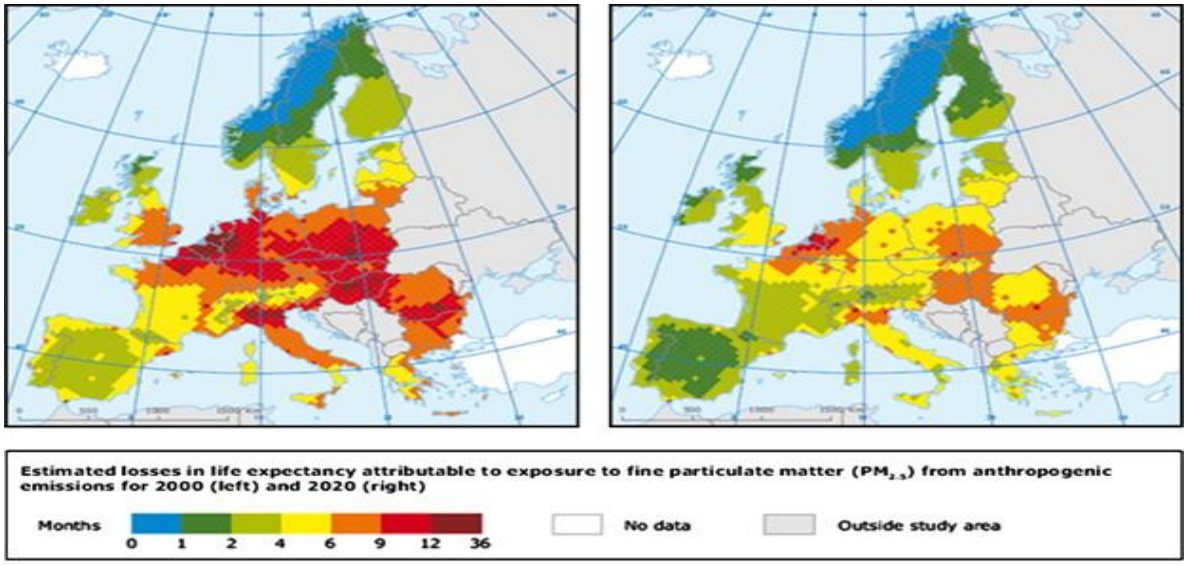

Figure 2-1 Health impact of PM mass concentrations (μg m^{-3}). Loss in statistical life expectancy (months) that can be attributed to anthropogenic contributions to $PM_{2.5}$ for the year 2000 (left) and 2020 (right) taken from Monks et al. (2009).

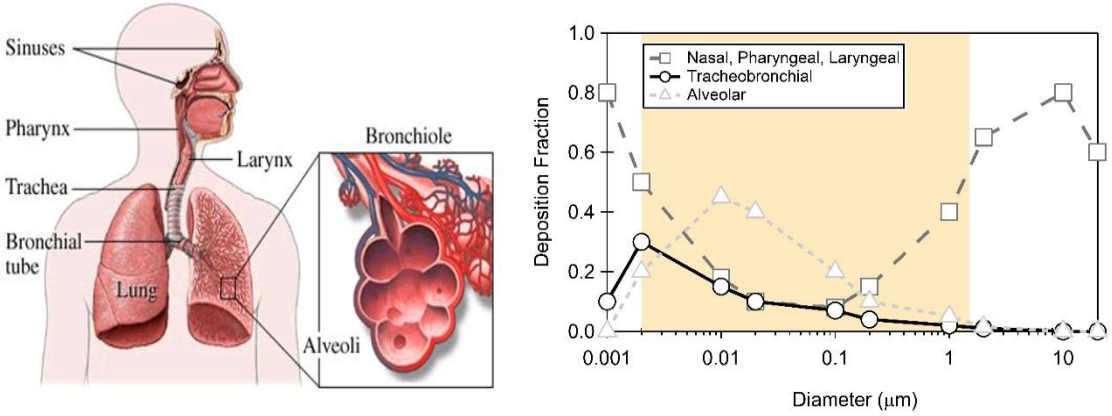

Figure 2-2 Particulate matter penetration into the human respiratory system**.** Based on their size, particles can penetrate into different parts of the human respiratory system (World Health Organization 2014).

2.2. Aerosol particles and climate

Aerosols have a complex role in our climate and have both direct and indirect effects. The direct effects are based on the aerosol particles themselves and governed by the ability of the particulate matter to absorb or scatter sunlight back into space. Solar radiation heats the atmosphere and Earth's surface, which in turn drives the planet's climate. However, aerosol particles, and the clouds that they help form, scatter about 25% of the sun's radiation back into space (Ramanathan et al., 1989). Because less of the sun's radiation reaches the ground, there is a net cooling effect. Due to the diverse properties of aerosols, their effects creates the greatest uncertainties in climate models (Carslaw et al., 2013), as shown in Figure 2-3 by the black error bars. In terms of indirect effects, cloud droplets are formed when water condenses on an existing aerosol, which are called cloud condensation nuclei (CCN) (Dusek et al., 2006). The increase in concentration of CCN reduces the supersaturation needed to form water droplets and, hence, clouds. The ability of a particle to act as a nucleus for water

droplet formation (i.e., to become activated as a CCN) depends on size, chemical composition and the local supersaturation (Bigg, 1986).

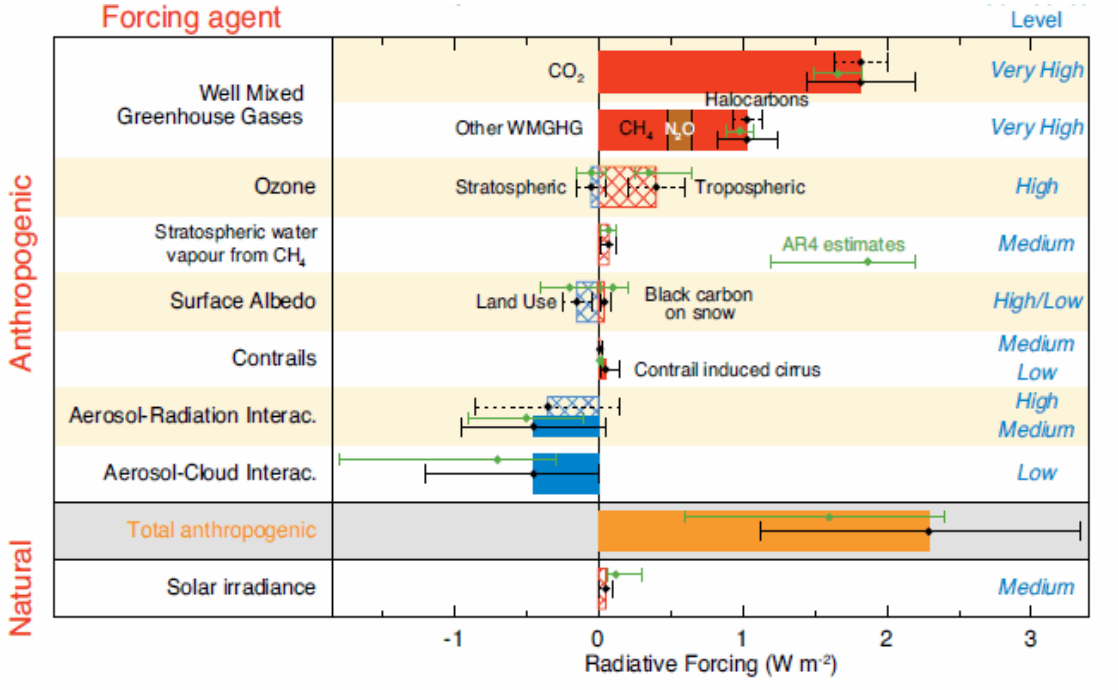

Figure 2-3 Diagram showing climate forcing agents, magnitude and confidence level (IPCC, 2014).

Hygroscopic materials such as sea salt and SO_4 are extremely efficient as CCN; mineral dust and combustion-released particulates can make effective CCN, especially if they are wet or have hygroscopic coatings. Organic substances have also been recognized as active cloud condensation and ice formation nuclei; organic acids or salts have the same CCN potential as inorganic acids or salts (Yu, 2000).

An increase in CCN leads to a greater number of smaller droplets (for a given cloud water content). Because of multiple light scattering within the cloud, the cloud albedo tends to increase with increased numbers of CCN, which leads to cooling. Additionally, clouds with more and smaller droplets are less prone to rain and drizzle formation and therefore persist longer, having more time to exert their cooling effect, however, the lack of rainfall may continue to warm the atmosphere (Teller & Levin, 2005).

2.3. Aerosol particles and light scattering properties

Light is an electromagnetic wave, made up of electric and magnetic fields, which exerts forces on charged species, such as protons, electrons, and molecular dipoles. For example, these fields can exert a force on a molecule that have dipole moments – meaning an uneven distribution of charge (Fierz-Schmidhauser et al., 2009). The electromagnetic forces cause the charged species to move. When these charged species moves, a new electric and magnetic field is created in the form of an electromagnetic wave (light). This new light wave can then travel in any direction, and is called scattered light.

The directions that the light is scattered depends on the size, shape and water content of the particle (Pan et al., 2009). In very small particles, the scattered light travels equally in all directions and is known as Rayleigh scattering. As particle size increases, more of the scattered light goes in the same direction as the initial light, which is called Mie scattering. Although the light can be scattered in any direction, a percentage of the sun's light is scattered away from the earth by aerosol particles in our atmosphere. This process and its dependence of particle composition is why the standard error for understanding aerosol effects on climate is significant. The scattering potential of particles depends on their water content. It has recently been reported that water soluble ions such as ammonium nitrate are found in the form of droplets in considerable concentration in the upper boundary layer. These particles have a strong light scattering potential, enhancing visibility and climate impacts (Morgan et al., 2010).

2.4. Aerosol particles and clouds

Aerosols are essential for cloud formation by interacting with them as CCN, ice nuclei (IN) or an absorbent to particles as described in section 2.2. They act to redistribute solar energy as latent heat inside different cloud layers (Peng et al., 2007) and are another indirect effect of aerosol on the atmosphere. The feedback mechanisms from clouds remain a source of uncertainty in climate response and sensitivity (Figure 2-3), whilst prior research reports a significant fraction of CCN activates on ultrafine (<0.1µm diameter) aerosol particles. This was found to occur mostly under clean or moderately polluted environments (Monks et al., 2009). These findings emphasize the need to quantify the main sources of ultrafine particles into the global atmosphere, as well as how these particles interact with clouds under different conditions.

2.5. References

Bigg, E. K. (1986). Discrepancy between observation and prediction of concentrations of cloud condensation nuclei. *Atmospheric Research*, *20*(1), 81–86. http://doi.org/10.1016/0169-8095(86)90010-4

Carslaw, K. S., Lee, L. A., Reddington, C. L., Pringle, K. J., Rap, A., Forster, P. M., … Pierce, J. R. (2013). Large contribution of natural aerosols to uncertainty in indirect forcing. *Nature*, *503*(7474), 67–71. http://doi.org/10.1038/nature12674

Dockery, D. W., Pope, C. A., Xu, X., Spengler, J. D., Ware, J. H., Fay, M. E., … Speizer, F. E. (1993). An association between air pollution and mortality in six U.S. cities. *The New England Journal of Medicine*, *329*(24), 1753–9. http://doi.org/10.1056/NEJM199312093292401

Dusek, U., Reischl, G. P., & Hitzenberger, R. (2006). CCN activation of pure and coated carbon black particles. *Environmental Science & Technology*, *40*(4), 1223–30. Retrieved from http://www.ncbi.nlm.nih.gov/pubmed/16572779

EEA. (2014). Air pollution fact sheet 2014.

Fierz-Schmidhauser, R., Zieger, P., Gysel, M., Kammermann, L., DeCarlo, P. F., Baltensperger, U., & Weingartner, E. (2009). Measured and predicted aerosol light scattering enhancement factors at the high alpine site Jungfraujoch. *Atmospheric Chemistry and Physics Discussions*, *9*(5), 20063–20101. http://doi.org/10.5194/acpd-9-20063-2009

IPCC. (2014). Climate Change 2014: Synthesis Report. Contribution of Working Groups I, II and III to the Fifth Assessment Report of the Intergovernmental Panel on Climate Change [Core Writing Team, R.K. Pachauri and L.A. Meyer (eds.)]. IPCC, Geneva, Switzer. Retrieved November 12, 2015, from http://www.ipcc.ch/report/ar5/syr/

Monks, P. S., Granier, C., Fuzzi, S., Stohl, A., Williams, M. L., Akimoto, H., … von Glasow, R. (2009). Atmospheric composition change – global and regional air quality. *Atmospheric Environment*, *43*(33), 5268–5350. http://doi.org/10.1016/j.atmosenv.2009.08.021

Morgan, W. T., Allan, J. D., Bower, K. N., Esselborn, M., Harris, B., Henzing, J. S., … Coe, H. (2010). Enhancement of the aerosol direct radiative effect by semi-volatile aerosol components: airborne measurements in North-Western Europe. *Atmospheric Chemistry and Physics*, *10*(17), 8151–8171. http://doi.org/10.5194/acp-10-8151-2010

Oberdörster, G. (2001). Pulmonary effects of inhaled ultrafine particles. *International Archives of Occupational and Environmental Health*, *74*(1), 1–8. Retrieved from http://www.ncbi.nlm.nih.gov/pubmed/11196075

Pan, X. L., Yan, P., Tang, J., Ma, J. Z., Wang, Z. F., Gbaguidi, a., & Sun, Y. L. (2009). Observational study of influence of aerosol hygroscopic growth on scattering coefficient over rural area near Beijing mega-city. *Atmospheric Chemistry and Physics*, *9*(19), 7519–7530. http://doi.org/10.5194/acp-9-7519-2009

Peng, Y., Lohmann, U., Leaitch, R., & Kulmala, M. (2007). An investigation into the aerosol dispersion effect through the activation process in marine stratus clouds. *Journal of Geophysical Research*, *112*(D11), D11117. http://doi.org/10.1029/2006JD007401

Pope, C. A., Turner, M. C., Burnett, R., Jerrett, M., Gapstur, S. M., Diver, W. R., … Brook, R. D. (2014). Relationships Between Fine Particulate Air Pollution, Cardiometabolic Disorders and Cardiovascular Mortality. *Circulation Research*. http://doi.org/10.1161/CIRCRESAHA.116.305060

Ramanathan, V., Cess, R. D., Harrison, E. F., Minnis, P., Barkstrom, B. R., Ahmed, E., & Hartmann, D. (1989). Cloud-Radiative Forcing and Climate: Results from the Earth Radiation Budget Experiment. *Science*, *243*(4887), 57–63. http://doi.org/10.1126/science.243.4887.57

Schwartz, J., Dockery, D. W., & Neas, L. M. (1996). Is Daily Mortality Associated Specifically with Fine Particles? *Journal of the Air & Waste Management Association*, *46*(10), 927–939. http://doi.org/10.1080/10473289.1996.10467528

Teller, a., & Levin, Z. (2005). The effects of aerosols on precipitation and dimensions of subtropical clouds; a sensitivity study using a numerical cloud model. *Atmospheric Chemistry and Physics Discussions*, *5*(4), 7211–7245. http://doi.org/10.5194/acpd-5-7211-2005

Worlds Health Organization. (2014). Burden of disease from Ambient Air Pollution for 2012, (Lmi), 2012–2014.

Yim, S. H. L., & Barrett, S. R. H. (2012). Public health impacts of combustion emissions in the United Kingdom. *Environmental Science & Technology*, *46*(8), 4291–6. http://doi.org/10.1021/es2040416

Yu, S. (2000). Role of organic acids (formic, acetic, pyruvic and oxalic) in the formation of cloud condensation nuclei (CCN): a review. *Atmospheric Research*, *53*(4), 185–217. http://doi.org/10.1016/S0169-8095(00)00037-5

Zhu, Y., Hinds, W. C., Krudysz, M., Kuhn, T., Froines, J., & Sioutas, C. (2005). Penetration of freeway ultrafine particles into indoor environments. *Journal of Aerosol Science*, *36*(3), 303–322. http://doi.org/10.1016/j.jaerosci.2004.09.007

3. Aerosol Formation Processes

3.1. Overview of particle formation processes

As was briefly described in Chapter 1, aerosol particles are either natural or anthropogenic in origin. Naturally occurring particles are typically produced by volcanoes, sea spray, biomass fires, and dust from arid soils, as well as biological sources, including pollen, bacterial and fungal spores. Anthropogenic emissions come from many sources, including the burning of fossil fuels in vehicles, domestic heating, power plants and industrial processes. Averaged over the globe, anthropogenic particulate matter [PM] accounts for about 10% of the total aerosol loading, while natural sources contribute the remaining majority. Aerosol particles can be further divided into primary and secondary sources according to their formation processes. Table 1 gives a complete list of aerosol sources, particle sizes and the strengths of the mass flux.

3.2. Natural primary and secondary emissions

Globally; dust is a major constituent of airborne particulates. The main sources are deserts, semi-arid regions and dried lake beds, although over-intensive farming can also contribute. Due to the nature of the sources, dust is more commonly found in the Northern Hemisphere, where the majority of land is situated, however, Australian dust has been observed in PM mass measurements in New Zealand (Marx et al., 2005).

An example of the scale of dust transportation in Europe is provided by research such as Querol et al. (2009), in which it is reported that Saharan dust is carried long distances, via upper atmospheric winds, and deposited throughout Europe. The Saharan dust episodes found in countries such as Spain can add considerable concentrations to aerosol loading (Viana et al. 2008). Saharan dust transportation through the mid-latitudes has also been implicated in influencing meteorological patterns (Gama et al. 2015), as well as altering formation processes of Atlantic hurricanes, via their input as a condensation sink (Sun et al., 2008).

The atmospheric lifetime of dust depends on particle size. Large particles are quickly removed from the atmosphere by gravitational settling, while sub-micrometer sized particles can have atmospheric lifetimes of several weeks. The mass median diameter of long-range transported dust is generally <10 μm (Pérez et al. 2006).

Table 3-1 A comprehensive list of primary and secondary aerosol sources and estimated yield per Tg/yr.

Source		Particle size (μm)	Strength (Tg/yr)
Natural			
Primary	Soil dust (mineral aerosols)	D <1	110
		D = 1-2	290
		D = 2-20	1750
	Sea to air flux of sea salt	D <1	54
		D = 1-16	3290
	Biogenic organic matter	Coarse	1000
	volcanic ash	Fine	20
Secondary	Sulfate aerosols from marine biogenic gases (mainly DMS)	Fine	16-32
	Sulfate aerosols from terrestrial biogenic gases	Fine	57
	Nitrate aerosols from NO_x (lightning, soil microbes)	Mainly coarse	3.9
	Organic matter from biogenic gases	Fine	16
	Sulfate aerosols from volcanic SO_2	Fine	9-21
Natural subtotal			At least 6600
Anthropogenic			
Primary	Aerosols from all kinds of fossil fuel burning, cement manufacturing, metallurgy, waste incineration, etc.	Coarse and fine	100
	Soot (black carbon) from fossil fuel burning (coal, oil)	Fine	8
	Soot from biomass burning	Fine	5
	Biomass burning without soot	Fine	80
Secondary	Sulfate from SO_2 (mainly from coal & oil burning)	Fine	140
	Nitrate aerosol from NO_x (fossil fuel and biomass combustion)	Mainly coarse	36
	Organic matter from anthropogenic gases	Fine	5
	Organic matter from biomass burning	Fine	54
	Organic matter from fossil fuel burning	Fine	28
Anthropogenic subtotal			460
Total			7100

3.2.1. Biogenic Sources

Biogenic emissions make up the vast majority of the total organic aerosol mass concentrations, overshadowing the total estimated mass from anthropogenic sources (Levine et al., 1995). Plants are the primary source of non-methane biogenic VOCs (NM-BVOC), such as monoterpenes, including α- and β-pinene and isoprene. There are numerous other minor NM-BVOC sources (Lathière et al. 2006), however, isoprene and terpenes attract the most attention due to their large global emissions, which can enhance particle production. This enables BVOCs to contribute up to 90% of aerosol composition in tropical forested areas (Ng et al. 2010).

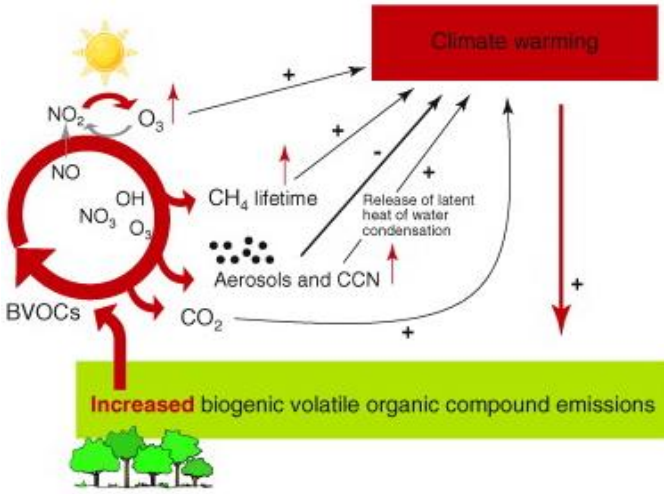

Figure 3-1 The chemical properties of increased BVOC emissions on atmospheric chemistry and climate (Peñuelas & Staudt 2010).

Figure 3.1 presents a schematic diagram that describes the processes involved in particle formation through BVOCs. Research suggests that a warmer planet will enhance BVOC emissions, which are defined by (+) symbols within the diagram. Increased BVOC emissions will enhance particle formation and development and therefore also enhance aerosol and CCN concentrations. Enhanced aerosol and CCN concentrations act to decrease temperatures (–) by the means described in Section 2. Other positive feedbacks, such as the direct greenhouse effect of BVOCs, and indirect greenhouse effect via O_3 formation and CH_4 (Laothawornkitkul et al. 2009; Peñuelas & Staudt, 2010).

3.2.2. Natural sulfate emissions

Natural sources of sulfate are the gas-to-particle conversion of SO_4^{2-} emitted from volcanoes and the oxidation of gaseous biogenic sulfur compounds. Sea spray is the abundant source of primary sulfate emissions. As shown in Table 1, sea salt sulfate is a primary source whilst non sea salt (nss) sulfate is a secondary product. Nss sulfate is produced from Dimethyl Sulfate (DMS), a gas released by marine phytoplankton in the oceans, and then transferred to the atmosphere via water-air surface friction and bubble burst processes (Vaattovaara et al., 2013). A large proportion of primary organic material is released from the world's oceans via bubble burst processes. The nss sufate constitutes the largest proportion of aerosol loading in locations with a high concentration of phytoplankton and other biologically active compounds (O'Dowd & de Leeuw 2007).
Depending on region, meteorology and locality to source, the concentrations of nss and sea salt sulfate are often comparable (Kerminen et al., 2005). The major difference between sea salt and nss sulfate is the mean size of the particle produced; sulfate from DMS exists in the sub-micrometer size fraction, whereas sea salt sulfate is largely coarse-mode aerosol.

3.3. Anthropogenic primary and secondary sources

Anthropogenic primary and secondary sources are usually found in the fine size fraction and account for the majority of total global fine aerosol mass. Typical emission sources are the burning

of fossil fuels for transport, incinerators, home furnaces and wood fires; these accounts for between 30-90% of total aerosol mass loading (Ng et al. 2010; Mohr et al. 2012). Industrial and mechanical human activities also contribute to this loading through the burning of coal, cement manufacturing, waste incineration and metallurgy. Though these processes an array of particulates are emitted, including poly-aromatic hydrocarbons (PAHs), dioxins and heavy metals (Park 2013).

Biomass burning is another significant primary source of particulates. This includes the clearance of forests and grasslands, agricultural waste and biomass fuel. Aerosols released during the burning of biomass consist of organic and elemental carbon, and are again generally fine mode aerosol. It has also been observed that biomass emissions are increasing with time (Capes et al. 2008), with resultant increases of the total aerosol loading.

Due to the direct emission input from high volumes of road traffic and industry the highest concentrations of anthropogenic particles are usually found in urban areas (Putaud et al. 2010). There are also specific hot-spots in less developed nations where population density is high and vehicular emissions are less regulated contributing to high levels of anthropogenic particles. Although the immediate effects are local, the long range transport of anthropogenic pollutants can occur and these particles may reach remote locations (Li et al. 2007).

Anthropogenic sources do not have to be emitted directly as a particle; they can also be derived from gaseous precursors of secondary organic and inorganic aerosols. The major sources are SO_2, NO_2 and none biological VOC's. Secondary aerosols are a major aerosol component within the central European region, and of significant relevance to the research carried out as part of this thesis.

3.3.1. Secondary Inorganic Aerosol

Secondary inorganic aerosol (SIA) include sulfate (SO_4^{2-}) nitrate (NO_3^-) and ammonium (NH_4^+), and are a major component in $PM_{2.5}$ aerosol worldwide. For example, an urban measurement site in Shanghai reports SIA contributions of up to 47% of total aerosol mass loading, whilst in an urban background site in Barcelona SIA made up 38-43% of the $PM_{2.5}$ mass (Long et al. 2014; Viana et al. 2008). SIA are formed from the available gas-phase precursors, therefore their relative abundance is directly dependent on the concentrations of NO_X, SO_2 and NH_3 gas precursors that are emitted.

3.3.2. Sulfate

As previously described, Sulfate (SO_4^{2-}) can be either primary or secondary in origin. SO_2 will usually react chemically with water to form sulfuric acid (H_2SO_4), Sulfuric acid quickly neutralizes with ammonia, forming either ammonium bisulfate or ammonium sulfate, however, research has recently discovered that sulfuric acid is often not fully neutralised (Pinder, et al., 2008). Due to the tangible problems caused by these acidic droplets (acid rain, erosion etc.) SO_2 emissions have been rigorously regulated, with a cap and trade scheme introduced. This has succeeded in reducing emissions and SO_4^{2-} levels are forecast to continue to fall (Boxman et al., 2008). Although decreases in long distance acid deposition rates have been modest, local health and wellbeing has greatly improved due to the lower particle concertation due to regulation (Stavins 2005).

Sulfate aerosol change the radiative properties of the atmosphere. Sulfate particles scatter solar radiation and alter the formation and development of clouds by serving as CCN. This also acts to change the cloud albedo and cloud lifetime. SO_4^{2-} particles have a more permeating effect on the biosphere by increasing acidity throughout the environment, whist their typical size and hygroscopisity increases their impact on human health (Dockery et al. 1993; Zhao & Gao 2008).

3.3.3. Ammonium

Ammonium (NH_4^+) is principally released by farming practices such as fertilization, the decaying of waste products from animals, and from coal and biomass burning. Emission levels of ammonium have been modelled in previous research (Luo et al., 2007), in which the importance of understanding ammonia chemistry on the concentration levels of SO_4^{2-} and NO_3^- were highlighted.

With decreases in SO_2 concentrations over recent years an increase in nitrate is predicted. This is due to increased availability of ammonia through lessened attachment of ammonia to sulfate and higher expected ammonia emissions caused by a warming climate. It is reported that the NH_4^+ burden is projected to increase globally from 0.24 to 0.36 Tg by 2020 (Pye et al. 2009).

3.3.4. Nitrate

Nitrate (NO_3^-) is formed from its precursor gas, nitric acid (HNO_3). Nitric acid is produced by the oxidation of NO_2 and the acid is subsequently neutralised by ammonia. The extent to which HNO_3 is neutralised by NH_3 is governed by thermodynamic equilibria, which, in turn, is determined by the temperature, relative humidity and molar concentrations of the subspecies (Seinfeld & Pandis 2012). It is important to note that H_2SO_4 and NH_4HSO_4 are neutralised before HNO_3 and that this preference not temperature dependent.

NO_3^- is most commonly found as the ionic compound NH_4NO_3, which is predominantly a fine mode particulate, with mean sizes ranging from 200nm (0.2 µm) to 600nm (0.6 µm) (Bai et al. 1995). This is comparable to related species such as $NaNO_3$ or $CaNO_3$, which are present in coarse modes (>1 µm) (Schwarz et al., 2012). The coarse mode fragment is generally caused by HNO_3 reacting with particulates already found as a coarse mode sea spray (NaCl) or minerals, such as $CaCO_3$. This results in the observed coarse particulate nitrate. These are usually observed during the summer months (Harrison & Pio 1983). Like sulfate, nitrate is also present in remote marine aerosols, but in much smaller concentrations than sulfate. This means that anthropogenic, not biogenic sources heavily influence total concentrations of NO_3^- worldwide.

Unlike ammonium sulfate, ammonium nitrate is volatile at typical ambient temperatures. This enables rapid dissociation from solid/deliquescent aerosol to gas phase species NH_4^+ and HNO_3, with the rate becoming more rapid during higher temperatures and lower relative humidity (Richardson & Hightower 1987; Cheng & Tsai 1997). This volatility can produce uncertainties within aerosol datasets by negative sampling and artefact production. There are also prominent diurnal

fluctuation in outdoor NO_3^- concentrations (Poulain et al. 2011; Kubelová et al. 2015). Figure 3.2 shows the chemical reactions governing NO_3^- formation during daytime and night time processes. These processes are non-linear and variable.

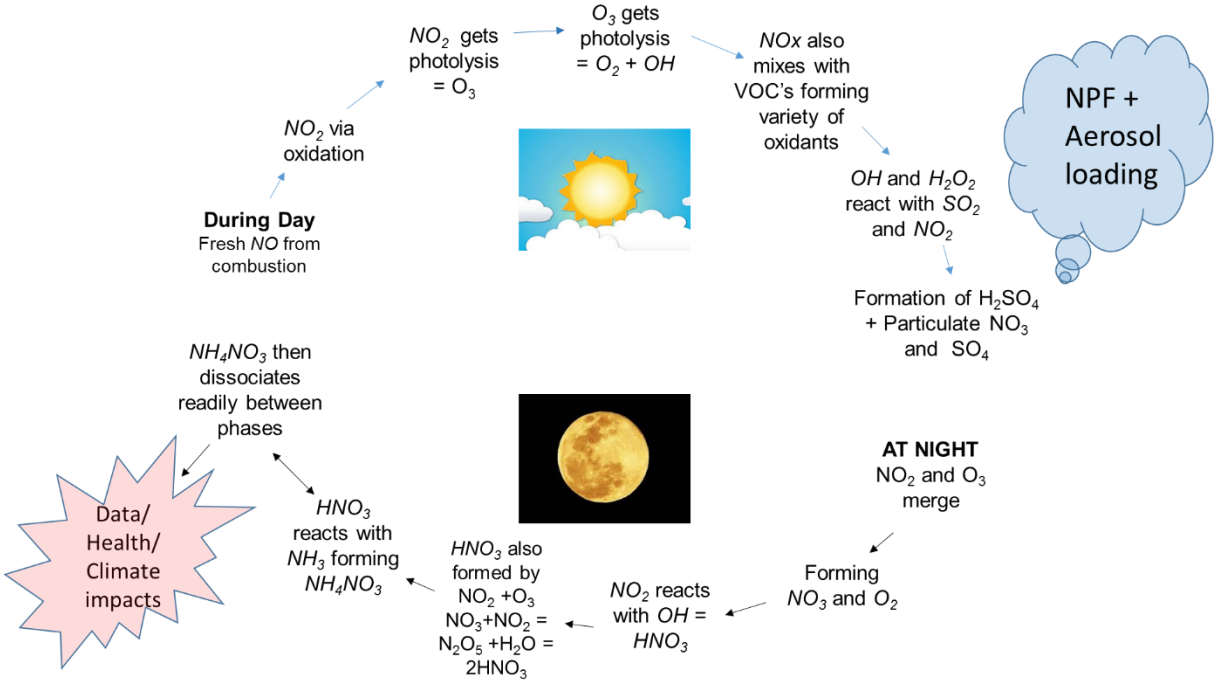

Figure 3-2 Schematic of chemical transformation processes that are carried out during the day and night. Created with input from (Seinfeld & Pandis 2012; Dassios & Pandis 1999; Mészáros 1999.).

3.4. References

Bai, H., Lu, C. & Ling, Y.M., 1995. A theoretical study on the evaporation of dry ammonium chloride and ammonium nitrate aerosols. *Atmospheric Environment*, 29(3), pp.313–321.

Boxman, A.W., Peters, R.C.J.H. & Roelofs, J.G.M., 2008. Long term changes in atmospheric N and S throughfall deposition and effects on soil solution chemistry in a Scots pine forest in the Netherlands. *Environmental Pollution*, 156(3), pp.1252–1259. Available at: http://dx.doi.org/10.1016/j.envpol.2008.03.017.

Capes, G. et al., 2008. Aging of biomass burning aerosols over West Africa: Aircraft measurements of chemical composition, microphysical properties, and emission ratios. *Journal of Geophysical Research*, 113, p.D00C15. Available at: http://doi.wiley.com/10.1029/2008JD009845 [Accessed December 1, 2015].

Cheng, Y.H. & Tsai, C.J., 1997. Evaporation loss of ammonium nitrate particles during filter sampling. *Journal of Aerosol Science*, 28(8), pp.1553–1567.

Dassios, K.G. & Pandis, S.N., 1999. The mass accommodation coe $ cient of ammonium nitrate aerosol. , 33, pp.2993–3003.

Dockery, D.W. et al., 1993. An association between air pollution and mortality in six U.S. cities. *The New England journal of medicine*, 329(24), pp.1753–9. Available at: http://www.scopus.com/inward/record.url?eid=2-s2.0-0027362097&partnerID=tZOtx3y1 [Accessed March 16, 2015].

Gama, C. et al., 2015. Seasonal patterns of Saharan dust over Cape Verde - a combined approach using observations and modelling. *Tellus B*, 67. Available at: http://www.tellusb.net/index.php/tellusb/article/view/24410/xml_1 [Accessed December 1, 2015].

Harrison, R.M. & Pio, C.A., 1983. Size-differentiated composition of inorganic atmospheric aerosols of both marine and polluted continental origin. *Atmospheric Environment (1967)*, 17(9), pp.1733–1738. Available

at: http://www.sciencedirect.com/science/article/pii/0004698183901804 [Accessed December 19, 2014].

Kerminen, V.-M. et al., 2005. Direct observational evidence linking atmospheric aerosol formation and cloud droplet activation. *Geophysical Research Letters*, 32(14), p.n/a–n/a. Available at: http://doi.wiley.com/10.1029/2005GL023130 [Accessed November 11, 2015].

Kubelová, L. et al., 2015. A study of summer and winter highly time-resolved submicron aerosol composition measured at a suburban site in Prague. *Atmospheric Environment*, 118, pp.45–57. Available at: http://www.sciencedirect.com/science/article/pii/S1352231015302296 [Accessed August 7, 2015].

Laothawornkitkul, J. et al., 2009. Biogenic volatile organic compounds in the Earth system. *The New phytologist*, 183(1), pp.27–51. Available at: http://www.ncbi.nlm.nih.gov/pubmed/19422541 [Accessed November 23, 2015].

Lathière, J. et al., 2006. Impact of climate variability and land use changes on global biogenic volatile organic compound emissions. *Atmospheric Chemistry and Physics*, 6(8), pp.2129–2146. Available at: http://www.atmos-chem-phys.net/6/2129/2006/acp-6-2129-2006.html [Accessed November 23, 2015].

Levine, J.S. et al., 1995. Biomass T Burning. *Environmental Science & Technology*, 29(3), pp.120–125.

Li, J. et al., 2007. Modeling study of ozone seasonal cycle in lower troposphere over east Asia. *Journal of Geophysical Research*, 112(D22), p.D22S25. Available at: http://doi.wiley.com/10.1029/2006JD008209 [Accessed February 2, 2016].

Long, S. et al., 2014. Characteristics of secondary inorganic aerosol and sulfate species in size-fractionated aerosol particles in Shanghai. *Journal of environmental sciences (China)*, 26(5), pp.1040–51. Available at: http://www.sciencedirect.com/science/article/pii/S1001074213605215 [Accessed November 12, 2015].

Luo, C. et al., 2007. Role of ammonia chemistry and coarse mode aerosols in global climatological inorganic aerosol distributions. *Atmospheric Environment*, 41(12), pp.2510–2533.

Marx, S.K., Kamber, B.S. & McGowan, H.A., 2005. Estimates of Australian dust flux into New Zealand: Quantifying the eastern Australian dust plume pathway using trace element calibrated 210Pb as a monitor. *Earth and Planetary Science Letters*, 239(3-4), pp.336–351. Available at: http://www.sciencedirect.com/science/article/pii/S0012821X05005558 [Accessed December 1, 2015].

Mészáros:, E., Fundamentals of Atmospheric Aerosol Chemistry. *Journal of Atmospheric Chemistry*, 39(1), pp.99–103. Available at: http://link.springer.com/article/10.1023/A%3A1010753724116 [Accessed December 16, 2015].

Mohr, C. et al., 2012. Identification and quantification of organic aerosol from cooking and other sources in Barcelona using aerosol mass spectrometer data. *Atmospheric Chemistry and Physics*, 12(4), pp.1649–1665.

Ng, N.L. et al., 2010. Organic aerosol components observed in Northern Hemispheric datasets from Aerosol Mass Spectrometry. *Atmospheric Chemistry and Physics*, 10(10), pp.4625–4641.

O'Dowd, C.D. & de Leeuw, G., 2007. Marine aerosol production: a review of the current knowledge. *Philosophical transactions. Series A, Mathematical, physical, and engineering sciences*, 365(1856), pp.1753–1774.

Park, Y.K., 2013. Release of Harmful Air Pollutants from Open Burning of Domestic Municipal Solid Wastes in a Metropolitan Area of Korea. *Aerosol and Air Quality Research*, pp.1365–1372. Available at: http://www.aaqr.org/Doi.php?id=18_AAQR-12-10-OA-0272&v=13&i=4&m=8&y=2013.

Peñuelas, J. & Staudt, M., 2010. BVOCs and global change. *Trends in Plant Science*, 15(3), pp.133–144.

Pérez, C. et al., 2006. A long Saharan dust event over the western Mediterranean: Lidar, Sun photometer observations, and regional dust modeling. *Journal of Geophysical Research*, 111(D15), p.D15214. Available at: http://doi.wiley.com/10.1029/2005JD006579 [Accessed December 1, 2015].

Pinder, R.W., Gilliland, A.B. & Dennis, R.L., 2008. Environmental impact of atmospheric NH_3 emissions under present and future conditions in the eastern United States. *Geophysical Research Letters*, 35(12), p.n/a–

n/a. Available at: http://doi.wiley.com/10.1029/2008GL033732.

Poulain, L. et al., 2011. Seasonal and diurnal variations of particulate nitrate and organic matter at the IfT research station Melpitz. *Atmospheric Chemistry and Physics*, 11(24), pp.12579–12599. Available at: http://www.atmos-chem-phys.net/11/12579/2011/acp-11-12579-2011.html [Accessed September 15, 2015].

Putaud, J.-P. et al., 2010. A European aerosol phenomenology – 3: Physical and chemical characteristics of particulate matter from 60 rural, urban, and kerbside sites across Europe. *Atmospheric Environment*, 44(10), pp.1308–1320. Available at: http://www.sciencedirect.com/science/article/pii/S1352231009010358 [Accessed November 21, 2014].

Pye, H.O.T. et al., 2009. Effect of changes in climate and emissions on future sulfate-nitrate-ammonium aerosol levels in the United States. *Journal of Geophysical Research*, 114(D1), p.D01205. Available at: http://doi.wiley.com/10.1029/2008JD010701 [Accessed November 9, 2015].

Querol, X. et al., 2009. Variability in regional background aerosols within the Mediterranean. *Atmospheric Chemistry and Physics Discussions*, 9(2), pp.10153–10192. Available at: http://www.atmos-chem-phys.net/9/4575/2009/acp-9-4575-2009.pdf.

Richardson, C.B. & Hightower, R.L., 1987. Evaporation of ammonium nitrate particles. *Atmospheric Environment (1967)*, 21(4), pp.971–975.

Schwarz, J. et al., 2012. Mass and chemically speciated size distribution of Prague aerosol using an aerosol dryer - The influence of air mass origin. *Science of the Total Environment*, 437, pp.348–362.

Seinfeld, J. & Pandis, S., 2012. *Atmospheric chemistry and physics: from air pollution to climate change*, Available at: http://www.google.com/books?hl=en&lr=&id=YH2K9eWsZOcC&oi=fnd&pg=PA1991&dq=seinfeld+and+pandis&ots=hK3xLmaXHx&sig=YBgCj_Ct7vI-a5Aso7JligN3958 [Accessed December 19, 2014].

Stavins, R.N., 2005. Lessons Learned from SO2 Allowance Trading. Available at: http://www.choicesmagazine.org/2005-1/environment/2005-1-11.htm [Accessed December 1, 2015].

Sun, D., Lau, K.M. & Kafatos, M., 2008. Contrasting the 2007 and 2005 hurricane seasons: Evidence of possible impacts of Saharan dry air and dust on tropical cyclone activity in the Atlantic basin. *Geophysical Research Letters*, 35(15), p.L15405. Available at: http://doi.wiley.com/10.1029/2008GL034529 [Accessed December 1, 2015].

Vaattovaara, P., Cravigan, L. & Ristovski, Z., 2013. Organic Contribution on Particles Formed on Pacific Ocean: From Phytoplankton Blooms to Climate. *Waset.Org*, 7(10), pp.2011–2014. Available at: http://www.waset.org/Publications/?path=Publications&p=82.

Viana, M. et al., 2008. Source apportionment of particulate matter in Europe: A review of methods and results. *Journal of Aerosol Science*, 39(10), pp.827–849. Available at: http://www.scopus.com/inward/record.url?eid=2-s2.0-51249110830&partnerID=tZOtx3y1 [Accessed January 26, 2015].

ZHAO, Y. & GAO, Y., 2008. Acidic species and chloride depletion in coarse aerosol particles in the US east coast. *Science of The Total Environment*, 407(1), pp.541–547. Available at: http://linkinghub.elsevier.com/retrieve/pii/S0048969708009029.

4. Ammonium Nitrate

4.1. Overview of ammonium nitrate

Ammonium nitrate accounts for an estimated 30% of fine particulate mass over continental landmasses (Wexler & Seinfeld, 1990), and over half the total particulate mass concentration in certain locations (Chow et al., 1993; Dall'Osto et al., 2013). As described in Figure 3.2, ammonium nitrate (NH_4NO_3) occurs in the atmosphere when NO and NO_2 are oxidized to form nitric acid, which is then neutralised by ammonia, the dominant atmospheric base, to form NH_4NO_3 (Lightstone et al., 2000) (Figure 3.2). With a relatively high vapour pressure and a known dependency on temperature and relative humidity, ammonium nitrate becomes volatile under typical atmospheric conditions and will readily partition into its primary gases NH_3 and HNO_3 in the following reversible reactions (Lunden et al., 2003),

$$NH_4NO_3(s) \rightleftharpoons HNO_3(g) + NH_3(g)$$
$$NH_4^+(aq)\ NO_3^-(aq) \rightleftharpoons HNO_3(g) + NH_3(g) \quad (4\text{-}1)$$

Ammonium nitrate is usually found in the accumulation mode between 200 and 600nm (Bergin et al.,1997), which, given the right conditions, would allow for long residence times. In particle form, NH_4NO_3 can be either crystalline (solid) or a supersaturated aqueous solution (Aq), with its phase being dependent on temperature and relative humidity (RH) (Seinfeld & Pandis, 2012). Previous research has demonstrated deliquescence of crystalline NH_4NO_3 at 62% RH. However, due to hysteresis, aqueous NH_4NO_3 does not recrystallize until RH is less than 20%. Moreover, recent studies indicates that where a solution of NH_4NO_3 has been used to generate aerosol, the resulting particles recrystallize at relative humidity values of less than 10% (Dassios and Pandis, 1999), Hu et al. (2011) found that recrystallization never occurred and Martin (2003) attributed this to the history of the particulate. The phase state of the ammonium nitrate particle is known to effect the size of the ammonium nitrate particle (Allen et al., 1989) and the equilibrium constant described in equation 1 (Stelson & Seinfeld, 1982)**.** Ammonium nitrate particles, under ambient conditions, can be internally mixed, whether with sulfides or elctrolytes or organics (Wexler & Seinfeld, 1990). The mixture has been found to effect the phase equilibria of the paricle by chaning the partcles thermodynamic properties (Lightstone et al 2000).

4.2. Prior knowledge of ammonium nitrate dissociation behaviour

The semi-volatile behaviour of NH_4NO_3 has led to this chemical species being of interest to researchers. Previous literature have discussed and contributed to an understanding about equilibrium constants, modelled ammonium nitrate concentrations, thermodynamic data and accommodation coefficients estimated. A considerable effort has been made to increase knowledge regarding dissociation behaviour. This section provides a review of major studies which have contributed to this understanding of ammonium nitrate, whilst also being considered relevant to the research presented within this document. Due to the depth and complexity of the research, only a brief synopsis of the literature is provided, however, by placing the articles in chronological order, it is hoped that the progression of the research through time is able to been observed.

- **Stelson, A., & Seinfeld, J. (1982)**
  - Thermodynamic method employed to predict temperature and relative humidity variation on dissociation rates.
  - Predict temperature and RH dependence of the NH_4NO_3 dissociation constant.
  - Theory agrees with atmospheric data.

- **Larson, T. V., & Taylor, G. S. (1983)**
  - Found that NH_4NO_3 particles experimental evaporation rates agreed with their theoretical predictions and with Knudsen's diffusion theory. The experimental values were obtained by using a diffusion stripped to remove gaseous NH_3 and HNO_3 from an aerosol containing NH_4NO_3 droplets, which led to the evaporation of NH_4NO_3.

- **Richardson, C. B., & Hightower, R. L. (1987)**
  - Levitated solid and aqueous phase ammonium nitrate particles and measured the resultant size and mass changes using mass balance and light scattering techniques.
  - The metastable liquid had a 17% increase in evaporation when the particle radius was near 2 μm, though the authors were unable to provide an external force that would result in such changes.
  - Inconsistent results for solid phase NH_4NO_3 gave rates 48 times slower than predicted by theory. This led to the introduction of an accommodation coefficient of 0.02-0.004 to compensate for this undefined kinetic restraint across the particle surface.

- **Allen, A. G., Harrison, R. M., & Erisman, J.-W. (1989)**
  - Measured atmospheric concentrations of HNO_3, HCL and NH_3 at Essex, UK (filter pack) and Cabuaw, Netherlands (denuder).
  - Integration times of 3, 12, and 24h used.
  - Experimental concentrations of products generally agreed with predictions of chemical thermodynamics.
  - No firm conclusions reached regarding differences between theoretical and experimental values.

- **Harrison R., Sturges W., Kitto A., & Li Y. (1990)**
  - Deployed a denuder to scrub HNO_3 and NH_3 from a sampled airstream and found shrinking rates of -0.45×10^{-10} / -0.49×10^{-10} ms^{-1} for solid and aqueous phase particles.
  - Rates were independent of particles size, and, similar to Richardson and Hightower's (1987) work, were much lower than theoretical predictions. This, again, points to an unknown kinetic constraint on achieving equilibrium at atmospheric conditions.

- **Mozurkewich, M. (1993)**
  - Compared ammonium nitrate dissociation calculations with a variety of literary sources, though his work encompassed three calculation methods and five independent data sets, which were reportedly in excellent agreement with each other.

- In addition to determining equations for the dissociation of NH_4NO_3, it was found that the Kelvin effect plays a large role in the dissociation of particles less than 100 nm.
- Particle size was found to have little effect on the deliquescence point.

➢ **Bai, H., Lu, C., & Ling, Y. M. (1995)**

- Introduced a complex mathematical model was that incorporated particle polydispersity, flow, number concentrations, size dynamics, gas-particle interaction and accommodation coefficient to determine the evaporation of dry ammonium nitrate.
- These theoretical results were then compared with the available literature, and discrepancies between the values were investigated. They conclude that to neglect the size parameter effects of the NH_4NO_3 particle and inappropriate deployment of kinetic theory would lead to significant departures from theoretically derived results.

➢ **Bergin M. H., Ogren J. A., Schwartz S. E., & Mcinnes L. M. (1997).**

- Reported a theoretical model with an associated accommodation coefficient of unity that accurately described their experimental data.
- Investigated ammonium nitrate particles of 300 nm.

➢ **Cheng, Y.-H., & Tsai, C.-J. (1997)**

- Examined evaporation loss of ammonium nitrate during filter sampling when the upstream saturation ratio was zero.
- Experimental and theoretical results were in agreement.
- Upstream particle concentration has large effect on the evaporation loss of ammonium nitrate particles.

➢ **Dassios, K. G., & Pandis, S. N. (1999)**

- Deployed a tandem differential mobility analyser/scanning mobility particle sizer (TDMA/SMPS) to observe NH_4NO_3 dissociation at temperatures between 20-27 ˚C and particles in the 80-220 nm size range. These results were then compared to a theoretical expression of the evaporation rate, which took into account both the Kelvin effect and the effect of RH on the equilibrium constant.
- Evaporation rates were slightly slower than predicted,
- Reported that their experimental findings were still consistent with their theoretical work. The authors explained this slight discrepancy by a mass accommodation coefficient of 0.8 to 0.5 when temperature increases from 20-27˚C.

➢ **Hering, S., & Cass, G. (1999)**

- Teflon filters collect 28% less nitrate on average than denuded nylon filters.
- Cascade impactor samples were within 5% of denuded nylon filters on average.
- Nitrate loss from Teflon filters may be due to scavenging of nitric acid and ammonia in the sampler inlet and/or heating of the filter substrate during sampling.

➢ **Schaap, M., Van Loon, M., Ten Brink, H. M., Dentener, F. J., & Builtjes, P. J. H. (2003)**

- Chemistry-transport model LOTOS extended with a thermodynamic equilibrium module
- Winter, fall and spring: high nitrate levels over north western, central and eastern Europe, whilst concentrations were predicted to be highest over Italy.
- Summer: appreciable concentrations only occur in areas with high ammonia emissions.

➢ **Lunden, M. M., Revzan, K. L., Fischer, M. L., Thatcher, T. L., Littlejohn, D., Hering, S. V., & Brown, N. J. (2003)**

- Monitored outdoor and indoor particulates in an unoccupied home in Clovis, California.
- Found that indoor ammonium nitrate concentrations were significantly lower than expected from penetration and deposition loss.
- Difference attributed to transformation of indoor ammonium nitrate into ammonia and nitric acid gases, which are then lost via deposition and sorption into indoor surfaces.

➢ **Bauer, S. E., Koch, D., Unger, N., Metzger, S. M., Shindell, D. T., & Streets, D. G. (2007)**

- Used GISS climate model to predict nitrate aerosol levels in 2030.
- Found that changes to ammonia sources will play a key role in determining future nitrate aerosol levels.
- Ammonium nitrate contributes about 10% of the net aerosol and ozone forcing.

➢ **Smolík, J., Dohányosová, P., & Schwarz, J. (2008)**

- Particulate matter samples collected indoors and outdoors in an apartment in Prague.
- Berner type low pressure impactors, ion chromatography (IC) and proton induced X-ray emission (PIXE).
- Very low indoor nitrate concentration when compared to outdoors.

➢ **Li, S., Wang, T., Zhuang, B., & Han, Y. (2009)**

- Coupled the regional climate change model (REGCM3) and a tropospheric atmosphere chemistry model (TACM), creating a regional climate chemistry modelling system (REgCCMS).
- Investigated impacts of anthropogenic nitrate aerosols over China.

➢ **Andelova, L., Smolik, J., Ondrackova, L., Ondracek, J., Lopez-Aparicio, S., Grontoft, T., & Stankiewicz, J. (2010)**

- Berner type low pressure impactors, ion chromatography (IC) and proton induced X-ray emission (PIXE).
- Sampling indoor and outdoor environments in parallel.
- Ammonium sulfate and nitrate formed about 30% of outdoor submicron fractions by mass.
- Indoor nitrate concentrations decreased to zero.
- Ammonium nitrate probably evaporated after penetration due to higher indoor temperatures and fast deposition of gaseous nitric acid on surfaces.
- Increased indoor ammonia concentrations.

➢ **Poulain, L., Spindler, G., Birmili, W., Plass-Dülmer, C., Wiedensohler, A., & Herrmann, H (2011)**

- Aerodyne Aerosol Mass Spectrometer (AMS) used in Melpitz, Germany.

- Nitrate levels always lowest during day, increased at night.
- Linked to gas-to-particle-phase equilibrium of ammonium nitrate and the dynamics of the atmosphere during the day.
- Summer nights: condensation of HNO_3 and NH_3 on pre-existing particles is the main source of nitrate.
- Winter nights: nighttime chemistry is the main source of nitrate.

➢ **Hu, D., Chen, J., Ye, X., Li, L., & Yang, X. (2011)**

- Used a self-assembled hygroscopic tandem differential mobility analyser (H-TDMA) system.
- 40-200 nm particles
- Volatile properties of NH_4CL and NH_4NO_3 led to great differences between measured hydroscopic growth factors and theoretical values.

➢ **Smolík, J., Mašková, L., Zikova, N., Ondráčková, L., & Ondráček, J. (2013).**

- Ammonium sulfate is deposited on vertical surfaces.
- Ammonium sulfate formed up to 60% of the mass of the water-soluble indoor submicron particulate matter.
- Ammonium sulfate is a stable compound, so it is used as a tracer of ambient fine aerosols indoors.

➢ **Mašková, L., Smolík, J., & Vodička, P. (2015)**

- Determined the composition of particulate matter in four different types of archives during four seasons.
- Fine nitrate was only detected when indoor temperatures were below 5 °C, above 5 °C nitrate practically disappeared from indoor measurements.

4.3. Concluding remarks

From prior research it is evident that the rapid dissociation / evaporation of ammonium nitrate at ambient conditions has created many challenges for the aerosol research community. Outdoors, there is strong evidence of a diurnal cycle of ammonium nitrate association during cool nights, which then dissociates during the warmer daytime period. Indoors, the higher temperatures, lower humidity, and abundance of different surface types, all act to accelerate the dissociation process. This eventuality causes changes to the acidification processes in the atmosphere, changes size distributions over short time periods and enhances ammonia and nitric acid concentrations indoors. The result of this process can then have implications for human health, aerosol composition characterisation and deterioration of valued artefacts.

There is a clear gap in knowledge regarding the transformation process of aerosol particles as they travel from the outdoor to indoor environment. Most research has identified changes in mass composition of chemical species through filter measurements. An accurate but not enlightening methodology to identify changes occurring to aerosol particles over short temporal periods.

4.4. References

Allen, A. G., Harrison, R. M., & Erisman, J.-W. (1989). Field measurements of the dissociation of ammonium nitrate and ammonium chloride aerosols. *Atmospheric Environment (1967)*, *23*(7), 1591–1599. http://doi.org/10.1016/0004-6981(89)90418-6

Andelova, L., Smolik, J., Ondrackova, L., Ondracek, J., Lopez-Aparicio, S., Grontoft, T., & Stankiewicz, J. (2010). Characterization of Airborne Particles in the Baroque Hall of the National Library. Retrieved March 16, 2015, from http://www.morana-rtd.com/e-preservationscience/2010/Andelova-26-04-2010.pdf

Bai, H., Lu, C., & Ling, Y. M. (1995). A theoretical study on the evaporation of dry ammonium chloride and ammonium nitrate aerosols. *Atmospheric Environment*.

Bauer, S. E., Koch, D., Unger, N., Metzger, S. M., Shindell, D. T., & Streets, D. G. (2007). Nitrate aerosols today and in 2030: a global simulation including aerosols and tropospheric ozone. *Atmospheric Chemistry and Physics*, *7*(19), 5043–5059. http://doi.org/10.5194/acp-7-5043-2007

Bergin, M. H., Ogren, J. A., Schwartz, S. E., & Mcinnes, L. M. (1997). Evaporation of ammonium nitrate aerosol in a heated nephelometer: Implications for field measurements. *Environmental Science and Technology*, *31*(10), 2878–2883.

Cheng, Y.-H., & Tsai, C.-J. (1997). Evaporation loss of ammonium nitrate particles during filter sampling. *Journal of Aerosol Science*, *28*(8), 1553–1567. Retrieved from http://www.sciencedirect.com/science/article/pii/S0021850297000335

Chow, J. C., Watson, J. G., Lowenthal, D. H., Solomon, P. A., Magliano, K. L., Ziman, S. D., & Richards, L. W. (1993). PM 10 and PM 2.5 Compositions in California's San Joaquin Valley. *Aerosol Science and Technology*, *18*(2), 105–128. http://doi.org/10.1080/02786829308959588

Dall'Osto, M., Querol, X., Alastuey, A., O'Dowd, C., Harrison, R. M., Wenger, J., & Gómez-Moreno, F. J. (2013). On the spatial distribution and evolution of ultrafine particles in Barcelona. *Atmospheric Chemistry and Physics*, *13*(2), 741–759. http://doi.org/10.5194/acp-13-741-2013

Dassios, K. G., & Pandis, S. N. (1999). The mass accommodation coe $ cient of ammonium nitrate aerosol, *33*, 2993–3003.

Harrison, R. M., Sturges, W. T., Kitto, A.-M. N., & Li, Y. (1990). Kinetics of evaporation of ammonium chloride and ammonium nitrate aerosols. *Atmospheric Environment. Part A. General Topics*, *24*(7), 1883–1888. Retrieved from http://www.cabdirect.org/abstracts/19911951941.html;jsessionid=8C15DD08D360833BC0CF0F92AF714929

Hering, S., & Cass, G. (1999). The Magnitude of Bias in the Measurement of PM25 Arising from Volatilization of Particulate Nitrate from Teflon Filters. *Journal of the Air & Waste Management Association*, *49*(6), 725–733. http://doi.org/10.1080/10473289.1999.10463843

Hu, D., Chen, J., Ye, X., Li, L., & Yang, X. (2011). Hygroscopicity and evaporation of ammonium chloride and ammonium nitrate: Relative humidity and size effects on the growth factor. *Atmospheric Environment*, *45*(14), 2349–2355. http://doi.org/10.1016/j.atmosenv.2011.02.024

Hu, D., Chen, J., Ye, X., Li, L., & Yang, X. (2011b). Hygroscopicity and evaporation of ammonium chloride and ammonium nitrate: Relative humidity and size effects on the growth factor. *Atmospheric Environment*, *45*(14), 2349–2355. Retrieved from http://www.sciencedirect.com/science/article/pii/S1352231011001580

Larson, T. V., & Taylor, G. S. (1983). On the evaporation of ammonium nitrate aerosol. *Atmospheric Environment (1967)*, *17*(12), 2489–2495. http://doi.org/10.1016/0004-6981(83)90074-4

Li, S., Wang, T., Zhuang, B., & Han, Y. (2009). Indirect radiative forcing and climatic effect of the anthropogenic nitrate aerosol on regional climate of China. *Advances in Atmospheric Sciences*, *26*(3), 543–552. http://doi.org/10.1007/s00376-009-0543-9

Lightstone, J. M., Onasch, T. B., Imre, D., & Oatis, S. (2000). Deliquescence, Efflorescence, and Water Activity in Ammonium Nitrate and Mixed Ammonium Nitrate/Succinic Acid Microparticles. *The Journal of Physical Chemistry A*, *104*(41), 9337–9346. Retrieved from http://pubs.acs.org/doi/abs/10.1021/jp002137h

Lightstone, J. M., Onasch, T. B., Imre, D., York, N., & Oatis, S. (2000). Deliquescence , Efflorescence , and Water Activity in Ammonium Nitrate and Mixed Ammonium Nitrate / Succinic Acid Microparticles, 9337–9346.

Lunden, M. M., Revzan, K. L., Fischer, M. L., Thatcher, T. L., Littlejohn, D., Hering, S. V., & Brown, N. J. (2003). The transformation of outdoor ammonium nitrate aerosols in the indoor environment. *Atmospheric Environment*, *37*(39-40), 5633–5644. http://doi.org/10.1016/j.atmosenv.2003.09.035

Martin, S. T. (2003). Crystallization of atmospheric sulfate-nitrate-ammonium particles. *Geophysical Research Letters*.

Mašková, L., Smolík, J., & Vodička, P. (2015). Characterisation of particulate matter in different types of archives. *Atmospheric Environment*, *107*, 217–224. http://doi.org/10.1016/j.atmosenv.2015.02.049

Mozurkewich, M. (1993). The dissociation constant of ammonium nitrate and its dependence on temperature, relative humidity and particle size. *Atmospheric Environment. Part A. General Topics*, *27*(2), 261–270. http://doi.org/10.1016/0960-1686(93)90356-4

Poulain, L., Spindler, G., Birmili, W., Plass-Dülmer, C., Wiedensohler, A., & Herrmann, H. (2011). Seasonal and diurnal variations of particulate nitrate and organic matter at the IfT research station Melpitz. *Atmospheric Chemistry and Physics*, *11*(24), 12579–12599. http://doi.org/10.5194/acp-11-12579-2011

Richardson, C. B., & Hightower, R. L. (1987). Evaporation of ammonium nitrate particles. *Atmospheric Environment (1967)*, *21*(4), 971–975.

Schaap, M., van Loon, M., ten Brink, H. M., Dentener, F. J., & Builtjes, P. J. H. (2003). The nitrate aerosol field over Europe: simulations with an atmospheric chemistry-transport model of intermediate complexity. *Atmospheric Chemistry and Physics Discussions*, *3*(6), 5919–5976. http://doi.org/10.5194/acpd-3-5919-2003

Seinfeld, J., & Pandis, S. (2012). *Atmospheric chemistry and physics: from air pollution to climate change*. Retrieved from http://www.google.com/books?hl=en&lr=&id=YH2K9eWsZOcC&oi=fnd&pg=PA1991&dq=seinfeld+and+pandis&ots=hK3xLmaXHx&sig=YBgCj_Ct7vI-a5Aso7JIigN3958

Smolík, J., Dohányosová, P., & Schwarz, J. (2008). Characterization of indoor and outdoor aerosols in a suburban area of Prague. *Water, Air, & Soil …*. Retrieved from http://link.springer.com/article/10.1007/s11267-007-9141-y

Smolík, J., Mašková, L., Zikova, N., Ondráčková, L., & Ondráček, J. (2013). Deposition of suspended fine particulate matter in a library. *Heritage Science*, *1*(1), 7. http://doi.org/10.1186/2050-7445-1-7

Stelson, A., & Seinfeld, J. (1982). Relative humidity and temperature dependence of the ammonium nitrate dissociation constant. *Atmospheric Environment (1967)*, *16*(5), 983–992. Retrieved from http://www.sciencedirect.com/science/article/pii/0004698182901846

Wexler, A. S., & Seinfeld, J. H. (1990). *The distribution of ammonium salts among a size and composition dispersed aerosol*. *Atmospheric Environment. Part A. General Topics* (Vol. 24). Retrieved from http://linkinghub.elsevier.com/retrieve/pii/0960168690900885

5. Indoor Aerosols

5.1. Indoor-to-outdoor relationship of aerosol particles

With an increasing number of the world's population spending more time indoors (Lazaridis & Aleksandropoulou, 2006), it is important that the air within these microenviroments is not detrimental to the occupants well-being. Indoor emitted sources dominate the composition and concentration of indoor particulate matter (Hussein et al., 2005), with common sources including smoking, cooking, kerosene heating, wood burning and re-suspension (He, 2004).

When indoor sources are absent, indoor concentrations correlate strongly to those outdoors (Diapouli et al, 2013; Diapouli et al., 2011; Lazaridis & Aleksandropoulou, 2008). A visualisation of a typical migration path a particle might take from outdoors to indoors is given in Figure 5.1. The relationship between indoor and outdoor aerosol has been extensively researched in various different environmental settings. For example, in Athens city (Diapouli et al. 2011), next to major freeways in Los Angeles (Zhu et al. 2005), residential areas in Brisbane (Guo et al., 2008; Hai Guo et al., 2010; Morawska, 2001), Helsinki (Hussein et al. 2004; Hämeri et al. 2004b), and at various background and urban sites throughout Europe (Hänninen et al. 2004).

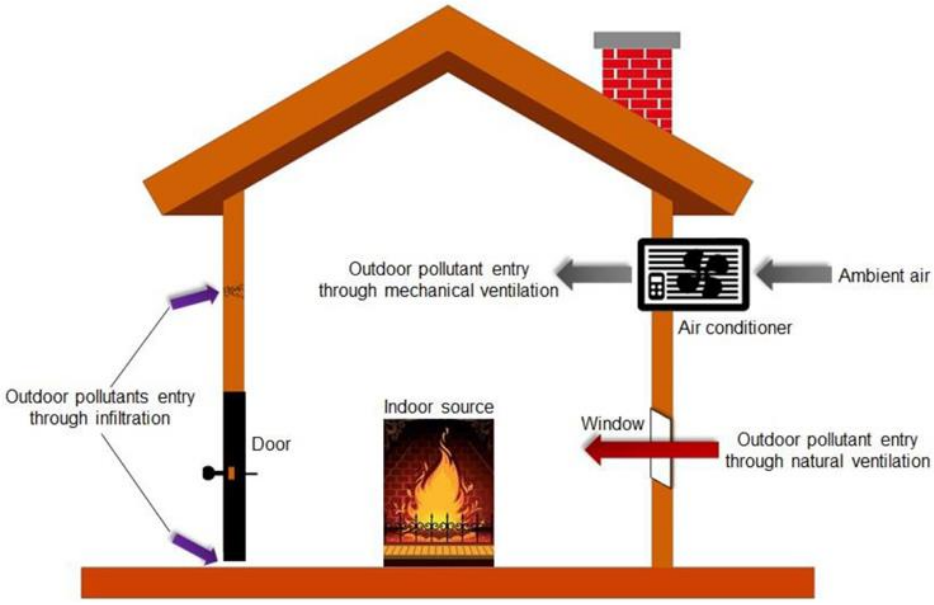

Figure 5-1 Sources and pathways of indoor air pollutants (Leung & Drakaki, 2015).

Despite the differing emission source for each researched location, all reported upon a background indoor concentration correlated to that outdoors. However, when indoor sources are present, sources outside are masked by the far larger concentrations of the indoor sources (Hussein et al., 2006).

Many papers have focused on indoor particle number concentrations and size distributions (Géhin et al., 2008; He et al., 2004; Morawska et al., 2001) to obtain insight into indoor / outdoor (I/O) aerosol behaviour. Other studies have taken into consideration indoor black carbon concentrations (Ho et al. 2004), and offline indoor chemical characterisation (Geller et al., 2002; Smolík et al, 2008). Prior

research has also focused upon particle transformations of semi volatile inorganic species such as ammonium nitrate. Ammonium nitrate causes uncertainties when considering indoor outdoor relationships by not following the principle of a correlated indoor/outdoor relationship (Lunden et al. 2003; Mašková, et al., 2015). Dissociation rates of particle phase NO_3^- have a strong temperature dependence (Stelson & Seinfeld, 1982), whilst NO_3^- precursor NHO_3 acid- reactions on indoor surfaces (Hering & Cass, 1999), add to uncertainties. Moreover, meteorology has been suspected of causing changes to Indoor outdoor ratios (Chan, 2002; Hussein et al., 2006).

Claculating the I/O ratio is the most common and simplest way to describe the concentration of aerosol that penetrates indoors from outdoors. Its obtained by the following expression,

$$\text{I/ O } Ratio = \frac{C\_in}{C\_\text{out}} \tag{5-1}$$

where the indoor/outdoor ratio is simply the division of concentrations indoors by those outdoors. Although in doing this, consideration must be given to the length of time it takes for outdoor partciles to penetrate indoors. Not all particles penetrate equally efficiently, the smaller particles tend to diffiuse to the surfaces of the building or windor frames, whilst coarse mode particles quickly gravitationally settle. Figure 5.2 graphs the penertration ratio of a particle per particle size (Nazaroff, 2004).

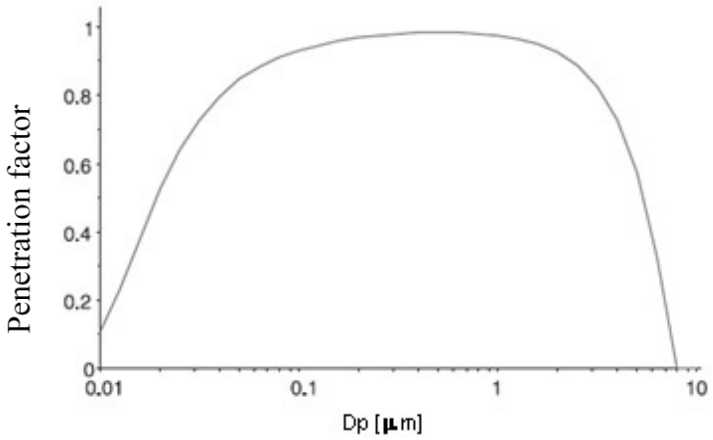

Figure 5-2 Schematic representation of the dependency penetration factor on the size of the particles (Nazaroff, 2004).

When exchange rates are slower than 2/h (2 complete changes of air by unit volume per hour) or when indoor soirces are present, changes to indoor number concentrations can be described by this simple mathematical formula (Hussein & Kulmala, 2007).

$$v\frac{dN_{in}}{dt} = \sum Sources - \sum Sink = P - E - \rho Q(N_{in} \_ N_{out}) \tag{5-2}$$

V - Volume of indoor air
P - Production of indoor particles
E - Elimination through reaction, filtration and settling.
Q -Air exchange rate
N_{in}/N_{out} - Number concentration indoors and outdoors with size selection.

ρ - Outdoor concentration of particles.

For the research presented within this thesis, indoor sources were consciously avoided, whilst a relatively rapid exchange rate and near simultanious indoor and outdoor measurements meant settling, resuspension and formation processes could be ignored. This reduced the complexity of understanding particulates indoors, understanding that they were almost all from outdoor sources and that the I/O ratio would be suitable for investigating I/O particulate measurements.

5.2. Literature review of key Indoor to outdoor research

Table 5-1 An overview of prior research with significance for research within this thesis.

Researchers	Date of Study	Method	Main Findings
Lunden et al.	2003	$PM_{2.5}$ collected experimentally Theoretical model applied	• Monitored outdoor and indoor particulates in an unoccupied home in Clovis, California. • Found that indoor ammonium nitrate concentrations were significantly lower than expected based off of penetration and deposition losses. • Difference attributed to transformation of indoor ammonium nitrate into ammonia and nitric acid gases, which are then lost via deposition and sorption into indoor surfaces.
Hämeri et al.	2004	Number and size distributions from DMPS measurements	• 1999-2003 measured aerosol number concentration and number size distribution in an urban area of Helsinki, Finland. • Simultaneous indoor and outdoor measurements were performed. • The use of a good quality air filter lowered concentrations by a factor of 10.
Hänninen et al.	2004	Studied $PM_{2.5}$ and SO_2 $NO_x$and 30 VOC's	• Indoor and outdoor settings in Helsinki, Basel, Prague, and Athens. • Ambient particles penetrate indoors very efficiently, removed by deposition, adsorption, and other mechanisms. • Some particles are generated indoors, even without combustion devices, the use of aerosol products, or cooking. • Calculated penetration efficiencies and air exchange.

			• Building materials, building, and family characteristics associated with indoor particle generation levels. • A significant fraction of the indoor concentrations remained unexplained.
Hussein et al.	(2005)	Number and size distributions from 2 x DMPS measurements [3-400nm]	• Family house with natural ventilation in Espoo, Finland. • Analysed the effects of indoor activities on indoor-to-outdoor relationship. • In the absence of indoor sources, particles migrated indoors from outdoors and number concentrations followed similar patterns as those outdoors. • Maximum penetration of particles between 100 and 400 nm in diameter.
Hussein et al.	2006	MC-SIAM model	• Estimated indoor-to-outdoor relationship of aerosol particles. • Natural ventilation did not provide a controlled indoor-to-outdoor relationship between outdoor and indoor particles. • A simple model is not sufficient for a multi-compartment residence. • Deposition rates were similar to previous studies. • Involved indoor sources. • Mean I/O value was 0.36 for ultrafine (UFP diameter <100 nm) and 0.60 for particles larger than 100 nm in diameter. • Natural ventilation did not lead to stable or controlled indoor-to-outdoor relationship.
Lazaridis et al.	2006	PM and gas concentrations	• 2002-2003 summer and winter in Oslo metropolitan area at two residential houses. • I/O measurements indicate the important contribution of outdoor air to indoor air quality. • No specific correlation was found between the I/O concentration and meteorological parameters.
Smolík et al.	2008	Berner type low pressure impactors, ion chromatography (IC) and proton induced X-ray emission (PIXE)	• Apartment in northwest suburb of Prague. • Temperature, pressure and relative humidity measured indoors and outdoors in parallel. • SMPS and APS used, radon technique used for ventilation rates. • Compared indoor and outdoor concentrations during a variety of indoor (particle-producing) activities.

Andelova et al.	2010	Berner type low pressure impactors, ion chromatography (IC) and proton induced X-ray emission (PIXE)	• Sampling indoor and outdoor environments in parallel. • Ammonium sulfate and nitrate formed about 30% of outdoor submicron fractions by mass. • Indoor nitrate concentrations decreased to zero • Ammonium nitrate probably evaporated after penetration due to higher indoor temperatures and fast deposition of gaseous nitric acid on surfaces.

5.3. Gaps in knowledge

It is clear that many important aspects of indoor air quality have been well researched. The majority of studies have focused on number size distributions, and have attributed source with the changing size of the particle. Filter measurements have also been commonly used to obtain details of composition within the indoor environment. However, these instruments run off-line so do not give detailed analysis when composition changes in a higher time resolution (such as diurnally).

To date, there is a lack of indoor research real time mass spectrometry to describe indoor aerosol composition. This would allow for high temporal observations of changing particle dynamics indoors, and would support size distribution and mass measurements. There are also times, indoors; when particulate are not beping produced, these should be accounted for, but requires a controlled environment to enable successful removal of indoor sources. The ability to use one set of instruments for both indoor and outdoor measurements removes uncertainty caused by inter-instrument comparisons, whilst a prolonged period of investigation of over 2 weeks would allow for greater contrast in conditions for comparisons.

5.4. References

Andelova, L., Smolik, J., Ondrackova, L., Ondracek, J., Lopez-Aparicio, S., Grontoft, T., & Stankiewicz, J. (2010). Characterization of Airborne Particles in the Baroque Hall of the National Library. Retrieved March 16, 2015, from http://www.morana-rtd.com/e-preservationscience/2010/Andelova-26-04-2010.pdf

Chan, A. T. (2002). Indoor–outdoor relationships of particulate matter and nitrogen oxides under different outdoor meteorological conditions. *Atmospheric Environment*, *36*(9), 1543–1551.

Diapouli, E., Chaloulakou, A., & Koutrakis, P. (2013). Estimating the concentration of indoor particles of outdoor origin: A review. *Journal of the Air & Waste Management Association*, *63*(10), 1113–1129. http://doi.org/10.1080/10962247.2013.791649

Diapouli, E., Eleftheriadis, K., Karanasiou, A. a., Vratolis, S., Hermansen, O., Colbeck, I., & Lazaridis, M. (2011). Indoor and outdoor particle number and mass concentrations in Athens. Sources, sinks and variability of aerosol parameters. *Aerosol and Air Quality Research*, *11*(6), 632–642. http://doi.org/10.4209/aaqr.2010.09.0080

Géhin, E., Ramalho, O., & Kirchner, S. (2008). Size distribution and emission rate measurement of fine and ultrafine particle from indoor human activities. *Atmospheric Environment*. Retrieved from http://www.sciencedirect.com/science/article/pii/S1352231008006535

Geller, M. D., Kim, S., Misra, C., Sioutas, C., Olson, B. a., & Marple, V. a. (2002). A Methodology for Measuring Size-Dependent Chemical Composition of Ultrafine Particles. *Aerosol Science and Technology*, *36*(6), 748–762. http://doi.org/10.1080/02786820290038447

Guo, H., Morawska, L., He, C., & Gilbert, D. (2008). Impact of ventilation scenario on air exchange rates and on indoor particle number concentrations in an air-conditioned classroom. *Atmospheric Environment*, *42*(4), 757–768. http://doi.org/10.1016/j.atmosenv.2007.09.070

Guo, H., Morawska, L., He, C., Zhang, Y. L., Ayoko, G., & Cao, M. (2010). Characterization of particle number concentrations and PM2.5 in a school: influence of outdoor air pollution on indoor air. *Environmental Science and Pollution Research International*, *17*(6), 1268–78. http://doi.org/10.1007/s11356-010-0306-2

Hämeri, K., Hussein, T., Kulmala, M., & Aalto, P. (2004a). Measurements of fine and ultrafine particles in Helsinki: Connection between outdoor and indoor air quality. In *Boreal Environment Research* (Vol. 9, pp. 459–467).

Hämeri, K., Hussein, T., Kulmala, M., & Aalto, P. (2004b). Measurements of fine and ultrafine particles in Helsinki: Connection between outdoor and indoor air quality. *Boreal Environment Research*, *9*(6), 459–467.

Hänninen, O. O., Lebret, E., Ilacqua, V., Katsouyanni, K., Künzli, N., Srám, R. J., & Jantunen, M. (2004). Infiltration of ambient PM2.5 and levels of indoor generated non-ETS PM2.5 in residences of four European cities. *Atmospheric Environment*, *38*(37), 6411–6423. http://doi.org/10.1016/j.atmosenv.2004.07.015

He, C., Morawska, L., Hitchins, J., & Gilbert, D. (2004). Contribution from indoor sources to particle number and mass concentrations in residential houses. *Atmospheric Environment*. Retrieved from http://www.sciencedirect.com/science/article/pii/S135223100400250X

Hering, S., & Cass, G. (1999). The Magnitude of Bias in the Measurement of PM25 Arising from Volatilization of Particulate Nitrate from Teflon Filters. *Journal of the Air & Waste Management Association*, *49*(6), 725–733. http://doi.org/10.1080/10473289.1999.10463843

Ho, K. F., Cao, J. J., Harrison, R. M., Lee, S. C., & Bau, K. K. (2004). Indoor/outdoor relationships of organic carbon (OC) and elemental carbon (EC) in PM2.5 in roadside environment of Hong Kong. *Atmospheric Environment*, *38*(37), 6327–6335. http://doi.org/10.1016/j.atmosenv.2004.08.007

Hussein, T., Glytsos, T., Ondráček, J., Dohányosová, P., Ždímal, V., Hämeri, K., … Kulmala, M. (2006). Particle size characterization and emission rates during indoor activities in a house. *Atmospheric Environment*, *40*(23), 4285–4307. http://doi.org/10.1016/j.atmosenv.2006.03.053

Hussein, T., Hameri, K., Aalto, P., Asmi, A., Kakko, L., & Kulmala, M. (2004). Particle size characterization and the indoor-to-outdoor relationship of atmospheric aerosols in Helsinki. *Scand J Work Environ Health*, *30 Suppl 2*, 54–62. http://doi.org/815 [pii]

Hussein, T., Hämeri, K., Heikkinen, M. S. A., & Kulmala, M. (2005). Indoor and outdoor particle size characterization at a family house in Espoo–Finland. *Atmospheric Environment*, *39*(20), 3697–3709. http://doi.org/10.1016/j.atmosenv.2005.03.011

Hussein, T., Karppinen, A., & Kukkonen, J. (2006). Meteorological dependence of size-fractionated number concentrations of urban aerosol particles. *Atmospheric …*. Retrieved from http://www.sciencedirect.com/science/article/pii/S135223100501037X

Hussein, T., & Kulmala, M. (2007). Indoor Aerosol Modeling: Basic Principles and Practical Applications. *Water, Air, & Soil Pollution: Focus*, *8*(1), 23–34. http://doi.org/10.1007/s11267-007-9134-x

Lazaridis, M., & Aleksandropoulou, V. (2006). characterization of indoor/outdoor particulate matter in two residential houses in Oslo, Norway: measurements overview and physical properties–URBAN-AEROSOL.

Indoor …. Retrieved from http://onlinelibrary.wiley.com/doi/10.1111/j.1600-0668.2006.00425.x/full

Lazaridis, M., & Aleksandropoulou, V. (2008). Sources and Variability of Indoor and Outdoor Gaseous Aerosol Precursors (O3, NOx and VOCs). *Water, Air, & Soil Pollution: Focus*, *9*(1-2), 3–13. http://doi.org/10.1007/s11267-008-9200-z

Lazaridis, M., Aleksandropoulou, V., Smolik, J., Hansen, J. E., Glytsos, T., Kalogerakis, N., & Dahlin, E. (2006). Physico-chemical characterization of indoor/outdoor particulate matter in two residential houses in Oslo, Norway: measurements overview and physical properties–URBAN-AEROSOL. *Indoor* …. Retrieved from http://onlinelibrary.wiley.com/doi/10.1111/j.1600-0668.2006.00425.x/full

Leung, D. Y. C., & Drakaki, E. (2015). Outdoor-indoor air pollution in urban environment: challenges and opportunity. *Frontiers in Environmental Science*, *2*(January), 1–7. http://doi.org/10.3389/fenvs.2014.00069

Lunden, M. M., Revzan, K. L., Fischer, M. L., Thatcher, T. L., Littlejohn, D., Hering, S. V., & Brown, N. J. (2003). The transformation of outdoor ammonium nitrate aerosols in the indoor environment. *Atmospheric Environment*, *37*(39-40), 5633–5644. http://doi.org/10.1016/j.atmosenv.2003.09.035

Mašková, L., Smolík, J., & Vodička, P. (2015). Characterisation of particulate matter in different types of archives. *Atmospheric Environment*, *107*, 217–224. http://doi.org/10.1016/j.atmosenv.2015.02.049

Morawska, L., He, C., Hitchins, J., Gilbert, D., & Parappukkaran, S. (2001). The relationship between indoor and outdoor airborne particles in the residential environment. *Atmospheric Environment*, *35*(20), 3463–3473. http://doi.org/10.1016/S1352-2310(01)00097-8

Nazaroff, W. W. (2004). Indoor particle dynamics. *Indoor Air*, *14*(Supplement 7). Retrieved from http://escholarship.org/uc/item/80f883g7

Riley, W. J., McKone, T. E., Lai, A. C. K., & Nazaroff, W. W. (2002). Indoor particulate matter of outdoor origin: Importance of size-dependent removal mechanisms. *Environmental Science & Technology*, *36*(2), 200–207. http://doi.org/10.1021/es010723y

Smolík, J., Dohányosová, P., & Schwarz, J. (2008). Characterization of indoor and outdoor aerosols in a suburban area of Prague. *Water, Air, & Soil* …. Retrieved from http://link.springer.com/article/10.1007/s11267-007-9141-y

Stelson, A., & Seinfeld, J. (1982). Relative humidity and temperature dependence of the ammonium nitrate dissociation constant. *Atmospheric Environment (1967)*, *16*(5), 983–992. Retrieved from http://www.sciencedirect.com/science/article/pii/0004698182901846

Zhu, Y., Hinds, W. C., Krudysz, M., Kuhn, T., Froines, J., & Sioutas, C. (2005). Penetration of freeway ultrafine particles into indoor environments. *Journal of Aerosol Science*, *36*(3), 303–322.

6. Overview of Instrumentation

6.1. Overview of Instrumentation

The need to investigate aerosol particles over 3 orders of magnitude (10nm-10µm) and composing of many different chemical species required of utilisation of a suite of Instrumentation during the different research campaigns discussed herein. The instruments were chosen to provide a complete and complimentary dataset within the confines of the natural and physical restrictions encountered, for example space and time availability.

The set of instrumentation typically consisted of online, fast time resolution instrumentation such as the SMPS and AMS systems (described below). These allowed observations of rapid changes in aerosol composition, number and mass.

Simultaneous offline cascade impactor measurements were made alongside the online instrumentation. These instrumentation collected samples over a longer period of time, usually 24 hours for the campaigns discussed within. Cascade impactors do not provide information of rapid changes in aerosol composition, however they provide reliable samples for composition analysis, and present a much wider size distribution than the online instrumentation, from the ultra-fine to coarse modes.

A key implement during the research was an automated switching valve. This enabled sampling from outdoors to indoors via an automated timer that was programmed to turn every 10 minutes. The almost simultaneous sampling of outdoor and indoor air was a fundamental part of Articles 2 and 3.

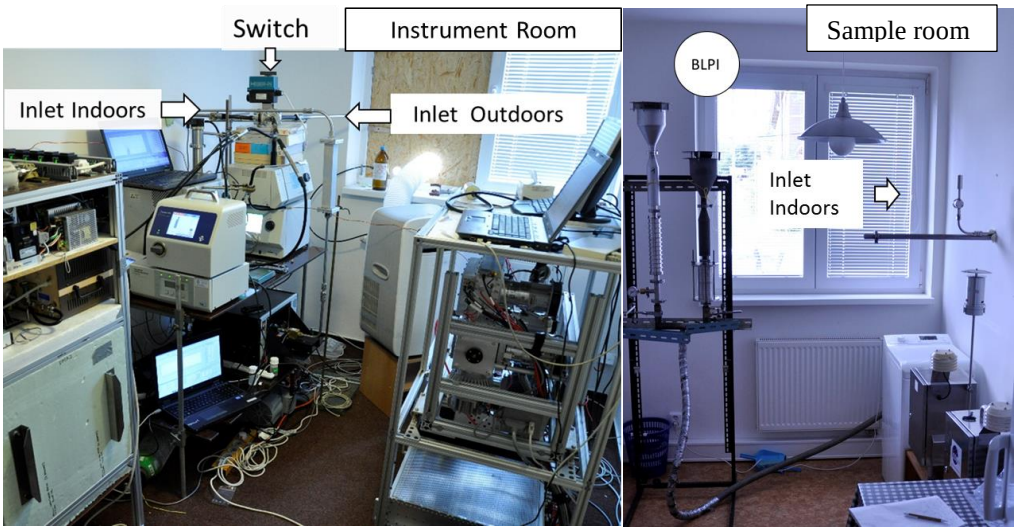

Figure 6-1 Photos of the instrument set-up for the summer and winter campaigns described in Articles 2 and 3 (Photocredit: J.Ondracek).

6.2. Scanning Mobility Particle Sizer

Particle number and mass size distributions were measured using a mobility particle size spectrometer operated in the scanning mode, referred to as a Scanning Mobility Particle Sizer (SMPS). The SMPS system comprises of an electrostatic classifier and particle detector. The electrostatic classifier contains an impactor, Differential Mobility Analyser (DMA) and a neutraliser. This system segregates particles according to their mobility in an electrostatic field. For particle detection after size separation a Condensation Particle Counter is used.

The sampled aerosol enters the system through the sampling inlet at a determined sample rate and is passed to a bipolar charger (neutralizer) which neutralizes the particles. The aerosol particles then enter the DMA where the particles are classified according to their electrical mobility. The electrical mobility of each particle is in accordance to their size with the smallest particles having the largest electrical mobility in accordance with the charging of each particle. Only particles of a certain mobility exit the DMA and pass through to the CPC to be counted, and this determines the particle concentration in that size range.

The DMA consists of a cylinder with a charged rod in the centre. The main flow of air through the DMA is particle free sheath air, with a laminar flow. The sampled poly-dispersed aerosol enters the DMA and particles with a positive charge move across the sheath flow towards the negatively charged central rod, at a rate determined by the particle's electrical mobility. Thus, particles of a certain mobility pass through the exit slit, whilst all other particles are carried away by the sheath flow. The size of particles exiting through the slit to the CPC is determined by the particle size and charge, the central rod voltage and flow within the DMA. By scanning the voltage across the central rod in the DMA, a full particle size distribution is collected.

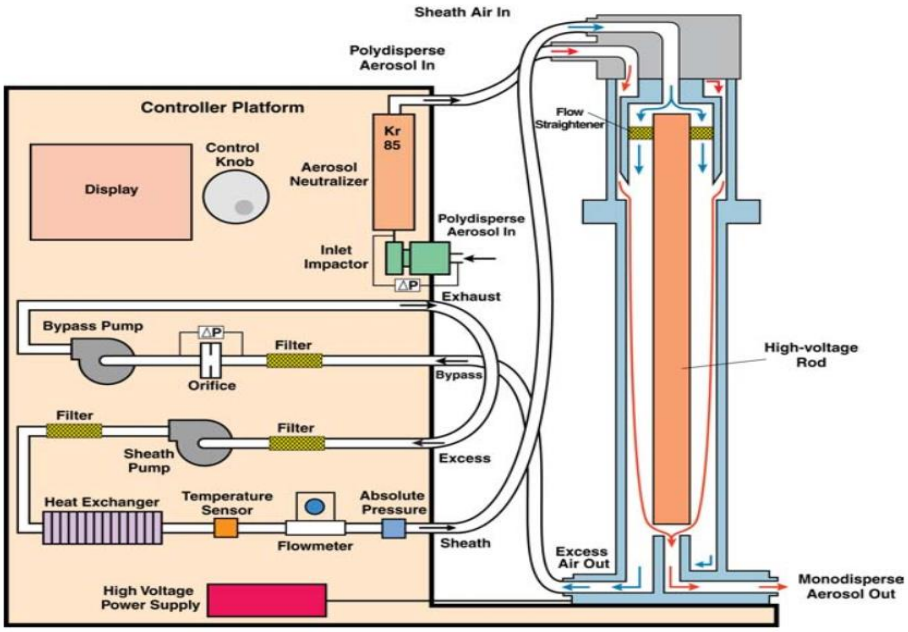

Figure 6-2 A schematic sketch of the TSI 3080 SMPS set-up (TSI Manual).

6.3. Compact Time of Flight Aerosol Mass Spectrometer (C-ToF-AMS).

The c-ToF-AMS (hereafter referred to as AMS) provides real-time measurements of chemical composition and size distribution of non-refractory (NR) submicron aerosol particles within the

vacuum aerodynamic diameter (d_{va}) range of 30–600 nm. Particles of other sizes are transmitted into the detection region with lower efficiencies with a total fraction count of ~$PM_{0.7}$.

The Aerodyne Time of Flight Aerosol Mass Spectrometer (TOF-AMS) is an instrument manufactured by Aerodyne Research Inc. and is used to study the chemical and physical nature of aerosol particles online, provides real-time measurements of NR-$PM_{1.}$with very high time resolution. The instrument works by focusing the sampled particles into a tightly collimated beam at its inlet and skimming off the majority of the gas phase material before impacting them onto a heated surface. The non-refractory components of the particles instantly vaporise and the vapours produced are analysed using electron ionisation mass spectrometry. The particle beam can also be modulated using a chopper wheel and the particle sizes calculated by measuring their velocities (Jayne et al., 2000).

Scientifically, the instrument can deliver quantitative mass concentrations of the major non-refractory chemical species present in submicron particles (ammonium, nitrate, sulphate, Non-refractory organics and non-sea-salt chloride). The results are given in µg/m^3 It is also capable of delivering these concentrations as a function of diameter as a dM/dlog(D) distribution. Further to this, information on the chemical nature of the organic fraction can be derived by inspecting the relative sizes of the peaks within the mass spectrum. In order to produce fully quality assured and meaningful results, the data must be processed offline.

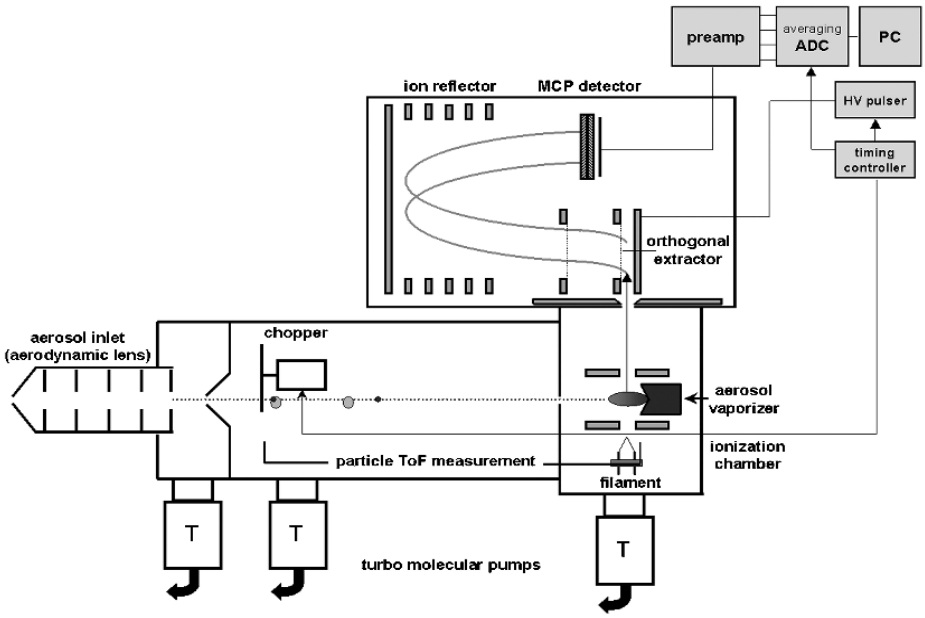

Figure 6-3 Schematic diagram of Aerodyne Aerosol Mass Spectrometer (Drewnick et al., 2005).

For the research presented within this document, the AMS alternated between the particle time-of-flight (PToF) mode and the mass spectra (MS) mode each sampling period (1 min). Under the PToF mode operation, the aerosol beam was chopped by a chopper wheel with radial slit. Particle size information was obtained as a function of particle time-of-flight in non-refractory (NR)-PM_1. Reported mass concentrations and size distributions were then averaged. The AMS was calibrated weekly during the campaigns using the brute force single particle mode (Decarlo et al., 2006; Drewnick et al., 2005)

6.4. Elemental Carbon /Organic Carbon

Elemental carbon and organic carbon (EC and OC) measurements were conducted by two semi-online field OC/EC analysers (Sunset Laboratory Inc. USA) in parallel (one sampling outdoor, second indoor), both with a $PM_{2.5}$ cyclone inlet (flow rate 8 lpm). The instruments were equipped with a carbon parallel-plate diffusion denuder (Sunset Lab.) to remove volatile organic compounds which may cause a positive bias in the measured OC concentrations. The denuder was placed at ambient outdoor conditions during outdoor measurements and inside of room during indoor measurements.

Samples were taken at 2-h intervals, including the thermal-optical analysis which lasts about 15 minutes. The analysis was performed using the shortened EUSAAR2 protocol – step [gas] temperature [°C] /duration [s]: He 200/90, He 300/90, He 450/90, He 650/135, He-Ox. 500/60, He-Ox. 550/60, He-Ox. 700/60, He-Ox. 850/100 (Vodička et al., 2013). The collected OC was evaporated and then oxidized to CO_2 either on a MnO_2 catalyst or together with EC on the filter by oxygen in the He/Ox phase, and analysed by a non-dispersive infrared (NDIR) detector. Automatic optical corrections for charring were made during each measurement and the split point between EC and OC was detected automatically (software: RTCalc522, Sunset Laboratory Inc. (USA).

6.5. Cascade Impactors

Cascade impactors operate on the principle of inertial impaction, which a function of particle size and velocity. Impactors consist of a series of stages each made up of a plate, with specific nozzle structures and different collection surface depending on impactor type. Sampled air is drawn into the impactor, flowing successively through the stages; nozzle size and total nozzle area decrease with stage number to accelerate the flow, thus increasing the inertia.

As particles pass through the nozzles they either remain entrained in the air stream, which is directed through a right angle at the exit of the nozzle, or break through the lines of flow, impacting on the collection medium. Particles with sufficient inertia are collected, the rest pass onto the next stage.

This function enables each stage of the impactor to have an associated cut-off diameter, characterizing the size of particles that are retained on the collection surface of that stage. Ideally, the collection efficiency would be a step function, where all of the particles above a certain size would be captured and those below it would pass through. In reality there is a curve from which D_{50}, the stage cut-off diameter, is determined (Figure 6-3).

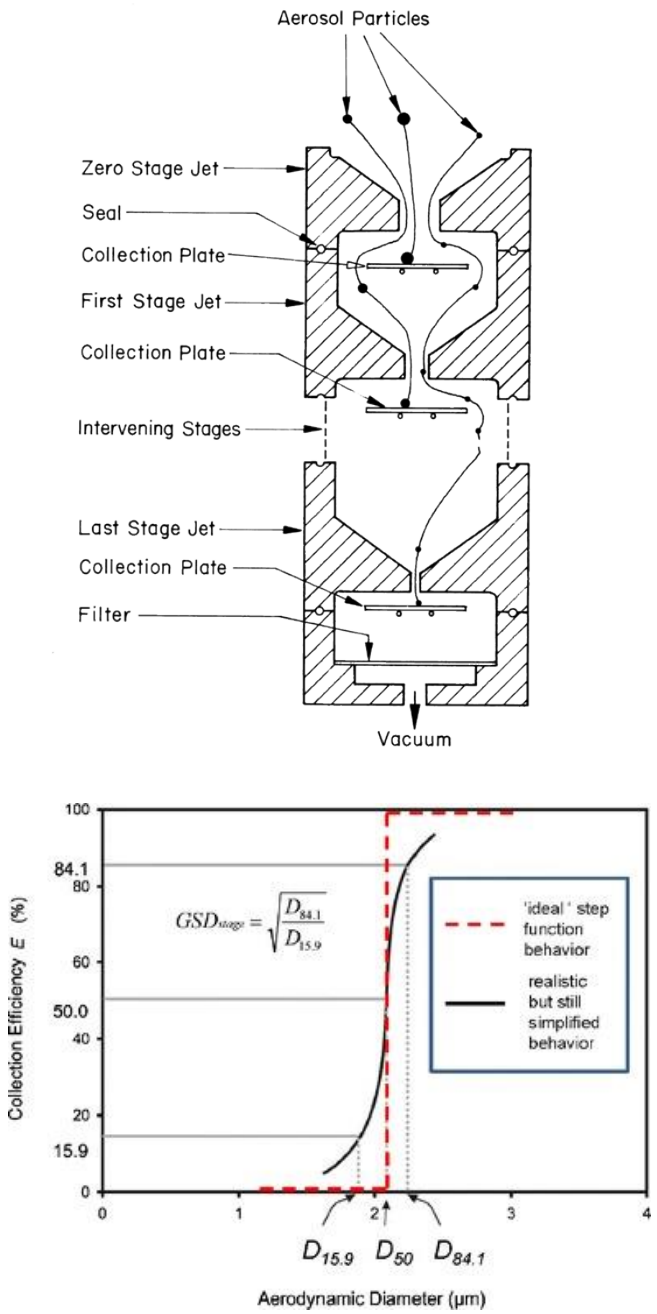

Figure 6-4 A schematic of the operation of the cascade impactor (Top) (Kulkarni and Baron, 2011), and CI stage collection efficiency curve showing "ideal" step function case and realistic but simplified model for establishing cut size (D_{50}) and related measures ($D_{15.9}$ and $D_{84.1}$), describing the stage cut-off (Roberts and Mitchell, 2013).

6.5.1. 10 stage Berner low pressure impactor

A Berner Low-Pressure Impactor (BLPI, 25/0.018/2, Hauke, Austria; (Berner *et al.*, 1979; Preining and Berner, 1979) was deployed in 3 experiments described within this thesis, and was used as the 'standard' instrument, due to its well understood characterisation in Štefancová, (2011).

This impactor collected particles onto PET foils (Mylar 13 µm thick) (flow rate 24.8 L min^{-1}) whilst separating particle mass into 10 size fractions. The cut diameters of the stages were 0.03, 0.056, 0.1, 0.16, 0.25, 0.43, 0.86, 1.73, 3.425, and 6.61 µm. The impactors were equipped with inlets with the cut-point calculated as 14 µm.

6.5.2. Nano' 8 stage Berner impactor

A modified BLPI (denominated as nano-BLPI, 10/0.01, Hauke, Austria) collecting particles on PET foils (Mylar 13 µm thick) (flow rate 17.2 L min^{-1}) from 0.01 µm to 1.95 µm in 8 size stages. The aerodynamic cut diameters of stages 1 to 8 were 0.011, 0.024, 0.039, 0.062, 0.095, 0.24, 0.49, 1.0 µm, and the inlet cut-point was calculated as 1.95 µm.

6.5.3. Nano-Micro-orifice Uniform Deposit Impactor

A Nano-Micro-orifice Uniform Deposit Impactor (Nano-MOUDI-II™, MSP Corp., Shoreview, MN, USA Model 125R; U.S. Patent # 6,431,014B1) equipped with Teflon filters (with diameters of 47 mm) were used to collect size-resolved aerosol samples. These impactors effectively separated the particulate matter into 13 stages with nominal cut diameters of 0.010, 0.018, 0.03, 0.06, 0.10, 0.18, 0.32, 0.56, 1.0, 1.8, 3.2, 5.6 and 10 µm when operated at an inlet flow rate of 10 L min^{-1}. The individual stages of this impactor rotate to smooth out the sample over the collection substrate and has a heated shell to protect the stages.

6.5.4. Soutas personal cascade impactors

Personal cascade impactor samplers (Sioutas™ PCIS, SKC Inc) (Misra et al., 2002) operating with a flow rate of 9 L min^{-1} at a pressure drop of 11 inches of H_2O (2.7 kPa). Particles can be separated in the following aerodynamic particle diameter ranges: <0.25; 0.25 to 0.5; 0.5 to 1.0; 1.0 to 2.5; and 2.5 to 10 µm. The collection substrates were 37 mm PTFE filters (Pall) or quartz fibre filters (Pall) for the < 0.25 µm stage and 25 mm PTFE filters (Pall) for the 0.25-2.5 µm and 2.5-10 µm stages. Two of the PCIS deployed in Prague separated particle mass in all of the 5 size fractions while another unit collected particles only at 3 of the stages (< 0.25 µm; 0.25-2.5 µm and 2.5-10 µm).

6.6. References

Decarlo, P. F., Kimmel, J. R., Trimborn, A., Northway, M. J., Jayne, J. T., Aiken, A. C., … Jimenez, J. L. (2006). Aerosol Mass Spectrometer. *Analytical Chemistry*, *78*(24), 8281–8289. http://doi.org/8410.1029/2001JD001213.Analytical

Drewnick, F., Hings, S. S., DeCarlo, P., Jayne, J. T., Gonin, M., Fuhrer, K., … Worsnop, D. R. (2005). A New Time-of-Flight Aerosol Mass Spectrometer (TOF-AMS)—Instrument Description and First Field Deployment. *Aerosol Science and Technology*, *39*(7), 637–658. http://doi.org/10.1080/02786820500182040

Jayne, J. T., Leard, D. C., Zhang, X. F., Davidovits, P., Smith, K. A., Kolb, C. E., & Worsnop, D. R. (2000). Development of an aerosol mass spectrometer for size and composition analysis of submicron particles. *Aerosol Sci. Tech.*, *33*(1-2), 49–70. http://doi.org/10.1080/027868200410840

Misra, C., Singh, M., Shen, S., Sioutas, C., & Hall, P. (2002). Development and evaluation of a personal cascade

impactor sampler (PCIS). *Journal of Aerosol Science*. Retrieved from http://www.sciencedirect.com/science/article/pii/S0021850202000551

Kulkarni, Baron, K. W. (2011). *Aerosol Measurement: Principles, Techniques, and Applications*. John Wiley & Sons. Retrieved from https://books.google.com/books?id=ETvXooNW4-EC&pgis=1

Roberts, D. L., & Mitchell, J. P. (2013). The effect of nonideal cascade impactor stage collection efficiency curves on the interpretation of the size of inhaler-generated aerosols. *AAPS PharmSciTech*, *14*(2), 497–510. http://doi.org/10.1208/s12249-013-9936-2

Štefancová, L., Schwarz, J., Mäkelä, T., Hillamo, R., & Smolík, J. (2011). Comprehensive Characterization of Original 10-Stage and 7-Stage Modified Berner Type Impactors. *Aerosol Science and Technology*, *45*(1), 88–100. http://doi.org/10.1080/02786826.2010.524266

Vodička, P., Schwarz, J., & Ždímal, V. (2013). Analysis of one year's OC/EC data at a Prague suburban site with 2-h time resolution. *Atmospheric Environment*, *77*, 865–872. http://doi.org/10.1016/j.atmosenv.2013.06.013

Wiedensohler, A., Birmili, W., Nowak, A., Sonntag, A., Weinhold, K., Merkel, M., … Bastian, S. (2012). Mobility particle size spectrometers: Harmonization of technical standards and data structure to facilitate high quality long-term observations of atmospheric particle number size distributions. *Atmospheric Measurement Techniques*, *5*(3), 657–685. http://doi.org/10.5194/amt-5-657-2012

7. Justification of the research

7.1. Importance and objectives of this thesis: research needs

The aims and objectives of this thesis and the papers contained within can be described by the following questions,

1. How does ammonium nitrate behave in an unmixed state when subjected to changes in particle size, temperature and residence time within a reactor, under low water contents?
2. How does a modelled response to ammonium nitrate dissociation behaviour compare to observations from laboratory experiments?
3. Can aerosol compositional dynamics be observed when utilising high temporal resolution instrumentation?
4. Do indoor chemical species represent those observed outdoors?
5. Are there seasonal differences in the behaviour of nitrate? Is there a seasonal response indoors?
6. How do online and offline instrumentation compare when observing indoor and outdoor mass concentrations of different species?

To address the first and second objectives, we developed an experiment that allowed nebulised and dried ammonium nitrate aerosol to be observed before and after a 2m long, laminar flow reactor set at various temperatures and switching flowrates to allow for various residence times within the reactor. Using 'clean' and dried air and ultrapure water the system was kept as pure as possible. Observed changes in mass allowed for dissociation constants to be created, these could be set against a model created from known parameters (Hinds, 2012).

The modelled tools can be powerful tools in understanding particle dynamics (Asmi et al., 2004), and whilst some researchers have either investigated dissociation behaviour via experimentation, (Dassios & Pandis, 1999; Hightower & Richardson, 1988; Stelson & Seinfeld, 1982) or have used models to observe changing dynamics of ammonium nitrate from outdoors to indoors (Lunden et al., 2003), there was little knowledge on the dissociation rates and behaviour of ammonium nitrate when travelling through the equivalence of a heated inlet. The changes in size and mass observed through these processes could then be applied to observed losses in field experiments where inlets have observed losses to ammonium nitrate or in such instances where ammonium nitrate is used for calibration standards, as is the case for the AMS.

The focus of the research then shifted towards field experimentation observations. To this end a metro campaign and two intensive campaigns were undertaken during summer 2014 and winter 2015. A switching system was utilised to observe indoor and outdoor air samples within a 10 minute switching cycle, whilst online instrumentation such as SMPS and AMS allowed for almost real time continuous measurements of both environments and for different seasons. The seasonal

aspect was believed to be important due to compositional changes observed over European sites during summer and winter (Schwarz et al. 2012; Vodička et al. 2013). The high temporal resolution allowed for diurnal observation in the changes of chemical characteristics outdoors. These included large mass concentration fluctuations that were observed diurnally during summer, and a nitrate flux throughout the day, rarely reported upon in previous literature (Kubelová et al., 2015; Poulain et al., 2011), but a seemingly important driver in mass concentrations over heavily populated areas.

There are very few studies that have investigated seasonal variations for indoor and outdoor chemical composition (Leung & Drakaki, 2015). However, with the knowledge that the outdoor composition changes according to season, it seemed reasonable to assume that that indoor chemical composition would also change should question four be true in accordance to findings in previous work (Hussein et al., 2005). To investigate this theory the seasonal campaigns required a sample room with no indoor sources, as to be certain that the indoor composition truly reflected those outdoors.

The meteorology for both seasonal analysis was carefully considered, and to obtain detailed analysis on indoor and outdoor dynamics, a statistical test was carried out using Spearman rank correlation and associated P-test. These tests were designed to find any given relationship between different typical meteorological parameters such as max/min temperatures, humidity, wind speed and atmospheric pressure, and outdoor / indoor concentrations of the key outdoor chemical species.

Finally, a selection of cascade impactors were intercompared in two different airmass types. This was carried out due to the existance of uncertianties in datasets on deposition substrates when investigating semi-volatile species. These uncertainties are amplified in the ultrafine partcile modes, however, to date no intercomparisons had been carried out to investigate these measurement uncertainties.

7.2. References

Asmi, A. J., Pirjola, L. H., & Kulmala, M. (2004). A sectional aerosol model for submicron particles in indoor air. *Scandinavian Journal of Work, Environment & Health*, *30 Suppl 2*, 63–72. Retrieved from http://www.ncbi.nlm.nih.gov/pubmed/15487687

Cape, J. ., Methven, J., & Hudson, L. . (2000). The use of trajectory cluster analysis to interpret trace gas measurements at Mace Head, Ireland. *Atmospheric Environment*, *34*(22), 3651–3663. http://doi.org/10.1016/S1352-2310(00)00098-4

Dassios, K. G., & Pandis, S. N. (1999). The mass accommodation coefficient of ammonium nitrate aerosol. *Atmospheric Environment*, *33*(18), 2993–3003.

Hightower, R. L., & Richardson, C. B. Evaporation of ammonium nitrate particles containing ammonium sulfate, 22 Atmospheric Environment 2587–2591 (1988).

Hinds, W. C. (2012). *Aerosol Technology: Properties, Behavior, and Measurement of Airborne Particles*. John Wiley & Sons. Retrieved from https://books.google.com/books?hl=en&lr=&id=qIkyjPXfWK4C&pgis=1

Hussein, T., Hämeri, K., Heikkinen, M. S. A., & Kulmala, M. (2005). Indoor and outdoor particle size characterization at a family house in Espoo–Finland. *Atmospheric Environment*, *39*(20), 3697–3709. http://doi.org/10.1016/j.atmosenv.2005.03.011

Kubelová, L., Vodička, P., Schwarz, J., Cusack, M., Makeš, O., Ondráček, J., & Ždímal, V. (2015). A study of summer and winter highly time-resolved submicron aerosol composition measured at a suburban site in Prague. *Atmospheric Environment*, *118*, 45–57. http://doi.org/10.1016/j.atmosenv.2015.07.030

Leung, D. Y. C., & Drakaki, E. (2015). Outdoor-indoor air pollution in urban environment: challenges and opportunity. *Frontiers in Environmental Science*, *2*(January), 1–7. http://doi.org/10.3389/fenvs.2014.00069

Lunden, M. M., Revzan, K. L., Fischer, M. L., Thatcher, T. L., Littlejohn, D., Hering, S. V., & Brown, N. J. (2003). The transformation of outdoor ammonium nitrate aerosols in the indoor environment. *Atmospheric Environment*, *37*(39-40), 5633–5644. http://doi.org/10.1016/j.atmosenv.2003.09.035

Morgan, W. T., Allan, J. D., Bower, K. N., Capes, G., Crosier, J., Williams, P. I., & Coe, H. (2009). Vertical distribution of sub-micron aerosol chemical composition from North-Western Europe and the North-East Atlantic. *Atmospheric Chemistry and Physics Discussions*, *9*, 9117–9150. http://doi.org/10.5194/acpd-9-9117-2009

Poulain, L., Spindler, G., Birmili, W., Plass-Dülmer, C., Wiedensohler, A., & Herrmann, H. (2011). Seasonal and diurnal variations of particulate nitrate and organic matter at the IfT research station Melpitz. *Atmospheric Chemistry and Physics*, *11*(24), 12579–12599. http://doi.org/10.5194/acp-11-12579-2011

Putaud, J.-P., Van Dingenen, R., Alastuey, A., Bauer, H., Birmili, W., Cyrys, J., … Raes, F. (2010). A European aerosol phenomenology – 3: Physical and chemical characteristics of particulate matter from 60 rural, urban, and kerbside sites across Europe. *Atmospheric Environment*, *44*(10), 1308–1320. http://doi.org/10.1016/j.atmosenv.2009.12.011

Schwarz, J., Štefancová, L., & Maenhaut, W. (2012). Mass and chemically speciated size distribution of Prague aerosol using an aerosol dryer—The influence of air mass origin. *Science of the Total …*. Retrieved from http://www.sciencedirect.com/science/article/pii/S0048969712009953

Stelson, A., & Seinfeld, J. (1982). Relative humidity and temperature dependence of the ammonium nitrate dissociation constant. *Atmospheric Environment (1967)*, *16*(5), 983–992. Retrieved from http://www.sciencedirect.com/science/article/pii/0004698182901846

Vodička, P., Schwarz, J., & Ždímal, V. (2013). Analysis of one year's OC/EC data at a Prague suburban site with 2-h time resolution. *Atmospheric Environment*, *77*, 865–872. http://doi.org/10.1016/j.atmosenv.2013.06.013

8. Article 1

An Experimental and Theoretical Assessment on the Dissociation Behaviour of Ammonium Nitrate

Nicholas Talbot[a,b], Jakub Ondracek[a], Jaroslav Schwarz[a], Kayleigh Kavanagh[a], Vladimir Zdimal[a].

[a]Institute of Chemical Process Fundamentals of the ASCR, v. v. i. Prague 6, Czech Republic
[b]Charles University, Faculty of Science, Department of Environmental Studies, Prague, 128 43, Czech Republic.

In preparation

Pages: 61-76

Published in: Unknown

Impact factor of Journal: Unknown

An Experimental and Theoretical Assessment on the Dissociation Behaviour of Ammonium Nitrate

Nicholas Talbot[a,b], Jakub Ondracek[a], Jaroslav Schwarz[a], Kayleigh Kavanagh[a], and Vladimir Zdimal[a].

[a]Institute of Chemical Process Fundamentals of the ASCR, v. v. i. Prague 6, Czech Republic
[b]Charles University, Faculty of Science, Department of Environmental Studies, Prague, 128 43, Czech Republic.

Keywords: Ammonium nitrate, dissociation, partial pressure, shrinkage.

Abstract

The volatility of ammonium nitrate at typical ambient conditions creates challenges for the aerosol research community. Attributed effects of ammonium nitrate dissociation include the creation of data artefacts, health implications, calibration uncertainties, and the accelerated degradation of antiquities. This paper sets out to achieve 2 objectives. Firstly, to provide a comprehensive overview of prior research into ammonium nitrate dissociation, to enable the assessment of the state of current knowledge. Secondly, to further the understanding of the dissociation process at the ultrafine particle scale, an area where prior research is limited.

To achieve the second objective, the results of an original experimentation are described. Nebulised ammonium nitrate particulate size and mass were recorded before and after transportation through a temperature controlled, 2-meter laminar flow reactor. The resultant changes in size and mass were then used to derive consequent shrinkage and dissociation rates. Results from size distribution data show an accelerated shrinkage of particles of 200nm (dp = 0 in 200 Sec), whilst each smaller particle size of 100 and 50nm shrank at a progressively slower rate. Moreover, dissociation rates (Kc) derived from integrated mass gave an inverse relationship to the shrinkage results. It was found the smaller particulate dissociated at a quicker rate, ranging from 200nm particle at 15˚C: Kc = 1.2 ppb^2 compared to 50nm particle at 25˚C: Kc = 3882 ppb^2. Accelerated dissociation through the continuum indicated the existence of a kinetic constraint underlining the importance of particle size on dissociation and shrinking rate of ammonium nitrate dissociation.

1. Introduction

Ammonium nitrate accounts for an estimated 30% of fine particulate mass over continental landmasses (Schaap, van Loon, ten Brink, Dentener, & Builtjes, 2004). Their influence can be of macro-scale such as radiative forcing and climatic (Pachauri & Meyer, 2014) or local, such as visibility, health, relic degeneration and artefact generation on filter measurements (T. Larson & Taylor, 1983; Lunden et al., 2003; Pope et al., 2014; Smolík, Mašková, Zikova, Ondráčková, & Ondráček, 2013). Ammonium nitrate (NH_4NO_3) occurs in the atmosphere when NO and NO_2 are oxidized to form HNO_3 which is then neutralised primarily by NH_4, the dominant atmospheric base, to form NH_4NO_3 (Lightstone, Onasch, Imre, York, & Oatis, 2000). NH_4NO_3 is commonly found in the accumulation mode between 100-500nm, allowing for prolongued residence time in the atmosphere (Bergin, Ogren, Schwartz, & Mcinnes, 1997). It is volatile under typical atmospheric conditons and will readily dissociate into its primary gases NH_3 and HNO_3 in the following reversable reactions (a. W. Stelson, Friedlander, & Seinfeld, 1979).

$NH_4NO_3(s) \rightleftharpoons HNO_3(g) + NH_3(g)$
$NH_4^+(aq)\ NO_3^-(aq) \rightleftharpoons HNO_3(g) + NH_3(g)$ **(1)**

In particle form, NH_4NO_3 can be either chrystalline (solid) or a supersaturated aqueous solution (Aq) with its phase being dependent on temperature and relative humidity (RH) (Seinfeld & Pandis, 2012). Previous research has demonstrated deliquescence of chrystalline NH_4NO_3 at 62% RH. However due to hysterisis, aqueous NH_4NO_3 does not recrystalise until RH is less than 20%. Moreover, recent studies indicates that where a solution of NH_4NO_3 has been used to generate aerosol, the resulting particles recrystalise at relative humidity values of less than 10% (Dassios & Pandis 1999) or less than 5% (Hu et al. 2011). It appears the history of the NH_4NO_3 particle is essential to understanding its chemistry (Martin, 2003).

The size distribution of NH_4NO_3 was found to have a significant effect on the overall dissociation rate in theoretical research by Bai et al. (1995). They conclude that to neglect size parameter effects of the NH_4NO_3 particle as well as innapropraite deployment of kinetic theory would lead to significant departures from theoretically derived results. Mozurkewich (1993) found for particles less than 100nm, the Kelvin effect has a substantial effect on the dissociation constants values.

With a relatively high vapour pressure, uncertainties regarding its phase state, its prominent use as a calibration medium for AMS measurements and its prominent occuarnce in total mass concentrations around the world makes ammonium nitrate a very important but challengine chemical species to understand, amd although there is a rich depth of ammonium nitrate research as will be demonstrated in section 2, there are still gaps in knowledge about shrinking rates of ammonium nitrate when compared to particle size, rates of shrinking and disscoiation behaviour.

This paper provides a comprehensive revision of prior research into ammonium nitrate, then describes results on the fundermental properties of NH_4NO_3 dissociation behaviour, utilising both experimental and theoretical approaches. A series of laboratory dissociation experiements and a dynamic theoretical model are considered and discussed. Resultant shrinking and dissociation rates through kinetic and continuem regimes are derived in relation to temperature, residence time and particle size.

2. Comprehensive review of prior research

To date, a variety of techniques have been employed in previous research which have often garnered differing, sometimes contradictory or uncertain, results. Within this section a chronological review of all major studies that have added to the current knowledge of ammonium nitrate disscocaition properties is presented in Table 1, results are shown in table 2 and section 2.1 shows the equations for dry and wet ammnium nitrate particles.

Table 2. A review of previous NH_4NO_3 research based only on research where fundamental dissociation behaviour was described,

Researchers	Date of Study	Method	Methodology and Findings
Stelson & Seinfeld	*1982*	Experimental	• Predict temperature and RH dependence of the NH_4NO_3 dissociation constant. Theory agrees with atmospheric data. • Results are provided in Table 2.
Larson and Taylor	*1982*	Experimental and Modelled	• Found that NH_4NO_3 particles' experimental evaporation rates agreed with their theoretical predictions and with Knudsen's diffusion theory. The experimental values were obtained by using a diffusion stripped to remove gaseous NH_3 and HNO_3 from an aerosol containing NH_4NO_3 droplets, which led to the evaporation of NH_4NO_3.
Richardson and Hightower	*1987*	Experimental	• Levitated solid and aqueous phase ammonium nitrate particles and measured the resultant size and mass changes using mass balance and light scattering techniques. • metastable liquid had a 17% increase in evaporation when the particle radius was near 2 µm, though the authors were unable to provide an external force that would result in such changes. • Additionally, inconsistent results for solid phase NH_4NO_3 gave rates 48 times slower than predicted by theory. This led to the introduction of an accommodation coefficient of 0.02-0.004 to compensate for this undefined kinetic restraint across the particle surface.
Allen, Harrison, & Erisman	*1989*	Field experiments(Denuder)	• Measured atmospheric concentrations of HNO_3, HCL and NH_3 at Essex, UK (filter pack) and Cabuaw, Netherlands (denuder) • Integration times of 3, 12, and 24 h • Experimental concentrations of products generally agreed with predictions of chemical thermodynamics • No firm conclusions reached regarding differences between theoretical and experimental values.
Harrison et al.	*1990*	Field experiments	• Shrinking rates of -0.45×10^{-10} / -0.49×10^{-10} ms^{-1} for solid and aqueous phase particles.

		(Denuder)	• Rates were independent of particles size, and, similar to Richardson and Hightower's (1987) work, • Much lower than theoretical predictions, pointing to an unknown kinetic constraint on achieving equilibrium at atmospheric conditions.
Mozurkewich	*1993*	Theoretical application of thermodynamics	• Work encompassed three calculation methods and five independent data sets, which were reportedly in excellent agreement with each other. • Determining equations for the dissociation of NH_4NO_3, it was found that the Kelvin effect plays a large role in the dissociation of particles less than 100 nm. Additionally, particle size was found to have little effect on the deliquescence point.
Bai et al.	*1995*	Mathematical model compared to experimental findings elsewhere	• Model incorporated particle polydispersity, flow, number concentrations, size dynamics, gas-particle interaction and accommodation coefficient to determine the evaporation of dry ammonium nitrate. • These theoretical results were then compared with the available literature, and discrepancies between the values were investigated. They conclude that to neglect the size parameter effects of the NH_4NO_3 particle and inappropriate deployment of kinetic theory would lead to significant departures from theoretically derived results.
Bergin et al.	*1997*	Theoretical model	• An associated accommodation coefficient of unity that accurately described their experimental data. Investigated ammonium nitrate particles of 300 nm.
Cheng & Tsai	*1997*	Filter sampling/ Modelled	• Experimental and theoretical results were in agreement. • Upstream particle concentration has large effect on the evaporation loss of ammonium nitrate particles.
Dassios and Pandis	*1999*	Experimental TDMA system and modelled system.	• Temperatures between 20-27 ˚C and particles in the 80-220 nm. • Evaporation rates were slightly slower than predicted, experimental findings were still consistent with their theoretical work. • Results were then compared to a theoretical expression of the evaporation rate, which took into account both the Kelvin effect and the effect of RH on the equilibrium constant

			• Mass accommodation coefficient of 0.8 to 0.5 when temperature increases from 20-27 ˚C.
Lunden et al	*2003*	$PM_{2.5}$ collected experimentally Theoretical model applied	• Monitored outdoor and indoor particulates in a unoccupied home in Clovis, California. • Found that indoor ammonium nitrate concentrations were significantly lower than expected based off of penetration and deposition loss. • Difference attributed to transformation of indoor ammonium nitrate into ammonia and nitric acid gases, which are then lost via deposition and sorption into indoor surfaces.
Hu, Chen, Ye, Li, & Yang,	*2011*	HT-DMA experimental	• Particle sizes 40-200 used nm. • Volatile properties of NH_4CL and NH_4NO_3 led to great differences between measured hydroscopic growth factors and theoretical values.

2.1. Dissociation constants

Many of the previous experiments offer dissociation constant expressions for solid or deiquescent partciles of ammonium nitarte, they are uually derived from known thermodynamic behaviour of the nitric acid/ammonia system. For ammonium nitrate below realtive humidity of 62% the particles can be considered dry and the following dissociation constants are considered.

Although there are several other constants, deriving from slightly different thermodynamic datasets, the 2 that are presented in Table 2 are most commonly referenced and therefore described here. The equations for wet ammonium nitrate particles are the core constituents. To view the full calculation procedure, refer to the cited manuscripts.

Table 3. Calculations for dissociation constants are shown from two separate studies.

Dry ammonium nitrate particulate	Wet ammonium nitrate particulate
(M Mozurkewich, 1993) $k\rho$ = 118.87- $\frac{2408}{T}$ + 6.025 ln(T)	(M Mozurkewich, 1993) k^*_P = (P1 - P2(1-a_w)+P3(1-a_w)^2 x (1-a_w)$^{1.75}$ x $k\rho$ ln(P1) = -135.94 + $\frac{8763}{T}$ + 19.12ln(T) ln(P2) = -122.65 + $\frac{9962}{T}$ + 16.22 ln (T) ln(P3) = -182.61 + $\frac{13875}{T}$ + 24.46 ln (T)
(Stelson et al. 1982) $k\rho$ = 70.82 + $\frac{24090}{T}$ + 6.04 (T)	(Stelson et al. 1982) ln$k\rho$ = ln$\frac{k}{aNH4NO3}$ = 54.18- $\frac{15.860}{T}$ +11.206ln

a_w = the water activity calculated between 1 and 0 with RH/100 (Kreidenweis et al.,2008).

2.2. Calculations of shrinking rates of particles

Two major research papers to date have presented calculations on the shrinking rate of ammonium nitrate. This involves creating a dynamic model which allows variable input through the calculation procedures.

The rate of evaporation of ammonium nitrate been calculated from the following equation (Seinfeld & Pandis, 2012)

$$J_{i,D_\mathrm{p}} = -2\pi D_\mathrm{p} D_{i,\mathrm{air}} F(Kn, \alpha_i)(c_i^\infty - c_i^s),$$

as was corrected into the following equation by Dassios & Pandis (1999) and Lunden et al. (2003)

$$J_{\mathrm{NH_4NO_3},R\mathrm{p}} = 2\pi R_\mathrm{p}\left[\beta - \sqrt{\gamma + 4D_{\mathrm{HNO_3}} D_{\mathrm{NH_3}} F(Kn_{\mathrm{HNO_3}}) F(Kn_{\mathrm{NH_3}}) K(T, \mathrm{RH}) \exp\left(\frac{2\sigma \upsilon_l}{RTR_\mathrm{p}}\right)}\right]$$

With the terms for diffusion, Fuchs transition and Kelvin effect included and the rate of change defined by

$$\frac{\mathrm{d}}{\mathrm{d}t}\left(\rho\frac{4}{3}\pi R_{\mathrm{p}}^{3}\right)=\frac{W}{W_{0}}J_{\mathrm{NH_4NO_3},R_{\mathrm{p}}}\mathrm{MW}_{\mathrm{NH_4NO_3}}$$

2.3. Results from previous research

Table 4. Observed theoretical results from previous research

Study	Experimental SR		Theory SR	α	K
	NH_4NO_3 (S)	NH_4NO_3 (aq)	NH_4NO_3		nb
Richardson and Hightower (1987)	0.06 - 0.34 x 10^{-10}	5.56 +/-0.78 x 10^{-10}	12 x 10-10	0.02 - 0.004	
Harrison et al (1990)	0.45 x 10^{-10}	0.49 x 10^{-10}			
Dassios and Pandis (1998)				0.5 - 0.8	
Bergin et al (1997)				1	
Wexler and Seinfeld (1989)	0.065 x 10^{-10}		36 x 10-10		59
Larson and Taylor (1983)		6 x 10^{-10}		1	
Stelson et al (1979)					41

SR = Shrinking rates / *SR results are converted from $Ås^{-1}$ to Ms^{-1}*
α = Accommodation Co-efficient
K= Dissociation constant (nb)

3. Experimental Methodology

The experimental technique measured dissociation of NH_4NO_3 through a tandem differential mobility analyzer/scanning mobility particle sizer system (Rader and McMurry, 1986, Dassios and Pandis, 1998). A poly-disperse NH_4NO_3 particle was produced by nebulizing a 1g/l solution of ammonium nitrate in ultrapure water. This particle was then introduced into a dried and filtered airflow with further drying using a silica diffusion dryer. The aerosol was then bought to a Boltzmann charge equilibrium using a Kr85 particle neutralizer (10 mCi), and selecting one mobility fraction in the Vienna type DMA.

This particle generation system was positioned in a thermally insulated box, kept at a controlled temperature below 10°C using a Model TC-36-25 RS232, bi-polar (heat and cool) proportional-integral-derivative temperature controller. This novel method was introduced to dry and preserve solid state NH_4NO_3, reducing the possibility of particle size change (shrinkage) during transportation to the reactor. The mono-disperse aerosol was then diluted with a dry, filtered, particle-free air and fed into a laminar flow reactor. The reactor consists of two, one meter long stainless steel cylinders which have a constant flow of water around a concentric outer cylinder which is controlled by a temperature bath.

Particle size distributions both upstream and downstream of the reactor were determined by a TSI EC 3080 SMPS with a TSI CPC 3775. The stability of the particle generating system was further checked by the UCPC 3025A monitoring continuously the total particle concentrations in front and behind the reactor. For the dissociation experiments, the changes in size and mass of ammonium nitrate aerosol for three selected particle sizes (50, 100 and 200nm), four reactor temperatures (15, 20, 25, and 30°C), and several flow rates (between 0.6 to 1.6 l/m) were investigated. These changes were then recorded before and after the reactor and from which shrinking rates were derived. Dissociation rates were then calculated using the integrated mass of modal concentration peaks, calculated to a molar equivalence then converted to ppb[2] for use as a comparative to previous literature.

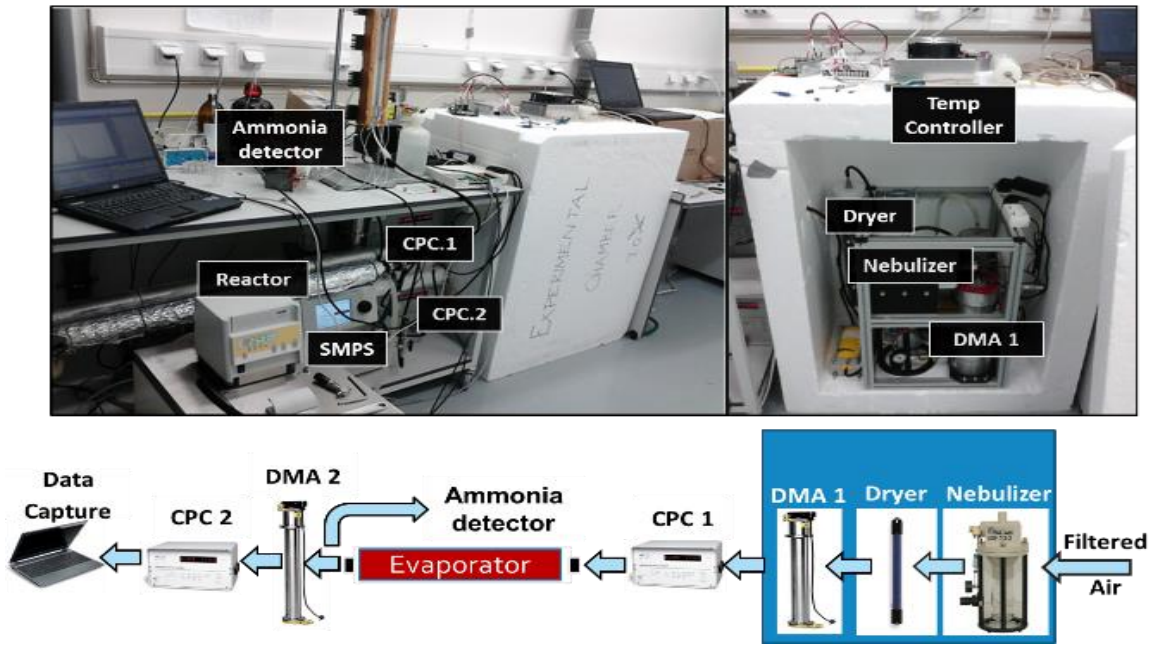

Figure 1. Photographs of the experimental layout (top) and schematic of sample flow (bottom).

3.1. Experimental controls

The high vapour pressure of NH_4NO_3 at normal ambient conditions translates to a well-documented sensitivity to deviations in temperature and relative humidity. Therefore these parameters were closely controlled and recorded at various stages in-line. Stability in the sampling system was rigorously controlled. Sampling only took place when relative humidity was less than 20%, whilst in the particle generator box temperature was always below 10 ˚C. Temperatures before and after the laminar flow reactor were monitored and constantly logged. Calibrations on the ammonia detector were carried out daily before monitoring.

Total particle counts were collected in-front and behind the reactor as well as a calibration scan before every profile change, where the aerosol containing flow would be redirected to bypass the reactor to give a full, non-associated scan. Any changes to particle size before the reactor could then be deducted from the reactor-effected particles. The solution of ammonium nitrate was kept under controlled laboratory conditions along with the ultrapure water which was collected in bulk the beginning of the experiment with a concentration of and continually used during the experiment to reduce resulting data bias from impurities within.

4. Results and discussion

4.1. Rate of NH_4NO_3 particle shrinking

Experimentally we investigated 50, 100, and 200nm NH_4NO_3 aerosol across 6 different residence times, ranging from 80 and 130 seconds through a reactor, which was set at 4 different temperature profiles, 15, 20, 25, 30˚C. The shrinking rate (SR) was calculated by the change in mean particle diameter before and after transportation through the reactor, the mean shrinking rates are shown in Fig.3 along with boxplot and whiskers to observe the scatter for each measured parameter.

For 100nm particles we find shrinking rates comparable to those of Richardson and Hightower's (1986) results for aqueous phase particles of 5.56 x 10^{-10}. The closest comparable experimental parameters were 100nm/30 ˚C, with a mean SR of 6.23 x 10^{-10}, 200nm/30 ˚C SR of 6.27x 10^{-10} and 200nm/25 ˚C SR of 4.32 x 10^{-10}. Larson and Taylor (1983) calculated the shrinking rate for aqueous particles to be 6 x 10^{-10}, also in good agreement with both the 30 ˚C parameter results. When considering shrinking rates for solid NH_4NO_3 particles (as listed in Table 2) all our experimentally obtained shrinking rates were considerably quicker, with our slowest recorded rate being for 50nm/15 ˚C parameter which had an SR of 1.05 x 10^{-10}.

It is evident from Figure 2 that the shrinking rate for 30˚C is notably higher than for all other temperatures. For 100nm/30 ˚C there is an observed increase in shrinking rate after 100 seconds from 0.42 x 10^{-9} m/s to 0.8 x 10^{-9} m/s (.4-.8 nm/s). An explanation could be the proximity of the 100nm /30 ˚C NSD mode to the calculated mean free path (68nm at 30 ˚C and standard pressure).

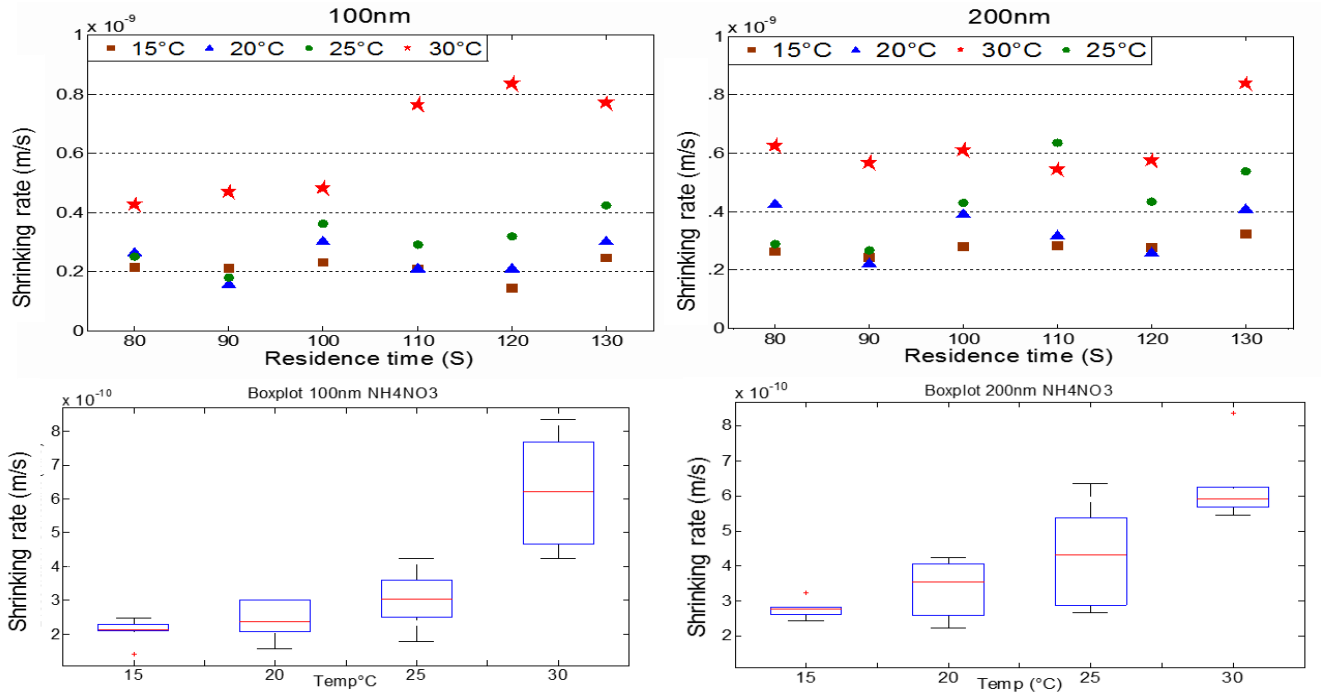

Figure 2. Shrinking rate for 100nm and 200nm (right) particle as a product of residence time.

It is with a residence time near 100 seconds when the NH_4NO_3 particle diameter becomes close to the mean free path in the system, introducing a kinetics change from diffusional to random molecular collision regimes. It is therefore possible that this increase can be attributed to this transition and, more precisely, its effects on the particle surface. Figure 3 shows the size distributions for 100nm/25 and 30˚C after the NH_4NO_3 has left the reactor. At 25 ˚C there is a steady reduction in particle diameter with residence time, the volatility is evident with mean size overlaps for 80 and 90 seconds and 100 and 110 seconds, regardless of this slight variability the overall trend is clear. Also evident from Figure 3 is that the greater the concentration of particles less than the mean free path for each subspecies and for each residence time the greater the sub-20nm peak. It is the sudden appearance of the <20nm peaks that was the driving force behind the abrupt jump in shrinking rate for 100nm/30˚C.

These <20nm peaks are most likely caused or enhanced by heterogeneous recondensation occurring on partially dissociated sub-10nm particles. Evidence for this is given by total counts of up to 20% more than the calibration count when these peaks occur, and most likely caused by sudden cooling on leaving the 30˚C reactor.

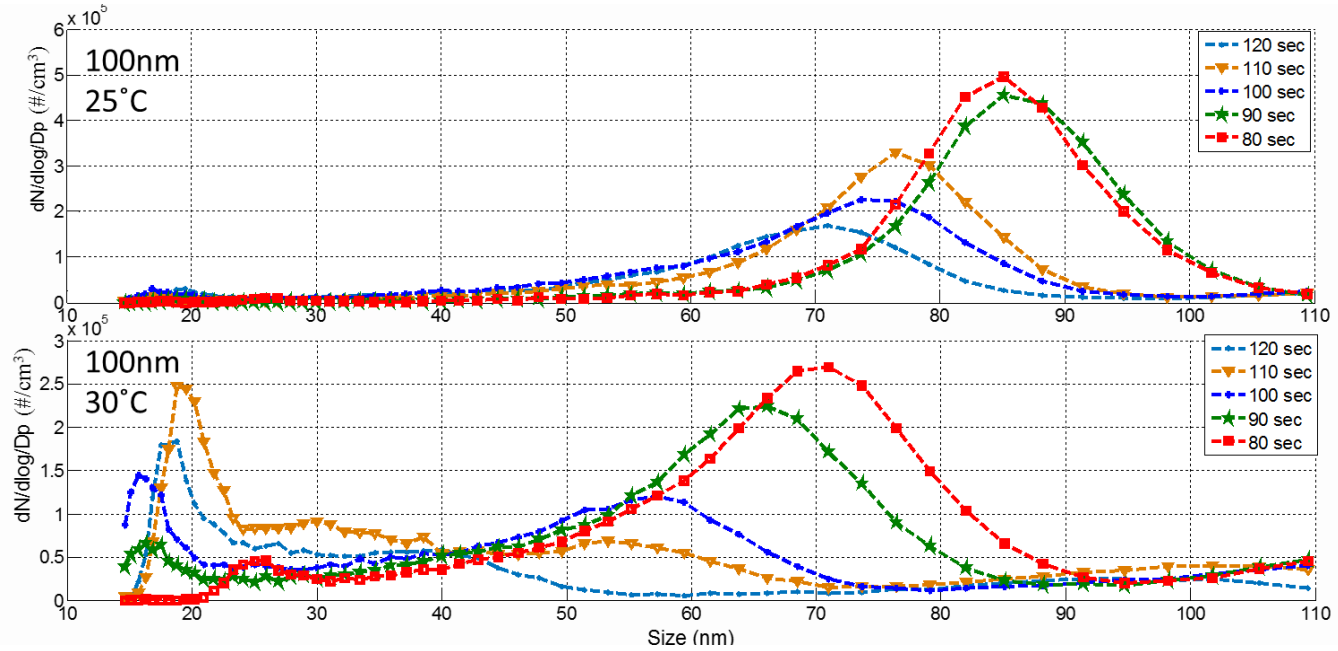

Figure 3: Final size distribution graphs for 100nm particles with residence times between 80 and 120 Seconds. 25˚C top and 30 ˚C bottom

4.2. Calculated shrinkage rate until *dp* = <14.7nm

Shrinking rates can now be used to calculate an extrapolated time, in seconds, that it would take for each particle to become so small as to be undetectable from our instrumentation (P_{te}). Figure 4 displays these rates taking into consideration temperature and residence time through the reactor. A linear fit line for each profile is displayed so overall trends can be observed. The correlation between temperature and shrinking rate is again evident, however, a size dependent factor can now also clearly shown. For 200nm particles with areactor temperature of 15, 20 and 30 ˚C there is a constant rate of

particle shrinkage which appears to be non-dependent on residence time, as denoted by the almost flat linear-fit. The fastest rates finds P_{te} for 200nm particle to be near 160 seconds except for the longest residence times, which shows an increase to near 100 seconds.

It should be remembered that 200nm particle, being larger, must undertake a greater loss of its component surface molecules to undergo the same rate of shrinkage as a 100nm particle under associated conditions, therefore must shrink at a considerably faster rate than their 100nm/30 ˚C equivalent.

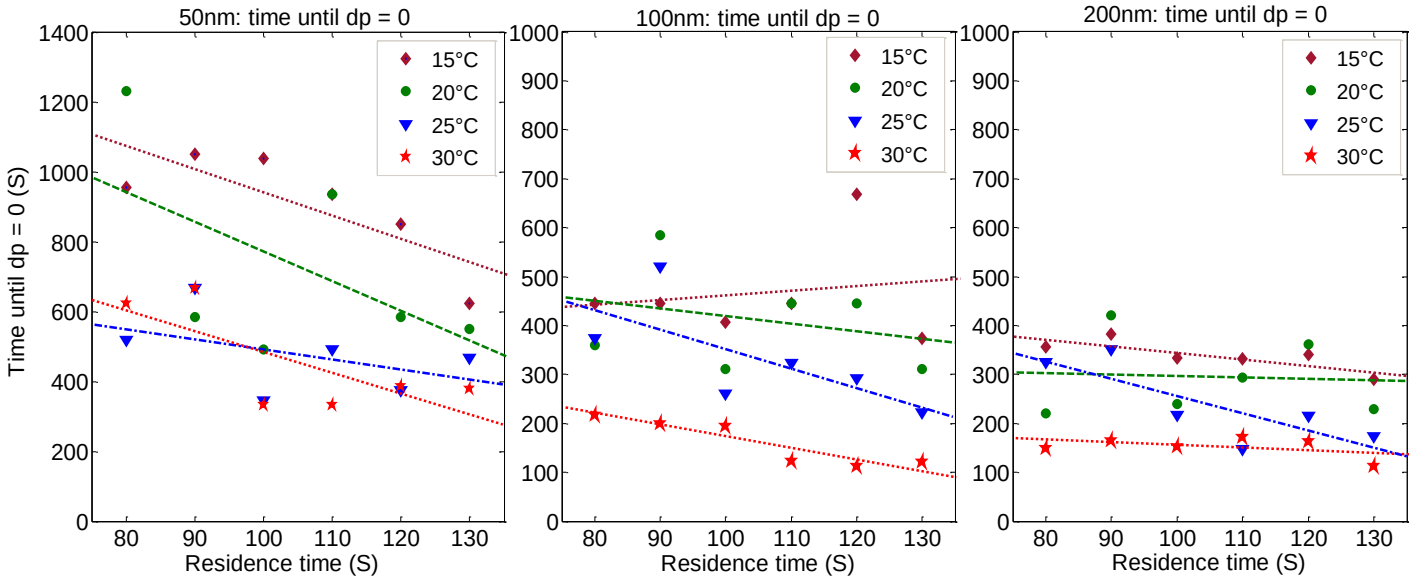

Figure 4: Time until each particle would become below detectable limit (<14.7nm) using calculated shrinking rates. Shown for each temperature profile as a product of residence time within the reactor. A linear-fit line gives the slope decrease in time until NH_4NO_3 particle would theoretically completely evaporate.

50nm/ 15 and 20 ˚C particles show greatest response to residence time within the reactor, exemplified by the largest decrease in time to completely dissociate. For example a 50nm NH_4NO_3 particle with a reactor residence time of 80 seconds and settings of 20˚C has an observed P_{te} of 1200 seconds, 10 seconds longer in the reactor P_{te} is halved to 600 seconds.

This steep decrease in time is indicative of the greater volatility of smaller NH_4NO_3 particles to temperature and possibly enhanced by Kelvin factors and mass kinetic regime of random molecular collisions. This volatility may also amplify experimental errors such as small temperature gradients through the system. From Fig.4 the following conclusions can be drawn. The larger particle show less dependence on residence time, less influence on temperature and are almost always predicted to completely dissociate quicker than the smaller 50nm and 100nm.

4.3. Calculated dissociation rates

We now derive dissociation rates from integral mass measurements taken from peak concentration curves. Dissociation constant (*Kc)* rates in ppb^2 are shown in Figure 5. The log scale y-axis reveals an order of magnitude difference for 30 ˚C 100nm and 200nm results. 200nm particles at 15 ˚C and 20˚C show appreciably lower dissociation constants of <10ppb and indicate little dependence on residence time. 50nm presents a far increased dissociation constant, however, the 50nm / 30 ˚C data should be treated with caution due to a lack an obvious peak mass due to almost complete dissociation.

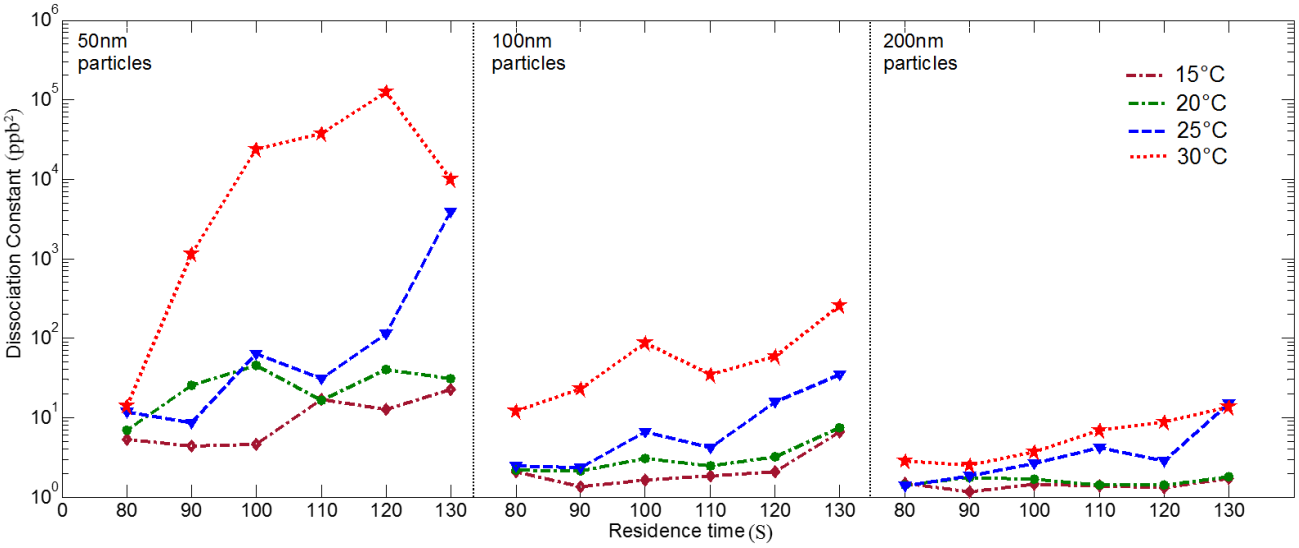

Figure 5. Dissociation Constants in ppb^2 calculated from the integral mass before and after the reactor

Contrary to shrinking rates, smaller particles have a much higher dissociation constant than larger particles when considering temperature and residence time. It is observed that 200nm NH_4NO_3 particles shrink quickest yet the rate of mass exchange between particle and bulk is considerably less. A possible explanation for this could be the particle dehydrating as it travels through the dry reactor environment, reducing the diameter quickly yet leaving the molecularly heavier crystalline solid NH_4NO_3.

Should this hypothesis be correct, this would imply that the diffusional drying of our particles direct from atomization was not sufficient to complete solidification. It is worth remembering that due to hysteresis, pure NH_4NO_3 does not recrystallize from aqueous form until relative humidity were less than 20%. Furthermore, Dassios and Pandis (1999) state this figure to be less than 10% when using NH_4NO_3 from solute, as was the case here. Our system was kept <20% relative humidity at all times however humidity levels were not less than 10%.

Figure 6 shows that 100nm and 200nm NH_4NO_3 particles were almost completely stable for all residence times through the reactor for temperatures of 15 and 20˚C with a narrow range of 1.47 to 2.88 ppb^2 for 200nm and an equally narrow range for 100nm apart for residence times of 130 seconds.

4.4. Experimental v theoretical dissociation constant

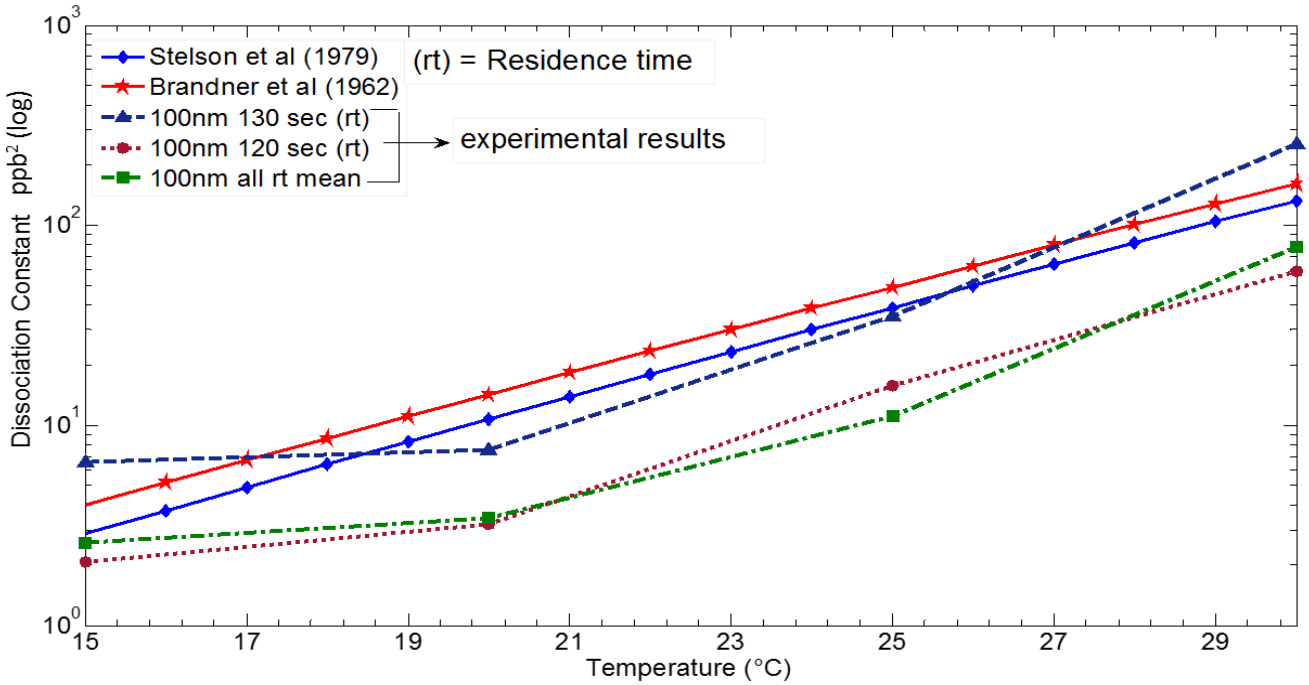

Figure 6. Dissociation constants in ppb^2. Comparing solid particle thermodynamic data (solid lines) with experimentally derived data (dashed).

We can now apply our closest fit data to those of the dissociation rates of Stelson et al (1979) and Bradner et al (1962) (Figure 6). Calculations are based on thermodynamic theory for solid particles. Stelson et al (1979) and Brandner (1962) provide moderate results for dissociation constant rates derived using the integration interpretation of the Van't Hoff equation, are commonly cited in previous papers and give a reasonable marker for trusted comparable dissociation behaviour. The results in Figure 6 are for 100nm particles with reactor residence times of 120, 130 seconds and an overall average. They show that for lower temperature profiles there is a slower increase in the dissociation constant but from 20 ˚C the dissociation rate increase is in-line with theoretical predictions. The results indicate the possibility of thermal gradients within the reactor at lower temperatures where dissociation rates are more sensitive to temperature changes.

Conclusions

Experimentally obtained results on ammonium nitrate shrinking rates are comparable with those of aqueous phase particles recorded in previous literature. 200nm particles are shown to shrink fastest and the 50nm particles slowest. For highest temperatures, our experiment identifies a rate shift in shrinking when 100nm particles change from diffusional to collisional kinetic regimes, moreover, heterogeneous re-condensation at the highest temperature profiles was observed. Calculated dissociation constants, derived from integrated mass measurements, show an inverse relationship to those of shrinking rates. The slowest dissociation rates being for 200nm particles. 200nm 15/20˚C show a constant *Kc* of 1.2 ppb^2, independent of residence time, indicating a steady but continuous reaction but without Eq.2 ever coming into equilibrium. It is likely that the reasonably short residence

times, small particle sizes investigated here and molecular interaction with the reactor walls all effect to hinder equilibrium being reached.

None of the chosen profiles of size and temperature in the experiments exactly replicate the dissociation rates obtained by applied thermodynamics for solid particles, however 100nm particles increase at a comparable dissociation rate once temperatures exceed 20 ˚C. Given the results of shrinking rates and dissociation constants it is highly likely that our particles were aqueous phase, at least when entering the reactor, indicating that RH<20% is not dry enough to recrystallize NH_4NO_3.

Finally our modelled results show that when considering just ammonia in the bulk, the rate of particle shrinkage considerably quicker than experimentally observed. The cause unknown however the possible presence of nitric acid remaining in the bulk for most of the journey of the reactor allowing continued dissociation, whilst the jump in rate through continuum indicates a previous kinetic restraint. Both modelled and experimentally obtained results show strong dependence of shrinking rate to both temperature and particle size.

Acknowledgements

The authors acknowledge support of this work by European Union Seventh Framework Programme (FP7/2007-2013) under grant agreement n° 315760 HEXACOMM.

5. References

Bai, H., Lu, C., & Ling, Y. M. (1995). A theoretical study on the evaporation of dry ammonium chloride and ammonium nitrate aerosols. *Atmospheric Environment*.

Bergin, M. H., Ogren, J. A., Schwartz, S. E., & Mcinnes, L. M. (1997). Evaporation of ammonium nitrate aerosol in a heated nephelometer: Implications for field measurements. *Environmental Science and Technology*, *31*(10), 2878–2883.

Cheng, Y. H., & Tsai, C. J. (1997). Evaporation loss of ammonium nitrate particles during filter sampling. *Journal of Aerosol Science*, *28*(8), 1553–1567.

Dassios, K. G., & Pandis, S. N. (1999). The mass accommodation coefficient of ammonium nitrate aerosol. *Atmospheric Environment*, *33*(18), 2993–3003.

Hu, D., Chen, J., Ye, X., Li, L., & Yang, X. (2011). Hygroscopicity and evaporation of ammonium chloride and ammonium nitrate: Relative humidity and size effects on the growth factor. *Atmospheric Environment*, *45*(14), 2349–2355. http://doi.org/10.1016/j.atmosenv.2011.02.024

Kreidenweis, S. M., Petters, M. D., & DeMott, P. J. (2008). Single-parameter estimates of aerosol water content. *Environmental Research Letters*, *3*(3), 035002. http://doi.org/10.1088/1748-9326/3/3/035002

Larson, T., & Taylor, G. (1983). On the evaporation of ammonium nitrate aerosol. *Atmospheric Environment (1967)*, *17*(12), 2489–2495. Retrieved from http://www.sciencedirect.com/science/article/pii/0004698183900744

Larson, T. V., & Taylor, G. S. (1983). On the evaporation of ammonium nitrate aerosol. *Atmospheric Environment (1967)*, *17*(12), 2489–2495. http://doi.org/10.1016/0004-6981(83)90074-4

Lightstone, J. M., Onasch, T. B., Imre, D., York, N., & Oatis, S. (2000). Deliquescence , Efflorescence , and Water Activity in Ammonium Nitrate and Mixed Ammonium Nitrate / Succinic Acid Microparticles, 9337–9346.

Lunden, M. M., Revzan, K. L., Fischer, M. L., Thatcher, T. L., Littlejohn, D., Hering, S. V., & Brown, N. J. (2003). The transformation of outdoor ammonium nitrate aerosols in the indoor environment. *Atmospheric Environment*, *37*(39-40), 5633–5644. http://doi.org/10.1016/j.atmosenv.2003.09.035

Martin, S. T. (2003). Crystallization of atmospheric sulfate-nitrate-ammonium particles. *Geophysical Research Letters*.

Mozurkewich, M. (1993). The dissociation constant of ammonium nitrate and its dependence on temperature, relative humidity and particle size. *Atmospheric Environment. Part A. General Topics*, *27*(2), 261–270. http://doi.org/10.1016/0960-1686(93)90356-4

Pachauri, R. K., & Meyer, L. (2014). Climate Change 2014: Synthesis Report. Contribution of Working Groups I, II and III to the Fifth Assessment Report of the Intergovernmental Panel on Climate Change, 151.

Pope, C. A., Turner, M. C., Burnett, R., Jerrett, M., Gapstur, S. M., Diver, W. R., … Brook, R. D. (2014). Relationships Between Fine Particulate Air Pollution, Cardiometabolic Disorders and Cardiovascular Mortality. *Circulation Research*. http://doi.org/10.1161/CIRCRESAHA.116.305060

Richardson, C. B., & Hightower, R. L. (1987). Evaporation of ammonium nitrate particles. *Atmospheric Environment (1967)*, *21*(4), 971–975.

Schaap, M., van Loon, M., ten Brink, H. M., Dentener, F. J., & Builtjes, P. J. H. (2004). Secondary inorganic aerosol simulations for Europe with special attention to nitrate. *Atmospheric Chemistry and Physics*, *4*(3), 857–874. http://doi.org/10.5194/acp-4-857-2004

Seinfeld, J., & Pandis, S. (2012). *Atmospheric chemistry and physics: from air pollution to climate change*. Retrieved from http://www.google.com/books?hl=en&lr=&id=YH2K9eWsZOcC&oi=fnd&pg=PA1991&dq=seinfeld+and+pandis&ots=hK3xLmaXHx&sig=YBgCj_Ct7vI-a5Aso7JIigN3958

Smolík, J., Mašková, L., Zikova, N., Ondráčková, L., & Ondráček, J. (2013). Deposition of suspended fine particulate matter in a library. *Heritage Science*, *1*(1), 7. Retrieved from http://www.heritagesciencejournal.com/content/1/1/7

Stelson, a. W., Friedlander, S. K., & Seinfeld, J. H. (1979). A note on the equilibrium relationship between ammonia and nitric acid and particulate ammonium nitrate. *Atmospheric Environment (1967)*, *13*(3), 369–371. http://doi.org/10.1016/0004-6981(79)90293-2

Stelson, A., & Seinfeld, J. (1982). Relative humidity and temperature dependence of the ammonium nitrate dissociation constant. *Atmospheric Environment (1967)*, *16*(5), 983–992. Retrieved from http://www.sciencedirect.com/science/article/pii/0004698182901846

9. Article 2

Outdoor and indoor aerosol size, number, mass and compositional dynamics at an urban background site during warm season

N. Talbot, L. Kubelova, O. Makes, M. Cusack, J. Ondráček, P. Vodička, J. Schwarz and V. Zdimal.

[a]Institute of Chemical Process Fundamentals of the ASCR, v.v.i., Rozojová 2, Prague 165 02 Czech Republic.
[b]Charles University, Faculty of Science, Department of Environmental Studies, Prague, 128 43, Czech Republic.

Published in *Atmospheric Environment Journal:* January 2016

Pages: 77--104

Published in: February 2016

Impact factor of Journal: 3.465

Outdoor and indoor aerosol size, number, mass and compositional dynamics at an urban background site during warm season

N. Talbot[a,b*], L. Kubelova[a,b], O. Makes[a,b], M. Cusack[a], J. Ondracek[a], P. Vodička[a], J. Schwarz[a] and V. Zdimal[a].

[a]*Institute for chemical process Fundamentals of the ASCR, v.v.i., Rozojova 2, Prague 165 02 Czech Republic.*
[b]*Institute for Environmental Studies, Faculty of Science, Charles University, Prague, 128 43, Czech Republic.*
*corresponding author

Keywords: aerosol, composition, dissociation, I/O ratio, nitrate.

Abstract

This paper describes the use of a unique valve switching system that allowed for high temporal resolution indoor and outdoor data to be collected concurrently from online C-ToF-AMS, SMPS and OC/EC, and offline BLPI measurements. The results reveal near real-time dynamic aerosol behaviour along a migration path from an outdoor to indoor environment.
An outdoor reduction in NR-PM_1 mass concentration occurred daily from AM (06:00-12:00) to PM (12:00-18:00). SO_4 (26%-37%) [AM/PM] increased proportionally during afternoons at the expense of NO_3 (18%-7%). The influences of mixing height, temperature and solar radiation were considered against the mean mass concentration loss for each species. Losses were then calculated according to species via a basic input/output model. NO_3 lost the most mass during afternoon periods, which we attribute to the accelerated dissociation of NH_4NO_3 through increasing temperature and decreasing relative humidity.

Indoor/outdoor (I/O) ratios varied from 0.46 for <40nm to 0.65 for >100nm. These ratios were calculated using average SMPS PNC measurements over the full campaign and corroborated using a novel technique of calculating I/O penetration ratios through the indoor migration of particles during a new particle formation event. This ratio was then used to observe changes in indoor composition relative to those outdoors.

Indoor sampling was carried out in an undisturbed room with no known sources. Indoor concentrations were found to be proportional to those outdoors, with organic matter [2.7 $\mu g/m^3$] and SO_4 [1.7 $\mu g/m^3$] being the most prominent species. These results are indicative of fairly rapid aerosol penetration, a source-free indoor environment and small afternoon I/O temperature gradients. Fine fraction NO_3 was observed indoors in both real-time AMS PM_1 and off-line BLPI measurements. Greater mass concentration losses were observed from filter measurements, highlighting an important time dependency factor when investigating semi-volatiles. Coarse mode NO_3 was observed by impactor measurements, ascribing value to observing the full particle mass size distribution for understanding aerosol origin.

1. Introduction

The global trend of urbanization (OECD, 2010) and rapid industrial modernization (X. Y. Zhang et al., 2012) is increasing the time populations are spending indoors (Kousa et al. 2002). Meanwhile, aerosol research indicates that a substantial fraction of a person's exposure to fine particulate occurs whilst

indoors (Hämeri et al., 2004b). Epidemiological studies repeatedly link exposure to fine particulate with adverse respiratory and cardiovascular health effects, including decreased lung function, asthma and myocardial infarction (O. Yu et al. 2000; Schwartz et al. 1996; Kampa and Castanas 2008; Dockery et al. 1993). To fully assess and understand these risks it is important to obtain a good understanding of the physical and chemical properties of particulates, as well as spatial and temporal variations for both indoor and outdoor environments (Chun Chen & Zhao, 2011; Morawska et al., 2001).

Indoor particle mass and number size distributions depend on many factors. The strength and occurrence of indoor sources such as open fires, cooking, cleaning and smoking are understood to be primary drivers of escalated indoor concentrations (Lazaridis and Aleksandropoulou 2006, Koistinen et al. 2004). Conversely, when indoor sources are absent, indoor concentrations strongly correlate to those outdoors (Hussein et al. 2006). This suggests an indoor/outdoor aerosol relationship that is closely related. Meteorological parameters, including wind speed, temperature, pressure and infiltration rates, control the influx of outdoor particulates indoors (Hänninen et al., 2004; Zhu et al., 2005). This highlights the importance of understanding the size and chemical composition of outdoor aerosol (Viana et al. 2008, Putaud et al. 2010, Schwarz et al. 2012, Poulain et al. 2011) and outdoor to indoor penetration processes (Hussein et al. 2005).

Once indoors, changes in temperature, humidity, and VOCs can enhance physico-chemical transformations of the aerosol (Huang et al., 2004a), which can enhance the harm potential of the aerosol whilst increasing the possibility of artefacts on indoor data (Tang & Munkelwitz 1993). This understanding has directed research to focus on particle dynamics and chemical composition (Gemenetzis, Moussas, Arditsoglou, & Samara, 2006), especially for semi-volatile species. For example, Lunden et al. (2003) measured I/O concentrations of nitrates, sulfates and carbon $PM_{2.5}$ in an apartment in California. Indoor NH_4NO_3 concentrations were significantly lower than modelled predictions based on deposition and penetration losses. The authors attribute these extra losses to phase transformation from solid or aqueous NH_4NO_3 to gaseous NH_3 and HNO_3, which is subsequently lost by sorption to indoor surfaces.

Numerous studies have supported these findings. Hering & Cass (1999) looked at losses of NH_4NO_3 from impactor substrate and found a temperature gradient of more than 5˚C between the sampled airflow and filter substrate to be significant in determining loss rate. Smolík et al. (2008) characterized I/O aerosol interaction in an apartment in Prague using PIXE/IC. The major fraction of fine particulate was found to be sulfate (SO_4), nitrate (NO_3) and ammonium (NH_4) outdoors, but very low NO_3 concentrations were recorded indoors. Similar results were recorded by Andělová et al. (2010) and by Mašková et al. (2015) using similar filter-based measurements. NO_3 was again found to be very low in summer both indoors and outdoors. These results were attributed to the dissociation behaviour of NO_3 in the form of ammonium nitrate (NH_4NO_3), which is understood to be volatile at typical ambient temperatures and relative humidity (RH).

It is not just volatile inorganics that are found to undergo physico-chemical transformation. Naumova et al. (2003) investigated I/O organic semi-volatile PAH gas / particle partitioning. They found enrichment of organic carbon indoors suggesting that sorption into organic matter of the particles may be more important in the indoor air than in the outdoor air. Sakurai et al. (2003) studied chemical composition and volatility of particles emitted from diesel vehicles and noted residual species

prominence, which represented non-volatile cores and low volatility organics. Appearances of smaller particles is thought to be a product of the condensation of organic vapours from combustion, suggesting that particles of outdoor origin can experience substantial changes and may be lost to building walls during indoor penetration.

Indoor sources disrupt this I/O relationship (Hussein et al. 2006), whilst a decoupling of the I/O aerosol relationship has also been recognised in which indoor concentrations of low volatile compounds were proportionally higher than reported outdoors. This is indicative of particle transformations occurring indoors. Most indoor research to date have favoured gravimetric techniques for compositional analysis. Usually using Ion chromatography (IC) from samples collected on filter substrate. This is a reliable technique but the lengthy sample time does not allow observations of transformations, and only implies volatility by observed absence of the expected species unless a backup filter has been applied. With many factors affecting I/O relationships, such as penetration efficiency, chemical composition and size, quantifying volatility has remained problematic for research.

Nonetheless, increasing the understanding of physico-chemical changes that occur on aerosol particles as they migrate indoors is important. Recent major studies in the United States (Chen et al. 2012) and China (Zhao et al. 2013) have highlighted the links between particulate migration from an outdoors to indoors environment and human exposure health risks. However, these studies were limited by not attaining compositional analysis.

The rapid collection of both indoor and outdoor aerosol samples was facilitated by the utilisation of a time controlled automated switching system. This allowed online C-ToF-AMS, OC/EC and SMPS instruments to observe, in almost real time, particle transformations during and after outdoor-originating particle had migrated indoors whilst no indoor sources were present. Important diurnal fluctuations in outdoor chemical composition and the indoor response to these changes are discussed, as well as the importance of the sampling time on aerosol composition data using comparative off-line chemical composition results obtained by BLPI measurements.

2. Methodology

Research took place between the 16th August and the 8th September, 2014 at a ground floor flat in Suchdol, Prague, Czech Republic. Details of the flat and area were previously described by Smolik et al. (2008) and Hussein et al. (2006), therefore only a brief overview of key details is provided here. Suchdol is a residential area in north-western Prague, about 6 km from the city centre. It is recognized as a suburban background site with residential houses and a university campus interspersed between plenty of green spaces. The traffic flow is moderate along one major 2-lane road (average traffic of 10000-15000 cars per day) with regular bus services.

Due to its location on a plateau above the river Vltava there are not many contributory roads alongside the site. Figure 1 shows the location in relation to Prague metropolis as well as wider terrain. The wind rose in Figure 1 shows a prominent south west prevailing wind, bringing influence from the airport. Note the very infrequent southerly winds indicating Prague city should not influence the site to any great extent.

2.1 Measurement site and sampling set-up.

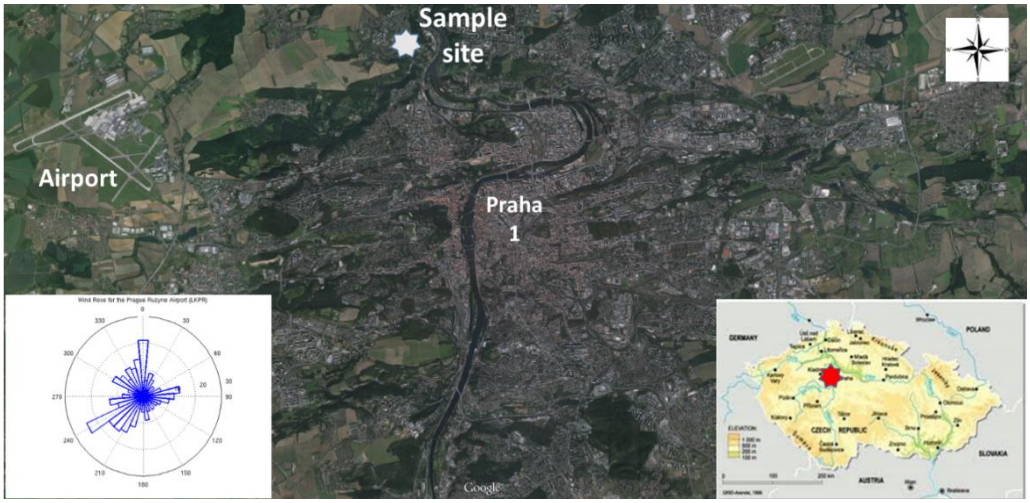

Figure 1. A satellite map of Prague (accessed from: https://www.google.cz/maps/ 2015) and (inset) topographical outlay of the surrounding terrain of Czech Republic and wind rose from Václav Havel Prague airport.

The flat used for the measurements is located in the Institute of Chemical Process Fundamentals in the Czech Academy of Sciences compound (50°7'36.47"N, 14°23'5.51"E, 277 MASL). Built in the 1960s but recently refurbished, the ground floor of the two story building is generally used as a guest house. The layout and dimensions of the flat are shown in Figure 2. Sampling was carried out from a bedroom with an inlet protruding to the kitchen area, used as the sealed indoor environment, and out through the bedroom window. The door to the kitchen from the hall and toilet area was kept closed unless entering to change filters (between 10-11am) or run experiments. These times were carefully logged. The outdoor sampling point was 1 m away from the window in the bedroom containing most of the instrumentation.

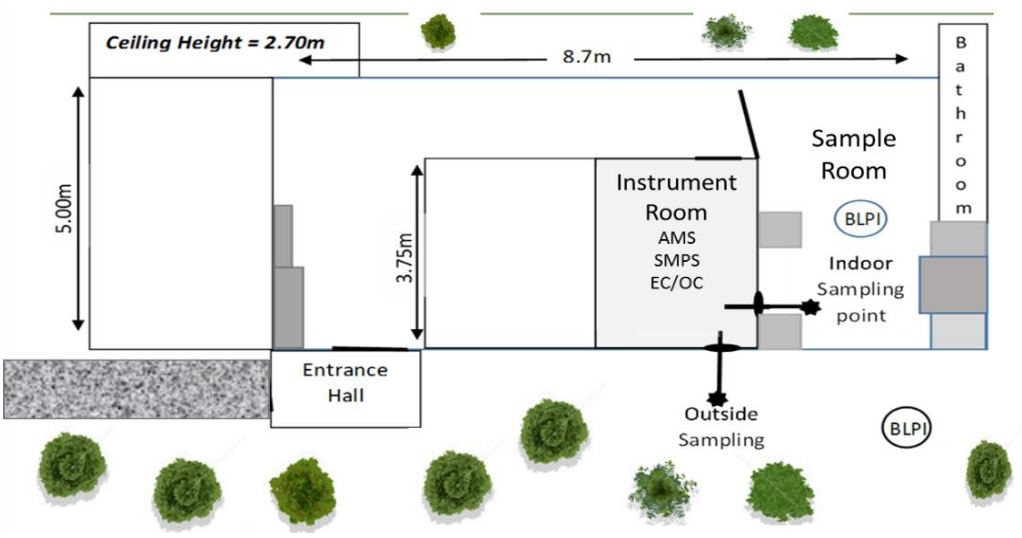

Figure 2. Sketch showing the layout of the apartment where indoor/outdoor comparative measurements took place.

2.2 Aerosol measurements and instrumentation

2.2.1. Online instrumentation

Size resolved particle number size distribution of indoor/outdoor aerosols were measured on-line using a Scanning Mobility Particle Sizer (SMPS) model 3936 TSI with long DMA 3081 and CPC 3775. This covered particles from 14.7 to 724 nm. All SMPS data was collected using a 3 minute up-scan, 30 second down-scan and 90 second purge to allow for the complete clearance of the inlets. Only the second 5-minute scan was considered for analysis in order to make sure the sample represented only the aerosol from its designated origin. Sequential outdoor / indoor sampling was conducted with two full SMPS scans from outdoors followed by two scans indoors, with 10 minute scan periods selected using automated switch-valve selectors.

The C-ToF AMS provides real-time measurements of NR-PM_1 chemical composition and size distribution (Drewnick et al., 2005). For this research the AMS alternated between the particle time-of-flight (PToF) mode and the mass spectra (MS) mode for each sampling period (1 min). Under the PToF mode operation the aerosol beam was chopped by a chopper wheel with radial slit. Particle size information was obtained as a function of particle time-of-flight in non-refractory PM_1 (NR-PM_1). Reported mass concentrations and size distributions were then averaged. The AMS was calibrated weekly during this campaign using the Brute force single particle mode (Decarlo et al., 2006; Drewnick et al., 2005).

Elemental carbon and organic carbon (EC and OC) measurements were conducted by two semi-online field OC/EC analysers (Sunset Laboratory Inc., USA) in parallel (one outdoor, second indoor), both with a $PM_{2.5}$ cyclone inlet (flow rate of 8 lpm). The instruments were equipped with a carbon parallel-plate diffusion denuder (Sunset Lab.) to remove volatile organic compounds that may cause a positive bias

in the measured OC concentrations. The denuder was placed at ambient outdoor conditions during outdoor measurements and inside the room during indoor measurements.

Samples were taken at 2-h intervals, including the thermal-optical analysis which lasted about 15 min. The analysis was performed using the shortened EUSAAR2 protocol – step [gas] temperature [°C]/duration[s]: He 200/90, He 300/90, He 450/90, He 650/135, He-Ox. 500/60, He-Ox. 550/60, He-Ox. 700/60, He-Ox. 850/100 (Vodička et al. 2013). The collected OC was evaporated and then oxidized to CO_2 either on a MnO_2 catalyst or together with EC on the filter by oxygen in the He/Ox phase, and analysed by a non-dispersive infrared (NDIR) detector. Automatic optical corrections for charring were made during each measurement and the split point between EC and OC was detected automatically (software: RTCalc522, Sunset Lab.).

2.2.2. Offline instrumentation

Two Berner type Low Pressure Impactors (BLPI, 25/0.018/2, Hauke, Austria) collected particles from the indoor and outdoor air. The BLPI samples were deposited on polycarbonate foils (flow rate 1.5 m^3/h). The foils were greased with Apiezon L vacuum grease to reduce particle bounce. The impactors separated PM into 10 size fractions. The cut diameters of the stages were 0.026, 0.057, 0.1, 0.16, 0.25, 0.44, 0.87, 1.8, 3.5 and 6.7 µm (Lucia Štefancová et al., 2011). BLPI Samples were collected indoors and outdoors concurrently over 4, 23 hour sampling periods during the campaign.

2.2.3. Data Considerations

Source experimentation, such as cooking, smoking, cleaning indoors, and an idling car engine and barbecue outside were carried out at various times during the three weeks (SI Table 1). All data recorded during experiments were later removed from the dataset analyses. AMS data was collected using a collection efficiency of 0.7. This was calculated using the total SMPS mass minus the elemental carbon mass taken from the EC-OC. For SMPS measurements a particle density of 1.5 was used throughout. The SMPS inversion routine used TSI AIM software with the mass concentration calculation using the same software assumes that all the particles are perfect spheres.

2.3 Meteorological measurements

Basic meteorological data (ambient temperature, pressure, RH, wind direction and velocity, and total solar radiation) were monitored at the weather station operated by the Czech Hydro-meteorological Institute. The container is permanently located at the ICPF compound 20 meters from the residence where the I/O samples were taken. Air-mass trajectories were computed using Hysplit back trajectory model provided by the NOAA Air resource laboratory (Stein et al. 2015) and each runtime had a duration of 72 hours.

3. Results and Discussion

3.1 Airmass trajectories and meteorology considerations

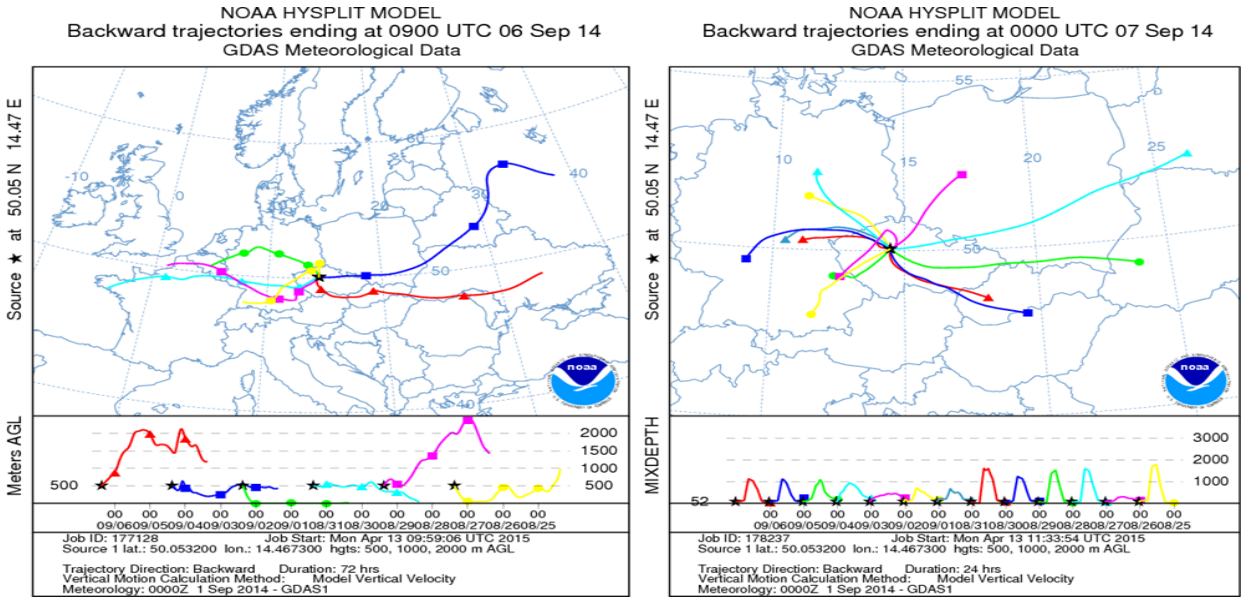

Figure 3. Air mass back trajectories ran for 72 hours, for the campaign period during which the AMS ran, featuring vertical profiling [left] and daily mixing depth [right].

Figure 3 provides an overview of back trajectories, giving vertical profiles and air mass origin over Prague during the campaign. Air mass origin is known to influence aerosol concentration and alter composition and holds implications for mass size distributions (Schwarz et al. 2012). Until the end of August Prague was under the influence of what is described as a westerly mixed maritime and continental air mass (Viana et al., 2008). This was typified by long range transportation, originating from the Biscay and the English Channel, advecting across Europe whilst mixing with continentally derived, low altitude air. From the beginning of September an easterly continental flow became established, reducing the influence of oceanic sources. The interaction of upper atmospheric air and continental land promotes enrichment of the marine aerosol as it interacts with continental derived emissions. For example, oceanic NaCl reacts with HNO_3 to create the secondary product $NaNO_3$ (Lehmann et al., 2005). From September 4th an easterly airflow mixed high and low altitude aerosol. It was during this period that a lower mixing layer was observed.

Table 1. Overview of meteorology for the full research period including overall averaged daytime high and low temperatures, relative humidity and wind speed, including averaged daily high gust speed. A daily synopsis of meteorological conditions is available in supplementary material (SI Figure 1).

Summer Campaign 2014	Temp. (°C)			Humidity (%)			Pressure	Wind (km/h)	
	Daytime high	avg	Night-time low	high	avg	low	avg	ave	High gust
	20.4	**15.2**	10.3	94.6	**74.1**	42.8	**1015.5**	**6.6**	11.5

Table 1 gives an overview of meteorological conditions during the experiment. Late summer temperatures were generally slightly below the long term average of around 22°C. There was only one brief rain event [SI Figure 1] after which the only new particle formation (NPF) event was observed during this study.

3.2 Indoor/outdoor particle number concentration and size distribution

Mean particle number concentrations (PNC) were 5.4 x 10^3 cm^{-3} outdoors and 3.0 x 10^3 cm^{-3} indoors. In context, Rimnáčová et al. (2011) viewed 2 years of data for Prague and found average PNC outdoors were 7.0 x 10^3 cm^{-3}, indicating rather low amounts of aerosol loading during this study. The difference can be explained by the low number of new particle formation events during this research (only one major event), compared to the Rimnáčová et al. (2011), who found from the same location that NPF events were a regular occurrences during summer months. Previous literature would indicate traffic emissions from local sources to be another major contributor of outdoor PNC over Prague (Ondráček et al. 2011).

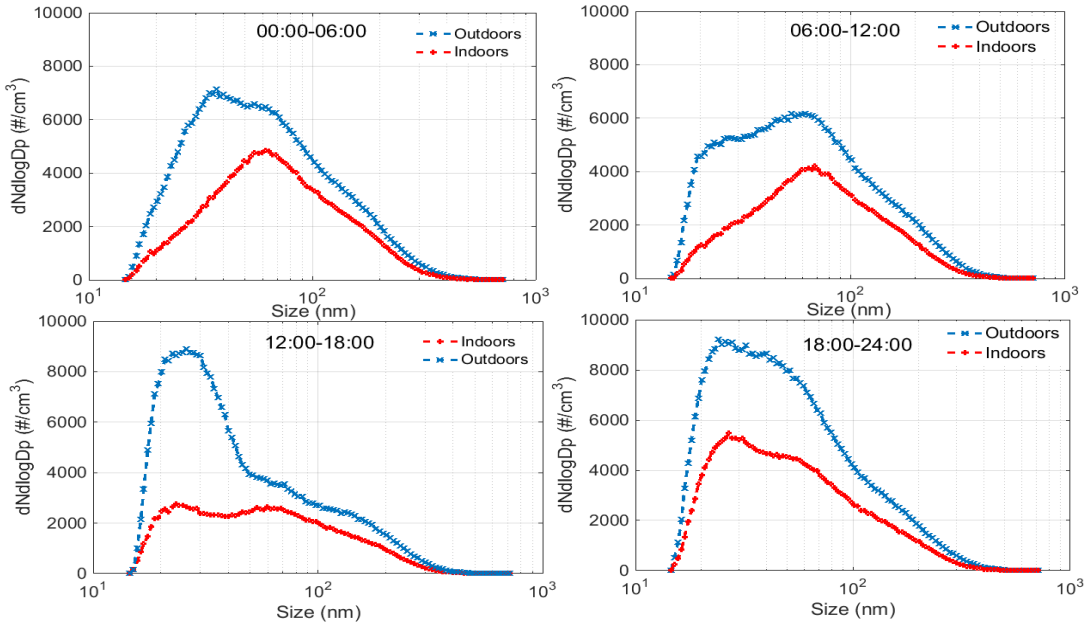

Figure 4. Averaged indoor/outdoor mean particle number size distribution for the full campaign. The distribution split into 4 sub-daily periods: 00:00-06:00, 06:00-12:00, 12:00-18:00 and 18:00-24:00.

Size distribution data for 4 sub-daily periods, 00:00–06:00, 06:00-12:00, 12:00-18:00 and 18:00-24:00, are presented in Figure 4. Each quarter shows the calculated mean size distribution over each 2nd scan of two x 5 min scans, therefore 17 scans for each period per day of research for both indoor and outdoor values. Particle size distribution was found to change significantly during the day. Outdoors, the distribution was tri-modal with peaks around 35 nm, 70 nm and a smaller peak around 200 nm. Throughout this campaign the dominant mode never exceeded 80nm. An afternoon mode between 20-30 nm then becomes the dominant for period 12:00-18:00, with a corresponding increase in PNC. Some new particle formation and traffic events outdoors would explain these modes. During the morning periods (00:00-12:00) the observed mode indoors was between 60-70 nm and particle size distribution (PSD) appeared to be bimodal with a smaller mode between 150-200 nm.

The increase in number concentration outdoors was found to increase differences between outdoor and indoor values, most notably for particles <60 nm. This is indicative of a lower penetration factor of ultrafine / lower order Aitken particles (Hussein et al. 2005), and possible coagulation. The apparent growth rate for a new particle event recorded during this investigation was 4.4 nm/hour. The I/O ratio is discussed later in section 3.4.1.

For the final quarter of the day, 18:00-24:00, there is evidence of coagulation of the particles formed in the previous period. The size distribution mode broadens to cover the size range 30-70 nm. During this period there was often evidence of a new input of Aitken particles, and although it not fully explained, this is suspected to be a result of evening traffic in Prague, and fires and barbeques in residential houses near the research site.

Comparable size distribution results from Helsinki showed a dominant nucleation mode (8-30 nm) of 7 x 10^3 cm^{-3} and Aitkin mode (20-100 nm) of 6.8 x 10^3 cm^{-3} (Hussein et al. 2007). Leipzig also had a dominant nucleation mode of 3-20 nm with a nucleation mode concentration of 9.8 x 10^3 cm^{-3} and a 20-100 Aitkin mode with a concentration of 9.4 x 10^3 cm^{-3} (Wehner & Wiedensohler, 2003). Atlanta showed a dominant Aitkin mode of 10-100 nm and a concentration of 13.4 x 10^3 cm^{-3} (W. Yu, Bao-yu, Wen-wen, & Qin-yan, 2007), whilst Beijing had a proportionally larger accumulation mode (100-1000nm) of 7.8 x 10^3 cm^{-3} .

3.3 Mass measurements

3.3.1. *Mass size distribution*

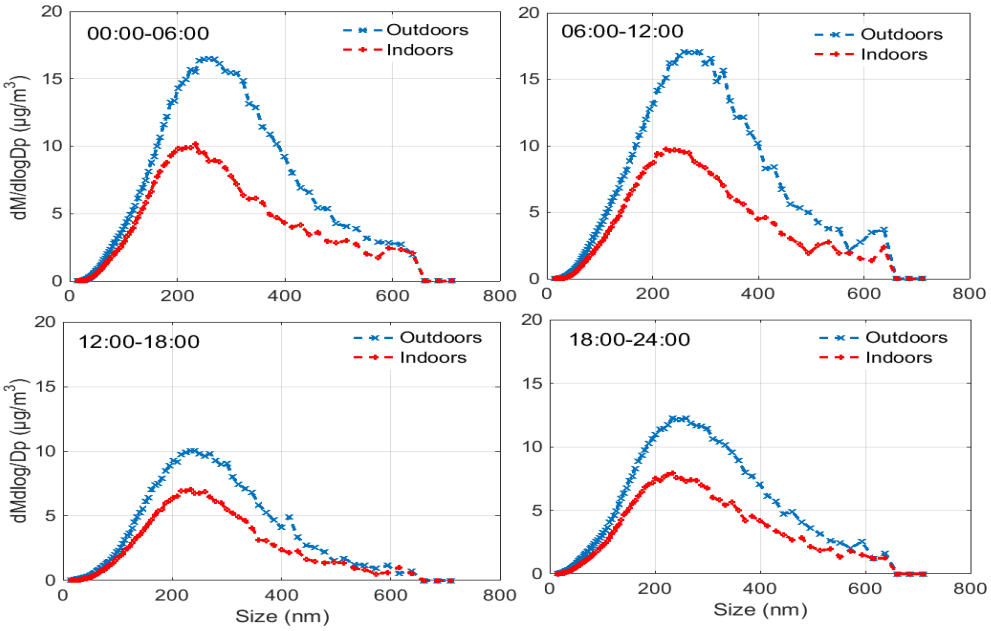

Figure 5. Averaged indoor/outdoor mean particle mass size distribution for the full campaign. The distribution split into 4 sub-daily periods. 00:00-06:00, 06:00-12:00, 12:00-18:00, and 18:00-24:00.

Mass size distributions derived from SMPS measurements are presented in Figure 5. During morning periods a mean concentration of 17 µg/m^3 outdoors and 9 -10 µg/m^3 indoors was observed. For the period of 12:00-18:00 hours outdoor concentrations fell from 17 µg/m^3 to 10 µg/m^3, whilst indoor values fell from 9 µg/m^3 to 7 µg/m^3. From 18:00-24:00 outdoor concentrations increased once more from 10 µg/m^3 to 13 µg/m^3, whilst indoor values remained stable. The 12:00-18:00 loss of mass concentration was observed daily throughout the campaign.

The I/O concentration ratio varies less indoors, presumably due to the more stable environment. The mass size distribution is bimodal, with the dominant mode between 200-300 nm. The outdoor mode was found to increase slightly during night time (Figure 5: 00:00-06:00). This increase was not observed indoors. The likely cause was diurnal fluctuations in RH values outdoor, with an overall nightly RH mean of 91.2% outdoors against 52.8% indoors. It is suspected this water content gradient, along with a greater night time I/O temperature gradient, helps dehydrate particulate as they penetrate indoors. It should also be acknowledged that some drying of the outdoor sample may also occur as the aerosol travels through the inlet to the indoor-located online instruments. This process would act to reduce the I/O modal difference.

3.3.2 Outdoor particle mass and NR-PM$_1$ species composition analysis

Overall results from AMS derived NR-PM$_1$ data show organic matter (3.6 µg/m^3) to be the dominant mass species outdoors, accounting for almost half of the total mass during the full study period [Table 2: All data]. Sulfate contributes a quarter of all mass loading (2.1 µg/m^3), whilst NO_3 (0.9 µg/m^3), elemental carbon (0.96 µg/m^3), and NH_4 (0.5 µg/m^3) contribute considerably less. To place these

results in context, Kubelová et al. (2015) used AMS measurements in the same location and found organic matter (4.2 μg/m^3) and SO_4 (2.0 μg/m^3) dominated in summer over NH_4 (1.2 μg/m^3) and NO_3 (0.8 μg/m^3). In Melpitz, Germany, Poulain et al. (2011) found organic matter (6.8 μg/m^3) and SO_4 (2.4 μg/m^3) to be prevalent over ammonium (0.9 μg/m^3) and NO_3 (0.6 μg/m^3). Both studies show comparable results of non-refractory PM_1 (NR-PM_1) derived from AMS measurements.

The key difference in aerosol composition between Melpitz and Prague is attributed to aerosol source. Prague's aerosol is urban background dominated by traffic emissions in summer (Kubelová et al., 2015; Ondráček et al., 2011), whilst Melpitz is a background site with major aerosol contribution in the form of biogenic and long range aerosol transport (Poulain et al., 2011). The similarity of Prague AMS PM_1 results to those observed in Melpitz may indicate the presence of regional aerosol during this campaign, or a similar influence of local sources.

Table 2 AMS compositional data for the full research period divided into AM/PM periods. % lost calculated by AM-PM/AM

		All data		All Data	All Data	AM/PM
		Ave	Proportional	AM	PM	%
Instrument	**Units**	**Outdoors**	**% Total**	**06:00 -12:00**	**12:00 - 18:00**	**Lost**
[EC-OC] EC	μg/m^3	0.96		0.8	0.6	25
AMS ORG	μg/m^3	3.6	51	3.3	2.0	40
AMS SO_4	μg/m^3	2.1	30	1.8	1.5	18
AMS NH_4	μg/m^3	0.5	7	0.5	0.3	40
AMS NO_3	μg/m^3	0.9	12	1.2	0.3	75
SMPS Mass	μg/m^3	7.9		9.8	4.7	52
Total AMS Mass	μg/m^3	7.3	100	6.8	3.6	47

Diurnal variation in mass concentration between morning and afternoons is quantified in Table 2 and graphically displayed in Figure 6. AMS compositional data are separated between AM (06:00-12:00) and PM (12:00-18:00) to assess composition mass changes. Daily mixing depth is shown as an insert in Figure 6; these fluctuations correspond to typical sunrise-sunset patterns for late August in Central

Europe. From 12:00-18:00 47% of mass is lost, compared to the preceding 06:00-12:00 period. The percentage loss of mass for each individual species is given in the right hand column of Table 2.

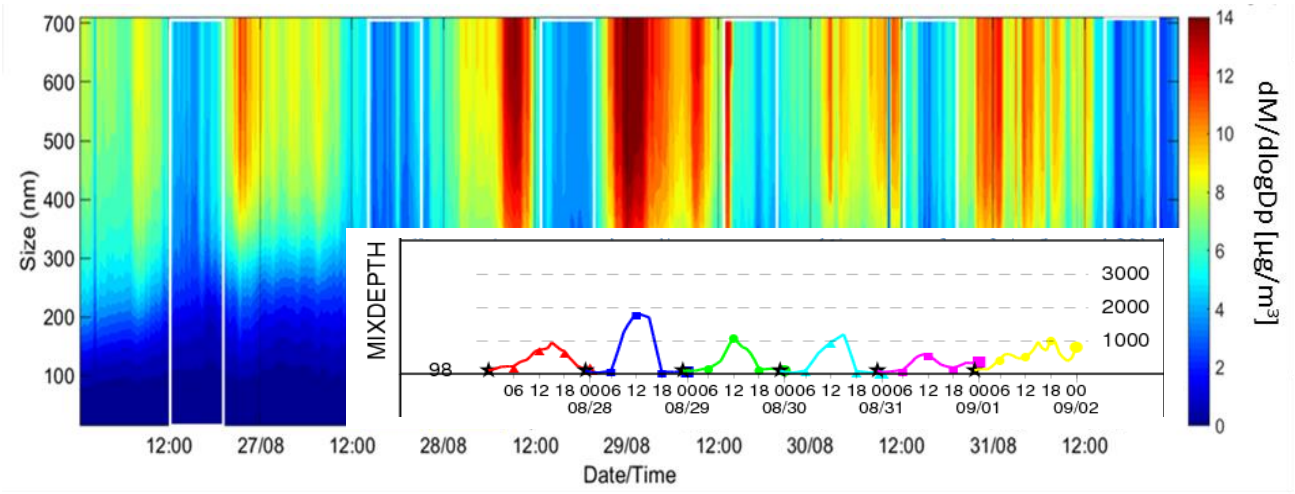

Figure 6. Cumulative contour plot using SMPS mass size distribution highlighting daily afternoon loss of mass (dates run left to right). A subset of mixing height [Inset] in meters, for the corresponding period, are also shown and include the 28th (maximum) and 31st (minimum).

3.3.3. Assessment of outdoor composition, diurnal mixing layer changes and species transformations

In this section we assess the impacts of two contrasting mixing layer height and physico-chemical transformations on total outdoor aerosol loading over a sub-daily timescale. To help achieve this a simplified boxplot model was utilized with fundamental processes graphically presented in Figure 7 (Guest, Mach, & Winchester, 1984). To assess the influence of mixing layer height we assume low variability in emission and deposition rates from mornings to afternoons. For example, we assume that traffic exhaust inputs during morning are largely replicated by those during the afternoon, with a return journey home. Furthermore, Kubelová et al. (2015) found, in a study carried out in the same location, also using AMS measurements, that SO_4 and Organics had both AM and PM peaks. We stress here that we do not presume a perfect mass balance between morning and afternoons, but that they are comparable. For this reason, we also excluded data from the day of the observed NPF event on the 30th August.

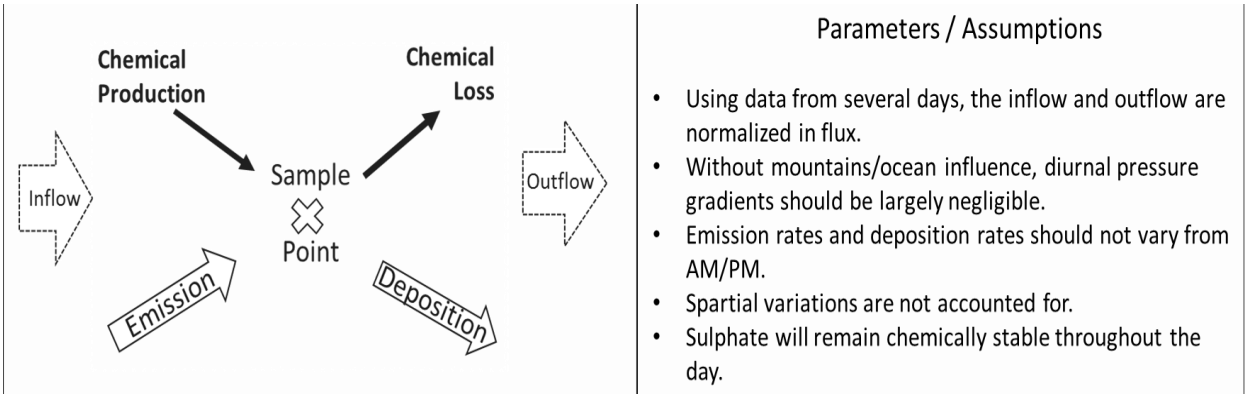

Figure 7. Basic principles of one box model showing input/outflow flux of aerosol (left) (Jacob, 1999), list of parameters and assumptions used in this experiment for the diurnal comparisons (right).

Results showed that through the campaign particle mass concentrations followed a relatively stable and predictable pattern of increases and decreases in accordance to time of day. We consider the probable causes of this to the occurrence of only one brief washout (wet deposition) episode, persistent stable meteorological conditions and a low fluctuation rate of sub-daily aerosol sources (such as daily morning/afternoon traffic exhaust). However, as expected, chemical composition was found to change over periods of days due to changes in airmass origin (Schwarz et al. 2012). To account for this we averaged the overall daily AM and PM aerosol composition mass. We also assume deposition rates to be consistent and relatively low due to organic matter and SO_4 usually being accumulation mode aerosol (Štefancová et al. 2010) (Figure 14). It is recognised that the assessment of changes to aerosol composition over short diurnal periods is complex and will not be exact, therefore this section uses AMS measurements to observe only the proportional changes to aerosol composition during AM and PM timeframes to obtain information on important diurnal processes.

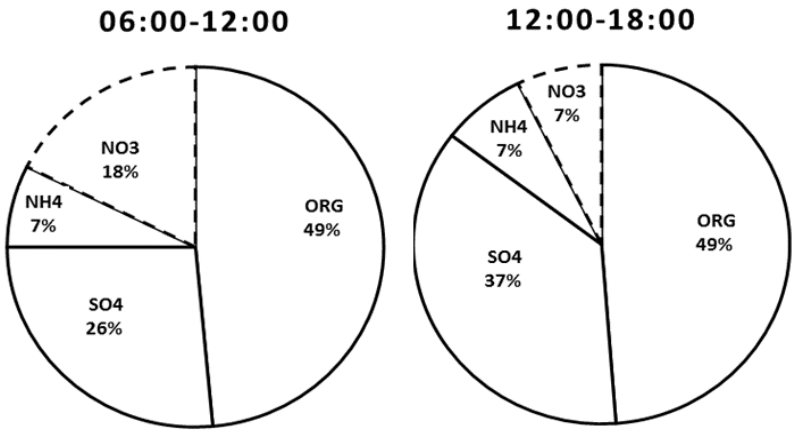

Figure 8. Proportional overall outdoor NR-PM_1 composition concentration from AM/PM for the full campaign. Taken from the AM/PM data in Table 2. Hatched area emphasizes change in NO_3.

Organic matter lost an average of 40% of its mass from morning to afternoon [Table 2] (3.3 µg/m^3/2.0 µg/m^3), however, it remained proportionally stable at 49% of total composition, as shown in Figure 8. We attribute this proportional stability of organics to inexact mass equilibrium between input and output of emission sources. To elaborate, Kubelová et al. (2015) observed peak during early morning (around 6-7am), resulting from lower temperatures during this time of day, which encouraged semi-volatile organics to partition to the particulate phase. This countered some dissociation of organics to the gas phase during the warmer afternoon period. However, Kubelová et al. (2015) also observed a second peak in organics during the afternoon, which can be associated to photo oxidation of both anthropogenic and biogenic precursor emissions.

SO_4 relative importance to total mass increased from 26% (AM) to 37% (PM). This increase can be attributed to the low volatility of SO_4 after an initial daily morning peak which coincided with morning peak SO_2 emissions (Kubelová et al., 2015). An added increase in afternoon SO_4 concentrations from the SO_4 reservoir effect would also enhance its proportion in PM_1 loading during afternoon periods (Xavier Querol et al., 1998). NH_4 remained proportionally stable at 7% of the total composition, whilst the largest proportional reduction was observed with NO_3 (18% AM to 7% PM). These results clearly show volatility losses contribute to aerosol mass reduction during a typical summer's day in Prague. If the 18% AM to PM reduction in mass of non-volatile SO_4 is attributed to losses due to increased dilution or/and mixing as well as other processes, the remaining losses of 22% of organic matter, 22% ammonium, and 57% of NO_3 mass loss can be attributed to physical transformation of aerosol during afternoon periods.

3.3.4 Mixing height, temperature and solar radiation

Mixing heights change dilution ratios, alter condensation sinks and influence aerosol mass loading (Boyouk, Léon, Delbarre, Podvin, & Deroo, 2010; Venzac et al., 2009). Afternoon losses can be explained by increased mixing, however, as Figure 6 shows, mixing height is already close to its maximum at 12:00 during this research period, therefore we suspect other processes also act to reduce mass concentrations. Mixing height is usually dependent on surface radiative forcing (temperature), which is generally correlated with solar radiation input (Thompson, 1998). All of these factors combine to introduce complex mechanisms that drive composition change. Two days of

contrasting mixing height, August 28th (mixing depth 1700m) and August 31st (mixing depth 650m), are compared.

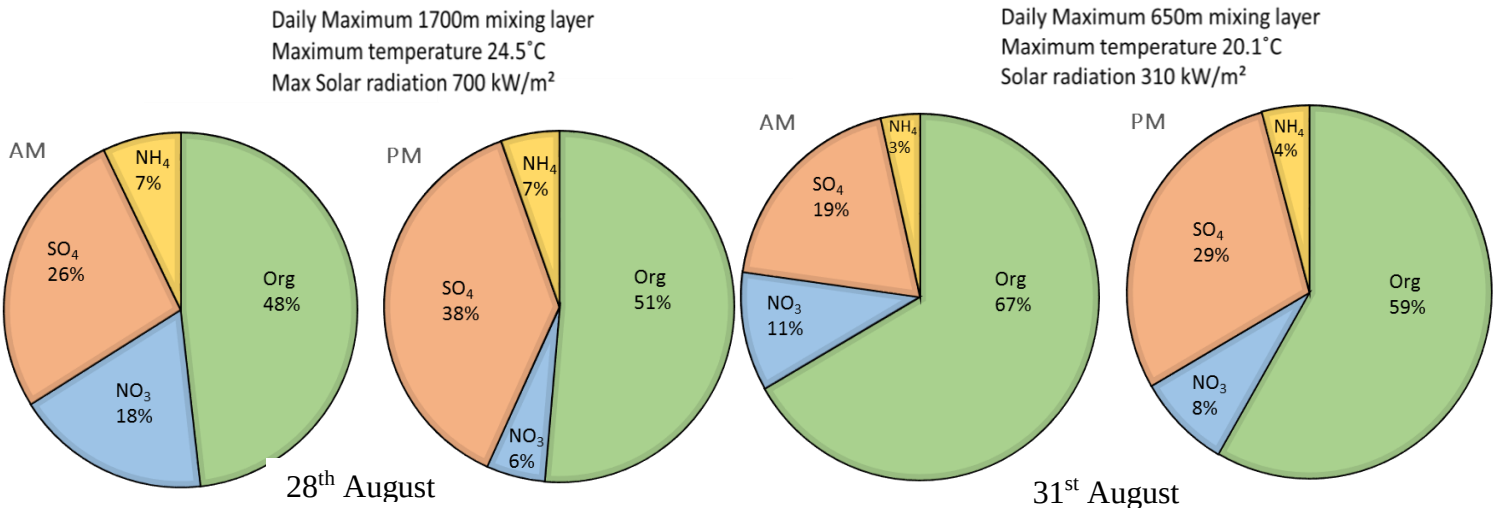

Figure 9. Changes in proportional composition in relation to mixing height change and temperature.

Table 3 AMS AM/PM data for the 28th and 31st August representing when the mixing height was at its maximum (28th) and minimum (31st)

[µg/m³]		Nr-Org	NO_3	SO_4	NH_4	Total
28th August	AM	2.7	1.0	1.5	0.4	5.6
	PM	1.9	0.2	1.4	0.2	3.6
31st August	AM	3.9	0.6	1.1	0.2	5.8
	PM	1.5	0.2	0.7	0.1	2.5

When the mixing height is at its greatest on the 28th August, SO_4 was found to change very little from AM to PM (Table 3). As already stated, a SO_4 reservoir in the boundary layer allowed advection of transported SO_4 to the study area. This is supported by the increased loss in SO_4 mass on the 31st August when the boundary layer is lower (Table 3).

Although there was an overall reduction in organics mass concentration from AM/PM, organic matter increased proportionally [Figure 9]. We associate this proportional increase to Increased O_3 and strong solar radiation which likely increasing SOA production during the afternoon of the 28th August (Liu et al., 2011). Conversely organic matter lost most mass when the mixing height was lower. This is most likely due to reduced SOA production through reduced solar radiation. However, other sources, such as fires, barbeques and traffic, may also affect the results. It was found that NO_3, mostly in the form of NH_4NO_3, showed the greatest variability with mixing height, as well as the highest loss rate from AM/PM on the warmer day during the campaign. The relationship between NH_4NO_3 phase and temperature and relative humidity is now explored.

3.3.5 Ammonium nitrate phase and equilibrium considerations

The K_p of ammonium nitrate is known to be dependent of temperature and relative humidity (Seinfeld and Pandis 2008). Of equal importance is the availability of NH_3, where HNO_3 competes with H_2SO_4 for neutralization. NH_3 is known to preference H_2SO_4 so it is whatever NH_3 is left that will be available to help form NH_4NO_3 (a. W. Stelson et al., 1979). Poulain et al. (2011) also detailed diurnal variations in different driving forces on NH_4NO_3 formation, and their work supports the research of Sartelet et al. (2007) who found HNO_3 formation is a very real limiting factor for to gas-particle phase equilibrium. HNO_3 is formed by several processes, most notably NO_2 + OH and N_2O_5 +H_2O during night time.

In an idealized system deliquescence of NH_4NO_3 should be 62% RH and the efflorescence RH is largely dependent of the history of the NH_4NO_3 particle (Poulain et al., 2011). However, the externally mixed nature of the atmosphere means that the physical state of the particle is unknown. This is important to understand as it effects dissociation rates. It should also be noted that HNO_3 does not just react with NH_3 but also sodium chloride, resulting in the chemical change of NaCl to $NaNO_3$. Previous research has shown that even far away from coastal regions, such as Prague, marine influences do exist (Poulain et al. 2011, Schwarz et al. 2012). Figure. 10 shows an example of NO_3 behaviour throughout a typical day. An increase of NO_3 was observed during the morning period, which was most likely caused by the chemical transformations previously mentioned. Increasing temperature coupled with decreasing humidity both help drive the following dissociation processes to the right hand side (Stelson et al, 1979)

$$NH_4NO_3 \text{ (s) or (aq)} \leftrightarrow NH_3 + HNO_3(g) \qquad (1)$$

Dissociation of NH_4NO_3 was observed by associated mass concentration loss at temperatures of 22˚C and 62% RH (Figure 10). Near midday the temperature drops briefly as a cold front passes over, however, there is only a small spike in NO_3. It is not until 21:00 when RH is 85% and temperature is 16.8 ˚C that gas to particle phase shift occurs. These temperatures and RH are higher than would be

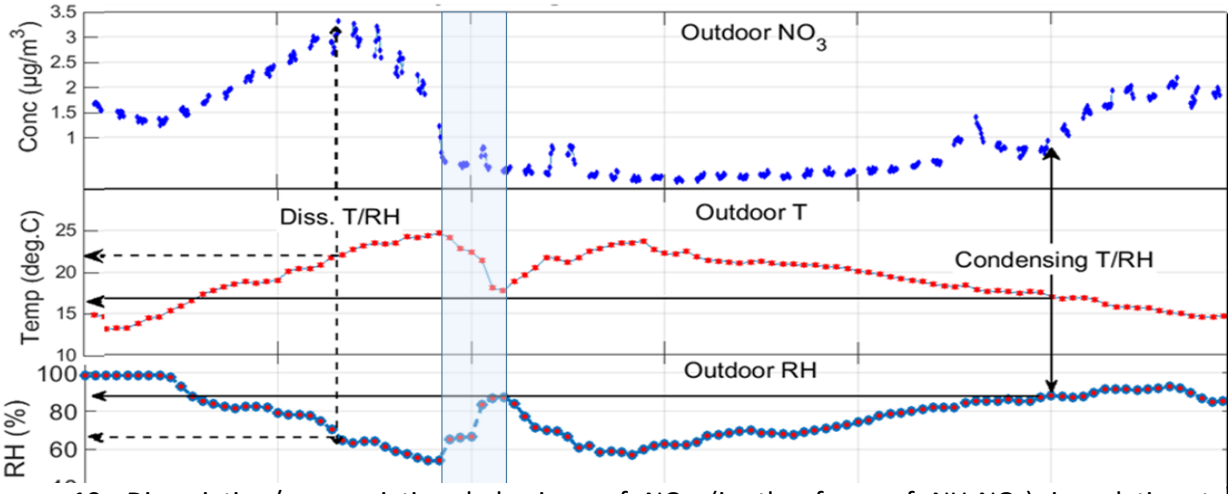

Figure 10. Dissociation/re-association behaviour of NO_3 (in the form of NH_4NO_3) in relation to temperature and relative humidity on Saturday 30th August. A brief rain event highlighted blue.

predicted through dissociation behaviour alone (Hightower & Richardson, 1988). However, this is possibly explained by Lightstone et al. (2000) and Han (2002), who found organics will be mixed with the inorganic salt of nitrate, which changes NH_4NO_3 deliquescence / efflorescence.

3.4 Indoor / outdoor characterization

Diurnal fluctuations outdoors are less apparent indoors, however, as a particle of outdoor origin penetrates indoors, it can be subjected to different temperatures, relative humidity and organic components, therefore instigating unique reactions (Lunden et al. 2003). This section utilizes real-time indoor/outdoor data to observe changes to outdoor particle concentration, composition, and mass and size distributions as they penetrate indoors.

3.4.1 Infiltration of particles and defining an Indoor/ outdoor ratio

In the absence of indoor sources, indoor concentrations are a product of those outdoors (Hussein et al. 2006), and are defined by the indoor/outdoor ratio, expressed by the following basic formula,

$$\text{I/ O } Ratio = \frac{C\_in}{C\_\text{out}} \quad (2)$$

Where $C_{\_in}$ and $C_{\_out}$ are indoor and outdoor concentrations respectively (Chen et al, 2011).

Temporal changes of indoor number concentrations can be described by this simple mathematical formula (Hussein and Kulmala 2007).

$$v\frac{dN_{in}}{dt} = \sum Sources - \sum Sink = P - E - \rho Q(N_{in} \_ N_{out}) \quad (3)$$

V - Volume of indoor air
P - Production of indoor particles
E - Elimination through reaction, filtration and settling.
Q - Air exchange rate
N_{in}/N_{out} - Number concentration indoors and outdoors with size selection.
ρ - Penetration

For this experiment we assume that with no disturbance in the sample room *P = 0*. The air exchange rate (Q) was hastened due to impactors and low flow filter instruments in the sample room, which means the E would likely be insignificant. The result of this is that the concentration indoors becomes reliant on the concentration outdoors and the infiltration factors of the size and composition of particle can best be described by the indoor/outdoor (I/O) ratio. It is understood that for the smallest and largest particles there would be expected to be some deposition losses through diffusive, transport or settling mechanisms (Diapouli et al. 2013). However, our main sampled chemical mass concentrations are in the accumulation mode particles where such factors would be expected to be minimal.

To further understand dispersal mechanisms within the sample room, CO_2 was released under normal sampling conditions, when no added ventilation or experimentation was taking place and other sampling instruments were running. The reduction curve was used to establish an air exchange rate of 1.26 air exchanges per hour.

The overall I/O ratio, separated into 3 size fractions and obtained from 3 weeks of SMPS PNC data, was .48 for <40 nm, .56 for 41-100 nm and .64 for >100-710 nm. It should be noted that infiltration rates are temporally variable, and known to be affected by meteorological conditions, particle size and compositional changes (Morawska et al., 2001). It is therefore of value to assess the overall I/O ratios with an event of a shorter time period. Figure 11 shows how particle size distribution changes over time for the observed NPF and growth on the 30th August both outdoors and indoors. A 20 minute infiltration delay from outdoor to indoors is recorded. This time was evaluated by matching the sharp increase of the new particle formation outdoors against the related increase indoors.

The observed particle formation and growth gives a time evolution of particle number concentration to identify I/O ratios between sizes 20 and 200 nm. This was carried out by taking a subsection of the particle plume outdoors (Figure 11 shown with white squares numbered 1-7) and comparing it against SMPS scans within the same size subsection from indoors. The average size of the square is defined by the averaged PNC within that size subset and time period, calculated from the average obtained over a number of scans. An infiltration time-lapse of 20 min was allocated. It is considered likely that the particle would shrink slightly on penetrating indoors due to thermal drying processes, however small I/O temperature gradients and similar daytime I/O relative humidity values meant minimal shrinkage was anticipated.

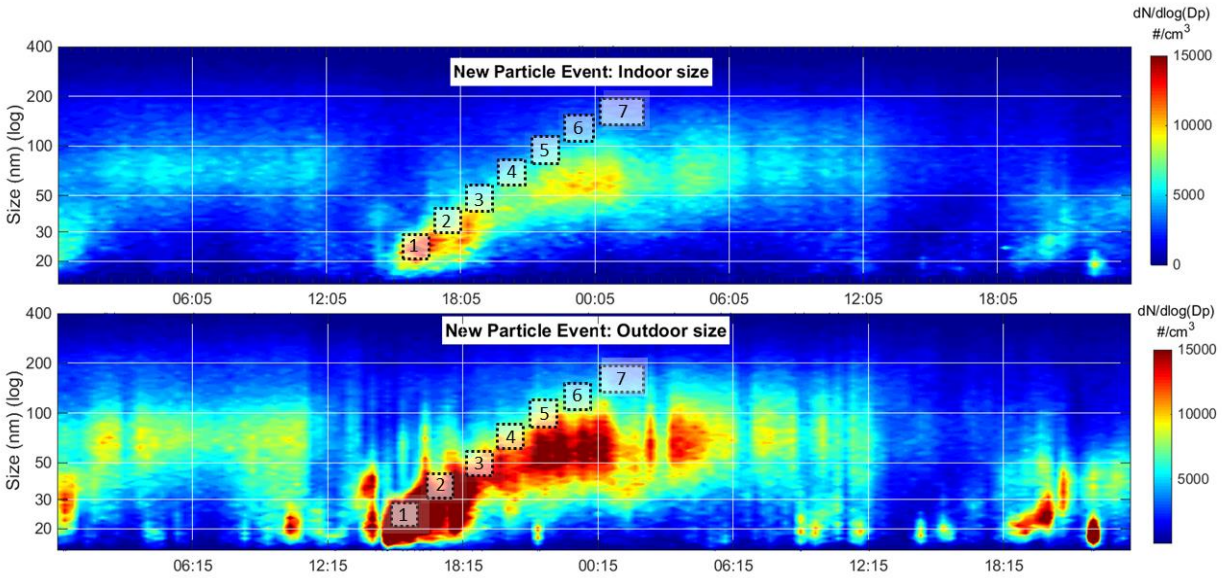

Figure 11. Contour plot of aerosol size distribution for the 30th and 31st August. The I/O data subsets used for subsequent penetration ratio calculations are labelled 1-7

Reference number	Size [nm]	I/O Ratio
1	20-30	0.46
2	30-40	0.54
3	40-60	0.67
4	60-80	0.65
5	80-110	0.62
6	110-150	0.67
7	150-200	0.64

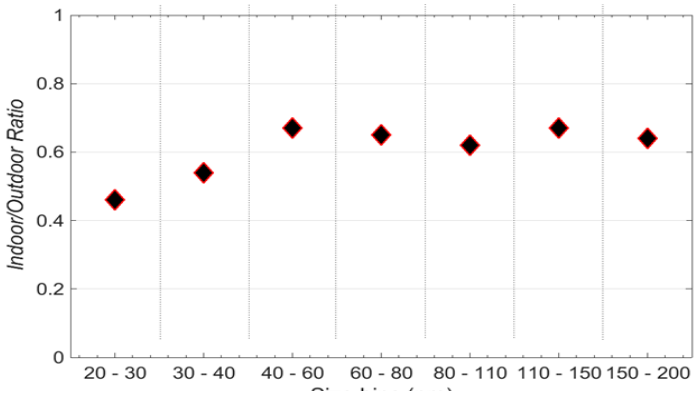

Figure 12. Indoor / outdoor ratio with given particle size from SMPS PNSD data displayed in Figure.11.

Figure 12 gives the calculated I/O ratio over this period. A ratio of 0.46 was calculated for the smallest size fractions, observed here at 20-30 nm. It was then observed that the I/O ratio becomes consistent for accumulation mode particles near 0.65. This is in good agreement with the overall mean I/O ratio for the nucleation and accumulation modes. Calculating a more detailed penetration factor, Hussein et al. (2006) found that I/O penetration factors remained constant for accumulation mode particles between 80 and 500 nm. They calculated a rate of 0.75 for the same apartment. Recent renovations, including the replacement of old windows, would make an I/O ratio of 0.65 reasonable. It should be kept in mind that highly time resolved SMPS data, used here to derive I/O ratios, and would provide a realistic penetration factor due to the high exchange rate observed during the campaign.

3.4.2 Indoor compositional analysis

Averaged indoor data for the full campaign are shown in Table 4. The I/O ratio can now be used to interpret compositional differences, with the understanding that the 0.65 I/O ratio value indicates that, once diffusive and other transport losses have been accounted for, a 0.65 fraction (or 65%) of particles outdoors successfully penetrate indoors.

Table 4. Indoor AMS, EC, and SMPS data for full research period with the I/O ratio fraction calculated.

Instrument	Chemical	Indoor Mass [µg/m^3]	Outdoor Mass [µg/m^3]	I/O Ratio
[EC-OC]	EC	0.9	0.96	0.90
AMS [PM_1]	Org	2.7	3.6	0.69
AMS [PM_1]	SO_4	1.7	2.1	0.84
AMS [PM_1]	NH_4	0.3	0.5	0.60
AMS [PM_1]	NO_3	0.4	0.9	0.33
AMS [PM_1]	Total Mass	5.1	7.3	0.65
SMPS [$PM_{0.71}$]	Total Mass	5.5	7.9	0.63

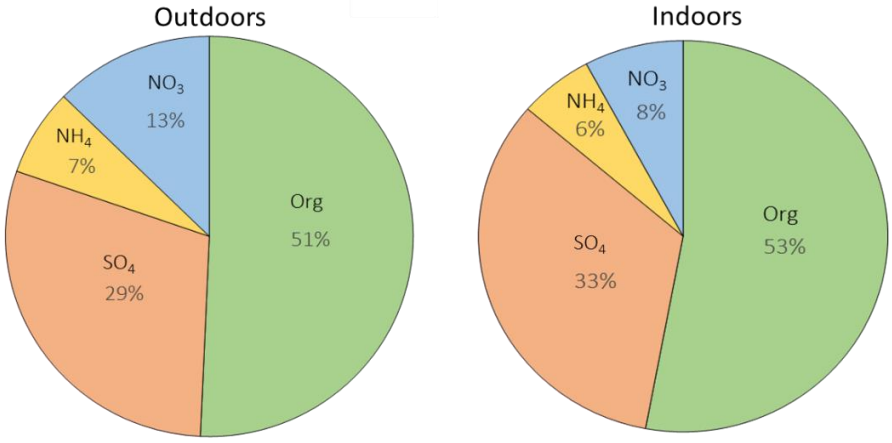

Figure 13. Changes in PM_1 chemical composition from outdoors to indoors during the campaign, as obtained by the AMS

As displayed in Table 4, SMPS mass reduced from 7.9 µg/m^3 outdoors to 5.5 µg/m^3 indoors with a given ratio of 0.63, which includes the smallest modes that penetrate less efficiently. AMS mass fell from 7.3 µg/m^3 outdoors to 5.1 µg/m^3 indoors, giving 0.65 ratio. The good agreement between different instruments is encouraging and gives weight to the precision of 0.65 I/O ratio. Stable compounds SO_4 and elemental carbon represent a greater ratio indoors, and their chemical stability and typical diameter in accumulation mode allows them to remain longer in the atmosphere, as previously described.

Figure 13 shows that organics and SO_4 proportionally increase slightly at the expense of NO_3, which is predicted to be mostly in the form of NH_4NO_3 (Seinfeld & Pandis, 2008). Observed NO_3 losses indoors are in-line or above the concentrations found in previous literature (Smolík et al. 2008; Mašková et al. 2015; Lunden et al. 2003), where measurements were taken offline, generally using filters and PIXE/IC analysis.

The presence of NO_3 indoors using real-time AMS data is of interest when set against previous research where filter measurements were made. Filter measurements, taken over longer sampling periods to collect adequate concentrations for analysis, have generally shown an absence of NO_3, except where backup filters have been used specifically to capture NO_3. However, as is shown here, NO_3 is observable when real-time measurements are made. This indicates the time dependence factor for the capture and recording of particles whilst dissociation / shrinking of NH_4NO_3 is occurring. This time factor must be considered in relation to particle residence time, especially in enclosed microenvironments. Dissociation of NH_4NO_3 indoors is not only driven by temperature, but also with the interaction of the aerosol with surfaces such as walls, furniture, ceilings and other structures. Acid-base reactions allow nitric acid to be stripped from the aerosol and quickly absorbed to surfaces, further accelerating dissociation (Hering & Cass, 1999). It should be noted this process also applies to the stainless steel inlet of the online AMS/SMPS system.

Filters collected from BLPI were run concurrently indoors and outdoors 4 times over 23 h sample periods during the campaign, with results presented in Figure 14. They show NO_3 is almost completely absent indoors on impactor measurements, in agreement to previous research and confirming the time dependent factor. There is also the coarse mode NO_3 on the median stage sizes between 2.5 µm and 5 µm. This is most likely attributed to $NaNO_3$ (Schwarz et al. 2012; Kubelová et al. 2015). Finally, Figure 14 also shows the strong relationship between SO_4 and NH_4, with similar mass size distributions, which demonstrates NH_4 preferred bonding to SO_4 over NO_3.

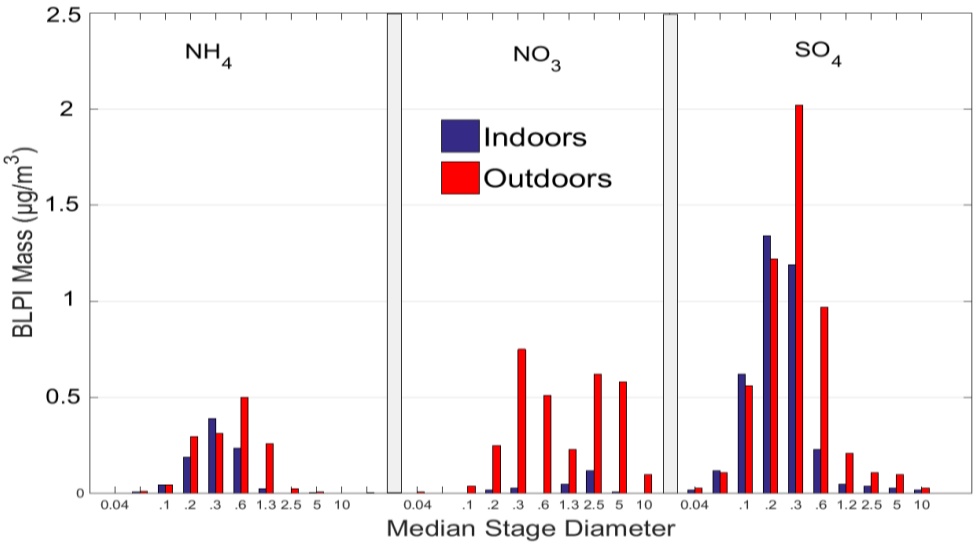

Figure 14. Average BLPI data for the major ions collected over the campaign period.

4 Summary and Conclusions

Total number particle concentrations during the campaign were lower than the long term average obtained from the same site. Sub-daily changes in modal size were observed when detailed analysis was carried out. Indoor size distributions modes were temporally responsive to changes outdoors, showing a distinct indoor/outdoor relationship. During the afternoon period of 12:00-18:00 a dominant 20-30 nm mode was evident. Although overall concentrations were still low, it is likely some new particle formation occurred during this period, with SOA production and shrinking of semi-volatile organic and inorganic species also likely. It is noted that only one new particle formation event was recorded during this study, which was attributed to dry conditions and high condensation sink during most days.

Mass concentrations show an inverse relationship from that of number size distribution. Lowest mass measurements both indoors and outdoors are observed during the afternoon periods when PNC were highest. It was found organics and SO_4 are the most prevalent species identified by compositional analysis from AMS PM_1 measurement. For the full campaign, organics represented half the total composition mass outdoors [3.6 µg/m^3] and indoors [2.7 µg/m^3] whilst SO_4 represented almost a third outdoors [2.1 µg/m^3] and indoors [1.7 µg/m^3]. This ratio was found to be similar to indoor and outdoor

composition, indicative of similar temperatures and relative humidity indoors and outdoors during daytime, which minimalized physico-chemical changes.

Using a simple dynamic model, dilution properties of mixing heights were assessed against volatility losses. SO_4 concentrations changed somewhat day to day. These changes were attributed to changes in SO_2 chemical conversion and increased input through the reservoir effect. However, sulfates known stability and longer temporal resolution allowed for its averaged diurnal loss of mass of 18%, from morning to afternoon, to be used as an approximation for proportional loses that could be accounted for by diurnal mixing height changes. NO_3, mostly in the form of NH_4NO_3, lost 57% of the mass after accounting for the 18% mixing /dilution loses. These losses were then set against AM/PM temperature changes, a key component of volatility. It was observed that once the temperature exceeded 22˚C a sharp reduction in mass concentration was observed. However, NO_3 mass was not observed to increase until temperatures were <17 ˚C – a delay most likely caused by the absence of precursor HNO_3 and the impure state of NO_3 aerosol. When observing the total aerosol composition, NR-Organics were the dominant species throughout the campaign, accounting for proportionally half total PM_1 mass, whilst SO_4 was found to proportionally increase more when mixing height is greatest, usually at the expense of NO_3. Organics lost more mass concentration during low mixing layer states, whilst higher mixing layer and associated temperature seemed to drive SOA production, decreasing proportional losses.

Indoors, a penetration ratio of between 0.4 for <40 nm and 0.65 for 80-200 nm was calculated during the growth period of the new particle formation event and was tested against the I/O comparisons of AMS, SMPS and BLPI, which all confirmed a I/O ratio of between .65 and .69. SO_4, EC and organics showed higher indoor values than the .65 ratio predicted. It is proposed that organics attachment to EC particles and SO_4 low volatility state may allow for higher proportional concentrations of these species to be observed indoors. Offline BLPI data showed fine fraction NO_3 in smaller concentrations than seen on AMS measurements, illustrating the extra mass losses that can be attributed to longer temporal resolution measurement techniques. However, BLPI measurements did clearly show coarse mode NO_3 on outdoor measurements, which is the likely product of $NaNO_3$ conversion.

Acknowledgements

The authors acknowledge support of this work by European Union Seventh Framework Programme (FP7/2007-2013) under grant agreement n° 315760 HEXACOMM.

5 References

Andelova, L., Smolik, J., Ondrackova, L., Ondracek, J., Lopez-Aparicio, S., Grontoft, T., & Stankiewicz, J. (2010). Characterization of Airborne Particles in the Baroque Hall of the National Library. Retrieved March 16, 2015, from http://www.morana-rtd.com/e-preservationscience/2010/Andelova-26-04-2010.pdf

Boyouk, N., Léon, J. F., Delbarre, H., Podvin, T., & Deroo, C. (2010). Impact of the mixing boundary layer on the relationship between PM2.5 and aerosol optical thickness. Atmospheric Environment, 44(2), 271–277. http://doi.org/10.1016/j.atmosenv.2009.06.053

Chen, C., & Zhao, B. (2011). Review of relationship between indoor and outdoor particles: I/O ratio, infiltration factor and penetration factor. Atmospheric Environment, 45(2), 275–288. http://doi.org/10.1016/j.atmosenv.2010.09.048

Chen, C., Zhao, B., & Weschler, C. (2012). Indoor exposure to "outdoor PM10": assessing its influence on the relationship between PM10 and short-term mortality in US cities. Epidemiology. Retrieved from http://journals.lww.com/epidem/Abstract/2012/11000/Indoor_Exposure_to__Outdoor_PM10___Assessing_Its.17.aspx

Decarlo, P. F., Kimmel, J. R., Trimborn, A., Northway, M. J., Jayne, J. T., Aiken, A. C., Jimenez, J. L. (2006). Aerosol Mass Spectrometer. Analytical Chemistry, 78(24), 8281–8289. http://doi.org/8410.1029/2001JD001213.Analytical

Diapouli, E., Chaloulakou, A., & Koutrakis, P. (2013). Estimating the concentration of indoor particles of outdoor origin: A review. Journal of the Air & Waste Management Association, 63(10), 1113–1129. http://doi.org/10.1080/10962247.2013.791649

Dockery, D. W., Pope, C. A., Xu, X., Spengler, J. D., Ware, J. H., Fay, M. E., … Speizer, F. E. (1993). An association between air pollution and mortality in six U.S. cities. The New England Journal of Medicine, 329(24), 1753–9. http://doi.org/10.1056/NEJM199312093292401

Drewnick, F., Hings, S. S., DeCarlo, P., Jayne, J. T., Gonin, M., Fuhrer, K., … Worsnop, D. R. (2005). A New Time-of-Flight Aerosol Mass Spectrometer (TOF-AMS)—Instrument Description and First Field Deployment. Aerosol Science and Technology, 39(7), 637–658. http://doi.org/10.1080/02786820500182040

Gemenetzis, P., Moussas, P., Arditsoglou, A., & Samara, C. (2006). Mass concentration and elemental composition of indoor PM2.5 and PM10 in University rooms in Thessaloniki, northern Greece. Atmospheric Environment, 40(17), 3195–3206. http://doi.org/10.1016/j.atmosenv.2006.01.049

Guest, P. S., Mach, W. H., & Winchester, J. W. (1984). Meteorological associations with aerosol composition in the boundary layer. Journal of Geophysical Research, 89(D1), 1459. http://doi.org/10.1029/JD089iD01p01459

Hämeri, K., Hussein, T., Kulmala, M., & Aalto, P. (2004). Measurements of fine and ultrafine particles in Helsinki: Connection between outdoor and indoor air quality. Boreal Environment Research, 9(6), 459–467.

Han, J.-H. (2002). Size effect of hematite and corundum inclusions on the efflorescence relative humidities of aqueous ammonium nitrate particles. Journal of Geophysical Research, 107(D10), 4086. http://doi.org/10.1029/2001JD001054

Hänninen, O. O., Lebret, E., Ilacqua, V., Katsouyanni, K., Künzli, N., Srám, R. J., & Jantunen, M. (2004). Infiltration of ambient PM2.5 and levels of indoor generated non-ETS PM2.5 in residences of four European cities. Atmospheric Environment, 38(37), 6411–6423. http://doi.org/10.1016/j.atmosenv.2004.07.015

Hering, S., & Cass, G. (1999). The Magnitude of Bias in the Measurement of PM25 Arising from Volatilization of Particulate Nitrate from Teflon Filters. Journal of the Air & Waste Management Association, 49(6), 725–733. http://doi.org/10.1080/10473289.1999.10463843

Hightower, R. L., & Richardson, C. B. Evaporation of ammonium nitrate particles containing ammonium sulfate, 22 Atmospheric Environment 2587–2591 (1988).

Huang, Z., Harrison, R. M., Allen, A. G., James, J. D., Tilling, R. M., & Yin, J. (2004). Field intercomparison of filter pack and impactor sampling for aerosol nitrate, ammonium, and sulphate at coastal and inland sites. Atmospheric Research, 71(3), 215–232. http://doi.org/10.1016/j.atmosres.2004.05.002

Hussein, T., Glytsos, T., Ondráček, J., Dohányosová, P., Ždímal, V., Hämeri, K., Kulmala, M. (2006). Particle size characterization and emission rates during indoor activities in a house. Atmospheric Environment, 40(23), 4285–4307. http://doi.org/10.1016/j.atmosenv.2006.03.053

Hussein, T., Hämeri, K., Heikkinen, M. S. A., & Kulmala, M. (2005). Indoor and outdoor particle size characterization at a family house in Espoo–Finland. Atmospheric Environment, 39(20), 3697–3709. http://doi.org/10.1016/j.atmosenv.2005.03.011

Hussein, T., Kukkonen, J., Korhonen, H., Pohjola, M., Pirjola, L., Wraith, D., Kulmala, M. (2007). Evaluation and modeling of the size fractionated aerosol particle number concentration measurements nearby a major road in Helsinki – Part II: Aerosol measurements within the SAPPHIRE project. Atmospheric Chemistry and Physics, 7(15), 4081–4094. http://doi.org/10.5194/acp-7-4081-2007

Hussein, T., & Kulmala, M. (2007). Indoor Aerosol Modeling: Basic Principles and Practical Applications. Water, Air, & Soil Pollution: Focus, 8(1), 23–34. http://doi.org/10.1007/s11267-007-9134-x

Kampa, M., & Castanas, E. (2008). Human health effects of air pollution. Environmental Pollution (Barking, Essex : 1987), 151(2), 362–7. http://doi.org/10.1016/j.envpol.2007.06.012

Koistinen, K. J., Edwards, R. D., Mathys, P., Ruuskanen, J., Künzli, N., & Jantunen, M. J. (2004). Sources of fine particulate matter in personal exposures and residential indoor, residential outdoor and workplace microenvironments in the Helsinki phase of the EXPOLIS study. Scandinavian Journal of Work, Environment & Health, 30 Suppl 2, 36–46. Retrieved from http://www.ncbi.nlm.nih.gov/pubmed/15487684

Kousa, A., Kukkonen, J., & Karppinen, A. (2002). A model for evaluating the population exposure to ambient air pollution in an urban area. Atmospheric Environment, Retrieved from http://www.sciencedirect.com/science/article/pii/S1352231002002285

Kubelová, L., Vodička, P., Schwarz, J., Cusack, M., Makeš, O., Ondráček, J., & Ždímal, V. (2015). A study of summer and winter highly time-resolved submicron aerosol composition measured at a suburban site in Prague. Atmospheric Environment, 118, 45–57. http://doi.org/10.1016/j.atmosenv.2015.07.030

Lazaridis, M., & Aleksandropoulou, V. (2006). characterization of indoor/outdoor particulate matter in two residential houses in Oslo, Norway: measurements overview and physical properties–URBAN-AEROSOL. Indoor Air Retrieved from http://onlinelibrary.wiley.com/doi/10.1111/j.1600-0668.2006.00425.x/full

Lehmann, K., Massling, a., Tilgner, a., Mertes, S., Galgon, D., & Wiedensohler, a. (2005). Size-resolved soluble volume fractions of submicrometer particles in air masses of different character. Atmospheric Environment, 39(23-24), 4257–4266. http://doi.org/10.1016/j.atmosenv.2005.02.011

Lightstone, J. M., Onasch, T. B., Imre, D., & Oatis, S. (2000). Deliquescence, Efflorescence, and Water Activity in Ammonium Nitrate and Mixed Ammonium Nitrate/Succinic Acid Microparticles. The Journal of Physical Chemistry A, 104(41), 9337–9346. Retrieved from http://pubs.acs.org/doi/abs/10.1021/jp002137h

Liu, P. F., Zhao, C. S., Göbel, T., Hallbauer, E., Nowak, A., Ran, L., Wiedensohler, A. (2011). Hygroscopic properties of aerosol particles at high relative humidity and their diurnal variations in the North China Plain. Atmospheric Chemistry and Physics, 11(7), 3479–3494. http://doi.org/10.5194/acp-11-3479-2011

Lunden, M. M., Revzan, K. L., Fischer, M. L., Thatcher, T. L., Littlejohn, D., Hering, S. V., & Brown, N. J. (2003). The transformation of outdoor ammonium nitrate aerosols in the indoor environment. Atmospheric Environment, 37(39-40), 5633–5644. http://doi.org/10.1016/j.atmosenv.2003.09.035

Mašková, L., Smolík, J., & Vodička, P. (2015). Characterisation of particulate matter in different types of archives. Atmospheric Environment, 107, 217–224. http://doi.org/10.1016/j.atmosenv.2015.02.049

Morawska, L., He, C., Hitchins, J., Gilbert, D., & Parappukkaran, S. (2001). The relationship between indoor and outdoor airborne particles in the residential environment. Atmospheric Environment, 35(20), 3463–3473. http://doi.org/10.1016/S1352-2310(01)00097-8

Naumova, Y. Y., Offenberg, J. H., Eisenreich, S. J., Meng, Q., Polidori, A., Turpin, B. J., … Farrar, C. (2003). Gas/particle distribution of polycyclic aromatic hydrocarbons in coupled outdoor/indoor atmospheres. Atmospheric Environment, 37(5), 703–719. http://doi.org/10.1016/S1352-2310 (02)00820-8

OECD, & Foundation, C. D. R. (2010). Trends in Urbanisation and Urban Policies in OECD Countries What Lessons for China? What Lessons for China? OECD Publishing. Retrieved from https://books.google.com/books?id=kqNKpU7yfOkC&pgis=1

Ondráček, J., Schwarz, J., Ždímal, V., Andělová, L., Vodička, P., Bízek, V.,Smolík, J. (2011). Contribution of the road traffic to air pollution in the Prague city (busy speedway and suburban crossroads). Atmospheric Environment, 45(29), 5090–5100. http://doi.org/10.1016/j.atmosenv.2011.06.036

Poulain, L., Spindler, G., Birmili, W., Plass-Dülmer, C., Wiedensohler, A., & Herrmann, H. (2011). Seasonal and diurnal variations of particulate nitrate and organic matter at the IfT research station Melpitz. Atmospheric Chemistry and Physics, 11(24), 12579–12599. http://doi.org/10.5194/acp-11-12579-2011

Putaud, J.-P., Van Dingenen, R., Alastuey, A., Bauer, H., Birmili, W., Cyrys, J., Raes, F. (2010). A European aerosol phenomenology – 3: Physical and chemical characteristics of particulate matter from 60 rural, urban, and kerbside sites across Europe. Atmospheric Environment, 44(10), 1308–1320. http://doi.org/10.1016/j.atmosenv.2009.12.011

Querol, X., Alastuey, A., Puicercus, J. A., Mantilla, E., Miro, J. V., Lopez-Soler, A., Artiñano, B. (1998). Seasonal evolution of suspended particles around a large coal-fired power station. Atmospheric Environment, 32(11), 1963–1978. http://doi.org/10.1016/S1352-2310 (97)00504-9

Rimnácová, D., Ždímal, V., Schwarz, J., Smolík, J., & Rimnác, M. (2011). Atmospheric aerosols in suburb of Prague: The dynamics of particle size distributions. Atmospheric Research, 101(3), 539–552. http://doi.org/10.1016/j.atmosres.2010.10.024

Sakurai, H., Tobias, H. J., Park, K., Zarling, D., Docherty, K. S., Kittelson, D. B., … Ziemann, P. J. (2003). On-line measurements of diesel nanoparticle composition and volatility. Atmospheric Environment, 37(9-10), 1199–1210. http://doi.org/10.1016/S1352-2310 (02)01017-8

Schwartz, J., Dockery, D. W., & Neas, L. M. (1996). Is Daily Mortality Associated Specifically with Fine Particles? Journal of the Air & Waste Management Association, 46(10), 927–939. http://doi.org/10.1080/10473289.1996.10467528

Schwarz, J., Štefancová, L., & Maenhaut, W. (2012). Mass and chemically speciated size distribution of Prague aerosol using an aerosol dryer— The influence of air mass origin. Science of the Total Environment, Retrieved from http://www.sciencedirect.com/science/article/pii/S0048969712009953

Schwarz, J., Štefancová, L., Maenhaut, W., Smolík, J., & Ždímal, V. (2012). Mass and chemically speciated size distribution of Prague aerosol using an aerosol dryer - The influence of air mass origin. Science of the Total Environment, 437, 348–362. http://doi.org/10.1016/j.scitotenv.2012.07.050

Seinfeld, J. H., & Pandis, S. N. (2006). Ch 17 Cloud Physics. Seinfeld & Pandis (Vol. 41). Retrieved from http://www.ncbi.nlm.nih.gov/pubmed/19286526

Smolík, J., Dohányosová, P., & Schwarz, J. (2008). Characterization of indoor and outdoor aerosols in a suburban area of Prague. Water, Air, & Soil, Retrieved from http://link.springer.com/article/10.1007/s11267-007-9141-y

Štefancová, L., Schwarz, J., Mäkelä, T., Hillamo, R., & Smolík, J. (2011). Comprehensive Characterization of Original 10-Stage and 7-Stage Modified Berner Type Impactors. Aerosol Science and Technology, 45(1), 88–100. http://doi.org/10.1080/02786826.2010.524266

Stein, A.F., Draxler, R.R, Rolph, G.D., Stunder, B.J.B., Cohen, M.D., and Ngan. (2015). NOAA's HYSPLIT atmospheric transport and dispersion modeling system. Amer. Meteor. Soc., 96, 2059–2077.

Stelson, a. W., Friedlander, S. K., & Seinfeld, J. H. (1979). A note on the equilibrium relationship between ammonia and nitric acid and particulate ammonium nitrate. Atmospheric Environment (1967), 13(3), 369–371. http://doi.org/10.1016/0004-6981 (79)90293-2

Tang, I. N., & Munkelwitz, H. R. (1993). Composition and temperature dependence of the deliquescence properties of hygroscopic aerosols. Atmospheric Environment. Part A. General Topics.

Venzac, H., Sellegri, K., Villani, P., Picard, D., & Laj, P. (2009). Seasonal variation of aerosol size distributions in the free troposphere and residual layer at the puy de Dôme station, France. Atmospheric Chemistry and Physics, 9(4), 1465–1478. http://doi.org/10.5194/acp-9-1465-2009

Viana, M., Kuhlbusch, T. A. J., Querol, X., Alastuey, A., Harrison, R. M., Hopke, P. K., Hitzenberger, R. (2008). Source apportionment of particulate matter in Europe: A review of methods and results. Journal of Aerosol Science, 39(10), 827–849. http://doi.org/10.1016/j.jaerosci.2008.05.007

Vodička, P., Schwarz, J., & Ždímal, V. (2013). Analysis of one year's OC/EC data at a Prague suburban site with 2-h time resolution. Atmospheric Environment, 77, 865–872. http://doi.org/10.1016/j.atmosenv.2013.06.013

Wehner, B., & Wiedensohler, A. (2003). Long term measurements of submicrometer urban aerosols: statistical analysis for correlations with meteorological conditions and trace gases. Atmospheric Chemistry and Physics, Retrieved from http://www.atmos-chem-phys.net/3/867/2003/acp-3-867-2003.pdf

Wu, Z., Hu, M., Lin, P., Liu, S., Wehner, B., & Wiedensohler, A. (2008). Particle number size distribution in the urban atmosphere of Beijing, China. Atmospheric Environment, 42(34), 7967–7980. http://doi.org/10.1016/j.atmosenv.2008.06.022

Yu, O., Sheppard, L., Lumley, T., Koenig, J. Q., & Shapiro, G. G. (2000). Effects of ambient air pollution on symptoms of asthma in seattle-area children enrolled in the CAMP study. Environmental Health Perspectives, 108(12), 1209–1214. Retrieved from http://www.scopus.com/inward/record.url?eid=2-s2.0-0034519473&partnerID=tZOtx3y1

Yu, W., Bao-yu, G. a O., Wen-wen, Y. U. E., & Qin-yan, Y. U. E. (2007). Je Sc Sc, 19, 1305–1310.

Zhang, X. Y., Wang, Y. Q., Niu, T., Zhang, X. C., Gong, S. L., Zhang, Y. M., & Sun, J. Y. (2012). Atmospheric aerosol compositions in China: Spatial/temporal variability, chemical signature, regional haze distribution and comparisons with global aerosols. Atmospheric Chemistry and Physics, 12(2), 779–799. http://doi.org/10.5194/acp-12-779-2012

Zhou, B., Zhao, B., Guo, X., Chen, R., & Kan, H. (2013). Investigating the geographical heterogeneity in PM 10-mortality associations in the China Air Pollution and Health Effects Study (CAPES): A potential role of indoor. Atmospheric Environment. Retrieved from http://www.sciencedirect.com/science/article/pii/S1352231013002987

Zhu, Y., Hinds, W. C., Krudysz, M., Kuhn, T., Froines, J., & Sioutas, C. (2005). Penetration of freeway ultrafine particles into indoor environments. Journal of Aerosol Science, 36(3), 303–322. http://doi.org/10.1016/j.jaerosci.2004.09.007

Supplementary material

SI Table 1: Metadata from the campaign including periods where data was removed

Metadata file								
Date	**Time Begum**	**Time ended**	**Experiment**	**Instruments effected**	**Data removed from/to**	**Indoors**	**Outdoors**	**Notes**
21-Aug	10:40	Campaign Begun. All instruments except AMS running						
22-Aug	10:20	10:50	Vacuum cleaner	All	10:10-12:45			
27-Aug	16:30		AMS running					
28-Aug	6:00	8:30	Lawn mowing	All	06:00-09:30			
	10:40	10:55	smoking	All	10:40-13:55			
29-Aug	12:15	13:40	Car exhaust emmision	All	10:00-14:00			Maintenance
	18:00	18:24	Shower	All	15:00-21:05			Maintenance
1-Sep	11:14	12:00	Car exhaust emmision	All	10:00-14:35			Maintenance
	18:30	18:35	Cleaning product	All	18:25-21:45			
			" "	AMS	18:25 (1st) - 13:10 (2nd)			NH_4 effected
3-Sep	16:00	19:00	BBQ	All	15:30 - 20:00			
4-Sep	10:40		Air freshner	All	08:40 - 20:45			
	15:09	16:10	Incense stick	All				
5-Sep	12:26	12:45	Cooking	All	09:00 - 17:15			Maintenance
6-Sep	9:50	9:55	Cleaning product	All	09:00 - end campaign			
8-Sep	11:08	Campaign Ended						

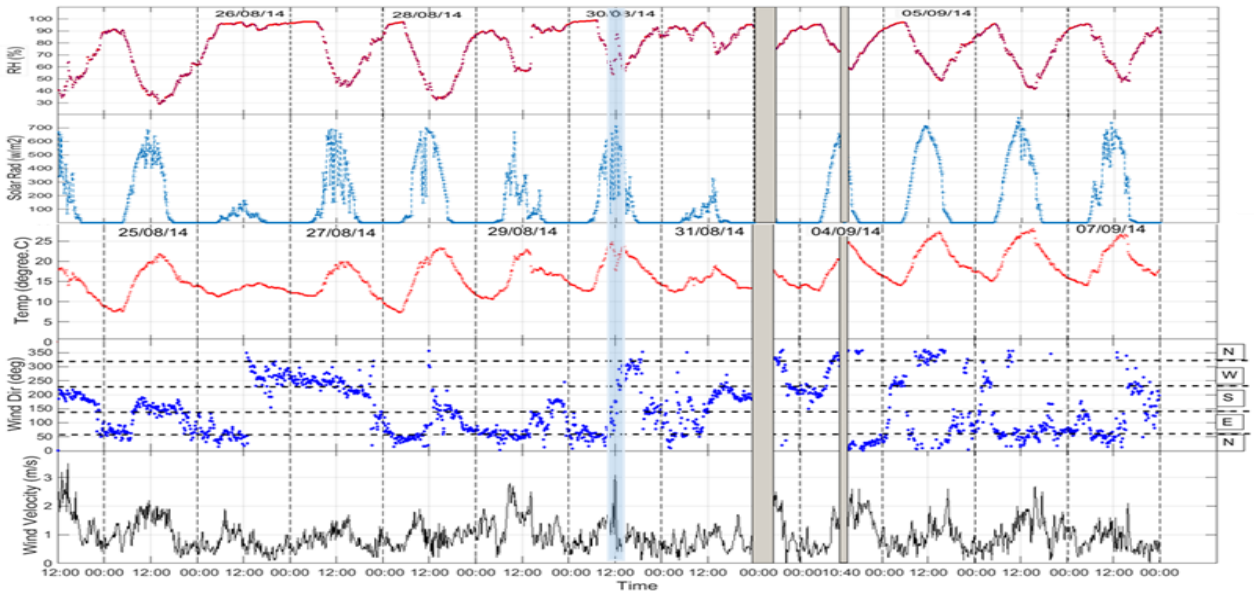

SI Figure 1 Overview of meteorology for the full research period including temperature, relative humidity, solar radiation, wind speed and wind direction. The only rain event is highlighted blue. Missing data shown by gray bars.

10. Article 3.

Transformations of Aerosol Particles from an Outdoor to Indoor Environment

N. Talbot[a,b], L. Kubelová[a,b], O. Makeš[a,b], J. Ondráček[a] , M. Cusack[a], J. Schwarz[a], P. Vodička[a,] N. Zíková[a], V. Ždímal[a].

[a]Institute of Chemical Process Fundamentals of the ASCR, v.v.i., Rozojová 2, Prague 165 02 Czech Republic.
[b]Charles University, Faculty of Science, Department of Environmental Studies, Prague, 128 43, Czech Republic.

Submitted to: Aerosol and Air Quality Research (January 2016)

Pages: 105-127

For publication in: 2016

Impact factor of Journal: 2.10

Transformations of aerosol particles from an Outdoor to Indoor Environment

N. Talbot[a,b*], L. Kubelová[a,b], O. Makeš[a,b], J. Ondráček[a] , M. Cusack[a], J. Schwarz[a], P. Vodička[a], N. Zíková[a], V. Ždímal[a].

[a]Institute of Chemical Process Fundamentals of the ASCR, v.v.i., Rozojová 2, Prague 165 02 Czech Republic.
[b]Charles University, Faculty of Science, Department of Environmental Studies, Prague, 128 43, Czech Republic.

Keywords: I/O ratio, transformations, shrinking, dissociation, aerosols.
*Corresponding Author

Abstract

This paper reports the findings of two campaigns that were carried out in order to better understand the transformational processes of aerosol particles as they migrate from outdoor to indoor environments. Summer and winter seasons were investigated using online and offline instrumentation, which, via an automated switching valve, obtained particle size and chemical composition information in near real time.

Online results showed that accumulation mode indoor / outdoor (I/O) ratios were significantly lower in winter than in summer. This difference was attributed to the shrinking undergone by particles when moving from outdoor (low temperature, high humidity) to indoor (high temperature, low humidity) environments. Differences were also notable within size distributions from offline impactor measurements, where more mass was recorded on <200nm stages for sulfate and ammonium.

C-ToF-AMS obtained chemical composition measurements showed lower indoor mass during winter. Whilst loss of water from particles can explain the changes to size, it would not adequately explain the extra loss of mass. Calculations showed a 31-37% decrease in I/O ratios for all chemical species during winter. The similarity in reduction for all species indicated the action of physical, rather than a chemical processes.

To assess the relative influence of physical factors on I/O relationships, statistical tests were carried out. These identified wind speed to be anti-correlated to indoor concentrations for all species. Further investigations applied wind roses with incorporated changes in I/O ratios, which indicated that the wind direction and wind speed had a minor influence on changes to indoor composition. This paper concludes that the relative concentration and composition of different aerosol species, increased temperature gradients and wind speed variability were the most influential factors when considering I/O aerosol transformations.

1. Introduction

Solid or liquid aerosol particles are of interest due to their impacts on climate (IPCC, 2014), meteorology (Tao, Chen, Li, Wang, & Zhang, 2012), visibility (Watson 2002), ecosystems (Mahowald et al., 2011) and human health (Dockery et al., 1993; Pope, Bates, & Raizenne, 1995; Schwartz et al., 1996). Natural and anthropogenic sources emit either particulate or primary gas-phase precursors, which then transition into the particle phase. As a result, the chemical composition and concentration of ambient particulate matter (PM) are considered to be time and location dependent (Mohr et al. 2012; Lehmann et al. 2005; Viana et al. 2008). Seasonal variability also effect aerosol composition,

with meteorological factors, such as temperature, wind speed and relative humidity, influencing anthropogenic emissions and physical aerosol properties (Hussein et al. 2006; Kubelová et al. 2015; Poulain et al. 2011; Hämeri et al. 2004).

When indoor sources are absent, indoor concentrations correlate strongly to those outdoors (Evangelia Diapouli et al., 2011; Lazaridis & Aleksandropoulou, 2006). The relationship between indoor and outdoor aerosol has been the subject of numerous studies, with prominent examples including a multi-location investigation throughout Europe (Hänninen et al. 2004), in central Athens (Diapouli et al. 2011), next to major freeways in Los Angeles (Zhu et al. 2005), residential areas in Brisbane (H. Guo et al., 2008; Hai Guo et al., 2010; Morawska et al., 2001) and in residential Helsinki (Hussein et al. 2004; Hämeri et al. 2004b). A common result from all these studies was a positive correlation between outdoor and indoor particulate concentrations. It is evident that to successfully evaluate indoor aerosol composition you must also understand outdoor aerosol composition at the same location, over the same time period.

Most indoor research to date has focused on indoor particle number concentrations and size distributions to obtain insight into indoor/outdoor (I/O) aerosol behaviour (Géhin et al., 2008; He et al., 2004; Morawska et al., 2001). Other studies have taken into consideration indoor black carbon concentrations (Ho et al. 2004), and have successfully deployed offline instrumentation to obtain indoor chemical characterisation (Geller et al., 2002; J Smolík et al., 2008). Prior research has also identified particle transformations of semi-volatiles, such as ammonium nitrate (NH_4NO_3). Dissociation rates of NH_4NO_3 aerosol are known to be strongly temperature dependent (A. Stelson & Seinfeld, 1982), whilst the NO_3 precursor gas, HNO_3, is known to quickly react on indoor surfaces (Hering & Cass, 1999), further increasing separation rates. This results in increased uncertainties when considering indoor chemical composition and particle number concentrations.

I/O ratios from previous research show a dependence on material surroundings, including building age, style, glazing and insulation (Chen & Zhao 2011; Diapouli et al. 2013; Leung & Drakaki 2015), whilst meteorology has been suspected of causing changes to I/O ratios (Hussein et al. 2006; Chan 2002). Moreover, meteorological influences can be masked by processes that dominate the inward migration of outdoor originating particulate (ventilation and air conditioning, for example).

Therefore, it is still not understood if meteorology directly influences indoor aerosol composition, or just outdoor aerosol composition, which then penetrates indoors. Moreover, how does seasonal variability effect the infiltration of outdoor particulates indoors? Are certain chemical species more likely to infiltrate under certain conditions? “How does using online over offline instrumentation influence the datasets? Finally, how influential is the sampling time when investigating indoor/outdoor relationships?”

This paper seeks to address these uncertainties by presenting results from two intensive campaigns carried out in a Central European urban background location during summer 2014 and winter 2015. Simultaneous outdoor to indoor size resolved particle number and mass concentrations along with chemical composition are compared according to season, whilst I/O ratios from particle number and chemical mass concentrations are described and discussed identifying key factors driving particle transformations indoors.

2. Methods

2.1. Measurement site and sampling set-up

Research took place from 16th August to the 8th September, 2014 and the 5th to 24th February, 2015 at a ground floor flat in Suchdol, Prague, Czech Republic. Details of the flat and location have been previously described in literature such as Hussein et al. (2006). Here we present a brief description of the key aspects. Suchdol is a residential area in north-western Prague, about 6 km north from the Prague city centre (Figure 1A) and is recognized as an urban background site. A predominantly south west prevailing wind can bring an influence from Václav Havel airport to the measurement site. Southerly originating airflows are not commonly observed on the site, however, it is likely some recirculation of urban air and micro-airflow dynamics will direct urban aerosol over the measurement site.

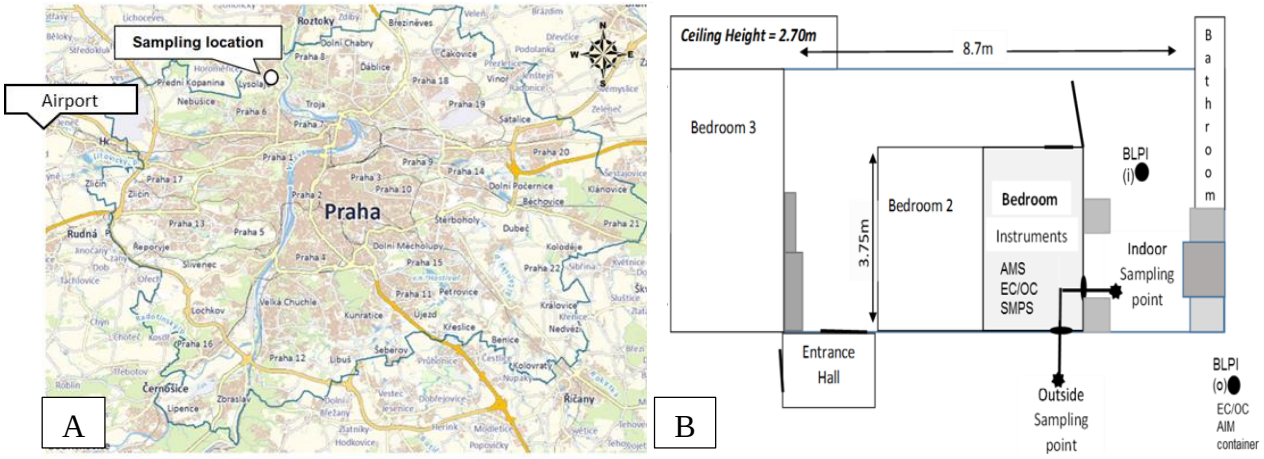

Figure 1.The location of the sampling site in Prague, used for both summer and winter campaigns (Left). Sketch showing the layout of the apartment where indoor/outdoor comparative measurements took place (Right).

The apartment used for both campaigns is located in the Institute of Chemical Process Fundamentals compound (50°7'36.47"N, 14°23'5.51"E, 277 MASL). The layout and dimensions of the flat are shown in Figure 1B and were described in detail in Hussein et al. (2006). A bedroom was used to house all online instrumentation, from which a 1.5m inlet protruded into the kitchen area, the chosen indoor sample point. A second inlet of the same length sampled outdoor air through a boarded up window from the instrument room (Figure 1B). For comparability the layout and structure of the experiment were kept consistent for both experiments.

2.2. Instrumentation and data collection

2.2.1. Scanning Mobility Particle Sizer

Size resolved particle number size distribution for the size range 14.7 – 724 nm was obtained with a Scanning Mobility Particle Sizer (SMPS), model 3936, TSI, with long DMA 3081 and CPC 3775, using a 3 minute up-scan, 30 second down-scan and 90 second purge. Only the second scan was considered for analysis to make sure the sample represented only the aerosol from its designated indoor or outdoor origin. For SMPS measurements, a particle density of 1.5 was used throughout. The SMPS inversion routine used TSI AIM software whilst the mass concentration calculation using the same software assumes that all the particles were perfect spheres.

2.2.2. Compact Time of Flight Aerodynamic Mass Spectrometer (C-ToF-AMS)

The Compact Time of Flight Aerodynamic Mass Spectrometer (C-ToF-AMS) provides real-time measurements of PM_1 chemical composition and size distribution (Drewnick et al., 2005). For both campaigns the AMS alternated between the particle time-of-flight (PToF) mode and the mass spectra (MS) mode, each with a sampling period of 1 min. Under the PToF mode operation, the aerosol beam was chopped by a chopper wheel with a radial slit. Particle size information was obtained as a function of particle time-of-flight in non-refractory PM_1 (NR-PM_1). Reported mass concentrations and size distributions were then averaged. The AMS was calibrated weekly during this campaign using the brute force single particle mode (Decarlo et al. 2006). AMS data was collected with a collection efficiency of 0.7 in summer and 0.67 for winter. This was calculated using the total SMPS mass then subtracting the elemental carbon mass taken from the EC/OC analysis.

2.2.3. EC/OC

Elemental carbon and organic carbon (EC and OC) measurements were conducted by two parallel, semi-online field OC/EC analysers (Sunset Laboratory Inc., USA; Figure 1) $PM_{2.5}$ cyclone inlets. The instruments were equipped with a carbon parallel-plate diffusion denuder (Sunset Lab.) to remove volatile organic compounds that may have caused a positive bias in the measured OC concentrations. The denuder was placed in ambient outdoor conditions during outdoor measurements and inside of room during indoor measurements. Samples were taken at 2-h intervals, including the thermal-optical analysis, which lasted about 15 min.

2.2.4. Berner Low Pressure Impactors

Two Berner type Low Pressure Impactors (BLPI, 25/0.018/2, Hauke, Austria) were run concurrently indoors and outdoors over 4 periods in the summer and 5 during the winter campaign. All sampling periods ran for 23 hours. The samples were captured on polycarbonate foils greased with Apiezon L vacuum grease to reduce particle bounce. 10 size fractions were separated with a flowrate of 15 l/m. Stage cut sizes for these impactors have been quantified by Štefancová et al. (2011) as 0.026, 0.057, 0.1, 0.16, 0.25, 0.44, 0.87, 1.8, 3.5 and 6.7 μm.

Particle mass concentrations on impactor substrates were gravimetrically determined by pre- and post-weighing the Mylar foils and filters (PTFE and quartz fiber) with a Sartorius M5P-000V001 electronic microbalance with a ±1 µg sensitivity. Blank samples (1 per sample) were collected for each sampling run and the deviation of mass values due to varying conditions was corrected with the help of the corresponding blanks. All samples were equilibrated for a period of 24 hours before weighing in a temperature and relative humidity controlled room. The electrostatic charges of the filters were removed using a U-shaped electrostatic neutralizer (Haug, type PRX U) and each sample was weighed three times with an accuracy of mass determination of ± 2 µg. After weighing, the sampled foils and filters were stored in the freezer at -18 °C.

Ion chromatography analysis

Ion chromatography analysis was only carried out using approximately 1/3 of each foil. Samples from each stage was cut out and number of aerosol spots on cut piece was calculated. The ratio between the cut piece and total number of spots at each impactor stage was used to recalculate results to overall ion amount on each stage. All samples were then extracted with 7 ml of ultrapure water, sonicated for 30 min in an ultrasonic bath and shaken for 1 hour. The extracts were then analyzed using a Dionex 5000 system both for cations (Na^+, NH_4^+, K^+, Ca^{2+} and Mg^{2+}) and anions (SO_4^{2-}, NO_3^-, Cl^-) in parallel. An IonPac AS11-HC 2 x 250 mm column was used for anions using hydroxide eluent and an IonPac CS18 2 x 250 mm was use for cations with methane sulfonic acid solution as an eluent. Both the anion and cation set-ups were equipped with electrochemical suppressors. External calibration was done using NIST traceable calibration solutions.

2.2.5. Meteorological measurements

Meteorological data (ambient temperature, pressure, relative humidity, wind direction and velocity, and total solar radiation) was recorded in the weather station operated by the Czech Hydrometeorological Institute. The container weather station is permanently located at the ICPF compound close to the research location.

2.2.6. Final data Considerations

Data was removed when experimental sources were introduced into the sample room. These periods were carefully listed in a metadata file and supported by analysing concentration and changes in composition using SMPS and AMS datasets, and if any of the chemical species showed a divergence from the norm after such experiments, systematic caution was taken and the set removed. No data smoothing procedures were used during either campaign.

2.3. Air exchange rates during experimentation.

To determine an air exchange rate for the experiment, CO_2 was released and its decomposition curve was used as the marker for the air exchange rates. Due to the location of filter measurement instrumentation within the sample room, 3 such experiments were carried out.

1. Windows and doors shut, no other instrumentation in the room: 1.27 air exchanges per hour.

2. Micro-ventilation conditions with no instrumentation in the room: 1.92 air exchanges per hour.
3. Windows sealed but instrumentation in the room: 1.26 air exchanges per hour.

2.4. Meteorology during campaigns

An overview of the mean meteorological conditions for both the winter and summer campaigns are shown in Table 1, averaged over the entire campaign.

Table 1. Key meteorological parameters from the summer (top) and winter campaigns in Prague

	Temp. (°C)			Humidity (%)			Pressure	Wind (km/h)	
Summer Campaign 2014	Daily high	Daily average	Night low	Daily high	Daily avg	Daily low	Daily avg	Daily ave	High gust
	20.4	15.2	10.3	94.6	74.1	42.8	1015.5	6.6	11.5
Winter Campaign 2015	Daily high	Daily average	Night low	Daily high	Daily avg	Daily low	Daily avg	Daily ave	High gust
	4.4	0.8	-2.8	92.2	76.0	50.6	1019.4	11.6	59.5

Summer conditions were notable for the prevalence of a stable air mass that allowed for only one rain event with winds slowly switching from westerly to easterly direction. This change in wind direction brought about a slow increase in temperature for the final week of the study. In contrast, the winter campaign had changing conditions, with a northerly flow at the beginning of the campaign changing to an easterly, southerly, and then a milder westerly for the final period of research.

3. Results and discussion

3.1. Indoor and outdoor aerosol composition overview

Table 2A: Results from the Prague summer campaign including mean, maximum and standard deviation.

Instrument	Species	Summer Outdoors			Summer Indoors		
		Mean	**Max**	**σ^2**	**Mean**	**Max**	**σ^2**
(EC-OC)	EC	0.95	2.5	0.4	0.8	5.2	0.4
AMS	Org	3.6	15.3	1.5	2.7	7.9	1.3
AMS	SO_4^{2-}	2.1	5	1.1	1.7	4.4	0.9
AMS	NH_4^+	0.5	1.1	0.2	0.3	0.6	0.1
AMS	NO_3^-	0.9	2.8	0.5	0.5	2	0.5
SMPS	Total number	$5.5x10^3$	$2.8x10^4$	$3.1x10^3$	$3.1x10^3$	$1.1x10^4$	$1.4x10^3$
SMPS	Total mass	6.4	15.9	2.9	3.7	9.7	1.2
AMS	Total mass	5.9			3.7		

Table 2B. Results from the Prague winter campaign including mean, maximum and standard deviation.

Instrument	Species	Winter Outdoors			Winter Indoors		
		Mean	**Max**	**σ^2**	**Mean**	**Max**	**σ^2**
(EC-OC)	EC	1.4	6.0	0.9	1.3	4.7	0.8
AMS	Org	7.5	38.3	4.5	3.6	16.7	2.3
AMS	SO_4^{2-}	3.6	12.6	1.9	1.7	10.9	1.0
AMS	NH_4^+	2.8	9.3	1.5	0.8	4.0	0.5
AMS	NO_3^-	6.5	26.3	4.0	1.3	7.3	0.8
SMPS	Total number	$5.4x10^3$	$2.9x10^4$	$3.1x10^3$	$3.0x10^3$	$1.8x10^4$	$1.9x10^3$
SMPS	Total mass	15.7	52.6	8.8	8.1	24.6	5.2
AMS	Total mass	19.4			5.6		

3.1.1 Particle size and number distributions

The overall PNC for both seasons were similar (Table 2A and B), however, sub-daily seasonal differences in concentration were evident (Fig.2). From 00:00 – 03:00, PNC was reduced as a result of dry deposition processes, whilst a morning traffic signature is shown by the increase in concentrations between 07:00-10:00. The time lag between seasons is a result of changes in seasonal Central European Time (CET), not adjusted in this study. Afternoon increases in summer concentrations can be accounted for by new particle formation, these events are less common in winter. (Monks et al., 2009; Putaud et al., 2010; Zíková & Ždímal, 2013).

These new particle formation events did not occur daily but are represented in arithmetic mean concentrations. Increases in evening PNC occurred earlier in winter than summer due to increased input from home heating sources (Lucia Štefancová et al., 2011), coupled with lower boundary layer height and possible temperature inversions. The corresponding later increase during summer would, conversely, be a product of higher boundary layer, more mixing, and possible reformation of particle nitrate through lowering temperatures (Kubelová et al., 2015). It is notable that I/O concentrations diverge throughout the evening. Home heating combustion sources are usually <50nm particles and will therefore penetrate less effectively due to diffusive processes, which explains the increasing difference between indoor and outdoor concentrations.

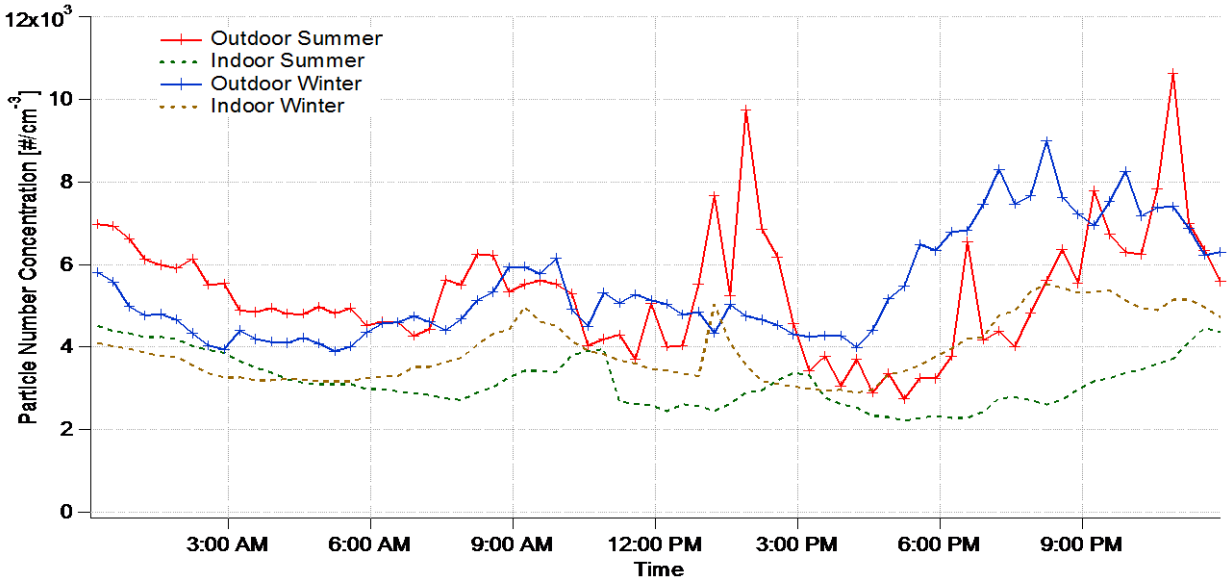

Figure 2. Size resolved $PM_{0.7}$ arithmetic mean PNC relative to time of day and season.

Particle size distribution modes, describing mobility diameter, are presented in Figure 3. Both seasons show a mode between 20-30nm. This mode was more prominent in summer, and was previously identified as a signal of fresh exhaust emissions (Ristovski, Morawska, Bofinger, & Hitchins, 1998) and secondary aerosol . A second mode between 50-60nm was found during summer but was extended in winter between 50-80nm. These modes are typical of aged coagulated combustion emissions, with larger sizes attributed to diesel emissions, which produce particulates between 50-120nm (Ondráček et al., 2011). Accumulation modes exist for both summer and winter distributions between 150-250nm mobility diameter in summer and between 250 and 300nm during winter. The likely source was secondary inorganics and other regional aerosol sources (Lehmann et al., 2005). Indoor modes were less pronounced than those outdoors and it is evident that the <40nm particulates do not penetrate as efficiently as those in accumulation modes. This is due to diffusion processes on the building surfaces (Zhu et al., 2005).

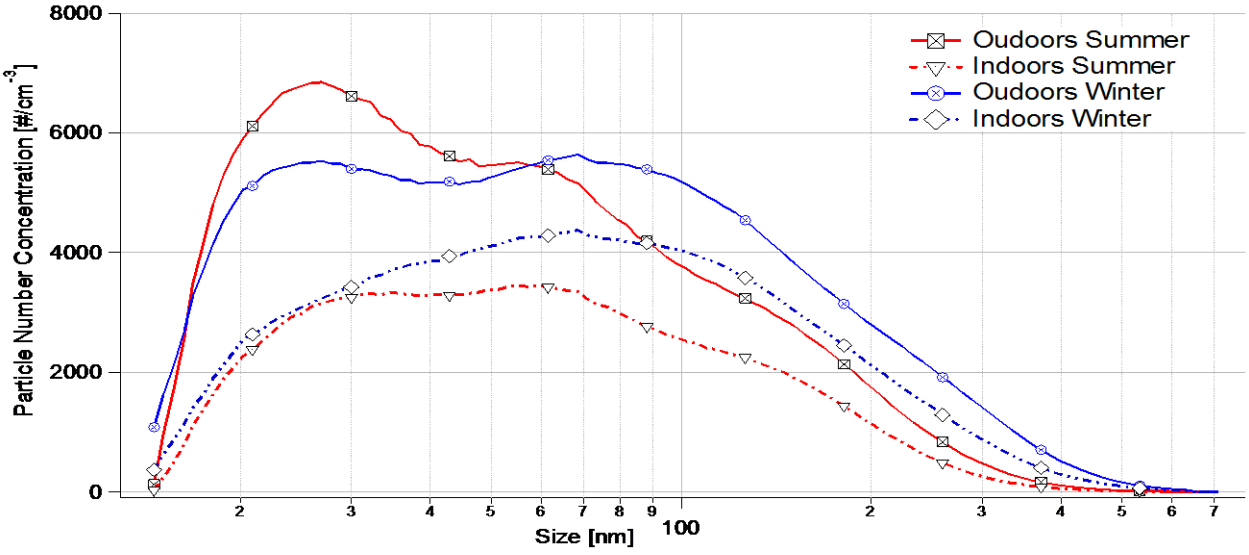

Figure 3. Average number size distribution. Outdoors and Indoors for summer and winter seasons

3.1.2 Chemical analysis from AMS measurements

Summer and winter indoor and outdoor chemical composition values are given in Tables 2A and B with the collection efficiency adjustments accounted for. Proportional chemical compositions are also presented in Figure 4. During winter, proportionally less NR-organics were observed outdoors (summer: 51% winter: 37%). Lower production values of biogenic aerosol and an increase in the concentration of other inorganic species such as NO_3^- and NH_4^+ were the likely contributing factors. The outdoor share of NO_3^- significantly decreased from winter to summer (winter: 32%, summer: 13%) which we explain by lower temperatures in winter supporting the aerosol phase of NH_4NO_3 over the gaseous phase (Huang et al., 2004b; Poulain et al., 2011; A. Stelson & Seinfeld, 1982).

This phase transformation process was also responsible for low concentrations of NO_3^- indoors during both seasons, with higher constant average temperatures, lower humidity and HNO_3 acid-surface reactions all acting to increase dissociation rates (Hering & Cass, 1999; Smolík, 2008). NH_4^+ (winter: 14%, summer: 6%), is the principal base in the atmosphere, neutralising SO_4^{2-} primarily, then NO_3^-, therefore it was expected NH_4^+ concentrations should be closely related to those species. An unexpected result was the drop in proportional share of SO_4^{2-} outdoors during winter (winter: 18%, summer: 30%). Although uncertain, we attribute this outcome to a decrease in daily mixing height. This would restrict the input of SO_4^{2-} from the boundary layer reservoir (Kvietkus et al. 2011), and, along with less available sunlight, would allow less photo-oxidation of SO_4^{2-} (Xavier Querol et al., 1998).

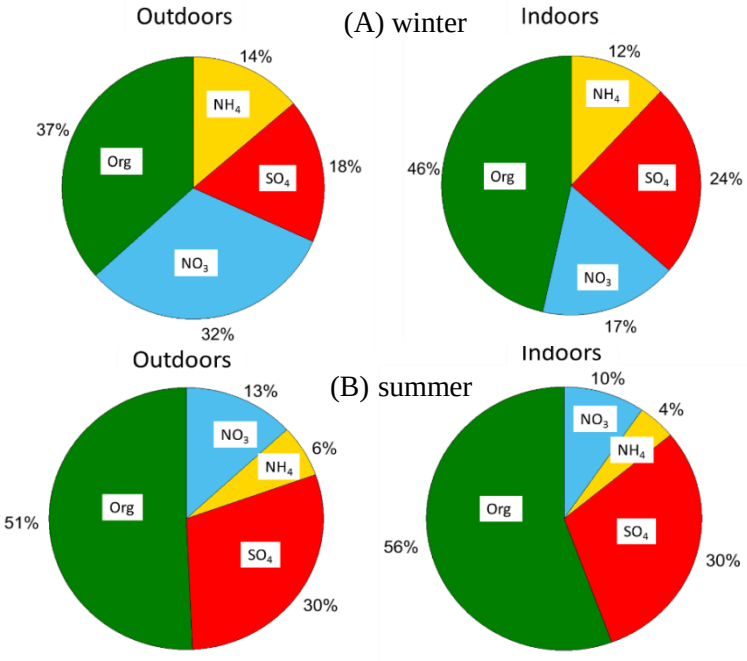

Figure 4. Averaged indoor and outdoor proportional chemical composition in, (A) winter and (B) summer

The outdoor chemical mass concentrations obtained from these two campaigns were within the standard deviation of results described in Kubelova et al., (2015), where non-refractory PM_1 (NR-PM_1) was measured during summer 2012 and winter 2013 in the Czech Republic. In that study, NR-organics

dominated for both winter and summer with NO_3^- as the second most prominent aerosol outdoors during winter, and SO_4^{2-} as the second most abundant during summer. Here we observed higher concentration of NR-organics and SO_4^{2-} in both seasons, however, this difference is within the range set by the standard deviation. The same applied to measured concentrations of NO_3^- and NH_4^+ in summer, whilst in winter, concentrations of NO_3^- and NH_4^+ in our measurement were lower than described in Kubelova et al., 2015. However, were again in the range set by the standard deviation.

3.2. Indoor / outdoor BLPI impactor measurements

Two Berner Low Pressure Impactors (BLPI) gave concurrent indoor and outdoor mass size distributions of major ions (SO_4^{2-}, NH_4^+ and NO_3^-) for sizes 25nm-10µm. The overall mean mass concentrations are presented in Figure 5A (SO_4^{2-}), 5B (NH_4^+) and 5C (NO_3^-) and Figure SI.1 (in the supplementary material). Mean particle sizes (340nm-median stage size) were smaller in summer than in winter (650nm-median stage size). The shift to smaller sizes can be explained by the seasonal differerences in aerosol composition (as previously described). This is in line with findings from Schwarz et al. (2012) where seasonal and airmass dependencies are detailed.

For both SO_4^{2-} and NH_4^+ larger mass concentrations were recorded on <200nm stages indoors than outdoors. Although observed in both seasons, the difference was greatest for SO_4^{2-} during winter with concentrations indoors almost double those outdoors for stages 1-3. With no indoor sources to generate the extra mass, particle bounce from the larger stage sizes would be a reasonable explanation. However, the collection substrate within the BLPI were greased during these experiments. If particle bounce is discounted, a shrinking of the indoor particles could be the cause through the dehydration of water soluble aerosol.

For example, mean indoor temperatures during winter (22.1˚C) were much higher than those outdoors (0.7 ˚C), considering summer values of 20.3˚C outdoors and 22.6˚C mean indoors. In summer, it was likely that the aerosol were more readily dried outdoors during daytime by the higher temperatures and lower humidity. This would result in dehydrated smaller particle penetrating indoors allowing for reducing further shrinkage.

During winter, NO_3^- (Figure 5C) largely mirrored the results of SO_4^{2-} and NH_4^+ outdoors, however NO_3^- lost considerably more mass indoors, we attribute this again to dissociation processes of NH_4NO_3. In summer, NO_3^- showed a unique mass size distribution with very little <200nm mass recorded indoors, whilst median mass diameters of 210nm and 340nm contained only very small mass concentrations. Unlike other major ions, NO_3^- has a marked coarse mode which is attributed to NaCl transformation, creating low volatility $NaNO_3$. It is due to the low volatility of this compound that the majority of NO_3^- mass found indoors is in the coarse mode. Again, these results support those of Schwarz et al. (2012), who attribute NaCl transformation to oceanic origins.

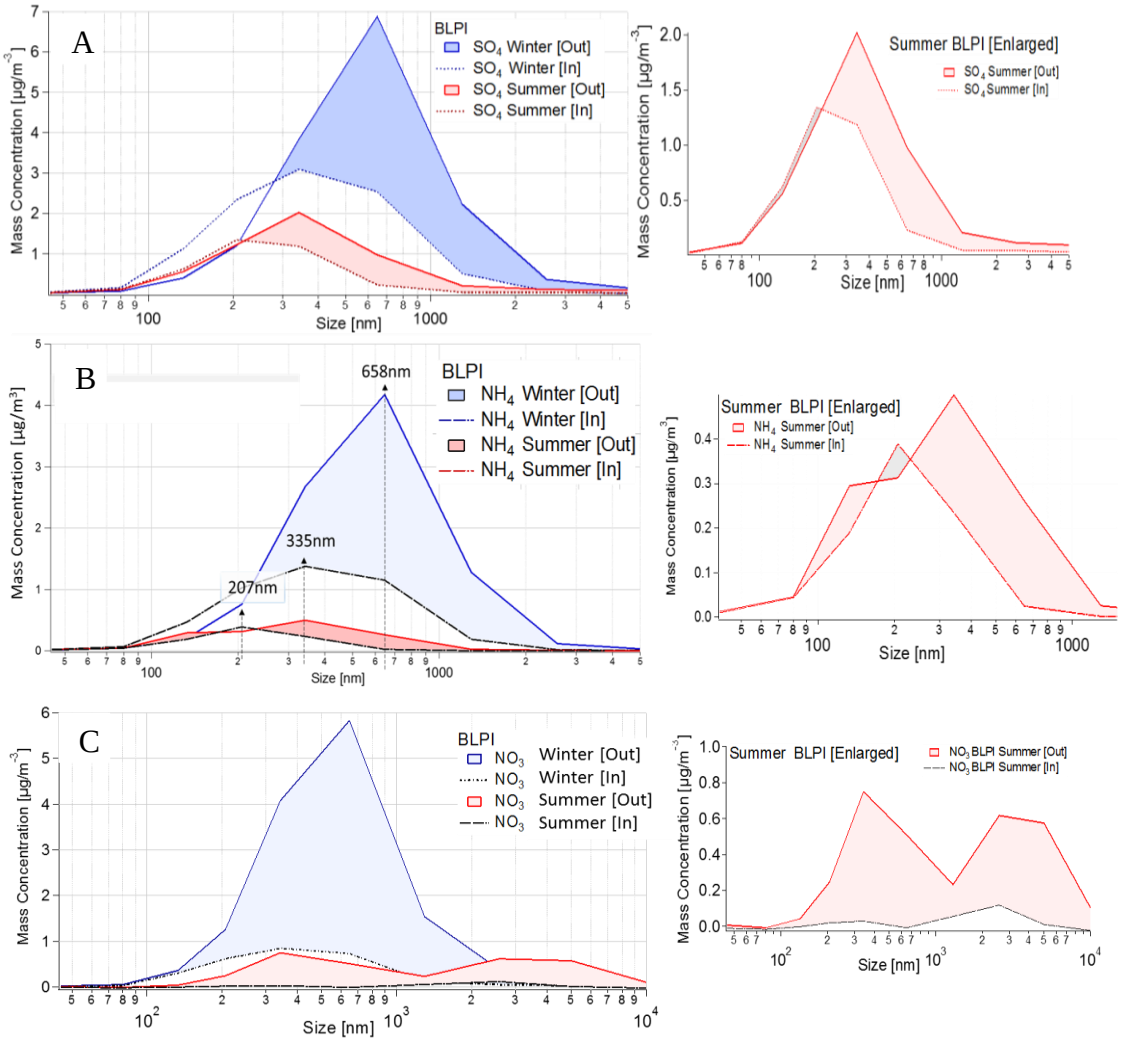

Figure 5. Graphical representation of BLPI particle mass size distributions for winter and summer. The summer data for all results were shown in proportional scale and also enlarged as a subplot.

To conclude this section, we associate particle shrinking during winter to the dehydration of aerosol particles as they travel from outdoors to indoors, and this, in turn, accounts for changes in observed particle size. This was observed on all instrumentation but was most clearly defined on the impactor measurements. The loss of mass from chemical species from outdoors to indoors found on BLPI measurements during the winter campaign cannot be explained by this shrinking processes.

3.3. Indoor / outdoor ratios

Without any indoor aerosol sources, indoor concentrations are known to be correlated to those outdoors via the migration of outdoor aerosol indoors (Hussein et al. 2006). Aerosol particles can penetrate through windows, framework, and building structure and ventilation mechanisms. This process can simply be defined by an indoor/outdoor ratio, expressed as (Chun Chen & Zhao, 2011)

$$\text{I/ O } Ratio = \frac{C\_in}{C\_\text{out}}. \qquad (1)$$

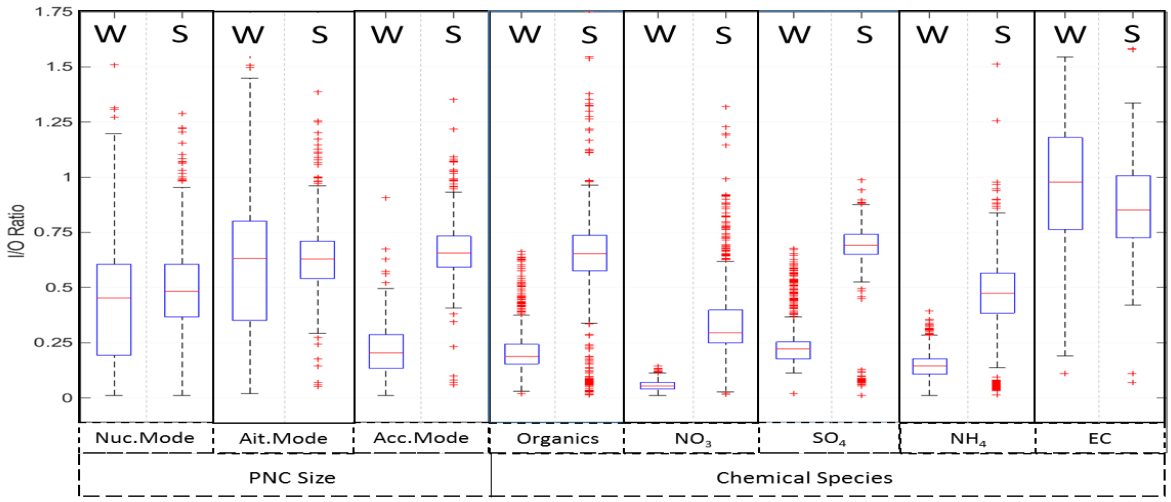

Figure 6. Boxplots showing averaged indoor/ outdoor ratio for PNC from SMPS and chemical PM_1 data from AMS and EC/OC measurements separated into winter (W) and summer (S) segments. The red line is the median value and the edge of the box represents the 25/75 percentiles. The whiskers show 95 percentile and the crosses denote outliers.

3.3.1. Indoor / outdoor ratio's and particle number concentration

I/O ratios based on PNC are shown in Figure 6 (boxplots: from left 1-3). Nucleation and Aitken modes were similar when calculating the median ratios, whilst for accumulation modes, a clear difference is observed between summer and winter. The difference in the I/O ratios for the accumulation mode supports the findings from the impactors. It would be expected that the shrinking of accumulation mode particles would increase the membership, and therefore the ratio, of smaller Aitken and nucleation modes. However this is not readily observed in the boxplots.

Linear regression models are presented in Figure 7 along with calculated correlation R^2 values and slope values, which are representative of I/O ratios. The nucleation mode (<40nm) is defined by a highly scattered and disordered relationship during summer. This is not the case for summer-season Aitken and accumulation modes, which show a high correlation between indoor and outdoor PNC (given by the slope of the fit). Nucleation mode slope is higher in winter than summer which may be due to the shrinking of larger particles. However, Aitken mode fractions are very similar between the two seasons, although there does appear to be more scatter during summer than in winter.

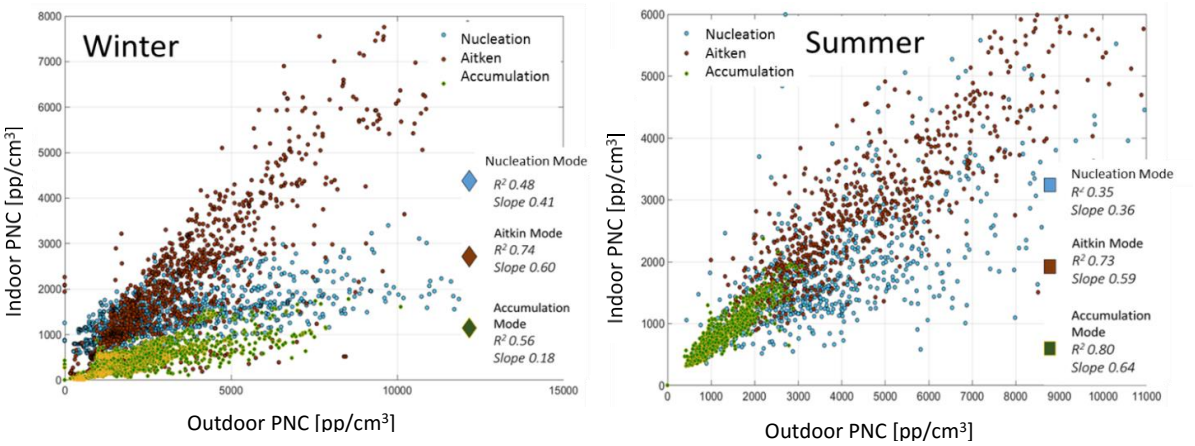

Figure 7. Linear regression models for PNC split into 3 size modes and separated into summer and winter

Summer accumulation mode was strongly correlated between indoors and outdoors, and a slope of .64 agrees with the boxplots in Figure 5. In contrast, during winter accumulation mode particulate are weakly correlated and a corresponding slope of .18 reveals a low I/O ratio, providing further evidence of shrinking of the indoor aerosol particles as previous described.

3.3.2. Indoor / outdoor ratios and chemical composition

Figure 5 shows a similar decrease in the I/O ratio for all AMS measured chemical species, however these are obtained by comparing mass results rather than size. The seasonal differences are more pronounced than can be attributed to dehydration processes alone. The mean I/O ratios for each species was; NR-organics (.48 / .72), NO_3^-. (.20 / .32), SO_4^{2-} (.50 / .76), and NH_4^+ (.32 / .48). If we now calculate the seasonal decrease in I/O ratio based on these results we find NR-organic (33.3%), NO_3^-. (37.5%), SO_4^{2-} (34.2%) and NH_4^+ (33.3%). This shows a very stable seasonal I/O ratio change for all species, which implies that physical factors, not physico-chemical processes, are primarily responsible for these differences.

EC results, shown in Figure 5 (right hand boxplot), shows only a small difference between the seasons. It is not clear why EC does not show seasonal variability whilst SO_4^{2-} does, whilst both have low volatility. We speculate that due to the outdoor sampling EC/OC instrument being housed away from the main research building (Figure 5), the instrument received different concentrations of chemical species as well as different influences from physical factors such as wind. These factors will be explored in greater details in section 3.3.

To better describe the I/O ratios in relation to chemical species, density graphs and histograms are shown in Figure 8. NO_3^- and NH_4^+ have a similar I/O ratio spread, however NO_3^- has a higher density of membership towards lower ratios, which is indicative of the NH_4NO_3 relationship during winter. The low ratios were due to higher concentrations outdoors and higher temperature indoors hastening dissociation.

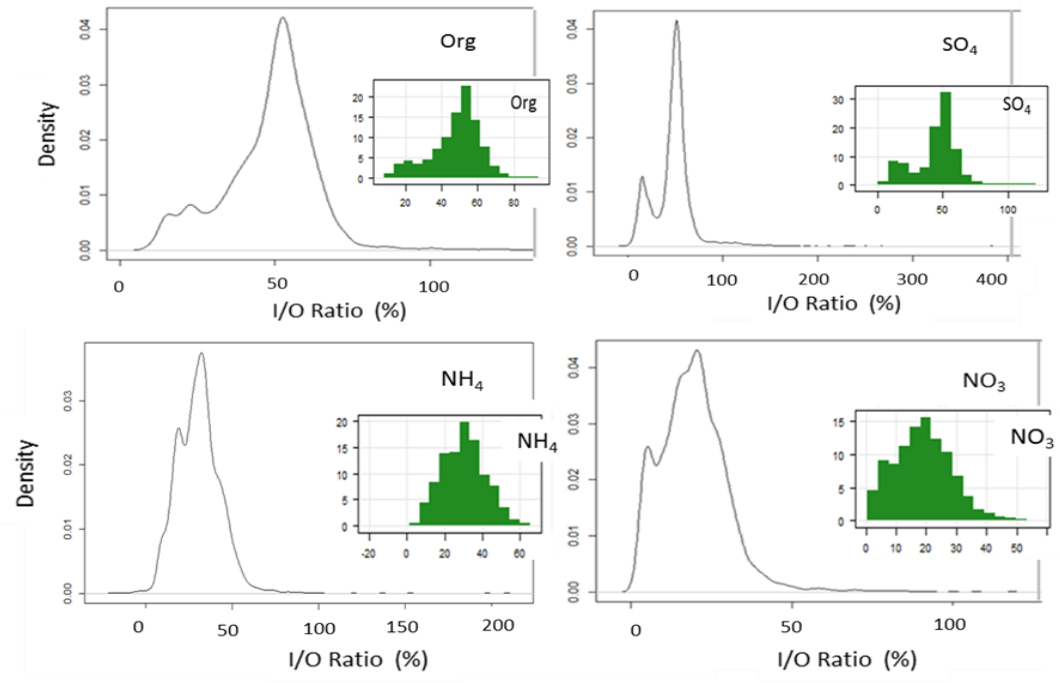

Figure 8. Winter density plot and inset histograms describing the spread of I/O ratios for each species, taken from AMS measurements.

The relative stability of SO_4^{2-} is evident by its defined peak close to 50%, this peak is very similar to organics. However, SO_4^{2-} has a more defined low-end I/O ratio. This maybe representative of periods where precipitation events caused wet deposition, quickly clearing the outside air, but leaving indoor concentrations unaffected. The mixing states of chemical species may also change indoors which may also change chemical mass, however this process would likely cause only a slight change in overall mass.

3.4. Indoor / outdoor rations and wind speed and direction

A non-parametric Spearman correlation analysis of winter-time results was carried out to better understand which physical factors statistically impacted on I/O ratios. (SI. Figure 2). The main outcome was the anti-correlation between wind speed and concentrations of all chemical species for both indoors and outdoors. For this analysis we only consider the winter campaign due to a low number of summer datapoints and low variability in wind speed and direction during summer, however the results should be applicable for all seasons.

For orientation purposes, the sample rooms main wall and windows face in a south westerly direction (Figure 9). It should be noted that due to the presence of buildings in the vicinity there is likely to have been some micro-circulation of the airflow around the sample area.

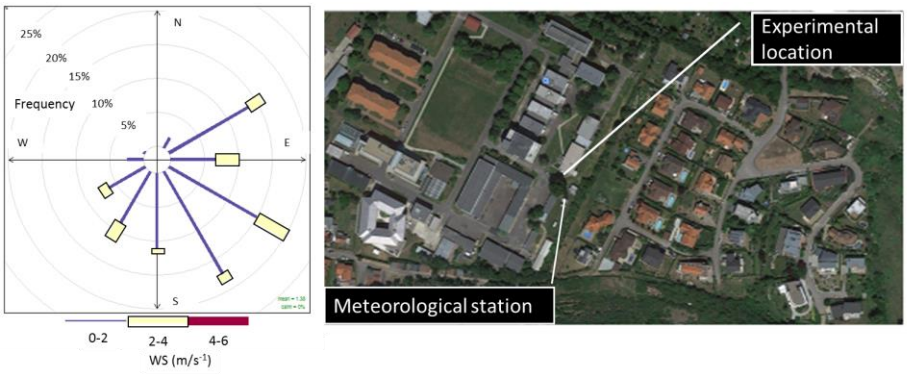

Figure 9. Wind rose taking 1hr averaged wind speed and directions (left), and map showing proximity of the meteorological station to the sampling location (right).

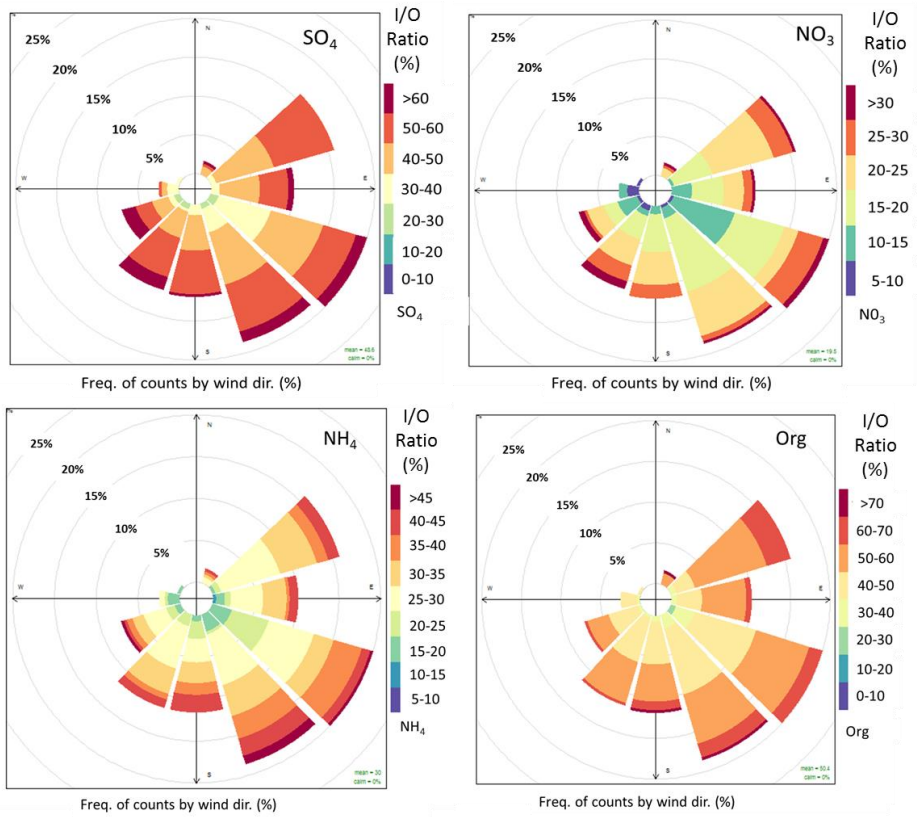

Figure 10. I/O ratio (as a percentage) per species in relation to wind speed and direction for each chemical species measured by the AMS.

A greater proportion of lower I/O ratios were observed when the wind direction came from the South East, this direction also saw a larger number of periods when wind speeds were between 2-4 m/s. This direction would direct aerosol particles onto both the front window and side wall of the sample room. These results suggest that there is a small but notable influence from wind direction on I/O ratios. Whilst wind speed did not vary enough for us to draw any definite conclusions, Figure 9 and 10, and SI Figure 3 all suggest that lower wind speeds increase the I/O ratio slightly.

It is perhaps more likely that I/O ratios would be more influenced by changes in aerosol particle concentrations outdoors due to increased wind speed variability. Higher wind speed decrease aerosol concentrations, with more variability in wind speed outdoors observed during winter, this would result in greater fluctuation on I/O ratios due to a time lag effect on indoor concentrations. During the summer campaign conditions were mostly stable, with low wind speeds. It is therefore likely that increased variability in wind speed during winter increased the deviation of I/O ratios between summer and winter.

3.5. Micro ventilation, I/O ratios and chemical compositional changes

For a 2-day period of the winter campaign, the window of our sample room was unsealed by moving the handle of the window into an upright position from a 'sealed' position at a right-angle. The purpose of this was to allow micro-ventilation of outdoor air to indoors to occur. To calibrate the difference, reduction curves from CO_2 gas release experiments found air exchanges rates increased 63%, from 1.3 to 1.9 exchanges an hour when compared to the sealed position. It was hoped this increase would allow a 'fresher' indoor sample with less residence time indoors and would provide a "stepping stone" point between composition outdoors and indoors.

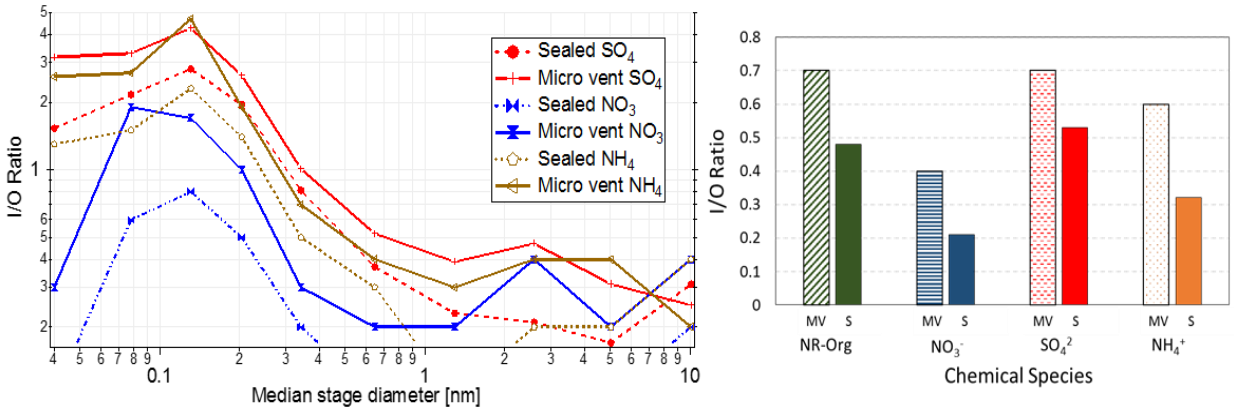

Figure 11. Changes in I.O ratio during micro-ventilation (MV) and sealed (S) periods from: (Left) BLPI data and (Right) AMS data

From the BLPI data, NO_3^- showed almost an order of magnitude difference in I/O ratio's during the micro-ventilation period, with the largest increase recorded on the 80nm (median) stage (Figure 11). The increased penetration for the smaller sizes allowed NO_3^- to have a greater ratio indoors than outdoors on impactor stages 200nm and lower as was the case with SO_4^{2-} and NH_4^+. Both SO_4^{2-} and NH_4^+ also increased their I/O ratios but to a far lesser extent than NO_3^-.

Although distribution curves for AMS NR-PM_1 measurements were not available for the micro-ventilation period, mass obtained I/O ratios support those of the BLPI. A key difference is a more significant increase in NH_4^+ I/O ratio, which increases almost in line with NO_3^-. Although uncertain

from one short period of a full campaign, it would appear that during micro-ventilation a few key factors are evident,

- All chemical species are more readily observed indoors during micro-ventilation.
- The presence of particle phase NO_3^- indoors appears to allow a related increased in indoor concentrations of NH_4^+ when detected by AMS measurements.
- This association was not observed on BLPI measurements.

We speculate that the 63% increase in ventilation rate allowed for less diffusion of particles to the building structure. Also we presume a lower decomposition rates of NH_4NO_3 occurred due to the reduced amount of time the aerosol has been exposed to the indoor conditions. This allows the NH_4NO_3 to stay in particle phase long enough to be measured indoors, although as a smaller particle than outdoors due to loss of molecules from the surface of the particle. This would allow for the NH_4^+ and NO_3^- to show similar results for AMS measurements.

4. Conclusions

Despite seasonal differences in sources and sinks acting to increase and reduce PNC during certain times of day, overall PNC were similar between summer and winter. Size distributions exemplified different sources with afternoon summer increases (Secondary Organic Aerosol /New Particle Formation) and wintertime early evening increases (home heating/low mixing layer). Observed daily modes outdoors describe a tri-modal structure typical for an urban background site. Indoors, a dominant broad mode between 70 and 100nm was observed, with smaller modes far less defined indoors than outdoors.

From BLPI data, impactor stages 1-3 which show particle sizes less than 200nm indicated higher concentrations indoors than outdoors, especially for SO_4^{2-} during winter. With no indoor sources and particle bounce discounted, this result was attributed to our indoor sample shrinking to smaller sizes due to water lost from the particle due to higher indoor temperatures than those of outdoors. The shrinking of aerosol particles indoors was also observed in accumulation mode particles obtained by SMPS measurements. From which we found a significant decrease in winter I/O ratio when compared to summer.

A significant reduction in indoor mass concentration was observed for all aerosol chemical species during the winter campaign. These could not be explained by dehydration processes alone, and a decrease in I/O ratios of between 31-33% for all species during winter indicates that a physical rather than a chemical process caused the decrease in I/O ratio. This result was surprising considering the known and observed loss of NO_3^- , which was found to lose the most mass indoors due to dissociation processes. It appears that despite NO_3^- being much more prevalent during winter, the relative loss rate, implied by I/O ratio changes, did not change significantly in accordance to season.

We provided a non-parametric statistical test that assessed various non chemical factors influencing outdoor and indoor chemical composition. This identified wind speed to be anti-correlated to outdoor

and indoor concentrations, which was further investigated by wind roses and calculations of associated I/O ratios. These revealed a greater dependence on the wind direction rather than wind speed. We conclude that the variability in wind speed during winter had the greatest effect on I/O mass concentrations during winter, whilst temperature changes had the greatest outcome on changes to particle size.

Acknowledgements

The authors acknowledge support of this work by European Union Seventh Framework Programme (FP7/2007-2013) under grant agreement n° 315760 HEXACOMM.

5. References

Chan, A. T. (2002). Indoor–outdoor relationships of particulate matter and nitrogen oxides under different outdoor meteorological conditions. Atmospheric Environment, 36(9), 1543–1551. http://doi.org/10.1016/S1352-2310 (01)00471-X

Chen, C., & Zhao, B. (2011). Review of relationship between indoor and outdoor particles: I/O ratio, infiltration factor and penetration factor. Atmospheric Environment, 45(2), 275–288. http://doi.org/10.1016/j.atmosenv.2010.09.048

Decarlo, P. F., Kimmel, J. R., Trimborn, A., Northway, M. J., Jayne, J. T., Aiken, A. C., Jimenez, J. L. (2006). Aerosol Mass Spectrometer. Analytical Chemistry, 78(24), 8281–8289. http://doi.org/8410.1029/2001JD001213.Analytical

Diapouli, E., Chaloulakou, A., & Koutrakis, P. (2013). Estimating the concentration of indoor particles of outdoor origin: A review. Journal of the Air & Waste Management Association, 63(10), 1113–1129. http://doi.org/10.1080/10962247.2013.791649

Diapouli, E., Eleftheriadis, K., Karanasiou, A. a., Vratolis, S., Hermansen, O., Colbeck, I., & Lazaridis, M. (2011). Indoor and outdoor particle number and mass concentrations in Athens. Sources, sinks and variability of aerosol parameters. Aerosol and Air Quality Research, 11(6), 632–642. http://doi.org/10.4209/aaqr.2010.09.0080

Dockery, D. W., Pope, C. A., Xu, X., Spengler, J. D., Ware, J. H., Fay, M. E., … Speizer, F. E. (1993). An association between air pollution and mortality in six U.S. cities. The New England Journal of Medicine, 329(24), 1753–9. http://doi.org/10.1056/NEJM199312093292401

Drewnick, F., Hings, S. S., DeCarlo, P., Jayne, J. T., Gonin, M., Fuhrer, K., Worsnop, D. R. (2005). A New Time-of-Flight Aerosol Mass Spectrometer (TOF-AMS)—Instrument Description and First Field Deployment. Aerosol Science and Technology, 39(7), 637–658. http://doi.org/10.1080/02786820500182040

Géhin, E., Ramalho, O., & Kirchner, S. (2008). Size distribution and emission rate measurement of fine and ultrafine particle from indoor human activities. Atmospheric Environment. Retrieved from http://www.sciencedirect.com/science/article/pii/S1352231008006535

Geller, M. D., Kim, S., Misra, C., Sioutas, C., Olson, B. a., & Marple, V. a. (2002). A Methodology for Measuring Size-Dependent Chemical Composition of Ultrafine Particles. Aerosol Science and Technology, 36(6), 748–762. http://doi.org/10.1080/02786820290038447

Guo, H., Morawska, L., He, C., & Gilbert, D. (2008). Impact of ventilation scenario on air exchange rates and on indoor particle number concentrations in an air-conditioned classroom. Atmospheric Environment, 42(4), 757–768. http://doi.org/10.1016/j.atmosenv.2007.09.070

Guo, H., Morawska, L., He, C., Zhang, Y. L., Ayoko, G., & Cao, M. (2010). Characterization of particle number concentrations and PM2.5 in a school: influence of outdoor air pollution on indoor air. Environmental Science and Pollution Research International, 17(6), 1268–78. http://doi.org/10.1007/s11356-010-0306-2

Hämeri, K., Hussein, T., Kulmala, M., & Aalto, P. (2004a). Measurements of fine and ultrafine particles in Helsinki: Connection between outdoor and indoor air quality. Boreal Environment Research, 9(6), 459–467.

Hämeri, K., Hussein, T., Kulmala, M., & Aalto, P. (2004b). Measurements of fine and ultrafine particles in Helsinki: Connection between outdoor and indoor air quality. In Boreal Environment Research (Vol. 9, pp. 459–467).

Hänninen, O. O., Lebret, E., Ilacqua, V., Katsouyanni, K., Künzli, N., Srám, R. J., & Jantunen, M. (2004). Infiltration of ambient PM2.5 and levels of indoor generated non-ETS PM2.5 in residences of four European cities. Atmospheric Environment, 38(37), 6411–6423. http://doi.org/10.1016/j.atmosenv.2004.07.015

He, C., Morawska, L., Hitchins, J., & Gilbert, D. (2004). Contribution from indoor sources to particle number and mass concentrations in residential houses. Atmospheric Environment. Retrieved from http://www.sciencedirect.com/science/article/pii/S135223100400250X

Hering, S., & Cass, G. (1999). The Magnitude of Bias in the Measurement of PM25 Arising from Volatilization of Particulate Nitrate from Teflon Filters. Journal of the Air & Waste Management Association, 49(6), 725–733. http://doi.org/10.1080/10473289.1999.10463843

Ho, K. F., Cao, J. J., Harrison, R. M., Lee, S. C., & Bau, K. K. (2004). Indoor/outdoor relationships of organic carbon (OC) and elemental carbon (EC) in PM2.5 in roadside environment of Hong Kong. Atmospheric Environment, 38(37), 6327–6335. http://doi.org/10.1016/j.atmosenv.2004.08.007

Huang, Z., Harrison, R. M., Allen, A. G., James, J. D., Tilling, R. M., & Yin, J. (2004). Field intercomparison of filter pack and impactor sampling for aerosol nitrate, ammonium, and sulphate at coastal and inland sites. Atmospheric Research, 71(3), 215–232. http://doi.org/10.1016/j.atmosres.2004.05.002

Hussein, T., Glytsos, T., Ondráček, J., Dohányosová, P., Ždímal, V., Hämeri, K., Kulmala, M. (2006). Particle size characterization and emission rates during indoor activities in a house. Atmospheric Environment, 40(23), 4285–4307. http://doi.org/10.1016/j.atmosenv.2006.03.053

Hussein, T., Hameri, K., Aalto, P., Asmi, A., Kakko, L., & Kulmala, M. (2004). Particle size characterization and the indoor-to-outdoor relationship of atmospheric aerosols in Helsinki. Scand J Work Environ Health, 30 Suppl 2, 54–62. http://doi.org/815 [pii]

Hussein, T., Karppinen, A., & Kukkonen, J. (2006). Meteorological dependence of size-fractionated number concentrations of urban aerosol particles. Atmospheric Environment, Retrieved from http://www.sciencedirect.com/science/article/pii/S135223100501037X

Kubelová, L., Vodička, P., Schwarz, J., Cusack, M., Makeš, O., Ondráček, J., & Ždímal, V. (2015). A study of summer and winter highly time-resolved submicron aerosol composition measured at a suburban site in Prague. Atmospheric Environment, 118, 45–57. http://doi.org/10.1016/j.atmosenv.2015.07.030

Kvietkus, K., Šakalys, J., RIimselyte, I., Ovadnevaite, J., Remeikis, V., & Špakauskas, V. (2011, January 1). Characterization of aerosol sources at urban and background sites in Lithuania. Lithuanian Journal of Physics. http://doi.org/10.3952/physics.v51i1.2008

Lazaridis, M., & Aleksandropoulou, V. (2006). Characterization of indoor/outdoor particulate matter in two residential houses in Oslo, Norway: measurements overview and physical properties–URBAN-AEROSOL. Indoor Air, Retrieved from http://onlinelibrary.wiley.com/doi/10.1111/j.1600-0668.2006.00425.x/full

Lehmann, K., Massling, A., Tilgner, A., Mertes, S., Galgon, D., & Wiedensohler, A. (2005). Size-resolved soluble volume fractions of submicrometer particles in air masses of different character. Atmospheric Environment, 39(23-24), 4257–4266. http://doi.org/10.1016/j.atmosenv.2005.02.011

Leung, D. Y. C., & Drakaki, E. (2015). Outdoor-indoor air pollution in urban environment: challenges and opportunity. Frontiers in Environmental Science, 2(January), 1–7. http://doi.org/10.3389/fenvs.2014.00069

Mahowald, N., Ward, D. S., Kloster, S., Flanner, M. G., Heald, C. L., Heavens, N. G., Chuang, P. Y. (2011). Aerosol Impacts on Climate and Biogeochemistry. Annual Review of Environment and Resources, 36(1), 45–74. http://doi.org/10.1146/annurev-environ-042009-094507

Mohr, C., DeCarlo, P. F., Heringa, M. F., Chirico, R., Slowik, J. G., Richter, R., Prévôt, a. S. H. (2012). Identification and quantification of organic aerosol from cooking and other sources in Barcelona using aerosol mass

spectrometer data. Atmospheric Chemistry and Physics, 12(4), 1649–1665. http://doi.org/10.5194/acp-12-1649-2012

Monks, P. S., Granier, C., Fuzzi, S., Stohl, A., Williams, M. L., Akimoto, H., von Glasow, R. (2009). Atmospheric composition change – global and regional air quality. Atmospheric Environment, 43(33), 5268–5350. http://doi.org/10.1016/j.atmosenv.2009.08.021

Morawska, L., He, C., Hitchins, J., Gilbert, D., & Parappukkaran, S. (2001). The relationship between indoor and outdoor airborne particles in the residential environment. Atmospheric Environment, 35(20), 3463–3473. http://doi.org/10.1016/S1352-2310 (01)00097-8

Ondráček, J., Schwarz, J., Ždímal, V., Andělová, L., Vodička, P., Bízek, V., Smolík, J. (2011). Contribution of the road traffic to air pollution in the Prague city (busy speedway and suburban crossroads). Atmospheric Environment, 45(29), 5090–5100. http://doi.org/10.1016/j.atmosenv.2011.06.036

Pope, C. A., Bates, D. V, & Raizenne, M. E. (1995). Health effects of particulate air pollution: time for reassessment? Environmental Health Perspectives, 103(5), 472–80. Retrieved from http://www.pubmedcentral.nih.gov/articlerender.fcgi?artid=1523269&tool=pmcentrez&rendertype=abstract

Poulain, L., Spindler, G., Birmili, W., Plass-Dülmer, C., Wiedensohler, A., & Herrmann, H. (2011). Seasonal and diurnal variations of particulate nitrate and organic matter at the IfT research station Melpitz. Atmospheric Chemistry and Physics, 11(24), 12579–12599. http://doi.org/10.5194/acp-11-12579-2011

Putaud, J.-P., Van Dingenen, R., Alastuey, A., Bauer, H., Birmili, W., Cyrys, J., Raes, F. (2010). A European aerosol phenomenology – 3: Physical and chemical characteristics of particulate matter from 60 rural, urban, and kerbside sites across Europe. Atmospheric Environment, 44(10), 1308–1320. http://doi.org/10.1016/j.atmosenv.2009.12.011

Querol, X., Alastuey, A., Puicercus, J. A., Mantilla, E., Miro, J. V., Lopez-Soler, A., Artiñano, B. (1998). Seasonal evolution of suspended particles around a large coal-fired power station. Atmospheric Environment, 32(11), 1963–1978. http://doi.org/10.1016/S1352-2310 (97)00504-9

Ristovski, Z. D., Morawska, L., Bofinger, N. D., & Hitchins, J. (1998). Submicrometer and Supermicrometer Particulate Emission from Spark Ignition Vehicles. Environmental Science & Technology, 32(24), 3845–3852. http://doi.org/10.1021/es980102d

Schwartz, J., Dockery, D. W., & Neas, L. M. (1996). Is Daily Mortality Associated Specifically with Fine Particles? Journal of the Air & Waste Management Association, 46(10), 927–939. http://doi.org/10.1080/10473289.1996.10467528

Schwarz, J., Štefancová, L., Maenhaut, W., Smolík, J., & Ždímal, V. (2012). Mass and chemically speciated size distribution of Prague aerosol using an aerosol dryer - The influence of air mass origin. Science of the Total Environment, 437, 348–362. http://doi.org/10.1016/j.scitotenv.2012.07.050

Smolík, J., Dohányosová, P., & Schwarz, J. (2008). Characterization of indoor and outdoor aerosols in a suburban area of Prague. Water, Air, & Soil Retrieved from http://link.springer.com/article/10.1007/s11267-007-9141-y

Smolík, J., Mašková, L., Zikova, N., Ondráčková, L., & Ondráček, J. (2013). Deposition of suspended fine particulate matter in a library. Heritage Science, 1(1), 7. Retrieved from http://www.heritagesciencejournal.com/content/1/1/7

Štefancová, L., Schwarz, J., Mäkelä, T., Hillamo, R., & Smolík, J. (2011). Comprehensive Characterization of Original 10-Stage and 7-Stage Modified Berner Type Impactors. Aerosol Science and Technology, 45(1), 88–100. http://doi.org/10.1080/02786826.2010.524266

Stelson, A., & Seinfeld, J. (1982). Relative humidity and temperature dependence of the ammonium nitrate dissociation constant. Atmospheric Environment (1967), 16(5), 983–992. Retrieved from http://www.sciencedirect.com/science/article/pii/0004698182901846

Tao, W. K., Chen, J. P., Li, Z., Wang, C., & Zhang, C. (2012). Impact of aerosols on convective clouds and precipitation. Reviews of Geophysics, 50(2). http://doi.org/10.1029/2011RG000369

Viana, M., Kuhlbusch, T. A. J., Querol, X., Alastuey, A., Harrison, R. M., Hopke, P. K, Hitzenberger, R. (2008). Source apportionment of particulate matter in Europe: A review of methods and results. Journal of Aerosol Science, 39(10), 827–849. http://doi.org/10.1016/j.jaerosci.2008.05.007

Vodička, P., Schwarz, J., & Ždímal, V. (2013). Analysis of one year's OC/EC data at a Prague suburban site with 2-h time resolution. Atmospheric Environment, 77, 865–872. http://doi.org/10.1016/j.atmosenv.2013.06.013

Watson, J. G. (2002). Visibility: Science and Regulation. Journal of the Air & Waste Management Association, 52(6), 628–713. http://doi.org/10.1080/10473289.2002.10470813

Zhu, Y., Hinds, W. C., Krudysz, M., Kuhn, T., Froines, J., & Sioutas, C. (2005). Penetration of freeway ultrafine particles into indoor environments. Journal of Aerosol Science, 36(3), 303–322. http://doi.org/10.1016/j.jaerosci.2004.09.007

Zíková, N., & Ždímal, V. (2013). Long-Term Measurement of Aerosol Number Size Distributions at Rural Background Station Košetice. Aerosol and Air Quality Research, 13(5), 1464–1474. http://doi.org/10.4209/aaqr.2013.02.0056

Supplementary Material

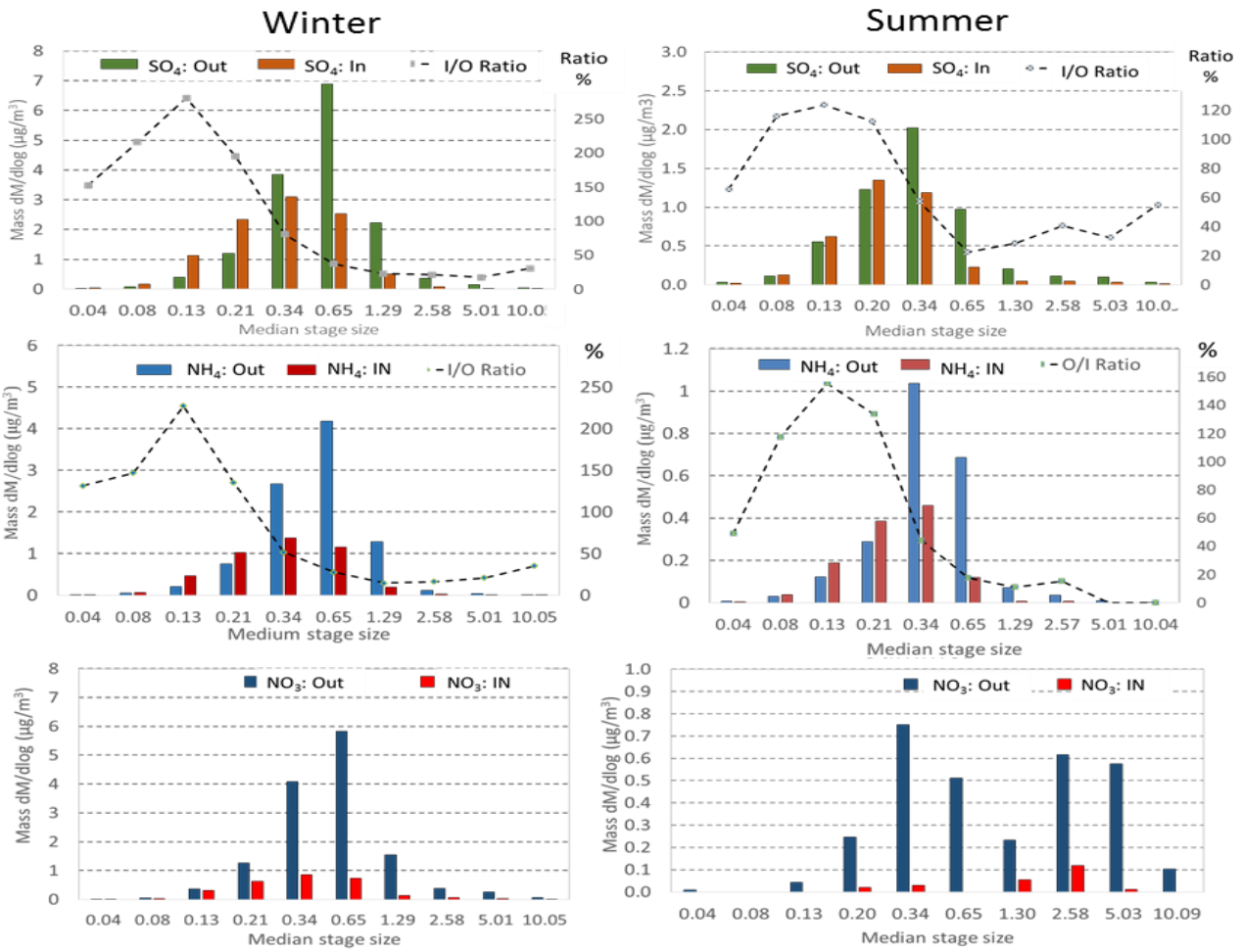

SI. 1. Winter (left) and summer sulfate, nitrate, and ammonium impactor measurements per median stage diameter. I/O ratios were given as percentages on the RHS of sulfate and ammonium graphs

	Species OUTDOORS (Spearman Correlation)						Species OUTDOORS (P Values of correlation)					
Parameter	Org Out	NO_3 Out	SO_4 Out	NH_4 Out	Chl out	Total	Org Out	NO_3 Out	SO_4 Out	NH_4 Out	Chl out	Total
Day	0.40	**0.53**	0.12	0.33	**0.57**	0.39	0.11	0.03	0.65	0.19	0.02	0.12
Temp (Day)	0.32	0.33	0.04	0.22	0.37	0.28	0.21	0.19	0.87	0.39	0.14	0.28
Temp (Night)	-0.25	0.00	-0.20	-0.11	-0.24	-0.15	0.34	0.98	0.45	0.67	0.36	0.56
Temp (Ave)	0.07	0.19	-0.16	0.03	0.10	0.06	0.78	0.47	0.54	0.90	0.71	0.81
Temp (Indoors)	-0.46	-0.29	**-0.61**	-0.41	-0.31	-0.39	0.07	0.25	0.01	0.10	0.23	0.13
RH (High)	0.48	**0.50**	0.48	**0.50**	0.25	0.48	0.05	0.04	0.05	0.04	0.33	0.05
RH (Low)	-0.20	-0.06	0.07	0.00	-0.35	-0.11	0.45	0.81	0.80	1.00	0.17	0.66
RH (Ave)	-0.14	0.02	0.12	0.07	-0.37	-0.06	0.60	0.95	0.64	0.80	0.14	0.83
RH (Indoors)	**-0.63**	**-0.70**	-0.37	**-0.59**	**-0.76**	**-0.69**	0.01	0.00	0.14	0.01	0.00	0.00
Outdoor Pressure	0.11	-0.02	0.44	0.17	-0.17	0.14	0.69	0.94	0.08	0.52	0.52	0.59
Indoor Pressure	0.09	-0.05	0.43	0.14	-0.17	0.10	0.73	0.85	0.08	0.59	0.52	0.69
Wind speed (Ave)	**-0.53**	-0.36	**-0.67**	-0.45	-0.41	**-0.48**	0.03	0.15	0.00	0.07	0.11	0.05
NR-Org In	**1.00**	**0.85**	**0.81**	**0.88**	**0.81**	**0.95**	NA	0.00	0.00	0.00	0.00	0.00
NO_3 Out		**1.00**	**0.73**	**0.95**	**0.66**	**0.94**		NA	0.00	0.00	0.00	0.00
SO_4 Out			**1.00**	**0.87**	**0.50**	**0.84**			NA	0.00	0.04	0.00
NH_4 Out				**1.00**	**0.64**	**0.97**				NA	0.01	0.00
Chl Out					**1.00**	**0.74**					NA	0.00
Total Out						**1.00**						NA

	Species INDOORS (Sp. correlation coefficient)						Species INDOORS (p-values of correlation)					
Parameter	NR-Org In	NO_3 In	SO_4 In	NH_4 In	Ch In	Total In	NR-Org In	NO_3 In	SO_4 In	NH_4 In	Ch In	Total In
Temp (day)	0.31	0.33	0.08	0.20	0.39	0.24	0.23	0.19	0.75	0.45	0.12	0.36
Temp (night)	-0.14	-0.06	-0.10	-0.06	-0.12	-0.06	0.58	0.82	0.70	0.81	0.65	0.81
Temp (ave)	0.12	0.16	-0.07	0.06	0.20	0.09	0.65	0.55	0.80	0.83	0.45	0.74
Temp (indoors)	**-0.59**	**-0.49**	**-0.69**	**-0.64**	-0.46	**-0.58**	0.01	0.04	0.00	0.01	0.07	0.01
RH (High)	0.44	0.41	**0.50**	0.48	0.28	0.45	0.08	0.10	0.04	0.05	0.28	0.07
RH (low)	-0.14	-0.06	0.14	0.08	-0.22	0.03	0.60	0.82	0.58	0.77	0.39	0.91
RH (ave)	-0.10	-0.02	0.21	0.14	-0.23	0.08	0.71	0.95	0.42	0.60	0.37	0.75
RH (Indoors)	**-0.60**	**-0.68**	-0.41	**-0.52**	**-0.72**	**-0.55**	0.01	0.00	0.10	0.03	0.00	0.02
Outdoor Pressure	0.04	0.14	0.38	0.29	-0.21	0.17	0.88	0.59	0.13	0.27	0.43	0.52
Indoor Pressure	0.05	0.12	0.38	0.28	-0.20	0.16	0.86	0.66	0.13	0.28	0.44	0.54
Wind Speed (ave)	**-0.56**	-0.47	**-0.65**	**-0.56**	-0.40	**-0.54**	0.02	0.06	0.00	0.02	0.11	0.03
NR-Org In	1.00	**0.89**	**0.83**	**0.88**	**0.89**	**0.92**	NA	0.00	0.00	0.00	0.00	0.00
NO3 In		1.00	**0.87**	**0.95**	**0.76**	**0.96**		NA	0.00	0.00	0.00	0.00
SO4 In			1.00	**0.97**	**0.56**	**0.92**			NA	0.00	0.02	0.00
NH4 In				1.00	**0.66**	**0.98**				NA	0.00	0.00
Ch In					1.00	**0.73**					NA	0.00
Total In						1.00						NA

Fig.9. Spearman correlation matrix (Left) and correlated P-Values (Right) for Indoor (Top) and outdoor (Bottom) average chemical mass composition. Highlighted boxes indicate statistically significantly correlated parameters on the 0.05 confidence level.

11. Article 4

Inter-comparison of four different cascade impactors for fine and ultrafine particle sampling in two European locations

A. S. Fonseca[1,2,*] **N. Talbot[3,4],** J. Schwarz[3], J. Ondráček[3], V. Ždímal[3], J. Kozáková[3,4], M. Viana[1], A. Karanasiou[1], X. Querol[1], A. Alastuey[1], T. V. Vu[5], J. M. Delgado-Saborit[5], R. M. Harrison[5,†],

[1] Institute of Environmental Assessment and Water Research (IDÆA-CSIC), Barcelona, 08034, Spain
[2] Universidad de Barcelona, Facultad de Química, Barcelona, 08028, Spain
[3] Institute of Chemical Process Fundamentals of the ASCR, v.v.i. (ICPF), Prague, 165 02, Czech Republic
[4]Charles University in Prague, Faculty of Science, Institute for Environmental Studies, Prague, 128 43, Czech Republic
[5]University of Birmingham, Division of Environmental Health & Risk Management, Birmingham, B15 2TT,UK
[†]Also at: Department of Environmental Sciences / Center of Excellence in Environmental Studies, King Abdulaziz University, PO Box 80203, Jeddah, 21589, Saudi Arabia

Accepted for Review in **Atmospheric Chemistry and Physics journal:** December 2015

Pages: 128-150

Published in: Spring 2016

Impact factor of Journal: 5.02

Inter-comparison of four different cascade impactors for fine and ultrafine particle sampling in two European locations.

A. S. Fonseca[1,2,*] **N. Talbot[3,4]**, J. Schwarz[3], J. Ondráček[3], V. Ždímal[3], J. Kozáková[3,4], M. Viana[1], A. Karanasiou[1], X. Querol[1], A. Alastuey[1], T. V. Vu[5], J. M. Delgado-Saborit[5], R. M. Harrison[5,†]

[1] Institute of Environmental Assessment and Water Research (IDÆA-CSIC), Barcelona, 08034, Spain

[2] Universidad de Barcelona, Facultad de Química, Barcelona, 08028, Spain

[3] Institute of Chemical Process Fundamentals of the ASCR, v.v.i. (ICPF), Prague, 165 02, Czech Republic

[4]Charles University in Prague, Faculty of Science, Institute for Environmental Studies, Prague, 128 43, Czech Republic

[5]University of Birmingham, Division of Environmental Health & Risk Management, Birmingham, B15 2TT,UK

[†]Also at: Department of Environmental Sciences / Center of Excellence in Environmental Studies, King Abdulaziz University, PO Box 80203, Jeddah, 21589, Saudi Arabia

Keywords: Mass size distribution; Chemical characterization; Ultra-fine particles; Cascade Impactors; Nanoparticles; Ultrafine particles

Abstract

Due to the need to better characterise the ultrafine particle (UFP) fraction and related personal exposure, several impactors have been developed to enable the collection of UFP (<100 nm). However, to the authors' knowledge there have been no field campaigns to-date inter-comparing impactor collection of UFP. The purpose of this study was two-fold: 1) to assess the performance of a number of conventional and nano-range impactors with regard to the particle mass size distribution under different environmental conditions and aerosol loads and types, and 2) to characterise aerosol size distributions including UFPs using impactors in 2 European locations. The impactors used were: (i) Berner low-pressure impactor (BLPI; 26 nm - 13.5 µm), (ii) nano-Berner low-pressure impactor (nano-BLPI; 11 nm - 1.95 µm) and (iii) Nano-microorifice uniform deposit impactor (nano-MOUDI; 10 nm-18 µm), and (iv) Personal cascade impactor Sioutas (PCIS; < 250 nm - 10 µm).

Taking the BLPI as an internal reference, the best agreement regarding mass size distributions was obtained with the nano-BLPI, independently of the aerosol load and aerosol chemical composition. The nano-MOUDI showed a good agreement for particle sizes >320 nm, whereas for particle diameters <320 nm this instrument recorded larger mass concentrations in outdoor air than the internal reference. This difference could be due to particle bounce, to the dissociation of semi volatiles in the coarser stages and/or to particle shrinkage during transport through the impactor due to higher temperature inside this impactor. Further research is needed to understand this behaviour.

With regard to the PCIS, their size-resolved mass concentrations were comparable with other impactors for PM_1, PM_2 and PM_{10}, but the cut-off at 250 nm did not seem to be consistent with that of the internal reference.

1. Introduction

Used in numerous areas of air quality research, cascade impactors are established, relatively simple, and robust instruments. They collect airborne aerosols and segregate them into a number of aerodynamic sizes for subsequent determination of mass size distribution, chemical and/or physical

properties (Hitzenberger *et al.*, 2004; Seinfeld and Pandis, 2006). The mechanical principle behind size impaction employs the known quantities of Stokes number and Cunningham correction factors to derive particle inertia, therefore ascribing a stopping distance in accordance to particle size (Hinds, 1999). Particulates are collected onto substrates, frequently made of quartz, polytetrafluoroethylene (PTFE; best known as Teflon), polyethylene terephthalate (commonly abbreviated PET, otherwise known as Mylar), polycarbonate or aluminium (Howell *et al.*, 1998; Schaap *et al.*, 2004; Tursic *et al.*, 2008). The choice of substrate is dependent on the type of impactor, sampling conditions and analytical techniques intended to be carried out (Fujitani *et al.*, 2006). A variety of cascade impactor designs have appeared since May (1945) first reported on an initial design to sample coarse aerosols (>2.5 µm). Since then, sampling size fractions for traditionally designed commercially available cascade impactors allowed for particle collection from coarse to fine fractions (<2.5 µm), for example 10 µm - 0.034 µm for the Berner low-pressure impactor (BLPI) (Hering *et al.*, 1978; Berner and Luerzer, 1980; Hillamo and Kauppinen, 1991) and size cuts as small as 0.056 µm for the micro-orifice uniform deposit impactor (MOUDI) (Marple *et al.*, 1991).

However, epidemiological studies have evidenced the need to focus on ultrafine particles (UFP; D_p<100 nm), due to their possibly larger impacts on health when compared to coarser particles (Oberdörster, 2000; Oberdorster *et al.*, 2005). Recently, due to the growing need to better characterise the UFP fraction, the second generation of MOUDI impactors (Model 122 and Model 125 Nano-MOUDI-II™, MSP Corp., Shoreview, MN, USA), both available in the rotating version (122-R and 125-R) and in the non-rotating version (122-NR and 125-NR) and nano-BLPI (not commercially available) were introduced, both adaptions of the original MOUDI (Marple *et al.*, 1991) and BLPI impactors (Hering *et al.*, 1978; Berner and Luerzer, 1980; Hillamo and Kauppinen, 1991), modified to enable the collection of UFP down to 11 nm. Also, the need to better understand and characterise personal exposure led to the development of portable, light-weight impactors such as the personal cascade impactor sampler (PCIS; Misra *et al*, 2002).

Due to the physical principle of particle collection associated with all impactors sampling artefacts can occur, including particle bounce, particle blow off, and particle wall loss (Wall *et al.*, 1988; Schwarz *et al.*, 2012). These artefacts vary according to the impactor type (Hillamo and Kauppinen, 1991; Howell *et al.*, 1998; Štefancová *et al.*, 2011) loads, composition of the aerosol sampled (Huang *et al.*, 2004; Sardar *et al.*, 2005; Fujitani *et al.*, 2006; Crilley *et al.*, 2013), and the type of substrate used (Fujitani *et al.*, 2006; Nie *et al.*, 2010). Also, because long sampling time is required for having enough mass of the finest UFP for chemical analysis may produce sampling artefacts of volatilization or absorption.

As well as those previously described, the sampling and accurate sizing of UFP/nanoparticles also present challenges. The need to create a fast flowing jet of air onto an impactor plate, creating the inertia allowing for collection of the smallest size fractions producing a high pressure differential at the lowest cut sizes. This pressure drop changes the vapour pressure in the bulk which can then enhance volatilisation (Hering and Cass, 1999). Attempts to address this were successfully carried out by decreasing the pressure drop over a reduced number of stages (Marple *et al.*, 1991; Štefancová *et al.*, 2011). Moreover, the low mass of UFP requires a greater collection concentration which then increases the possibility of mass overloading on the larger fractions. The commercially available Nano-MOUDI-II™seeks to reduce jet velocity, pressure drop, particle bounce, re-entrainment and evaporative loss by incorporating micro-orifice nozzles (up to 2000 as small as 50 µm in diameter in the 10 L/min Model 125 and up to 6 000 of 50 µm diameter in the 30 L/min Model 122). The rotating Nano-MOUDI-II™versions (Model 122-R and 125-R) have internal embedded stepper motors for the rotation of the sampling stages, thereby spreading the sample over the filter to reduce build-up

(Marple *et al.*, 2014). However, as will be described below, this spreading of the sample may create new uncertainties and complications.

Cascade impactors have been deployed in a diverse array of measurement campaigns utilising their versatility, characterising size-fractionated chemical composition of urban aerosols (Sardar *et al.*, 2005; Schwarz *et al.*, 2012), particle volatility (Hering and Cass, 1999; Huang *et al.*, 2004), vapour-particle phase partitioning (Delgado-Saborit *et al.*, 2014), influence of relative humidity (Štefancová *et al.*, 2010), indoor - outdoor relationship (Smolík *et al.*, 2008), archive contamination (Mašková *et al.*, 2015), metals in particles collected near a busy road (Lin *et al.*, 2005; Karanasiou *et al.*, 2007; Ondráček *et al.*, 2011), size-segregated emission particles in a coal-fired power station (Tursic *et al.*, 2008), whilst extensive theoretical investigations and experimental characterization of cascade impactors tended to focus on the performance of one type of cascade impactor (Biswas and Flagan, 1984; Wang and John, 1988; Štefancová *et al.*, 2011; Jiménez and Ballester, 2011; Marple *et al.*, 2014). Howell *et al.* (1998) carried out an intercomparison of 'traditional' BLPI and MOUDI impactors during a field campaign. Field campaigns usually provide a greater variation of conditions than controlled laboratory based conditions, offering a more robust analysis of comparable instrumentation. Another notable intercomparison study was conducted by Pennanen *et al.* (2007) who tested a modified 4-stage Harvard high-volume cascade impactor against a reference 10-stage BLPI in 6 different European locations over different seasons. The authors note the implicit effects on individual impactors of meteorology and aerosol composition. Other studies have run two or more impactors in tandem measuring simultaneously indoors and outdoors (Smolík *et al.*, 2008; Mašková *et al.*, 2015), to cover extended particle size distributions (Geller *et al.*, 2002), or characterise artefacts caused by particle volatility (Huang *et al.*, 2004; Schaap *et al.*, 2004) or changes in size distribution due to different relative humidity (Štefancová *et al.*, 2010).

To the authors' knowledge there has been no field campaign to-date intercomparing impactor collection efficiency of UFP. As a result, this paper seeks to address this by assessing the performance of a number of conventional and nano-range impactors, namely Berner low-pressure impactor (BLPI, 25/0.018/2, Hauke, Austria), nano-Berner low-pressure impactor (nano-BLPI, 10/0,01, Hauke, Austria), nano-microorifice uniform deposit impactor (Nano-MOUDI-II™, MSP Corp., Shoreview, MN, USA Model 125R; U.S. Patent # 6,431,014B1) and Personal cascade impactor Sioutas (SioutasTM PCIS, SKC Inc.; Misra *et al*, 2002) impactors, by means of two intercomparison exercises in Prague, during winter 2015 and in Barcelona during summer 2015. The aim of the campaigns was to test the instruments' performance under different environmental conditions and aerosol loads and types. Our work reports on the impactor performances not only with regard to different particle size distributions but also aerosol composition and meteorology.

2. Methodology

2.1. Sampling sites and sampling set-up

2.1.1. Prague

The field intercomparison initially took place in outdoor air (6th-23rd February 2015) and it was subsequently moved indoors (23rd February 2015 - 2nd March 2015) in Prague, Suchdol at the Institute of Chemical Process Fundamentals (ICPF), Academy of Sciences of the Czech Republic (ASCR) compound (50°7'36.47"N, 14°23'5.51"E, 277 m.a.s.l). Suchdol is a residential area in north-western Prague, about 6 km from the city centre. It is recognized as a suburban background site with residential houses and a university campus interspersed between plenty of green spaces. The traffic flow is

moderate along one major 2-lane road (average traffic of 10000-15000 vehicles/day) with regular bus services. Due to its location on a plateau above the river Vltava there are not many contributory roads alongside (Figure S1). Detailed information of the area where the impactors were located were previously provided by Smolík *et al.* (2008) and Hussein *et al.* (2006).

Outdoor sampling consisted of 3 weekend sampling periods (6 - 9th, 13 - 16th and 20th - 23rd February 2015), and 2 week-day samplings, (10 - 12th and 17 - 20st).

In addition, indoor samples were also collected during 2 week-day samplings (23rd - 25th and 25th - 27th February 2015) and a final 3-day weekend sampling period (27th February 2015 - 2nd March 2015). This resulted in a total of 5 valid outdoor samples (three weekend and two week-day) and two valid indoor samples (one weekend and one week-day). For both outdoor and indoor sampling, the weekend runs started on the preceding Friday between 11:00h-13:00h local time and finished at 9:00h local time on the following Monday. The week-day samplings started between 11h00-14h00 and terminated at 9h00. The sample duration in Prague was defined based on the experience from previous research (Smolík *et al.*, 2008; Štefancová *et al.*, 2011). Based on ambient PM concentrations it was considered that samples should be collected over no more than 72 hours, to avoid substrate overload.

2.1.2. Barcelona

The Barcelona intercomparison was conducted exclusively outdoors at an air quality monitoring station at IDAEA-CSIC located in an urban background site in the southwest of Barcelona (41°23'14" N, 02°06'56"E,, 78 m.a.s.l) from 18th May to 3rd July 2015 (Figure S2). The sampling site, described in detail by Reche *et al.* (2015), is influenced by vehicular emissions from one of the city's main traffic avenues (Diagonal avenue), located at approximately 200 m from the site and with a mean traffic density of 90 000 vehicles/day (Amato *et al.*, 2015). Thus, the site is classified as urban background, but it is located in a city with very high road traffic and influenced by the emissions of one of the largest arterial roads of the city.

Outdoor sampling in Barcelona consisted of 4 valid week-day sampling runs, each run accounting for 96h (4 days duration sampling time). The runs started every Monday between 10:00h-12:00h local time and finished on Fridays around 14:00h-16:00h local time. The sample duration in Barcelona was set longer than in Prague since the averages of particle mass collected during a sampling less than 4 days as duration would not be sufficient for further chemical analysis.Indoor intercomparisons were not carried out due to the absence of an appropriate location for indoor air sampling.

2.2. Instrument set-up and experimental specifications

In the present study, the mass size distribution of the aerosol was measured by different types of cascade impactors:

- A Berner low-pressure impactor (BLPI, 25/0.018/2, Hauke, Austria; (Berner et al., 1979; Preining and Berner, 1979) which collects particles onto PET foils (Mylar 13 µm thick) (flow rate 24.8 L min^{-1}). The impactors separated particle mass into 10 size fractions. The cut diameters of the stages were 0.026, 0.056, 0.1, 0.16, 0.25, 0.43, 0.86, 1.73, 3.425, and 6.61 µm (Štefancová *et al.*, 2011). The impactors were equipped with inlets with the cut-point calculated as 14 µm.
- A modified BLPI (denominated as nano-BLPI, 10/0.01, Hauke, Austria) collecting particles on PET foils (Mylar 13 µm thick) (flow rate 17.2 L min^{-1}) from 0.01 µm to 1.95 µm in 8 size stages. The aerodynamic cut diameters of stages 1 to 8 were 0.011, 0.024, 0.039, 0.062, 0.095, 0.24, 0.49, 1.0 µm, and the inlet cut-point was calculated as 1.95 µm. Given that the nano-BLPI is a custom made

instrument, the design parameters of each of its impaction stages are shown in Table S1 in the supporting information.

- A nano-microorifice uniform deposit impactor (Nano-MOUDI-II™, MSP Corp., Shoreview, MN, USA Model 125R; U.S. Patent # 6,431,014B1) equipped with PTFE filters (with diameters of 47 mm) was used to collect size-resolved aerosol samples. These impactors effectively separated the particulate matter into 13 stages with nominal cut diameters of 0.010, 0.018, 0.03, 0.06, 0.10, 0.18, 0.32, 0.56, 1.0, 1.8, 3.2, 5.6, 10 µm and the inlet cut-point as 18 µm when operated at an inlet flow rate of 10 L min^{-1}.
- Three personal cascade impactor samplers (SioutasTM PCIS, SKC Inc; Misra *et al*, 2002) operating with a flow rate of 9 L min^{-1} at a pressure drop of 11 inches of H_2O (2.7 kPa). Particles can be separated in the following aerodynamic particle diameter ranges: <0.25; 0.25 to 0.5; 0.5 to 1.0; 1.0 to 2.5; and >2.5 µm. The collection substrates were 37 mm PTFE filters (Pall) or quartz fibre filters (Pall) for the < 0.25 µm stage and 25 mm PTFE filters (Pall) for the 0.25-2.5 µm and >2.5µm stages. Two of the PCIS deployed in Prague separated particle mass in all of the 5 size fractions while another unit collected particles only at 3 of the stages (< 0.25 µm; 0.25-2.5 µm and >2.5 µm). In order to facilitate interpretation of the data, a lower cut diameter of 30 nm was assumed for the last filter stage of particles < 0.25 µm (quasi-UFP).

All the cascade impactors were loaded with uncoated substrates to avoid possible interferences in future chemical analysis (mainly, determination of organics), so the particle bounce that might occur during dry collection has to be considered excepting for the case of BLPI which foils were coated with a thin layer of vacuum grease (Apiezon L, Apiezon products, M&I Materials Ltd, Manchester, England) to ensure adherence of deposited particles and reduce the artefact of bounce.

For the Prague winter intercomparison, the abovementioned six different impactors were deployed simultaneously in both outdoor and indoor sampling periods. The cascade impactors and their inlets were positioned outside above the roof of ICPF building, 285 m.a.s.l. The nano-MOUDI, in order to protect the electrical components it was kept inside an air-conditioned cabin with a temperature continually lower than 20˚C and a metal pipe (about 300 cm long) was extended through the roof of the building. With regard to indoor sampling, the impactors were placed inside Laboratory of Aerosol Chemistry and Physics experimental hall on the 2nd floor where office and other experimental activities take place. In both campaigns (indoor and outdoor), the pump exhausts were extended far of the sampling spots in order to avoid sampling artefacts.

For the Barcelona summer intercomparison, the same cascade impactors were deployed (except for the PCIS) at the urban background monitoring site located in IDAEA-CSIC (78 m.a.s.l; South West part of the city) within the University Campus and they were positioned under a plastic shelter to protect them from rain while allowing free ventilation. All the impactor pumps were placed 5 m distance from the impactors whilst long tubes (10 m) were connected to the exhausts to avoid contamination of the samples.

The error in the sampling flow rate and sampled volume in both campaigns was < 5%. Thus, it is assumed that flow rates did not affect the particle size cut-offs. The uncertainty in the particle mass concentration determination was < 15% except in some cases for the smallest stages of nano-BLPI and nano-MOUDI impactor which reached mass value deviations > 20 % (standard deviation).

The specifications of the campaigns and the impactors deployed in the intercomparison study are summarized in Table 1. The BLPI was used as internal reference for the size distribution in this study as it was calibrated with the method described by Hillamo and Kauppinen (1991) for the fine stages and by Štefancová *et al.* (2011) for coarse stages. For the intercomparison, the modal pattern of

aerosol mass size distribution was divided into four size groups: (i) PM_{10} (D_p<10 µm), (ii) PM_2 (D_p<2 µm), (iii) PM_1 (D_p<1 µm) and (iv) $PM_{0.25}$ (D_p<0.25 µm) particles. Approximate lower cut points for those selected size fractions are shown in Table S2 in the supporting information.

Table 1. Impactors deployed in Prague and Barcelona and their specifications.

Impactor type	**BLPI**	**nano-BLPI**	**nano-MOUDI**	**PCIS (5 stages)** [c]	**PCIS (3 stages)** [d]
Number of samplings in Prague	5x outdoor (3x weekend-days + 2x week-days) 2 x indoor (1xweekend-days + 1x week-days)	5x outdoor (3x weekend-days + 2x week-days) 2 x indoor (1xweekend-days + 1x week-days)	5x outdoor (3x weekend-days + 2x week-days) 2 x indoor (1xweekend-days + 1x week-days)	5x outdoor (3x weekend-days + 2x week-days) 2 x indoor (1xweekend-days + 1x week-days)	5x outdoor (3x weekend-days + 2x week-days) 2 x indoor (1xweekend-days + 1x week-days)
Number of samplings in in Barcelona	4 x outdoor (4 x week-days)	4 x outdoor (4 x week-days)	4 x outdoor (4 x week-days)	N/A	N/A
Flow rate (L min^{-1})[a]	24.8	17.2	10	9	9
Sampling substrates	PET foils (MYLAR) 13 µm thick	PET foils (MYLAR) 13 µm thick	PTFE 47 mm	37 mm PTFE filters (Pall) < 0.25 µm stage and 25 mm PTFE filters (Pall) for the 0.25-2.5 µm and 2.5-10 µm stages	37 mm quartz-fibre filters (Pall) < 0.25 µm stage and 25 mm PTFE filters (Pall) for the 0.25-2.5 µm and >2.5 µm stages
Nº Stages	10	8	13	5	3
Lower cut sizes (µm) [b]	0.026 0.056 0.10 0.16 0.25 0.43 0.86 1.73 3.42 6.61	0.011 0.024 0.039 0.062 0.095 0.24 0.49 1.0	0.01 0.018 0.032 0.056 0.10 0.18 0.32 0.56 1.00 1.80 3.20 5.60 10	0.03 0.25 0.50 1.00 2.50	0.03 0.25 2.50
Inlet cut-point (µm)	14	1.95	18	10	>2.5

[a] Volumetric flow rate at 20°C and ambient pressure
[b] All sizes are aerodynamic equivalent diameters
[c] Two units deployed; A cyclone was installed ahead which cut PM_{10}
[d] One single unit deployed
N/A – Not available

2.3. Sample conservation and gravimetric analysis

Particle mass concentrations on impactor substrates were gravimetrically determined by pre- and post-weighing the Mylar foils and filters (PTFE and quartz fiber) with a Sartorius M5P-000V001 electronic microbalance in Prague and a Mettler MT5 electronic microbalance in Barcelona, both with a ±1 µg sensitivity. Blank samples (1 per sample) were collected per each impactor type in both intercomparison (Prague and Barcelona) for each of the sampling periods. The deviation of mass values due to varying conditions was corrected with the help of the corresponding blanks.

All samples were equilibrated for a period of 24 hours before weighing in a temperature and relative humidity controlled room. The electrostatic charges of the filters were removed using an U-shaped electrostatic neutralizer (Haug, type PRX U) in Prague and a zerostat anti-static instrument (Z108812-

1EA, Sigma-Aldrich Co. LLC.) in Barcelona. Each sample was weighed three times with an accuracy of mass determination of ± 2 µg. After weighing, the sampled foils and filters were stored in the freezer at -18 °C.

2.4. Ion chromatography analysis

Ion chromatography analysis were only carried out for the Prague samples and for the BLPI, nano-BLPI and nano-MOUDI impactors with the aim to support the interpretation of the particle mass size distributions data. The PCIS filters were not analysed due to the differences observed for the finest size fraction with the other impactors, as will be discussed below.

The whole nano-MOUDI impactor samples were extracted in 7 ml of ultrapure water. In case of the Berner impactors, approximately 1/3 of each foil with samples from each stage was cut out and number of aerosol spots on cut piece was calculated. The ratio between cut and total number of spots at each impactor stage was used to recalculate results to overall ion amount on each stage. All samples were then extracted with 7 ml of ultrapure water, sonicated for 30 min ultrasonic bath and shaken for 1 hour using a shaker. The extracts were then analyzed using a Dionex 5000 system both for cations (Na^+, NH_4^+, K^+, Ca^{2+} and Mg^{2+}) and anions (SO_4^{2-}, NO_3^-, Cl^-) in parallel. An IonPac AS11-HC 2 x 250 mm column was used for anions using hydroxide eluent, IonPac CS18 2 x 250 mm for cations using methane sulfonic acid solution as an eluent. Both anion and cation set-up were equipped with electrochemical suppressors. External calibration was done using NIST traceable calibration solutions.

3. Results

3.1. Meteorological data and mean aerosol concentrations in outdoor air

Tables 2 displays the meteorological data (ambient temperature, relative humidity, ambient pressure and wind speed), the mean and standard deviations (±σ) of aerosol concentrations for Prague and Barcelona and season during sampling with BLPI.

Table 2. Meteorological data and mean daily aerosol concentrations in outdoor air in Prague from 6th to 23rd February 2015 and in in Barcelona from 18th May to 3rd July 2015.

Sampling site	Temperature (ºC)		Relative humidity (RH, %)		Barometric pressure recalculated to sea level (mbar)	Wind Speed (km h^{-1})	Mean PM_{14}* (µg/m^3)
	Min	Max	Min	Max			
Prague (winter)	-3.4±2.6	3.9±3.3	51±15.4	92±2.1	1023±9.4	12.5±6.6	34.6 ± 15.8
Barcelona (summer)	18±3.3	26±3.3	39±9.9	85±7.1	1018±3.1	12±2.6	15.2 ± 2.1

During the winter campaign in outdoor air from 6th to 23rd February 2015 in Prague, the daily maximum average temperature was 3.9±3.3 ºC and the minimum average temperature was -3.4±2.6 ºC. The relative humidity varied in the range of 51-92% from day to day.

As expected, higher temperatures during summer were monitored in Barcelona from 18th May to 3rd July 2015 than in Prague (minimum of 18±3 ºC and maximum of 26±3 ºC). However, slightly lower RH

(minimum of 39±10 % and maximum of 85±7%), similar pressure (1018±3 mbar) and wind speed (12±3 km h^{-1}) values were recorded. The results imply that aqueous particles may have been collected on an impaction stage different from the stage where they ought to be collected due to the flow-induced relative humidity changes during the day (Fang *et al.*, 1991; Štefancová *et al.*, 2010). Aqueous particles can shrink due to evaporation caused by pressure drop through the impactor and/or grow due to condensation caused by aerodynamic cooling. Also, a distortion of the size distribution due to bounce-off should not be neglected for Barcelona given that foils were not greased prior to sampling.

In Prague, the mean PM_{14} mass concentration measured outdoors (with BLPI) was 34.6 ± 15.8 µg/m^3 whilst in Barcelona (with BLPI) it was 15.2 ± 2.1 µg/m^3 (Table 2), in agreement with previous results from 2008 winter campaign in ICPF (Schwarz *et al*. 2012; PM_{14}=34 µg/m^3) and of the same order of magnitude as PM_{10} from a 2014 summer campaign in the monitoring station at IDAEA-CSIC (PM_{10}=19.6 µg/m^3). The reason of higher averages of particle mass concentrations in winter in Prague than in summer in Barcelona are due to higher emissions (mainly due to coal and biomass burning used for residential heating) and meteorological conditions such as the lower mixing heights of the boundary layer or even temperature inversions occurring in Prague (Schwarz *et al.*, 2012).

3.2. Average particle mass concentrations per stage for the different impactors

To estimate the cumulative mass concentration for the different size ranges in each of the impactors, the integrated curve of the measured particle mass size distributions was determined by Eq. 1:

$$M_i = M_{i-1} + \int_{D_{pi-1}}^{D_{pi}} \frac{dM}{dlogD_p} \times dlogD_p \qquad \text{Eq. (1)}$$

Where, *M* is the estimated mass concentration for each impactor stage *i*, D_{pi-1} and D_{pi} are respectively the lower and upper cut-off diameters of the impactor stage *i*

The cumulative curves of the particle mass distributions from Prague (indoor and outdoor) and Barcelona are shown in Figures 1 and 2, respectively.

Results show that the nano-BLPI behaved similarly to the internal reference considered for this work (BLPI), especially for particles larger than 250 nm. Outdoors and indoors, the nano-MOUDI was in agreement with the BLPI for particles larger than 320 nm (independent of the aerosol load and type). However, for particles below 320 nm, the particle mass concentration of the nano-MOUDI tended to be higher than for the BLPI, especially during winter in Prague. In indoor air, the nano-MOUDI cumulative curve of the mass size distributions was closer to the curve obtained for the BLPI impactor.

While in Prague, the nano-MOUDI mass size distributions for particles >1 µm were lower than the rest of the impactors, in Barcelona, this trend was not so evident (Figure 1 and 2). This different behaviour could be ascribed to a number of causes: (a) in outdoor air the effect of particle bounce and/or the shrinkage of semi volatile compounds may have caused a shift in particle mass towards the lower sizes of the nano-MOUDI, especially in winter in Prague; and/or (b) indoors, the mechanism of the nano-MOUDI of spreading the sample (rotating plates), with the increase in temperature, both in indoor air and inside the nano-MOUDI shell, could favour particle dissociation/evaporation from the PTFE filters and thus result in lower mass loads across the lower size ranges, and thus the nano-MOUDI curve would appear to be closer to the internal reference BLPI. This effect would not be so prominent in outdoor air, given that the instrument does not reach such high temperatures. Nie *et al.* (2010) also attributed the loss of volatile compounds to the increase of the temperature inside the MOUDI. However, nitrate concentrations were low in indoor air (see sections below), and therefore the

volatilization of this species would have had a low impact on particle mass (leaving only the organic fraction to account for this). Further research is necessary to clarify the different behaviours observed.

The size-fractionated average mass concentrations ($PM_{0.25}$, PM_1, PM_2 and PM_{10}) collected by each impactor along with standard errors deviation (±σ) in the respective size fractions, using data from a total of 5 experiments outdoors and 2 indoors in Prague, and a total of 4 valid samples outdoors in Barcelona are summarised in Figure 3. Approximate cut points for the selected size fractions are shown in Table S2 in the supporting information. However, it is important to take into account that some differences in the results could be partially attributed to the differences in the real cut points for the selected size fractions.

The average PM_{14} mass concentrations and corresponding standard deviation obtained using the internal reference (BLPI) in Prague outdoors were 34.6 ± 15.8 µg/m^3. In Barcelona, the PM_{14} mass concentrations and standard deviation in summer were 15.2 ± 2.1 µg/m^3. Comparison of independent data from Grimm (corrected with high volume sampling) and the impactors with PM_1 and PM_{10} size cuts, was carried out for the outdoor campaign in Barcelona (4 samples). A slope of 0.98 and a R^2 of 0.7 was obtained for the PM_{14} for BLPI with PM_{10} from an online laser spectrometer (corrected with regard to reference instrumentation) whereas for PM_1, a slope of 0.7 and a better fit of the data was obtained (R^2=0.9). Similarly to BLPI, the nano-BLPI shows a slope of 0.7 and a R^2 of 1 for the cut point PM_1. The mass differences detected for PM_1 suggest that impactors sampling artefacts such as particle blow off, particle wall losses and/or particle bounce occurred.

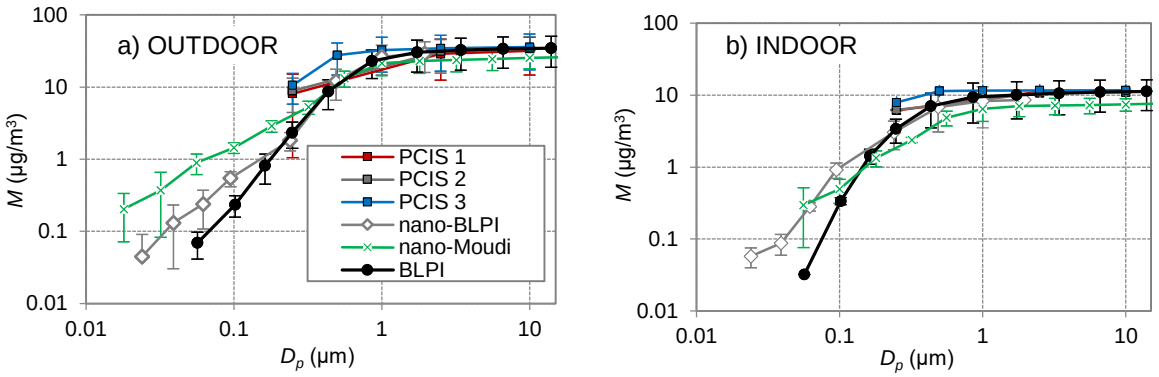

Figure 1. Cumulative mass concentrations measured by the six impactors in Prague: (a) outdoors and (b) indoors. Error bars indicate the standard deviation (±σ).

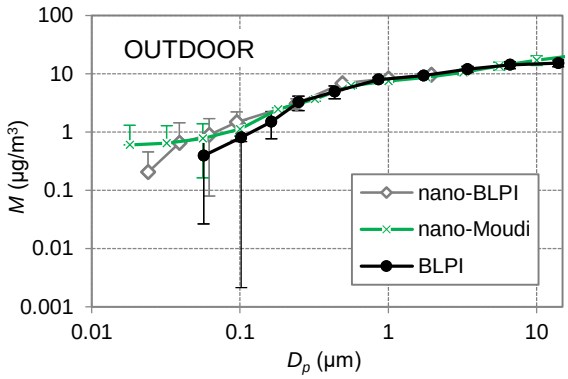

Figure 2. Cumulative mass concentrations measured by the three impactors in Barcelona, outdoors. Error bars indicate the standard deviation (±σ).

As shown in Figure 3, the largest relative difference between the average mass concentrations collected with the three impactors (PCIS, nano-BLPI and nano-MOUDI) and the internal reference (BLPI) was calculated for the $PM_{0.25}$ size fraction measured outdoors in Prague by PCIS and nano-MOUDI, when concentrations were larger by 354 and 126 %, respectively. The best agreement between the three impactors and the internal reference was obtained in the Barcelona summer campaign.

Intercomparisons between the nano-BLPI impactor and the reference BLPI indicate an overall good agreement with absolute differences in mass concentrations per size fraction being <30%, independent of the aerosol type. A consistent underestimation of the particle mass concentrations for the $PM_{0.25}$ size fractions was obtained with the nano-BLPI for all campaigns and locations (Figure 3). This consistent underestimation was in the order of 5 and 22% outdoors in Barcelona and Prague, respectively, and 10% indoors in Prague, for $PM_{0.25}$. As for PM_1, a slight overestimation of mass concentrations with regard to the BLPI was obtained by the nano-BLPI in both sampling campaigns outdoors. The largest deviation in this size fraction was obtained in Prague outdoors (15%) whereas the smallest difference was obtained in Barcelona (5%). Similar to the $PM_{0.25}$ fraction, the PM_1 and PM_2 concentrations obtained indoors by the nano-BLPI were lower (12 and 15%, respectively) than those of the BLPI.

As for the nano-MOUDI, it consistently measured lower PM_1 and PM_2 concentrations in all campaigns (max difference obtained indoors for PM_1 = 31% and PM_2 = 30 %). These differences can be explained by the difference in the cut points given that PM_1 and PM_2 fractions from the BLPI are actually 0.86 µm and 1.7 µm, respectively. For quasi-UFP mass concentrations were significantly higher (126%) in Prague outdoors, whereas the disagreement with the BLPI was reduced in Barcelona outdoors (14%). Finally, in indoor air, concentrations registered by the nano-MOUDI were lower (30%) than the BLPI, in Prague.

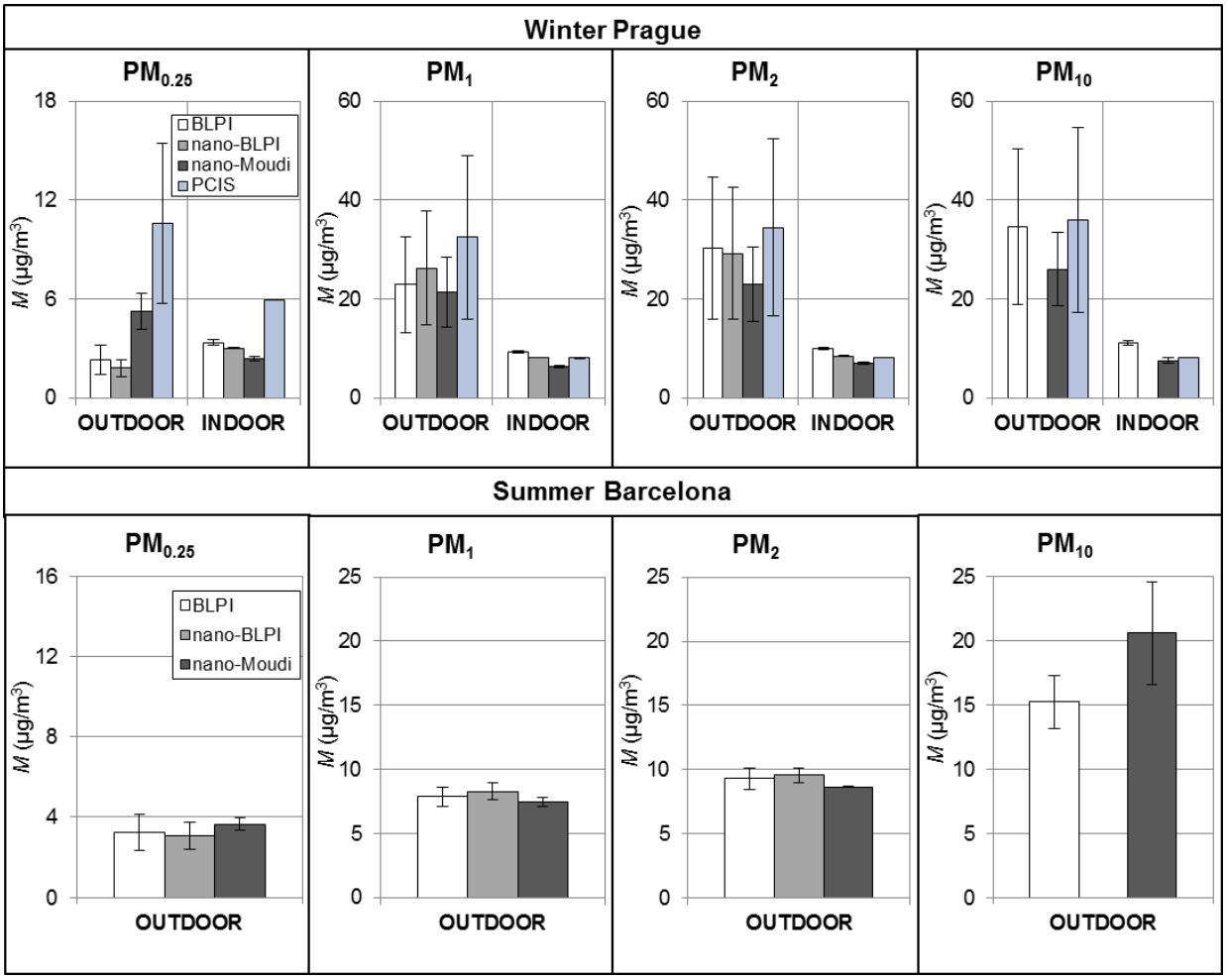

Figure 3. Average mass concentrations collected by the impactors in approximate size ranges: $PM_{0.25}$, PM_1, PM_2 and PM_{10}, during winter Prague campaign (top) and summer Barcelona Campaign (bottom). Error bars indicate the standard deviation (±σ) of the measured concentrations. The PCIS data correspond to PCIS 3 from Figure 1, where more particle size fractions were collected.

Finally, the portable PCIS were only used in Prague during winter given the major differences obtained with regard to the BLPI for the quasi-ultrafine size mode $PM_{0.25}$ (354%). A similar pattern was observed for indoor air, although with a relatively smaller, but still high difference (75%). The differences with regard to the coarse fractions were much smaller when compared to the quasi-UFP fractions (<[±42%] and <[±27%] in outdoors and indoors, respectively). In outdoor air, the PCIS showed consistently higher PM_1, PM_2 and PM_{10} concentrations (42, 14 and 4%, respectively). Similar results were reported by Sioutas (2004) where an average ratio PCIS to MOUDI (Model 110, MSP Corp, Minneapolis, MN) of 2.02 (± 0.59) and 1.21 (± 0.35) was reported for an aerodynamic size range < 0.25 µm and 2.5-1 µm, respectively. However, in indoor air a consistently underestimation (12, 16 and 21 % for PM_1, PM_2 and PM_{10}), was observed.

In summary, for the aerosols and sampling conditions in this work, the PCIS provided comparable size-resolved mass concentrations for PM_1, PM_2 and PM_{10} while the cut-off at 250 nm did not seem to be consistent with the internal reference BLPI.

3.3. Aerosol mass size distributions

3.3.1. Particle size distribution in outdoor air

The average particle mass size distributions obtained in the outdoor intercomparison study (Prague and Barcelona) can be found in Figure 4.

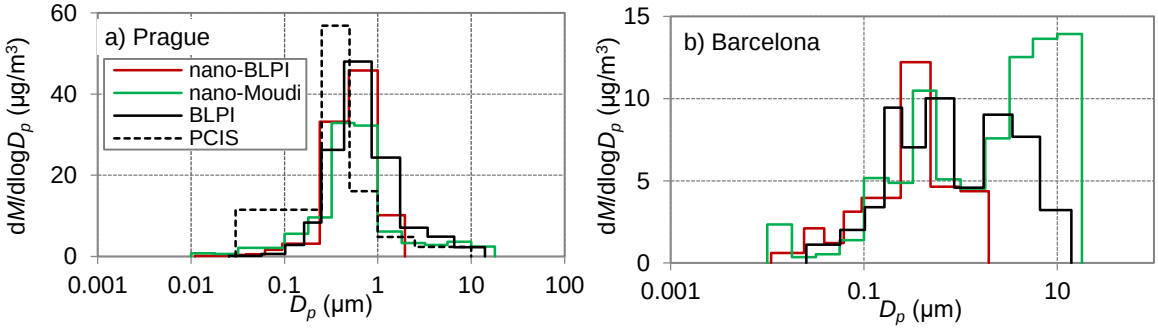

Figure 4. Average mass size distributions obtained outdoors: (a) winter in Prague and (b) summer in Barcelona.

As can be seen, the particle mass size distributions are very different depending on the season and sampling location. During winter in Prague (outdoors), the mass size distributions have a predominantly fine mode, with the coarse mode being almost negligible (by all impactors). The maximum mass concentration obtained in the fine size fraction mode was between 0.4-0.9 µm, whereas in summer in Barcelona, this maximum was shifted towards smaller size fractions between 0.2 and 0.4 µm. In addition to the different aerosol types, this shift to lower sizes might be caused by a lower average relative humidity during sampling in Barcelona that could have caused the particle drying (Tables 2) and therefore, be a reason for particle bounce (Fang *et al.*, 1991; Štefancová *et al.*, 2010).

While in Prague during winter the coarse mode was mostly insignificant, in Barcelona during summer the mass size distributions were clearly bimodal, with larger coarse mode concentrations (Figure 4). The coarse mode obtained may be due to mineral and marine aerosol contributions in the study area (Querol *et al.*, 2008).

The majority of mass concentrations were found in the accumulation mode (PM_1) for both campaigns (7.9 ± 0.7 µg/m^3 and 22.9 ± 9.8 µg/m^3 according the internal reference BLPI in summer Barcelona and winter Prague, respectively). With the increase in mass there was an increase in agreement between the impactors, where the closest agreement was observed (between 200-600 nm) (Figure 4).

Figure 4 reveals that the nano-MOUDI recorded higher particle mass concentrations in the ultrafine range (<100 nm) than the reference BLPI during winter in Prague (5 samples in total outdoors). Although differences were smaller, the same is true for the Barcelona summer campaign (4-week sampling, Figure 4). As previously mentioned, to protect the electrical components of the nano-MOUDI during winter campaign in Prague outdoors, it was kept inside a climate controlled cabin with a temperature continually lower than 20˚C. At these temperatures dissociation of ammonium nitrate can still occur at a slow rate (Smolík *et al.*, 2008)(Andelova et al., 2010; J Smolík et al., 2008)(Andelova et al., 2010; J Smolík et al., 2008)(Andelova et al., 2010; J Smolík et al., 2008).

In addition, during the sampling, an increase of temperature inside the nano-MOUDI shell was detected due to the internal mechanism of spreading the sample (rotating plates) which generates heat. It is therefore likely that the internal temperature in the nano-MOUDI was higher than that of the cabin and thus led to particle volatilisation (Štefancová *et al.*, 2010). The lower nitrate and chloride concentrations in the accumulation mode on the nano-MOUDI filters (see below) would support this interpretation. It is also known that a 5ºC difference between the PTFE filter (of the type used in the nano-MOUDI) and sampling temperature may accelerate the dissociation of ammonium nitrate on PTFE filters up to 20% (Hering and Cass, 1999). The BLPI and nano-BLPI have no internal warming mechanisms and were located outdoors in Prague and Barcelona, so it is expected that lower volatilisation would occur in these scenarios. However, drying of particles before they are deposited on a substrate may happen also in the BLPI and nano-BLPI due to higher pressure drops (at equivalent sizes) in comparison with the nano-MOUDI. This would increase the driving force for evaporation at those stages, which would encourage particle shrinkage.

All these previous facts (temperature, RH, high surface area) appear to enhance the evaporation of semi-volatiles (and dissociation of ammonium nitrate) and therefore particle shrinkage during transport through the nano-MOUDI. Also, the residence time of particles inside the nano-MOUDI low pressure stages is longer due to the low volume flow rate in this instrument. All of this could thus explain the mass size distributions from the nano-MOUDI being skewed towards smaller particle fractions during the Barcelona and Prague campaigns (Figure 4). It should be stated that the rotation of the impaction plates and the nozzle plates of the nano-MOUDI was specifically designed to achieve a uniform deposit on the collection substrates and therefore, eradicate the particle bounce-off artefact (Marple *et al.*, 2014) that may otherwise occur. Particle bounce-off would only be expected when collecting particles in dry conditions such as in Barcelona (< 50% RH) (Table 2) or indoors. Finally, the overall internal volumes in the low pressure stages seem similar in all of the impactors tested; however, this would need experimental confirmation.

3.3.2. Particle s*ize distribution in indoor air*

In Prague, indoor concentrations were lower than outdoors mainly due to a change in weather conditions resulting in cleaner air masses during sampling periods (Figure 4 and Figure 5). Reduced penetration efficiency and faster settling times probably explain the lower indoor coarse mode mass obtained (Figure 5; Hussein *et al*, 2007). Once again, the nano-BLPI measured similar mass concentrations to the reference BLPI (Figure 3) while the nano-MOUDI recorded notably lower mass from fine to coarse modes. In addition, the nano-MOUDI size distribution showed a slight shift towards larger particle sizes (Figure 5). The difference between the BLPIs and the nano-MOUDI could suggest that the latter underestimated mass during this campaign for all particle cut sizes. Initially this would appear to reduce the possibility of volatility losses being responsible for this difference, as ammonium nitrate dissociates readily indoors thereby causing equal losses to all impactors (Lunden *et al.*, 2003). However, because of the way the sample is spread across the substrate in the nano-MOUDI, as described above, the ammonium nitrate collected would be more prone to volatilization than that collected on the other impactors. Therefore it could be considered that the mechanism of the nano-MOUDI of spreading the sample (rotating plates), with the increase in temperatures, both indoors and inside the nano-MOUDI shell, could enhance dissociation/evaporation from the nano-MOUDI PTFE filters. This conclusion can be supported by Figures 6 and 7, which show significantly lower mass

concentrations of major species of ammonium nitrate with the nano-MOUDI, in comparison with the BLPI.

A number of sources of uncertainty in this interpretation should be taken into account:

a) Increased uncertainty in the mass determination due to lower mass concentrations and shorter sampling times
b) No blank correction available for nano-MOUDI IC data
c) No uncertainty calculations for mass determinations available for nano-MOUDI, possibly resulting in negative mass concentrations in the lower stages
d) Only 2 valid samples available for indoor air (for all impactors)

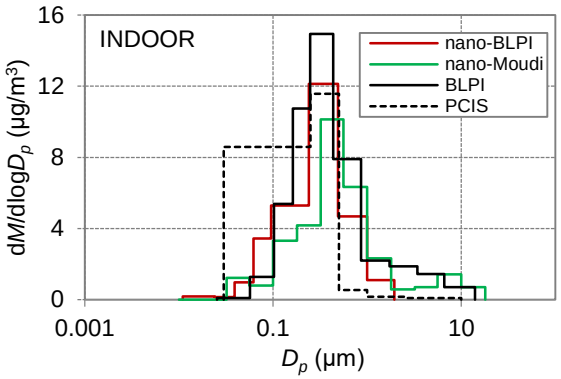

Figure 5. Average mass size distributions in Prague during winter in indoor air.

3.3.3. Size distribution of chemical components

Figures 6 and 7 show the particle mass size distributions of major (SO_4^{2-}, NO_3^- and NH_4^+) and minor (Cl^-, Na^+, K^+, Mg^{2+} and Ca^{2+}) aerosol constituents for the winter campaign in Prague in outdoor and indoor air, respectively. In the winter in Prague, the mass size distributions of components have a predominantly fine mode (< 1 µm), with the coarse mode being almost negligible in winter in Prague (by all impactors) but highly significant in Barcelona during summer, such as the case for BLPI.

While the fine mode was dominant for the particle mass concentration and all the predominant aerosol constituents (SO_4^{2-}, NO_3^- and NH_4^+) for both indoor and outdoor air during winter in Prague, the average mass size distributions for minor species (Cl^-, Na^+, K^+, Mg^{2+} and Ca^{2+}), were clearly multimodal (Figures 6 and 7). Similar mass size distributions of these species were obtained by the nano-BLPI and the reference BLPI both outdoors and indoors in Prague. However marked differences in the mass size distributions of these species were observed with the nano-MOUDI impactor.

In outdoor air there is a clear decrease of NO_3^- and NH_4^+ concentrations measured with the nano-MOUDI, confirming the interpretations provided in the previous sections. This is also visible, even if less pronounced, indoors. In addition, outdoors in Prague, the mass size distributions obtained by the BLPI showed that Ca^{2+}, Na^+ and Mg^{2+} were dominated by coarse modes and for the case of K^+, the fine mode is the dominant one (suggesting biomass combustion as a possible emission source). As for Cl^-, the mass size distributions were clearly bimodal. The nano-MOUDI outdoors had different size distributions from the BLPI for Cl^-, Na^+, Ca^{2+} and Mg^{2+}. Only for K^+ the size distribution is similar. Mass size distributions of Cl^- and Na^+ may have been influenced by filter contamination. The Ca^{2+} peak detected at around 100 nm obtained by the nano-BLPI in outdoor air may possibly be ascribed also to filter contamination, although no specific data are available to support this interpretation. Similar peaks at 10 and 50 nm were observed indoors with the nano-MOUDI and nano-BLPI which may suggest bounce, contamination or blank variability.

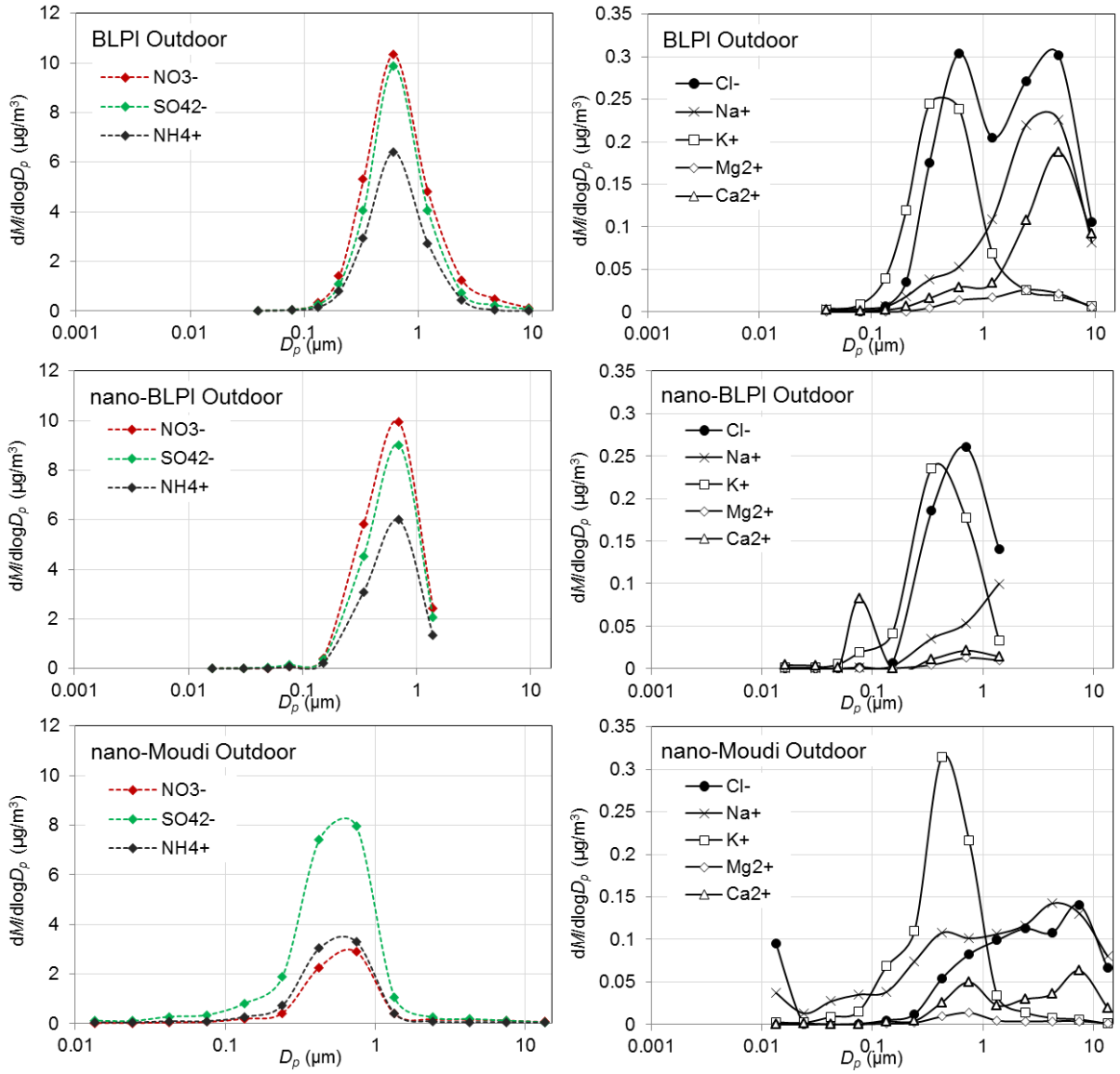

Figure 6. Average mass size distributions for different ionic species (left: SO_4^{2-}, NO_3^- and NH_4^+ and right: Cl^-, Na^+, K^+, Mg^{2+} and Ca^{2+}) during winter in outdoor air in Prague.

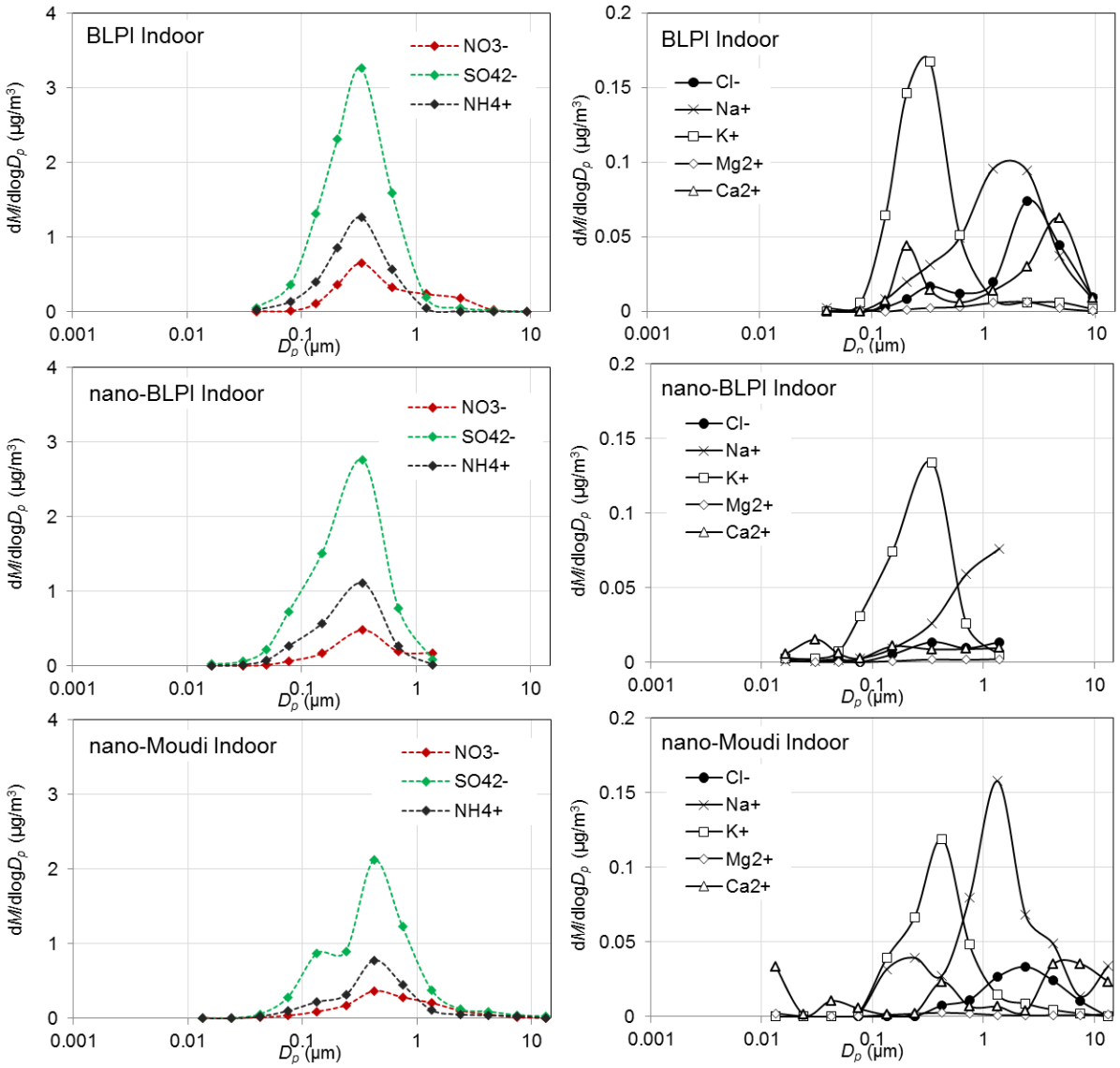

Figure 7. Average mass size distributions for different ionic species (left: SO_4^{2-}, NO_3^- and NH_4^+ and right: Cl^-, Na^+, K^+, Mg^{2+} and Ca^{2+}) during winter in indoor air in Prague.

4. Conclusions

This work aimed to assess the performance of four conventional and nano-range impactors, by means of two intercomparison exercises in Prague, during winter 2015 and in Barcelona during summer 2015. The aim of the campaigns was to test the instruments' performance with regard to the particle mass size distributions under different aerosol compositions resulting from different emission sources, meteorology, seasons, and air mass origins. All the cascade impactors were loaded with uncoated substrates excepting for the case of BLPI which foils were coated.

Taking the BLPI as an internal reference, the best agreement regarding mass size distributions was obtained with the nano-BLPI, especially for particles larger than 250 nm. The nano-MOUDI showed a good agreement for particle sizes >320 nm, whereas for particle diameters <320 nm this instrument recorded larger mass concentrations than the internal reference. Different particle effects may have caused the differences regarding particle mass concentrations collected in indoor and outdoor air by the nano-MOUDI. Particle volatilisation may have occurred due to the internal rotating mechanisms

which heat the impactor casing up. Decomposition of ammonium nitrate and chloride, as evidenced by the lower nitrate and chloride concentrations in the accumulation mode, is probably also enhanced in the nano-MOUDI due to the spreading of the sample on the whole filter surface, in comparison with thick individual spots of material obtained with the BLPI and nano-BLPI impactors. Further research is needed to clarify this issue. With regard to the PCIS, their size-resolved mass concentrations were comparable with other impactors for PM_1, PM_2 and PM_{10}, but the cut-off at 0.25 µm was not consistent with that of the internal reference.

In Barcelona, the sampling took place under dry conditions (< 50% RH) and thus, particle bounce would be expected since some particles (depending on composition) could get dry(I. N. Tang & Munkelwitz, 1994)(I. N. Tang & Munkelwitz, 1994)(I. N. Tang & Munkelwitz, 1994). Inversely, bounce can be probably neglected for the Prague outdoor intercomparison since the RH was always >50 % indicating the presence of droplet aerosols that tend to adhere to the impaction substrate. To avoid such an effect impactor substrates should always be greased especially in areas with low humidity.

Aerosol mass size distributions were assessed for the Prague and Barcelona campaigns. During winter in Prague (outdoors), the mass size distributions showed a predominantly fine mode, with the coarse mode being almost negligible (by all impactors). However, in Barcelona, the coarse size fractions showed larger mass concentrations, evidencing the higher influence of mineral and marine aerosols.

This study concludes that comparability between the different types of impactors assessed was dependent on particle size. Specifically, the influence of the differences in impactor construction (number of jets, flow, vapour pressure, etc.) on UFP mass concentrations should be further addressed. In addition, further research is necessary with regard to the particle processes (evaporation, bounce, etc.) behind the differences in particle mass observed across size fractions in this study.

Acknowledgements

The research leading to these results received funding from the European Community's Seventh Framework Program (FP7-PEOPLE-2012-ITN) no. 315760 (HEXACOMM project). It was also supported by Charles University in Prague, under the project GA UK no. 274213 and the Spanish MINECO, under the frame of SIINN, the ERA-NET for a Safe Implementation of Innovative Nanoscience and Nanotechnology, in the framework of ERANET-SIINN project CERASAFE (id.:16).

5. References

Amato, F., Alastuey, A., Karanasiou, A., Lucarelli, F., Nava, S., Calzolai, G., Severi, M., Becagli, S., Gianelle, V.L., Colombi, C., Alves, C., Custódio, D., Nunes, T., Cerqueira, M., Pio, C., Eleftheriadis, K., Diapouli, E., Reche, C., Minguillón, M.C., Manousakas, M., Maggos, T., Vratolis, S., Harrison, R.M., Querol, X. (2015). AIRUSE-LIFE+: a harmonized PM speciation and source apportionment in 5 Southern European cities. *Atmos. Chem. Phys. Discuss., 15*(17), 23989-24039. doi: 10.5194/acpd-15-23989-2015

BcnMap. (2015). Barcelona Map, Ajuntament de Barcelona, from http://w20.bcn.cat/Guiamap/Default_en.aspx#x=27601.01&y=83987.71&z=0&w=980&h=574&base=GuiaMartorell

Berner, A., Luerzer, C. (1980). Mass size distributions of traffic aerosols at Vienna. *The Journal of Physical Chemistry, 84*(16), 2079-2083. doi: 10.1021/j100453a016

Berner, A., Lürzer, C., Pohl, F., Preining, O., Wagner, P. (1979). The size distribution of the urban aerosol in Vienna. *Science of The Total Environment, 13*(3), 245-261. doi: http://dx.doi.org/10.1016/0048-9697(79)90105-0

Biswas, P., Flagan, R.C. (1984). High-velocity inertial impactors. *Environmental Science & Technology, 18*(8), 611-616. doi: 10.1021/es00126a009

Crilley, L.R., Ayoko, G.A., Jayaratne, E.R., Salimi, F., Morawska, L. (2013). Aerosol mass spectrometric analysis of the chemical composition of non-refractory PM1 samples from school environments in Brisbane, Australia. *Science of The Total Environment, 458–460*, 81-89. doi: http://dx.doi.org/10.1016/j.scitotenv.2013.04.007

Delgado-Saborit, J.M., Stark, C., Harrison, R.M. (2014). Use of a versatile high efficiency multiparallel denuder for the sampling of PAHs in ambient air: gas and particle phase concentrations, particle size distribution and artifact formation. [Research Support, Non-U S Gov't]. *Environ Sci Technol, 48*(1), 499-507.

Fang, C.P., McMurry, P.H., Marple, V.A., Rubow, K.L. (1991). Effect of Flow-induced Relative Humidity Changes on Size Cuts for Sulfuric Acid Droplets in the Microorifice Uniform Deposit Impactor (MOUDI). *Aerosol Science and Technology, 14*(2), 266-277. doi: 10.1080/02786829108959489

Fujitani, Y., Hasegawa, S., Fushimi, A., Kondo, Y., Tanabe, K., Kobayashi, S., Kobayashi, T. (2006). Collection characteristics of low-pressure impactors with various impaction substrate materials. *Atmospheric Environment, 40*(18), 3221-3229. doi: http://dx.doi.org/10.1016/j.atmosenv.2006.02.001

Geller, M.D., Kim, S., Misra, C., Sioutas, C., Olson, B.A., Marple, V.A. (2002). A Methodology for Measuring Size-Dependent Chemical Composition of Ultrafine Particles. *Aerosol Science and Technology, 36*(6), 748-762. doi: 10.1080/02786820290038447

Hering, S., Cass, G. (1999). The Magnitude of Bias in the Measurement of PM25 Arising from Volatilization of Particulate Nitrate from Teflon Filters. *Journal of the Air & Waste Management Association, 49*(6), 725-733. doi: 10.1080/10473289.1999.10463843

Hering, S.V., Flagan, R.C., Friedlander, S.K. (1978). Design and evaluation of new low-pressure impactor. I. *Environmental Science & Technology, 12*(6), 667-673. doi: 10.1021/es60142a004

Hillamo, R.E., Kauppinen, E.I. (1991). On the Performance of the Berner Low Pressure Impactor. *Aerosol Science and Technology, 14*(1), 33-47. doi: 10.1080/02786829108959469

Hinds, W.C. (1999). *Aerosol technology : properties, behavior, and measurement of airborne particles*. New York: Wiley.

Hitzenberger, R., Berner, A., Galambos, Z., Maenhaut, W., Cafmeyer, J., Schwarz, J., Müller, K., Spindler, G., Wieprecht, W., Acker, K., Hillamo, R., Mäkelä, T. (2004). Intercomparison of methods to measure the mass concentration of the atmospheric aerosol during INTERCOMP2000—influence of instrumentation and size cuts. *Atmospheric Environment, 38*(38), 6467-6476. doi: http://dx.doi.org/10.1016/j.atmosenv.2004.08.025

Howell, S., Pszenny, A.A.P., Quinn, P., Huebert, B. (1998). A Field Intercomparison of Three Cascade Impactors. *Aerosol Science and Technology, 29*(6), 475-492. doi: 10.1080/02786829808965585

Huang, Z., Harrison, R.M., Allen, A.G., James, J.D., Tilling, R.M., Yin, J. (2004). Field intercomparison of filter pack and impactor sampling for aerosol nitrate, ammonium, and sulphate at coastal and inland sites. *Atmospheric Research, 71*(3), 215-232. doi: http://dx.doi.org/10.1016/j.atmosres.2004.05.002

Hussein, T., Glytsos, T., Ondráček, J., Dohányosová, P., Ždímal, V., Hämeri, K., Lazaridis, M., Smolík, J., Kulmala, M. (2006). Particle size characterization and emission rates during indoor activities in a house. *Atmospheric Environment, 40*(23), 4285-4307. doi: http://dx.doi.org/10.1016/j.atmosenv.2006.03.053

Hussein, T., Kukkonen, J., Korhonen, H., Pohjola, M., Pirjola, L., Wraith, D., Härkönen, J., Teinilä, K., Koponen, I.K., Karppinen, A., Hillamo, R., Kulmala, M. (2007). Evaluation and modeling of the size fractionated aerosol particle number concentration measurements nearby a major road in Helsinki – Part II: Aerosol

measurements within the SAPPHIRE project. *Atmos. Chem. Phys., 7*(15), 4081-4094. doi: 10.5194/acp-7-4081-2007

IPR. (2015). Geoportal Praha, Prague geographic data in one place, Prague Institute of Planning and Development (IPR Praha), from http://www.geoportalpraha.cz/en/maps-online#.VlIWWLerR1s

Jiménez, S., Ballester, J. (2011). Use of a Berner Low-Pressure Impactor at Low Inlet Pressures. Application to the Study of Aerosols and Vapors at High Temperature. *Aerosol Science and Technology, 45*(7), 861-871. doi: 10.1080/02786826.2011.566900

Karanasiou, A.A., Sitaras, I.E., Siskos, P.A., Eleftheriadis, K. (2007). Size distribution and sources of trace metals and n-alkanes in the Athens urban aerosol during summer. *Atmospheric Environment, 41*(11), 2368-2381. doi: http://dx.doi.org/10.1016/j.atmosenv.2006.11.006

Lin, C.-C., Chen, S.-J., Huang, K.-L., Hwang, W.-I., Chang-Chien, G.-P., Lin, W.-Y. (2005). Characteristics of Metals in Nano/Ultrafine/Fine/Coarse Particles Collected Beside a Heavily Trafficked Road. *Environmental Science & Technology, 39*(21), 8113-8122. doi: 10.1021/es048182a

Lunden, M.M., Revzan, K.L., Fischer, M.L., Thatcher, T.L., Littlejohn, D., Hering, S.V., Brown, N.J. (2003). The transformation of outdoor ammonium nitrate aerosols in the indoor environment. *Atmospheric Environment, 37*(39–40), 5633-5644. doi: http://dx.doi.org/10.1016/j.atmosenv.2003.09.035

Marple, V., Olson, B., Romay, F., Hudak, G., Geerts, S.M., Lundgren, D. (2014). Second Generation Micro-Orifice Uniform Deposit Impactor, 120 MOUDI-II: Design, Evaluation, and Application to Long-Term Ambient Sampling. *Aerosol Science and Technology, 48*(4), 427-433. doi: 10.1080/02786826.2014.884274

Marple, V.A., Rubow, K.L., Behm, S.M. (1991). A Microorifice Uniform Deposit Impactor (MOUDI): Description, Calibration, and Use. *Aerosol Science and Technology, 14*(4), 434-446. doi: 10.1080/02786829108959504

Mašková, L., Smolík, J., Vodička, P. (2015). Characterisation of particulate matter in different types of archives. *Atmospheric Environment, 107*, 217-224. doi: http://dx.doi.org/10.1016/j.atmosenv.2015.02.049

May, K.R. (1945). The Cascade Impactor. *Journal of Scientific Instruments, 22*(12), 247.

Misra, C., Singh, M., Shen, S., Sioutas, C., Hall, P.M. (2002). Development and evaluation of a personal cascade impactor sampler (PCIS). *Journal of Aerosol Science, 33*(7), 1027-1047. doi: 10.1016/s0021-8502(02)00055-1

Nie, W., Wang, T., Gao, X., Pathak, R.K., Wang, X., Gao, R., Zhang, Q., Yang, L., Wang, W. (2010). Comparison among filter-based, impactor-based and continuous techniques for measuring atmospheric fine sulfate and nitrate. *Atmospheric Environment, 44*(35), 4396-4403. doi: http://dx.doi.org/10.1016/j.atmosenv.2010.07.047

Oberdörster, G. (2000). Pulmonary effects of inhaled ultrafine particles. *Int Arch Occup Environ Health, 74*(1), 1-8. doi: 10.1007/s004200000185

Oberdorster, G., Oberdorster, E., Oberdorster, J. (2005). Nanotoxicology: an emerging discipline evolving from studies of ultrafine particles. [Research Support, N I H , Extramural

Research Support, U S Gov't, Non-P H S

Research Support, U S Gov't, P H S

Review]. *Environ Health Perspect, 113*(7), 823-839.

Ondráček, J., Schwarz, J., Ždímal, V., Andělová, L., Vodička, P., Bízek, V., Tsai, C.J., Chen, S.C., Smolík, J. (2011). Contribution of the road traffic to air pollution in the Prague city (busy speedway and suburban crossroads). *Atmospheric Environment, 45*(29), 5090-5100. doi: http://dx.doi.org/10.1016/j.atmosenv.2011.06.036

Pennanen, A.S., Sillanpaa, M., Hillamo, R., Quass, U., John, A.C., Branis, M., Hunova, I., Meliefste, K., Janssen, N.A., Koskentalo, T., Castano-Vinyals, G., Bouso, L., Chalbot, M.C., Kavouras, I.G., Salonen, R.O. (2007).

Performance of a high-volume cascade impactor in six European urban environments: mass measurement and chemical characterization of size-segregated particulate samples. [Evaluation Studies

Research Support, Non-U S Gov't]. *Sci Total Environ, 374*(2-3), 297-310.

Preining, O., Berner, A. (1979). Aerosol Measurements in the Submicron Size Range. *EPA report, EPA-600/2-79-105*. Washington, DC: EPA.

Querol, X., Alastuey, A., Moreno, T., Viana, M.M., Castillo, S., Pey, J., Rodríguez, S., Artiñano, B., Salvador, P., Sánchez, M., Garcia Dos Santos, S., Herce Garraleta, M.D., Fernandez-Patier, R., Moreno-Grau, S., Negral, L., Minguillón, M.C., Monfort, E., Sanz, M.J., Palomo-Marín, R., Pinilla-Gil, E., Cuevas, E., de la Rosa, J., Sánchez de la Campa, A. (2008). Spatial and temporal variations in airborne particulate matter (PM10 and PM2.5) across Spain 1999–2005. *Atmospheric Environment, 42*(17), 3964-3979. doi: http://dx.doi.org/10.1016/j.atmosenv.2006.10.071

Reche, C., Viana, M., Brines, M., Perez, N., Beddows, D., Alastuey, A., Querol, X. (2015). Determinants of aerosol lung-deposited surface area variation in an urban environment. [Research Support, Non-U S Gov't]. *Sci Total Environ, 517*, 38-47.

Sardar, S.B., Fine, P.M., Mayo, P.R., Sioutas, C. (2005). Size-Fractionated Measurements of Ambient Ultrafine Particle Chemical Composition in Los Angeles Using the NanoMOUDI. *Environmental Science & Technology, 39*(4), 932-944. doi: 10.1021/es049478j

Schaap, M., Spindler, G., Schulz, M., Acker, K., Maenhaut, W., Berner, A., Wieprecht, W., Streit, N., Müller, K., Brüggemann, E., Chi, X., Putaud, J.P., Hitzenberger, R., Puxbaum, H., Baltensperger, U., ten Brink, H. (2004). Artefacts in the sampling of nitrate studied in the "INTERCOMP" campaigns of EUROTRAC-AEROSOL. *Atmospheric Environment, 38*(38), 6487-6496. doi: http://dx.doi.org/10.1016/j.atmosenv.2004.08.026

Schwarz, J., Štefancová, L., Maenhaut, W., Smolík, J., Ždímal, V. (2012). Mass and chemically speciated size distribution of Prague aerosol using an aerosol dryer--the influence of air mass origin. *Sci Total Environ, 437*, 348-362. doi: 10.1016/j.scitotenv.2012.07.050

Seinfeld, J.H., Pandis, S.N. (2006). Atmospheric Chemistry and Physics: From Air Pollution to Climate Change, 2nd edition. *J. Wiley, New York*.

Sioutas, C. (2004). Development of New Generation Personal Monitors for Fine Particulate Matter (PM) and its Metal Content. *NUATRC Research Report No. 2*.

Smolík, J., Dohányosová, P., Schwarz, J., Ždímal, V., Lazaridis, M. (2008). Characterization of Indoor and Outdoor Aerosols in a Suburban Area of Prague. *Water Air Soil Pollut: Focus, 8*(1), 35-47. doi: 10.1007/s11267-007-9141-y

Štefancová, L., Schwarz, J., Maenhaut, W., Chi, X., Smolík, J. (2010). Hygroscopic growth of atmospheric aerosol sampled in Prague 2008 using humidity controlled inlets. *Atmospheric Research, 98*(2–4), 237-248. doi: http://dx.doi.org/10.1016/j.atmosres.2010.04.009

Štefancová, L., Schwarz, J., Mäkelä, T., Hillamo, R., Smolík, J. (2011). Comprehensive Characterization of Original 10-Stage and 7-Stage Modified Berner Type Impactors. *Aerosol Science and Technology, 45*(1), 88-100. doi: 10.1080/02786826.2010.524266

Tursic, J., Grgic, I., Berner, A., Skantar, J., Cuhalev, I. (2008). Measurements of size-segregated emission particles by a sampling system based on the cascade impactor. [Research Support, Non-U S Gov't]. *Environ Sci Technol, 42*(3), 878-883.

Wall, S.M., John, W., Ondo, J.L. (1988). Measurement of aerosol size distributions for nitrate and major ionic species. *Atmospheric Environment (1967), 22*(8), 1649-1656. doi: http://dx.doi.org/10.1016/0004-6981(88)90392-7

Wang, H.-C., John, W. (1988). Characteristics of the Berner Impactor for Sampling Inorganic Ions. *Aerosol Science and Technology, 8*(2), 157-172. doi: 10.1080/02786828808959179

Supporting information

Figure S1. Sampling location in Prague and impactors deployed in outdoor (top right) and indoor environment (bottom right) (IPR, 2015).

Figure S2. Sampling location in Barcelona (BcnMap, 2015).

Table S1. Design parameters of the stages from nano-BLPI.

Stage number	Lower cut sizes (µm)	Number of nozzles	Nozzle Diameter (mm)
9	1.95	1	3.60

8	1.00	39	0.70
7	0.49	17	0.60
6	0.24	8	0.54
5	0.095	43	0.27
4	0.062	88	0.25
3	0.039	142	0.25
2	0.024	237	0.25
1	0.011	408	0.25

Table S2. Approximate lower cut sizes for selected size fractions.

Selected size fractions	BLPI (µm)	nano-BLPI (µm)	nano-MOUDI (µm)	PCIS (µm)
$PM_{0.25}$	0.025-0.25	0.011-0.24	0.01-0.32	0.03-0.25
PM_1	0.025-0.86	0.011-1.0	0.01-1.0	0.03-1.0
PM_2	0.025-1.7	0.011-1.95	0.01-1.8	0.03-2.5
PM_{10}	0.025-14	N/A	0.01-10	0.03-10

N/A – Not available

12. Article 5.

Variability of aerosols and chemical composition of PM_{10}, $PM_{2.5}$ and PM_1 on the platform of the Prague underground metro.

M. Cusack, **N. Talbot**, J. Ondráček, M.C. Minguillón, V. Martins, K. Klouda, J. Schwarz, V. Ždímal.

Published in ***Atmospheric Environment journal***: September 2015

Pages: 152- 167

Published in: 2015

Impact factor of Journal: 3.465

Variability of aerosols and chemical composition of PM_{10}, $PM_{2.5}$ and PM_1 on the platform of the Prague underground metro.

M. Cusack[a], **N. Talbot[ae]**, J. Ondráček[a], M.C. Minguillón[b], V. Martins[b,c], K. Klouda[d], J. Schwarz[a], V. Ždímal[a].

[a] {Institute of Chemical Process Fundamentals of the ASCR, v.v.i., Rozvojova 2, 165 02 Prague 6 – Suchdol, Czech Republic}
[b] {Institute of Environmental Assessment and Water Research, IDAEA, CSIC, Jordi Girona, 18-26, 08034, Barcelona, Spain}
[c] {Department of Analytical Chemistry, Faculty of Chemistry, University of Barcelona, Av. Diagonal 647, 08028 Barcelona, Spain}
[d] {National Institute for Nuclear, Chemical and Biological Protection, Kamenná 71, 262-31 Milín, Czech Republic}
[e] -Charles University in Prague, Faculty of Science, Institute for Environmental Studies, Prague, 128 43, Czech Republic

Corresponding author: Michael Cusack

Key words: underground train microenvironment, PM concentrations, sub-micron particle number concentration and size distribution, PM chemical characterisation

Abstract

Measurements of PM_{10}, $PM_{2.5}$ and PM_1 and particle number concentration and size distribution were measured for 24 hours on a platform of the Prague underground metro in October 2013. The three PM fractions were analysed for major and minor elements, secondary inorganic compounds (SIA) and total carbon (TC). Measurements were performed both when the metro was inoperative and closed to the public (background), and when the metro was in operation and open to passengers. PM concentrations were elevated during both periods, but were substantially enriched in the coarse fraction during hours when the metro was in operation. Average PM concentrations were 214.8, 93.9 and 44.8 μg m^{-3} for PM_{10}, $PM_{2.5}$ and PM_1, respectively (determined gravimetrically). Average particle number concentrations were 8.5 x 10^3 cm^{-3} for background hours and 11.5 x 10^3 cm^{-3} during operational hours. Particle number concentrations were found to not vary as significantly as PM concentrations throughout the day. Variations in PM are strongly governed by passing trains, with highest concentrations recorded during rush hour. When trains are less frequent, PM concentrations are shown to fluctuate in unison with the entrance and exit of trains (as shown by wind velocity measured on the platform). PM was found to be highly enriched with iron, especially in the coarse fraction, comprising 46% of PM_{10} (99 μg m^{-3}). This reduces to 6.7 μg m^{-3} during background hours, proving that the main source of iron is the trains themselves, most probably from wheel-rail mechanical abrasion. Other enriched elements relative to background hours included Ba, Cu, Mn, Cr,

Mo, Ni and Co, among others. Many of these elements exhibited a similar size distribution, further indicating their sources are common and are attributed to train operations.

1 Introduction

One of the principal measures employed by developed countries to combat traffic congestion and emissions in urbanised areas is through the promotion of public transport. Of the various modes of public transport available in many urban areas, underground trains are considered one of the cleanest from an environmental perspective. This is due to a number of factors, including the metro system's capability of carrying a large number of passengers who may otherwise use automobiles, reducing traffic congestion and emissions at surface level. Furthermore, the trains are powered electrically with subsequent lower local emissions compared to traffic. However, numerous studies have reported higher concentrations of PM on underground platforms and inside the trains themselves than above-ground ambient PM concentrations (Aarnio et al., 2005; Johansson & Johansson, 2003; Kam, Cheung, Daher, & Sioutas, 2011; X. Querol et al., 2012; Imre Salma et al., 2009; Imre Salma, Weidinger, & Maenhaut, 2007; Seaton et al., 2005), among many others. Most of these studies have described high concentrations of PM and metals in the air. Considering the routine use of many passengers on metro systems (during commuting for example), it is important to understand and characterise the air quality in these specific microenvironments in order to determine what type of aerosols passengers are regularly exposed to. In the aforementioned studies, numerous metals have been found to be enriched in these environments compared to surface air, such as Fe, Mn, Ni, Cu and Cr.

Excessive exposure to Fe and other metals has been linked to oxidative stress, inflammatory reactions, neurodegenerative diseases and multiple sclerosis (Donaldson et al., 1997). Cr and Ni are known to be carcinogenic, and Mn is classified as neurotoxic and can cause respiratory illnesses (WHO, 2000). This may increase the personal exposure to these contaminants by commuters. Minguillón et al (2012) used personal sampling to identify aerosols in the metro microenvironment as a source of personal exposure. The sources of these metals include mechanical wear and friction of the electric cables which power the trains, brake pad erosion, mechanical abrasion of wheel and rails, erosion of construction material in the tunnels, and significant resuspension from air turbulence as a result of passing trains (X. Querol et al., 2012; Imre Salma et al., 2007). The levels of PM on the platforms are often strongly governed by ventilation systems and the entrainment of surface air to the underground stations.

The Prague metro rail network is relatively new by European standards, which began construction in 1974, and is continuously being extended since its introduction. The Prague metro currently consists of three lines, comprising 57 stations, totalling a tunnel network of 59.4 km. According to the operator Prague Public Transit Company (PPTC, www.dpp.cz), the Prague metro carried 589,165,000 passengers in 2012 alone, with an average duration of 16 minutes per trip. Thus, regular use of the metro for commuting would be roughly 30 minutes per day. A previous study on particulate pollution levels in the Prague metro system reported that the passenger in that study spent on average 11.3 ± 3.1 min in the underground section of the metro including escalators and waiting on the platform, but

not including on-train travel (Braniš, 2006), which corresponded well with the most frequent average time spent per journey by passengers as reported by the Prague Ministry of Transport (www.mdcr.cz). That same study compared PM_{10} levels in the ground level urban environment, the underground spaces of the metro network and inside the trains. Concentrations were highest inside the metro trains, followed by the underground spaces and finally the outdoor environment.

The aim of this study is to describe aerosol concentrations and variability, and chemically characterise PM sampled during a 24 hour period on a platform of the Prague underground metro system. To this end, PM and particle number concentration and size distribution are described, and the chemical composition of PM in various size fractions is discussed, both for periods when the metro was out of operation and operational.

2 Methodology

2.1. Sampling site

Measurements were performed at the city centre metro station Museum (platform of line A, direction Depo Hostivař), which is at the intersection of line A and line C. The platform is at a depth of 34 metres below ground and is separated from the train moving in the opposite direction by two walls and a central tunnel. According to PPTC, ventilation for this station was continuous and stable throughout the day, both when the metro was closed and open. The measurement site was located at the end of the platform where the trains exit, to minimise impact and inconvenience for passengers. The passenger entrance onto the platform is around halfway down the platform. Trains commence at 4:40 h and the last train leaves the terminus station at 00:00 h, with a frequency between two to ten minutes depending on the time of day. Both on-line and off-line sampling were performed during hours when the metro was shut down and closed to the public (for background sampling), and when the metro was in operation and open to the public.

2.2. On-line measurements

Particle number size distributions within the range 0.5 – 20 µm (aerodynamic diameter) were measured in real-time by an Aerodynamic Particle Sizer (APS 3321 TSI). Ambient aerosol was sampled using the instruments inlet with a time resolution of 3 min. The data collected by the APS was used to calculate PM concentrations using the AIM software (TSI, density 1 g cm^{-3}) with a high time resolution, although this data was not corrected by comparison with gravimetric sampling as the duration of the campaign was short. Furthermore, the particle density used is more typical of ambient aerosol, which can be significantly different to the metro environment. Thus, the data presented in this work from the APS are more useful for observing variations in concentrations of PM, as opposed to reporting definitive concentrations, which can instead be deduced from the gravimetric sampling (described below). Total particle number concentrations were measured using a Condensation Particle Counter (CPC 3025 TSI) for particles of diameter 3 nm and above. The sub-micrometre particle number size distribution was measured using a Scanning Mobility Particle Sizer (SMPS 3936 TSI), comprised of a Differential Mobility Analyser (DMA 3080 TSI) coupled with a CPC (3775 TSI), which provided the size distribution of particles of mobility diameter 14-637 nm. The time resolution was set at 3 min. with an aerosol flow of 0.3 l/min and a sheath air flow of 3 l/min. A range of meteorological parameters (wind

speed, wind direction, temperature, relative humidity, atmospheric pressure) were measured alongside all the instrumentation employed.

2.3. Off-line sampling

PM_{10}, $PM_{2.5}$ and PM_1 samples were collected using low volume samplers (2.3 m^3 h^{-1}, LECKEL) equipped with quartz microfibre filters (Pallflex) during two sampling periods. The first period corresponded to the time when the metro was out of operation and closed to the public (3:03 to 4:35 a.m.), and the second period included operational hours (5:03 to 0:08 (+1 day) a.m.). PM_x concentrations were determined gravimetrically using a microbalance (Model XP105DR, Mettler Toledo) with a sensitivity of ±10 µg. The filters were pre-equilibrated before weighing for at least 48 h in a conditioned room (20°C and 50% relative humidity).

Different analytical techniques were employed for the chemical characterisation of PM collected on each filter, as described by Querol et al. (2008). ½ of each filter was acid digested ($HF:HNO_3$: $HClO_4$) for the determination of major and trace elements. The major components were determined by Inductively Coupled Plasma Atomic Emission Spectroscopy (IRIS Advantage TJA solutions, THERMO). Concentrations of trace elements were measured by Inductively Coupled Plasma Mass Spectroscopy (X Series II, THERMO). A portion of each filter (1.5 cm^2) was used for the determination of total carbon (TC) by a thermal-optical method using a Sunset instrument. The remaining filter was water extracted and subsequent analyses were performed for the determination of water soluble SO_4^{2-}, NO_3^- and Cl^- by Ion Chromatography HPLC and NH_4^+ by selective electrode.

Size segregated samples were collected using a 12 stage small deposit area cascade impactor (SDI, Maenhaut et al., 1996) with aerodynamic lower cut diameters of 0.045, 0.09, 0.15, 0.23, 0.34, 0.52, 0.73, 0.99, 1.50, 2.38, 4.21 and 7.98 µm. The particles were collected on greased Kapton foils (PIXE International, USA). Two samples were taken during operating hours in order to limit the bounce effect. The first sample was taken from 5:05-16:00 and the second from 16:05 to 00:10, and the sum of the two impactor samples are presented here. Elemental composition of the different size fractions (SDI stages) was determined by Particle Induced X-Ray Emission (PIXE). The analysis was performed at 3MV by a Tandetron 4130MC accelerator (NPI ASCR in Řež, Czech Republic). The 2.9MeV proton beam was collimated to 6x6mm squared spot on the sample (particular stages). Each stage was measured for 600s at the beam current up to 30nA depending on the intensity of emitted X-rays.

3 Results

3.1. Variation in PM and particle number concentrations

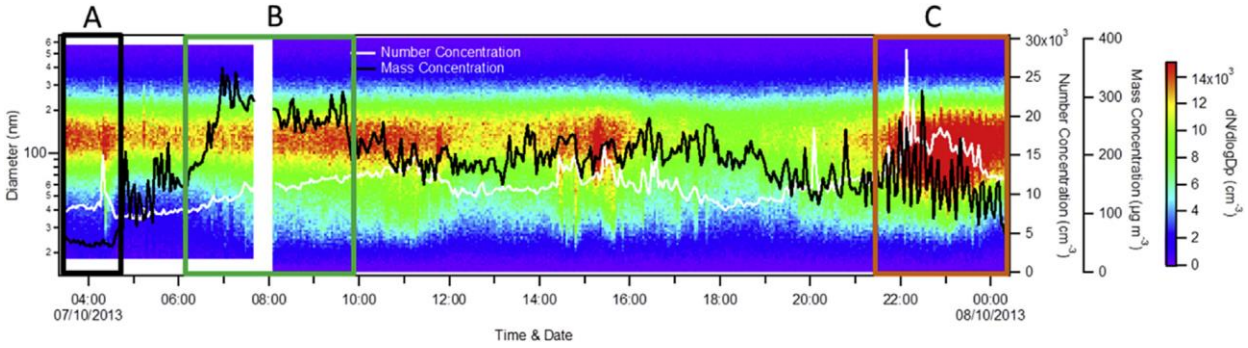

Fig. 1. Contour plot of the particle number size distribution, N14_637, sub-micron particle number concentration and particle mass concentration recorded on 7/10/2013. Periods of interest highlighted (A, B and C).

Fig. 1 shows the variation of the particle number size distribution, and total mass concentration ($PM_{0.5-20}$, as calculated from APS) and number concentration (from the CPC) measured on the metro platform for 24 hours. Concentrations during background hours (period A in Fig.1) were at their lowest as a result of no passing trains and no passengers on the platform. Average PM_{10} (determined gravimetrically) during this period were 96.3 µg m^{-3}, and particle number concentrations were 8.5 x 10^3 cm^{-3} with a modal diameter consistently around 126 nm. An abrupt peak in particle number concentrations was a result of tobacco smoke entering the platform from behind an emergency exit located beside the measurement site. Mass concentrations increase instantly with the arrival of the first train at 4:47 hr, resulting in an average PM_{10} concentration of 214.8 µg m^{-3} during metro operational hours. PM concentrations (as determined by APS) were at their highest during rush hour (B in Fig. 1), when trains were most frequent (every 2-3 min. until 9:30 hr) and passenger numbers were at their highest. Particle number concentrations did not increase as abruptly, with a gradual steady increase during period B. Both mass and number concentrations reach a relatively steady state following rush hour, when trains run with a frequency of 4-5 min. until 20 hr. Similar daily patterns have been observed systematically in other metro systems (Martins et al., 2014). During the final part of the day (period C in Fig. 1) a significant change in the variation of mass and number concentrations occurs. PM commences a decreasing trend with a well-defined oscillating profile. This is not reflected in the particle number concentration, but number concentrations increase to their highest recorded for the entire day (11.4 x 10^3 cm^{-3}). The opposing trend for particle mass and particle number concentration may be related to differing sources of PM and sub-micrometre particle concentrations. This decoupling of variations in PM and sub-micrometre particle concentrations has been described previously in Milan (Colombi et al., 2013).

Fig. 2a shows the variation of $PM_{0.5-1}$, $PM_{1-2.5}$ and $PM_{2.5-10}$ and wind speed for the duration of the campaign. The coarse fraction is affected to a much greater extent by the arrival of trains than the fine fraction. Indeed, concentrations of $PM_{1-2.5}$ and $PM_{2.5-10}$ are enriched from background to operational hours by a factor of 12 and 7 respectively. In contrast, PM_1 is only increased by a factor of 1.6. It is evident in Fig. 2a that PM variation is strongly governed by wind speed, which is generated by the entrance and exit of trains into and out of the metro tunnel. Indeed, the variation of both wind speed and PM is in very good agreement for most of the day. This indicates that PM concentrations are directly a result of the trains, both in source and variations in concentrations. Furthermore, low nocturnal concentrations relative to operating hours indicate efficient removal processes of coarse particles when the metro shuts down. Similar behaviour has been observed in the Budapest metro system (Imre Salma et al., 2007) and the Barcelona metro (Martins et al., 2014). However, as evidenced in Fig. 1, this is not the case for number concentration.

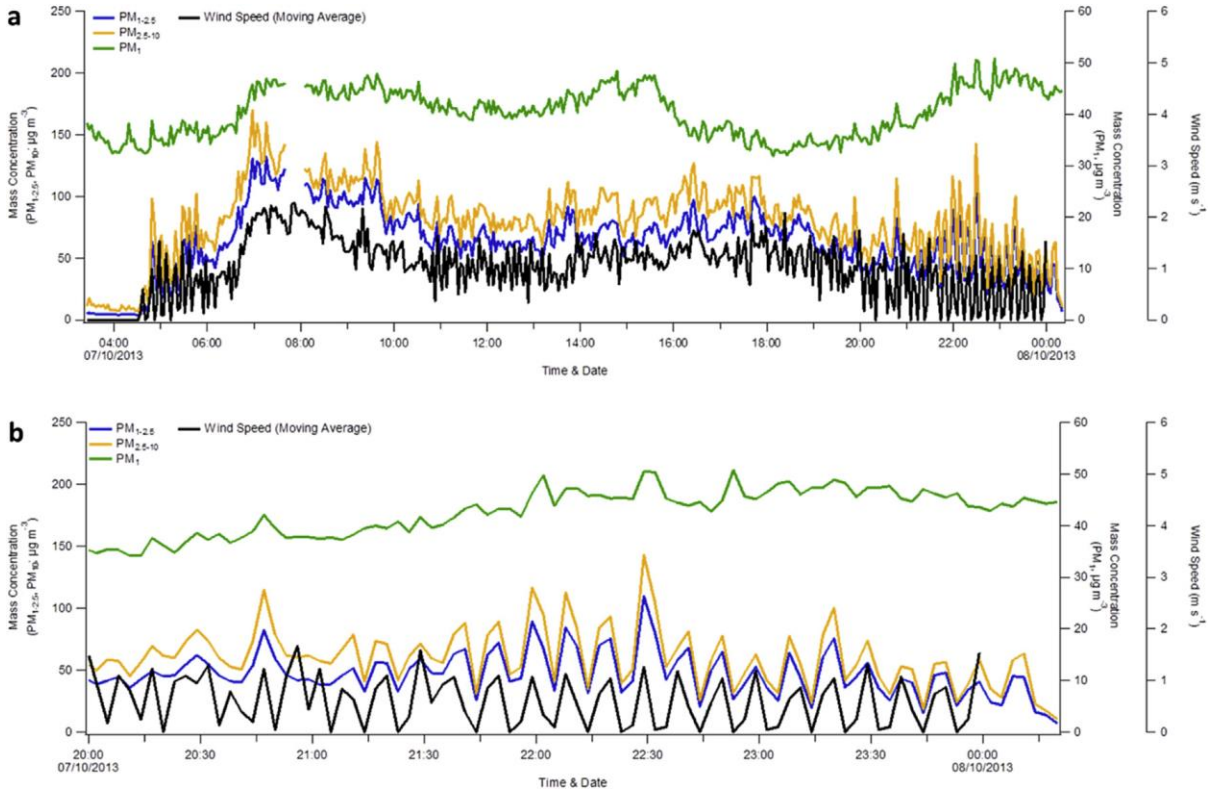

Fig. 2a. Variation in mass concentration (PM1, PM1_2.5 and PM2.5_10) and wind velocity (m s_1). b. As in a for a shorter time period.

Fig. 2b highlights a specific period towards the end of the day (Period C in Fig. 1) for the same parameters shown in Fig. 2a. Fig. 2b shows that as trains become less frequent later in the day (every 7-10 min.) a clear correlation between PM and wind speed emerges. PM concentrations peak with maximum wind speed as a result of train arrivals, indicating that the incoming and outgoing trains directly affect PM on the platform, and when the air settles again (when velocity is at 0 m s^{-1}) PM concentrations reduce. It is noteworthy that when trains are more frequent (when there is almost constant movement of air), the overall net effect on PM is a direct increase. However, when trains are less frequent, PM concentrations reduce, but are also subject to short-lived increases in concentrations. This indicates a two-fold effect of the passage of trains: production of particles by mechanical processes and resuspension by turbulence.

PM concentrations have been reported for a large number of underground train platforms. For purposes of comparison, PM concentrations determined gravimetrically in this study are discussed. A measurement campaign was previously performed in the Prague metro by Braniš, 2006. PM_{10} concentrations on the platform reported in that study averaged at 102 µg m^{-3} (summer concentrations of 71.1 µg m^{-3} and winter concentrations of 120.2 µg m^{-3}) as measured during train operational hours for typical commuting trips i.e. during morning and evening rush hours on weekdays. PM_{10} for this study on the platform was significantly higher at 214.8 µg m^{-3}, but this is the mean concentration for the entire time the metro was in operation, and as described previously, concentrations vary significantly throughout the day.

Furthermore, the instrumentation employed differed for this campaign and that described by Braniš (2006). In that case, a handheld photometric instrument (Dusttrak, TSI) was employed, which is not as

accurate as the standard gravimetric method used in this work. Numerous studies have been performed in metro systems around the world, with many reporting high concentrations of PM_{10} such as in Berlin, London, Stockholm, Rome, Beijing, Budapest, Seoul, Paris, Shanghai and Barcelona (Adams et al., 2001a; Adams et al., 2001b; Fromme et al., 1998; Johansson & Johansson, 2003; Kim et al., 2008; Li et al., 2007; Park & Ha, 2008; Querol et al., 2012; Raut et al., 2009; Salma et al., 2007; Seaton et al., 2005; Ripanucci et al., 2006; Ye et al., 2010; Nieuwenhuijsen et al., 2007; Martins et al., 2014). Of these studies, Berlin and Budapest gave similar average concentrations of PM_{10} at 147 μg m^{-3} and 180 μg m^{-3}, respectively. Night-time concentrations of PM_{10} of 28 μg m^{-3} in Paris by Raut et al. (2009) were much lower compared to those recorded in this work (96.3 μg m^{-3}), but daytime concentrations were similar at 200 μg m^{-3} during normal hours and higher during rush hour (320 μg m^{-3}). It should be noted however that the representativeness of this study should be taken with caution owing to brevity of the campaign (24 h).

Measurements of particle number concentrations on metro platforms to the authors' knowledge are much less common. Number concentrations reported for the Paris metro platform as reported by Raut et al., (2009) were 7 x 10^3 cm^{-3} during operational hours and as low as 4 x 10^3 cm^{-3} at night. These concentrations are significantly lower than this study, whereby concentrations of 8.5 x 10^3 cm^{-3} and 11.5 x 10^3 cm^{-3} were measured for night-time and operational hours respectively. However, similarly to this study, Raut et al., (2009) found relatively little change between particle number concentrations for sub-micrometre particles between day and night, compared with the large fluctuations in mass concentrations. Particle number concentrations measured on three platforms of the London underground (Seaton et al., 2005) ranged from 14 x 10^3 to 29 x 10^3 cm^{-3}, which is significantly higher than concentrations measured in this study. However, similarly to this study, concentrations increased gradually and independently of the mass concentration from early morning to midday. The authors attributed this behaviour to the entrainment of surface air to the platform tunnel. Simultaneous surface measurements of particle number concentration were not measured in this study, but considering the evidence presented in the literature, it is probable that the main source of particles on the platform is from the surface.

Borsós et al. (2012) reported the daily and seasonal variation of particle number concentrations at surface level at a suburban site in Prague. The diurnal variation in that study resembles the variation observed in the Prague metro, albeit with a time lag of between one and two hours for the Prague metro. The authors attributed high nocturnal concentrations in Prague to the influence of domestic heating emissions, traffic and a reduction in the boundary layer height, the combined effect being an increase in concentrations. Similarly to the Prague metro, daytime concentrations were lowest in the late afternoon, which was linked to increased mixing as a result of maximum boundary layer height. Autumn median particle number concentrations in that study ranged from 6 - 7 x 10^3 cm^{-3}. Particle number concentration levels of 31 x 10^3 cm^{-3} were recorded in an underground station in Helsinki (Aarnio et al., 2005) and the authors similarly attributed to these concentrations to surface air entrainment owing to the close correlation with particle number concentrations at the surface.

3.2. PM Speciation

Table 1 shows the mean concentrations of the various major and minor species analysed for PM_1, $PM_{2.5}$ and PM_{10} during both background and operational hours. As the oxidation state cannot be

determined from the analysis performed, only elemental concentrations are shown in Table 1, but for the chemical mass balance, the metal oxide concentrations (Fe_2O_3, Al_2O_3, CuO, MnO, ZnO, TiO_2, Cr_2O_3) were calculated. The chemical mass balance is graphically represented in Fig. 3. The sum of all the components allowed for the determination of 64 to 87 % of the total mass during operational hours and 47 to 55 % during background hours (Fig. 3). The remaining mass is probably attributable to water retention on the filters, and the larger undetermined mass during background hours may be a result of higher uncertainty related to the short sampling time (1:32 hr).

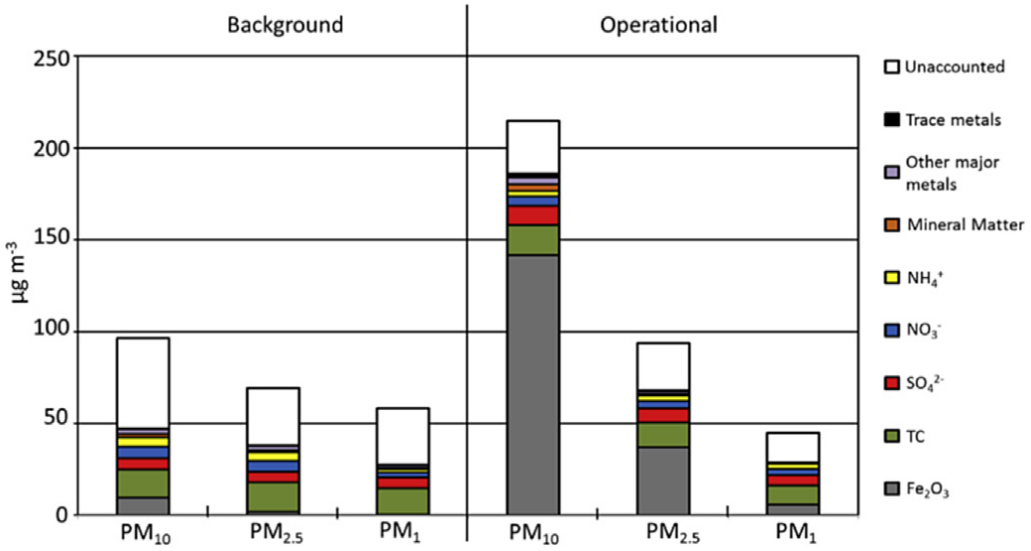

Fig. 3. Chemical composition of PM10, PM2.5 and PM1 (mg m_3) for Background and Operational hours.

As evidenced in Table 1 and Fig 3, the majority of PM is in the coarse fraction during operational hours. During this period PM_{10} reached 214.8 µg m^{-3}, followed by 93.9 µg m^{-3} for $PM_{2.5}$ and 44.8 µg m^{-3} for PM_1. Background levels were significantly lower for PM_{10} (96.3 µg m^{-3}) and $PM_{2.5}$ (69.4 µg m^{-3}). However background PM_1 concentrations were actually higher at 58.2 µg m^{-3}. It should be highlighted that although total concentrations of PM_1 were found to be higher during background hours relative to operational hours, the sum of the chemical components (as shown in Fig. 3) is actually lower.

Fe is the dominant species in the coarse fraction by a significant margin, comprising 46% of PM_{10} (98.9 µg m^{-3}) and 28% of $PM_{2.5}$ (25.9 µg m^{-3}). This percentage composition reduces to 9% (4.0 µg m^{-3}) for PM_1. For the background samples, Fe becomes a much less significant species, indicating that the source of Fe is dominant during metro operational hours only. The abundance of iron compounds in underground metro tunnels has been documented previously (Aarnio et al., 2005; Querol et al., 2012) and is directly related to emissions from wheel-rail mechanical abrasion. Elemental Fe concentrations measured in this study for $PM_{2.5}$ (25.9 µg m^{-3}) compare well with those measured in Budapest ($PM_{2.0}$; 15.5 µg m^{-3}, Salma et al., 2007), although PM_{10} concentrations in that study were significantly lower (49 µg m^{-3}) than this study (98.9 µg m^{-3}). Aarnio et al. (2005) also reported similar Fe concentrations in $PM_{2.5}$ (20.3 µg m^{-3}). Fe concentrations also fall within the range of the Barcelona metro reported by Querol et al. (2012) for PM_{10} (28.7-144 µg m^{-3}) and $PM_{2.5}$ (28-55.9 µg m^{-3}).

The second most abundant compound for both background and operational samples was total carbon (TC). For both periods, TC can be considered relatively fine during background hours (95% in PM_1), and

slightly more dispersed across the three fractions during operational hours (64% in PM_1). Analysis of organic and elemental carbon (OC/EC) was not performed owing to the interference of Fe in high concentrations when splitting OC and EC by thermal optical methods (Querol et al., 2012). Concentrations of TC in $PM_{2.5}$ (13.5 μg m^{-3}) and PM_{10} (16.5 μg m^{-3}) during operational hours in this study fall within the lower range reported by Querol et al. (2012) for the Barcelona metro system (13 – 34 μg m^{-3} for $PM_{2.5}$ and 13 – 53 μg m^{-3} for PM_{10}).

Mineral matter (MM: Al_2O_3 + CO_3^{2-} + Ca + Mg + TiO_2) concentrations were higher during background hours for PM_1 and $PM_{2.5.}$ PM_{10} was higher during operational hours most likely as a result of resuspension of the coarsest particles in the tunnel, as well as erosion of construction materials. Furthermore, the lower concentrations of MM during background hours may be a result of quicker deposition of the coarsest particles when there are no passing trains and thus less air turbulence. Indeed, this may be an important factor for all species. Other metals (Ba + Cu + Mn + Zn + Cr + Na + K) and trace element concentrations were mostly all higher in all fractions during operational hours, indicating that the main sources of these compounds are from the trains.

Concerning secondary inorganic aerosols (SIA), nitrate concentrations were similar for both periods, with concentrations being slightly elevated during background hours for the coarse fraction. A similar distribution of concentrations is observed for ammonium. SO_4^{2-} concentrations were elevated relative to ammonium and nitrate, and were mostly fine during background hours. PM_{10} sulphate levels were elevated during operational hours and this may indicate the presence of coarser SO_4^{2-} species or the adsorption of sulphate to coarser particles. Sulphate concentrations presented here were calculated from bulk S concentrations and so the presence of sulphate species other than secondary sulphate is possible. As shown in Table 1, sulphate concentrations were highest in the coarse fraction during operational hours, which may indicate the presence of other sulphate species as a result of passing trains. $BaSO_4$ for example is often used as a bulk material in the manufacture of brake pads in trains (Sternbeck et al., 2002; Aarnio et al., 2005).

The variation observed for the majority of SIA is most likely a result of the entrainment of polluted surface air down to the platform, as few sources of SIA would be expected to exist in the metro microenvironment. Thus, surface meteorology and mixing layer development would likely affect SIA concentrations in the metro, similarly to particle number concentrations. As stated previously, the metro ventilation system operated continuously and uniformly throughout the entire measurement period, which would further indicate that changes in concentrations at the surface would be reflected in the metro environment. Schwarz et al. (2012) reported mean surface concentrations of SIA in $PM_{13.7}$ from a suburban site in Prague for winter and summer. In that study, concentrations of SO_4^{2-}, NO_3^- and NH_4^+ were 3.8, 5.8 and 2.7 μg m^{-3} (respectively) in winter, and 2.3, 1.6 and 1.1 μg m^{-3} in summer.

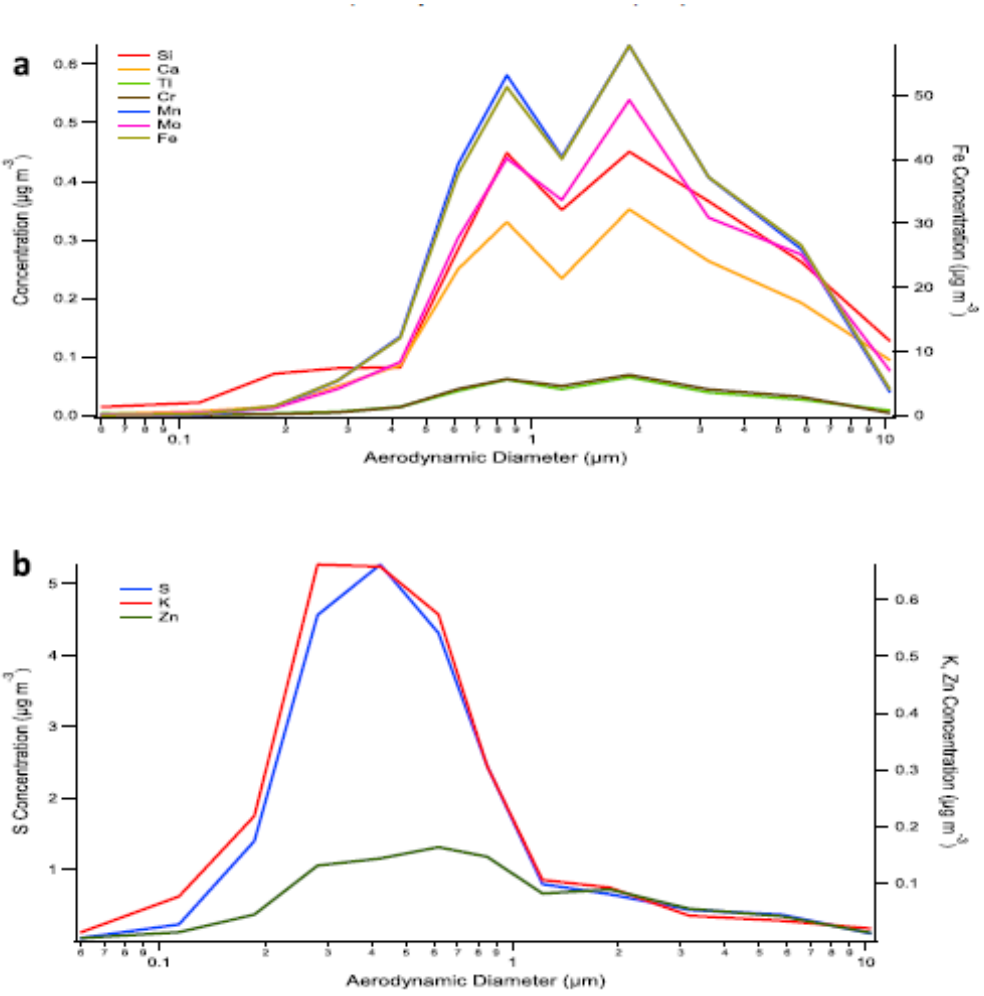

Fig. 4a. Mass size distribution of certain elements (mg m_3) sampled during operational hours. b. Mass size distribution of certain elements (mg m_3) sampled during operational hours.

Certain trace elements exhibit significantly higher concentrations than others, and are specifically enriched in the coarse fraction during operational hours such as Ba, Cu, Mn, Zn, Cr, Mo, Sb, Sn, Ni, Co, Li and Cd. Mo concentrations were very elevated, especially in PM_{10}. Mo has many applications such as in steel alloys and as an electrically conducting ceramic. The probable sources of these elements are emissions from sparking from electrical cables and wheel-rail abrasion (Aarnio et al., 2005; Raut et al., 2009) and brake pads (Sitzmann et al., 1999).

Table 1. Average concentrations of PM_x and chemical components for background and operational hours, measured on the Prague underground metro platform on the 08/10/2013. ws, water soluble; MM, mineral matter.

	PM_1		**$PM_{2.5}$**		**PM_{10}**	
µG M^{-3}	Background	Operational	Background	Operational	Background	Operational
PM_X	58.2	44.8	69.4	93.9	96.3	214.8
TC	14.4	10.5	16.3	13.5	15.1	16.5
WS-NO_3^-	2.6	3.3	6.0	4.2	6.2	4.9
WS-NH_4^+	1.9	2.9	4.8	3.0	5.1	3.0

SO_4^{2-}	5.9	5.5	5.6	7.5	6.5	10.6
FE	0.2	4.0	1.2	25.9	6.7	98.9
CO_3^{2-}	0.3	0.1	0.5	0.6	1.2	2.2
CA	0.1	0.1	0.2	0.3	0.5	1.1
AL	0.6	0.0	0.7	0.2	0.7	0.7
BA	0.01	0.01	0.02	0.07	0.04	0.24
MG	0.1	0.0	0.1	0.1	0.2	0.2
CU	<0.01	0.03	0.01	0.07	0.03	0.19
MN	0.01	0.04	0.02	0.27	0.08	0.75
ZN	0.07	0.06	0.07	0.11	0.13	0.22
NA	0.10	0.03	0.39	0.10	0.20	0.31
K	0.35	0.28	0.37	0.39	0.47	0.58
TI	0.02	<0.01	0.03	0.01	0.04	0.05
CR	<0.01	0.01	0.01	0.03	0.02	0.12
MM	1.6	0.1	2.3	1.2	3.3	4.9
NG M^{-3}						
SR	3.4	0.5	6.7	2.3	6.7	7.4
MO	44	65	99	435	195	1615
SB	0.6	2.0	1.2	3.4	2.5	6.3
SN	1.5	1.7	2.8	3.9	5.0	9.5
NI	0.7	0.9	3.2	5.1	4.9	17.5
AS	5.8	6.5	6.5	9.0	7.0	11.3
PB	29.9	18.1	34.8	23.1	39.0	28.9
V	<0.01	0.5	<0.01	1.2	2.8	3.3
CO	<0.01	0.3	<0.01	1.8	<0.01	6.7
W	<0.01	0.2	<0.01	1.1	<0.01	2.3
LI	<0.01	0.3	<0.01	1.8	<0.01	6.7
RB	<0.01	0.5	<0.01	0.8	<0.01	1.3
CD	<0.01	0.5	<0.01	0.9	<0.01	1.7
BI	<0.01	0.0	<0.01	0.2	<0.01	0.4

Fig. 4a shows the average mass size distribution for certain species (Si, Ca, Ti, Cr, Mn, Mo and Fe) measured during metro operational hours. All of these elements display very similar size distributions with a broad size distribution leaning toward the coarse fraction. The double peak is most likely a result of particle bounce in the impactor, which can be a common problem occurring in impactors (Dunbar et al., 2005). This similar size distribution indicates that the particles are from the same source i.e. from trains and resuspension, as described previously. On the contrary, S, K and Zn share a similar mass size distribution (Fig. 4b), as the sources of these elements are most likely found outdoors and transported to the metro microenvironment, which has similarly been observed in the Budapest

metro system (Salma et al., 2007). A study of the size distribution of SIA at a suburban site outside Prague by Schwarz et al (2012) showed a similar size distribution for secondary sulphate and K, further indicating that the source of S and K in the metro environment is from outdoors.

4 Health implications and Conclusions

There are currently no directives governing concentrations of aerosols in underground train systems, even though concentrations are often much higher than those permissible in ambient air by EU directives (2008/50/EC). A comprehensive study of the exposure of metro train drivers and commuters to PM and its chemical components was performed for the London Underground (Seaton et al., 2005) which highlighted the high levels of aerosols passengers can be exposed to. Concentrations measured in that study on the platform were in the region of 270-480 μg m^{-3} of $PM_{2.5}$. These concentrations are appreciably higher than those measured in this study (93.9 μg m^{-3}). Measurements were not taken in this study inside the trains, thus making exact exposure levels for the duration of the commute not possible.

However, a study by Minguillón et al. (2012) suggested that the highest exposure of passengers to metro aerosols takes place on the platforms as opposed to inside the trains. Seaton et al. (2005) described that the exposure of passengers to the levels of iron oxide measured in the London underground for $PM_{2.5}$ (67% of the total mass) were well below acceptable levels for a workplace environment and do not pose a significant threat to passengers' health. Considering levels of iron oxide are lower for the Prague metro (40% of $PM_{2.5}$: 37.1 μg m^{-3}), it can be assumed there is negligible health risk also. Metals that are enriched during metro operation hours (and thus, presumably emitted as a result of the passing trains), such as Ba, Cu, Mn, Zn, Cr, Mo, Sb, Sn, Ni, Co, and Cd, may be cause for concern from a human health perspective. The accumulative amount of time passengers spend exposed to these metals of such high concentrations throughout their lifetime, and the possible adverse health effects associated with such exposure, may be significant and is certainly worthy of further investigation.

The results presented here describe the variation of particle mass and particle number concentration and size distribution for a 24 hr period on a metro platform in Prague measured on the 7th October 2013. The chemical composition of PM_{10}, $PM_{2.5}$ and PM_1 is also described, for periods when the metro was in operation and also when it was closed to the public and out of operation. This study shows that the air quality in the Prague underground microenvironment is quite severely polluted, with elevated concentrations of PM relative to normal outdoor levels. The main driving force behind the variation in PM levels is undoubtedly the trains themselves, both through wind turbulence by incoming and outgoing trains causing resuspension, and from emissions as a result of the operation of the trains (mechanical wheel/rail abrasion, brake pad wear). Particle number concentrations do not appear to be significantly affected by the trains and do not vary substantially throughout the day in the metro environment, indicating the source of submicron particles is separate to that of PM, most likely from outdoors. PM exists primarily in the coarse fraction, and is highly enriched by Fe, emitted from mechanical abrasion at the wheel-rail interface. TC and SIA are the second most abundant compounds, the sources of which are mostly likely found at ground level. Certain trace elements, such as Ba, Cu, Mn and Zn (among others) were enriched from brake wear and electrical cable erosion.

Acknowledgements

This work was financially supported by the European Union 7th Framework program HEXACOMM FP7/2007-2013 under grant agreement N° 315760, and the Ministry of Interior of the Czech Republic under grant N° VF2010201513. The PIXE analysis was performed in the CANAM (Centre of Accelerators and Nuclear Analytical Methods LM2011019) research infrastructure.

5 References

Aarnio, P., Yli-Tuomi, T., Kousa, A., Mäkelä, T., Hirsikko, A., Hämeri, K., Räisänen, M., Hillamo, R., Koskentalo, T., Jantunen, M., 2005. The concentrations and composition of and exposure to fine particles ($PM_{2.5}$) in the Helsinki subway system. Atmospheric Environment 39, 5059–5066.

Adams, H. S., Nieuwenhuijsen, M. J., Colvile, R. N., 2001. Determinants of fine particle ($PM_{2.5}$) personal exposure levels in transport microenvironments , London , UK. Atmospheric Environment 35, 4557–4566.

Adams, H. S., Nieuwenhuijsen, M. J., Colvile, R. N., McMullen, M. A. S., Khandelwal, P., 2001. Fine particle ($PM_{2.5}$) personal exposure levels in transport microenvironments, London, UK. The Science of the Total Environment 279, 29–44.

Braniš, M., 2006. The contribution of ambient sources to particulate pollution in spaces and trains of the Prague underground transport system. Atmospheric Environment 40, 348–356.

Colombi, C., Angius, S., Gianelle, V., Lazzarini, M., 2013. Particulate matter concentrations, Physical characteristics and elemental composition in the Milan underground transport system. Atmospheric Environment 70, 166–178.

Donaldson, K., Brown, D.M., Mitchell, C., Dinerva, M., Beswick, P.H., Gilmour, P., McNee, W., 1997. Free radical activity of PM_{10}: iron mediated generation of hydroxyl radicals. Environmental Health Perspectives 105, 1285-1289.

Dunbar, C., Kataya, A., Tiangbe, T., 2005. Reducing bounce effects in the Anderson cascade impactor. International Journal of Pharmaceutics 301, 25-32.

Fromme, H., Oddoy, A., Piloty, M., Krause, M., Lahrz, T., 1998. Polycyclic aromatic hydrocarbons (PAH) and diesel engine emission (elemental carbon) inside a car and a subway train. The Science of the Total Environment 217, 165–173.

Furuya, K., Kudo, Y., Okinagua, K., Yamuki, M., Takahashi, K., Araki, Y., Hisimatsu, Y., 2001. Seasonal variation and their characterisation of suspended particulate matter in the air of subway stations. Journal of Trace Microprobe Techniques 19, 469-485.

Johansson, C., Johansson, P., 2003. Particulate matter in the underground of Stockholm. Atmospheric Environment 37(1), 3–9.

Kam, W., Cheung, K., Daher, N., Sioutas, C., 2011. Particulate matter (PM) concentrations in underground and ground-level rail systems of the Los Angeles Metro. Atmospheric Environment 45, 1506–1516.

Kim, K. Y., Kim, Y. S., Roh, Y. M., Lee, C. M., Kim, C. N., 2008. Spatial distribution of particulate matter (PM_{10} and $PM_{2.5}$) in Seoul Metropolitan Subway stations. Journal of Hazardous Materials 154, 440–443.

Li, T.-T., Bai, Y.-H., Liu, Z.-R., Li, J.-L., 2007. In-train air quality assessment of the railway transit system in Beijing: A note. Transportation Research Part D: Transport and Environment 12, 64–67.

Maenhaut, W., Hillamo, R., Mäkelä, T., Jaffrezo, J. L., Bergin, M. H., Davidson, C. I., 1996. A new cascade impactor for aerosol sampling with subsequent PIXE analysis. Nuclear Instruments and Methods in Physics Research Section B: Beam Interactions with Materials and Atoms 109, 482-487.

Martins, V., Moreno, T., Minguillón, M.C., Amato, F., de Miguel, E., Capdevila, M., Querol, X., 2014. Exposure to airborne particulate matter in the subway system. Science of the Total Environment, in press. Doi: 10.1016/j.scitotenv.2014.12.013

Minguillón, M.C., Schembari, A., Triguero-Mas, M., de Nazelle, A., Dadvand, P., Figueras, F., Salvado, J.A., Grimalt, J.O., Nieuwenhuijsen M.J., Querol, X., 2012. Source apportionment of indoor, outdoor and personal $PM_{2.5}$ exposure of pregnant women in Barcelona, Spain. Atmospheric Environment 59, 426-436.

Nieuwenhuijsen M.J., Gómez-Perales, J.E., Colvile, R.N., 2007. Levels of particulate air pollution, its elemental composition, determinants and health effects in metro systems. Atmospheric Environment 41, 7995-8006.

Park, D.-U., Ha, K.-C., 2008. Characteristics of PM_{10}, $PM_{2.5}$, CO_2 and CO monitored in interiors and platforms of subway train in Seoul, Korea. Environment International 34, 629–634.

Querol, X., Moreno, T., Karanasiou, A., Reche, C., Alastuey, A., Viana, M., Font, O., Gil, J., de Miguel, E., Capdevila, M., 2012. Variability of levels and composition of PM_{10} and $PM_{2.5}$ in the Barcelona metro system. Atmospheric Chemistry and Physics 12, 5055–5076.

Raut, J. C., Chazette, P., Fortain, A., 2009. Link between aerosol optical, microphysical and chemical measurements in an underground railway station in Paris. Atmospheric Environment 43, 860–868.

Ripanucci, G., Grana, M., Vicentini, L., Magrini, A., Bergamaschi, A., 2006. Dust in the underground railway tunnels of an Italian town. Journal of Occupational and Environmental Hygiene3, 16-25.

Salma, I., Weidinger, T., Maenhaut, W., 2007. Time-resolved mass concentration, composition and sources of aerosol particles in a metropolitan underground railway station. Atmospheric Environment 41, 8391–8405.

Salma, I., Pósfai, M., Kovács, K., Kuzmann, E., Homonnay, Z., Posta, J., 2009. Properties and sources of individual particles and some chemical species in the aerosol of a metropolitan underground railway station. Atmospheric Environment 43, 3460–3466.

Schwarz, J., Štefancová, L., Maenhaut, W., Smolík, J., Ždímal, V., 2012. Mass and chemically speciated size distribution of Prague aerosol using an aerosol dryer - The influence of air mass origin. Science of the Total Environment 437, 348–362.

Seaton, a, Cherrie, J., Dennekamp, M., Donaldson, K., Hurley, J. F., Tran, C. L., 2005. The London Underground: dust and hazards to health. Occupational and Environmental Medicine 62, 355–362.

Sitzmann, B., Kendall, M., Watt, J., Williams, I., 1999. Characterisation of airborne particles in London by computer-controlled scanning electron microscopy. Science of The Total Environment 241, 63–73.

Sternbeck, J., Sjödin, Å., Andréasson, K., 2002. Metal emissions from road traffic and the influence of resuspension—results from two tunnel studies. Atmospheric Environment 36, 4735–4744.

WHO (World Health Organisation), 2000. Air Quality Guidelines for Europe. second ed., European series No. 91, WHO Regional Office for Europe, Copenhagen.

Ye, X., Lian, Z., Jiang, Ch., Zhou, Z., Chen, H., 2010. Investigation of indoor environmental quality in Shanghai metro stations, China. Environmental Monitoring and Assessment 167, 643-651.

13. Conclusions

This thesis has focused on the transformation of aerosol particles, with attention given to the migration from their outdoor origin to an indoor environment. Within this process, physico-chemical changes to size distribution and chemical composition have been observed in high temporal resolution, which cannot be found in previous literature. The observational speed has enabled insight into both physical and chemical processes that occur in accordance to season, chemical species and micro environment. Within these parameters of research, various instrumentation has been utilised to identify transformation processes, and this has brought about increased knowledge of instrument variability when observing dynamic aerosol processes. The behaviour of nitrate, mostly assumed to be in the solid or aqueous phase as ammonium nitrate, has been a key focus of this thesis, with its volatility at ambient temperatures rigorously defined in article 1, its diurnal phase-shift in summer analysed in article 2, its indoor/ outdoor dissociation clearly defined in article 3, and instrument vulnerability to artefact generation in article 4.

This section will present a brief overview of each research article and then highlight the key results from each. After this, a brief synopsis of all the research will be given, with an overview of the original knowledge that was gained during the research. Finally, a critical evaluation of where future research may advance the findings of this document will be presented.

13.1. Article 1

This article set out to further the understanding of the fundamental process of ammonium nitrate dissociation at the ultrafine particle scale, an area where prior research is limited. An amalgamation of past literature was condensed and reviewed, whilst ammonium nitrate particle size and mass were recorded before and after transportation through a temperature controlled, 2-meter laminar flow reactor. Shrinkage rates and dissociation constants were obtained and set against modelled results and findings from previous literature,

1. The NH_4NO_3 was most likely not completely dehydrated by the time it reached the reactor. Further drying took place in the reactor, helping explain, in part, the accelerated shrinking rates of the 200 nm particles.

2. Dissociation rates showed a dependence on Kelvin surface / kinetics regime change effects. There was an observed dissociation rate increase through the change from diffusion to kinetic regime and a marked acceleration in rate as the particle shrank. This was shown in both our dissociation rates and was highlighted very efficiently in our model, which was designed directly to account for such factors.

3. Temperature was, as expected, the key driving force for dissociation rates, however the particle size is clearly an important factor to consider when assessing dissociation behaviour. Because the particle size changes with changing temperatures the system can be said to be dynamic.

4. Through changing the flow rate of of sample, residence time within the reactor was adjusted between 80-130 seconds. This residence time was found to greatly effect the rate of dissociation.

5. Relative humidity was held constant for this experiment, however with all water soluble ions, and observed indirectly here through hysteresis, relative humidity is crucial to understanding ammonium nitrate particle phase, which is important for size-dissociation rates, and, therefore, must be considered.

13.2. Article 2

This paper describes results from indoor and outdoor measurements, obtained almost simultaneously by using a valve switching system that allowed for high temporal resolution data to be collected concurrently from online C-ToF-AMS, SMPS and OC/EC, and offline BLPI measurements. The results reveal near real-time dynamic aerosol behaviour along a migration path from an outdoor to indoor environment, indoor composition in relation to those outdoors without indoor sources, and warm-season diurnal variations in aerosol composition outdoors.

1. A unique automated switching system allowing for concurrent I/O sampling, which resulted in high temporal resolution of aerosol particle transformations via online C-ToF-AMS, SMPS and OC/EC, revealed the dynamic behaviour of outdoor aerosols migrating indoors into a source-free micro-environment during summer over Prague.

2. Diurnal fluctuations in chemical composition outdoors were investigated through a mass balance model, which revealed that nitrate concentrations were raised during the cooler morning periods but were subsequently lost during the afternoon period. The model attributed 18% AM/PM losses to increased mixing during daytime.

3. A real-time Indoor/Outdoor (I/O) ratio was derived from the indoor penetration of outdoor originating new particles, which revealed a ratio from 0.46 for the smallest <40 nm particles to 0.67 for upper-Aitken and accumulation modes.

4. Indoor concentrations were found to be proportional to those outdoors, with organic matter [2.7 $\mu g/m^3$] and SO_4 [1.7 $\mu g/m^3$] as the most prominent species indoors. Fine fraction NO_3 was observed indoors in both real-time AMS PM_1 and offline BLPI measurements. Greater mass concentration losses were observed from filter measurements.

5. We conclude that the results are indicative of fairly rapid aerosol penetration, a source-free indoor environment and small afternoon I/O temperature gradients.

13.3. Article 3

This article reports the findings of two campaigns that were carried out in order to better understand the transformational processes of aerosol particles as they migrated from outdoor to indoor environments. Summer and winter seasons were investigated using online and offline instrumentation, which, via an automated switching valve, obtained particle size and chemical composition information in near real time.

1. Online results showed that accumulation mode indoor / outdoor (I/O) ratios were significantly lower in winter than in summer. This difference was attributed to the shrinking undergone by particles when moving from outdoor (low heat, high humidity) to indoor (high heat, low humidity) environments.

2. Differences were also notable within size distributions from offline impactor measurements, where more mass was recorded on <200 nm stages for sulfate and ammonium.

3. C-ToF-AMS-obtained chemical composition measurements showed lower indoor mass during winter. Whilst loss of water from particles explained the changes to size, it would not adequately explain the extra loss of mass. Calculations showed a 31-37% decrease in I/O ratios for all chemical species during winter. The similarity in reduction for all species indicated the action of physical, rather than chemical, processes.

4. To assess the relative influence of physical factors on I/O relationships, statistical tests were carried out. These identified wind speed as an anti-correlated to indoor concentrations for all species. Further investigations applied wind roses with incorporated changes in I/O ratios, which indicated that the wind direction and wind speed had a minor influence on changes to indoor composition.

5. This paper concludes that the relative concentration and composition of different aerosol species, increased temperature gradients and wind speed variability were the most influential factors when considering I/O aerosol transformations.

13.4. Article 4

The purpose of this study was two-fold: 1) to assess the performance of a number of conventional and nano-range cascade impactors with regard to the particle mass size distribution under different environmental conditions, variations in chemical composition and different aerosol loads, and 2) to characterise aerosol size distributions, including UFPs, using impactors in 2 European locations. The impactors used were: (i) Berner low-pressure impactor (BLPI; 26 nm - 13.5 µm), (ii) nano-Berner low-pressure impactor (nano-BLPI; 11 nm - 1.95 µm), (iii) Nano-microorifice uniform deposit impactor (nano-MOUDI; 10 nm-18 µm) and (iv) Personal cascade impactor Sioutas (PCIS; < 250 nm - 10 µm).

1. Several impactors have been developed to enable the collection of ultrafine particles (UFP) (<100 nm). However, until now, there have been no field campaigns to-date intercomparing impactor collection of UFP.

2. Taking the BLPI as an internal reference the best agreement regarding mass size distributions was obtained with the nano-BLPI, independently of the aerosol load and aerosol chemical composition. The nano-MOUDI showed a good agreement for particle sizes >320 nm, whereas for particle diameters <320 nm this instrument recorded larger mass concentrations in outdoor air than the internal reference.

3. The differences were attributed to particle bounce, to the dissociation of semi volatiles in the coarser stages and/or to particle shrinkage during transport through the impactor due to higher temperature inside this impactor.

4. These results support the dissociate behaviour of nitrate observed in article 1 and the extra mass lost on impactor mass when compared to real-time instrumentation for articles 2-3.

5. With regard to the PCIS, their size-resolved mass concentrations were comparable with other impactors for PM_1, PM_2 and PM_{10}, but the cut-off at 250 nm did not seem to be consistent with that of the internal reference.

13.5. Article 5

For this final article measurements of PM_{10}, $PM_{2.5}$ and PM_1 and particle number concentration and size distribution were measured for a 24-hr period on a platform of the Prague underground metro. The three PM fractions were analysed for major and minor elements, secondary inorganic compounds (SIA) and total carbon (TC). Measurements were performed both when the metro was inoperative and closed to the public (background), and when the metro was in operation and open to passengers. The purpose was to obtain information regarding the publics' exposure risks to various aerosols. There are currently no directives governing concentrations of aerosols in underground train systems, even though concentrations are often much higher than those permissible in ambient air by EU directives (2008/50/EC).

1. Levels of iron oxide for the Prague metro were 40% of $PM_{2.5}$ at 37.1 μg m^{-3}; it can be assumed there is negligible health risk at these levels. Metals that are enriched during metro operation hours (and thus, presumably emitted as a result of the passing trains), such as Ba, Cu, Mn, Zn, Cr, Mo, Sb, Sn, Ni, Co and Cd, may be cause for concern from a human health perspective.

2. The results presented here describe the variation of particle mass and particle number concentration and size distribution for a 24-hr period on a metro platform in Prague measured on the 7th October, 2013. The chemical composition of PM_{10}, $PM_{2.5}$ and PM_1 is also described for periods when the metro was in operation and when it was closed to the public and out of operation.

3. This study shows that the air quality in the Prague underground micro-environment is quite severely polluted, with elevated concentrations of PM relative to normal outdoor levels. The main driving force behind the variation in PM levels is undoubtedly the trains themselves, both through wind turbulence by incoming and outgoing trains causing resuspension, and from emissions as a result of the operation of the trains (mechanical wheel/rail abrasion, brake pad wear).

4. Particle number concentrations do not appear to be significantly affected by the trains and do not vary substantially throughout the day in the metro environment, indicating the source of submicron particles is separate to that of PM, most likely from outdoors. PM exists primarily in the coarse fraction, and is highly enriched by Fe emitted from mechanical abrasion at the wheel-rail interface.

5. Total carbon (TC) and Secondary inorganic aerosol are the second most abundant compounds in Prague metro. The sources were mostly likely from ground level, outdoors. This illustrated that the migration of aerosol particles from an outdoor to indoor environments is a crucial factor impacting public health.

13.6. Concluding comments

The research described herein has clearly demonstrated that indoor aerosol concentrations are dependent on those outdoors during times when indoor sources are not present. When aerosol particles migrate indoors, transformations occur, however, these transformations are far greater in winter than in summer. We attribute this to the increased thermal and humidity gradient from outdoors to indoors during the cool season and to the change in composition outdoors during winter, most notably due to the prevalence in nitrate during winter, which we assume to be in the form of ammonium nitrate. The amount of shrinking was indicative of a rapid dehydration of particles, which was notable on both impactor measurements and on the online instrumentation. This was demonstrated by the recording of more mass indoors than outdoors on the <200 nm impactor stages for sulfate and ammonium. Size distributions from SMPS measurements clearly showed most of the loss occurring in the accumulation mode sizes, where most of the inorganic fraction can be found.

Inter-instrumentation comparisons are complex due to the collection method and calculation function of individual instruments. Therefore, in this document we do not try and directly assess one instrument against another type, we only observe and compare the results over certain time periods. From this aerosol transformational dynamics were observed in great detail by the online instrumentation, via the timed switching valve. We associate these losses to physical factors, mostly meteorological, where Spearman statistical analysis showed the greatest statistical significance.

For impactor measurements, direct comparisons were made due to the similarity in collection techniques between the instruments. The differences between the different impactors showed that the volatile component of aerosol loading make a significant difference between the differing instruments, with these different results a product of pressure drop, internal instrument heating and capture medium (filter type). These findings are relevant and should be considered to those results obtained by impactor measurements in Prague metro.

All of the findings are closely aligned with the foundational research carried out during the ammonium nitrate dissociation experiments described in article 1. Clearly, there is a strong temperature dependence to dissociation behaviour of ammonium nitrate, however, the aerosol size played a large part in the rate of shrinkage, with rapid increase in loss as the particle shrinks. This informs us of the important time dependent factor when collecting nitrate data, which is directly allied to findings from the impactors compared to online data collection techniques

14. Future Work

This research has shown that nitrate plays an integral part in aerosol loading. However, investigating nitrate is often complex due to its presence as semi-volatile ammonium nitrate. It is understood that the sub-species nitric acid readily attaches itself to surfaces in acid-base reactions. It is reasonable to assume that this hastens the dissociation process.

Outdoors, this process would have little consequence apart from at the point where the aerosol is sampled, however, indoors this process could have significant implications for the results. The chain of experiments carried out for this thesis did not separate causes of dissociation, rather, it focused on the temperature variable. An experimental technique to reduce the influence of this process would be using a Millikan style experiment. Briefly, this would involve suspending a balanced charged particle of ammonium nitrate within the controlled atmosphere of a Millikan, and by using a nethelometer laser, the changes to the particle can be observed whilst temperature and humidity are adjusted. This would isolate the particle away from surfaces, lessening the effect of acid-base reactions.

For our fundamental experiment described in article 1, gas measurements would have supported the findings from the dissociation process. There were attempts to obtain NH_3 results, however, the instrumentation proved too unreliable to add to the results. Moreover, it would be possible to re-run the dissociation experiment with an AMS online, which would provide further information concerning nitrate and ammonium peaks during various temperature profiles. By comparing the SMPS results with those of the AMS it would also be possible to obtain information about the ammonium nitrate phase by using density.

To obtain concurrent gas measurements for all experiments, ideally including NOx, NH_3 and O_3 would have allowed greater insight into phase change processes. However, arranging online gas instrumentation into the same configuration as the aerosol instrumentation is a non-trivial process and would require further time, planning and instrumentation that was not available here.

Slightly longer sampling periods during the seasonal comparisons would have been useful, especially in summer when stable atmospheric conditions did not allow for very diverse conditions. In particular, there was only one new particle formation event observed, which coincided with the only precipitation received during the 3 weeks. Further investigation of these events with high time resolution could have proved interesting.

Finally, the impactor inter-comparison provided a very interesting range of results from the two locations. The range of results obtained from the different impactors was perhaps a little surprising. To provide further insight into the causes for the differing results it would be interesting if further inter-comparisons were carried out simultaneously indoors and outdoors. This should give insight into internal losses through composition abundance and volatility.